Nagra
Nationale
Genossenschaft
für die Lagerung
radioaktiver Abfälle

Cédra
Société coopérative
nationale
pour l'entreposage
de déchets radioactifs

Cisra
Società cooperativa
nazionale
per l'immagazzinamento
di scorie radioattive

TECHNICAL REPORT 85-59

FINAL REPORT OF THE BUFFER MASS TEST
Volume II: Test Results

R. Pusch (Swedish Geological Co)
L. Börgesson (Swedish Geological Co)
G. Ramqvist (El-tekno AB)

August 1985

Parkstrasse 23 5401 Baden/Schweiz Telephon 056/20 55 11

Nagra
Nationale
Genossenschaft
für die Lagerung
radioaktiver Abfälle

Cédra
Société coopérative
nationale
pour l'entreposage
de déchets radioactifs

Cisra
Società cooperativa
nazionale
per l'immagazzinamento
di scorie radioattive

TECHNICAL REPORT 85-59

FINAL REPORT OF THE BUFFER MASS TEST
Volume II: Test Results

R. Pusch (Swedish Geological Co)
L. Börgesson (Swedish Geological Co)
G. Ramqvist (El-tekno AB)

August 1985

Parkstrasse 23 5401 Baden/Schweiz Telephon 056/20 55 11

Der vorliegende Bericht betrifft eine Studie, die für das Stripa-Projekt ausgeführt wurde. Die Autoren haben ihre eigenen Ansichten und Schlussfolgerungen dargestellt. Diese müssen nicht unbedingt mit denjenigen des Auftraggebers übereinstimmen.

Le présent rapport a été préparé pour le projet de Stripa. Les opinions et conclusions présentées sont celles des auteurs et ne correspondent pas nécessairement à ceux du client.

This report concerns a study which was conducted for the Stripa Project. The conclusions and viewpoints presented in the report are those of the authors and do not necessarily coincide with those of the client.

Das Stripa-Projekt ist ein Projekt der Nuklearagentur der OECD. Unter internationaler Beteiligung werden von 1980-86 Forschungsarbeiten in einem unterirdischen Felslabor in Schweden durchgeführt. Diese sollen die Kenntnisse auf folgenden Gebieten erweitern:
- hydrogeologische und geochemische Messungen in Bohrlöchern
- Ausbreitung des Grundwassers und Transport von Radionukliden durch Klüfte im Gestein
- Verhalten von Materialien, welche zur Verfüllung und Versiegelung von Endlagern eingesetzt werden sollen
- Methoden zur zerstörungsfreien Ortung von Störzonen im Fels

Seitens der Schweiz beteiligt sich die Nagra an diesen Untersuchungen. Die technischen Berichte aus dem Stripa-Projekt erscheinen gleichzeitig in der NTB-Serie der Nagra.

The Stripa Project is organised as an autonomous project of the Nuclear Energy Agency of the OECD. In the period from 1980-86, an international cooperative programme of investigations is being carried out in an underground rock laboratory in Sweden. The aim of the work is to improve our knowledge in the following areas:
- hydrogeological and geochemical measurement methods in boreholes
- flow of groundwater and transport of radionuclides in fissured rock
- behaviour of backfilling and sealing materials in a real geological environment
- non-destructive methods for location of disturbed zones in the rock

Switzerland is represented in the Stripa Project by Nagra and the Stripa Project technical reports appear in the Nagra NTB series.

Le projet Stripa est un projet autonome de l'Agence de l'OCDE pour l'Energie Nucléaire. Il s'agit d'un programme de recherche avec participation internationale, qui sera réalisé entre 1980 et 1986 dans un laboratoire souterrain, en Suède. Le but de ces travaux est d'améliorer et d'étendre les connaissances dans les domaines suivants:
- mesures hydrogéologiques et géochimiques dans les puits de forage
- chimie des eaux souterraines à grande profondeur
- écoulement des eaux souterraines et transport des radionucléides dans les roches fracturées
- comportement des matériaux de colmatage et de scellement des dépôt finals
- méthodes de localisation non destructive des zones de perturbation de la roche

La Suisse est représentée dans le projet Stripa par la Cédra. Les rapports techniques du projet Stripa sont publiés dans la série des rapports techniques de la Cédra (NTB).

ABSTRACT

The evaluation of the Buffer Mass Test mainly concerned the heating of the bentonite/rock system that simulated hot canisters in deposition holes, the swelling and swelling pressures of the expanding bentonite in the heater holes, and the water uptake of the bentonite in the holes as well as in the tunnel backfill. These processes had been predicted on the basis of laboratory-derived data and FEM calculations with due consideration of the actual geometry.

The recorded temperatures of the bentonite and surrounding rock were found to be below the maximum temperature that had been set, but higher than the expected values in the initial period of testing. The heater surface temperatures dropped in the course of the tests due to the uptake of water from the rock even in the "driest" hole which was located in almost fracture-free rock.

The water uptake in the highly compacted bentonite in the heater holes was manifested by a successively increased swelling pressure at the bentonite/rock interface. It was rather uniformly distributed over this interface and reached a maximum value of about 10 MPa.

The water content determination confirmed that water had been absorbed by the bentonite from the rock even in the driest holes where the counteracting thermal gradient was rather high. In the wettest holes the saturation became almost complete and a high degree of saturation was also observed in the tunnel backfill. Both in the heater holes and the tunnel, the moistening was found to be very uniform along the periphery, which is at least partly explained by the self-sealing ability of bentonitic buffer materials.

A general conclusion is that the involved physical processes are well understood and that the ultimate physical state of the buffer materials under repository conditions can be safely predicted.

RESUME

L'évaluation de l'essai sur la masse-tampon a essentiellement porté sur le chauffage du système bentonite/roche (pour simuler la chaleur émanant des conteneurs placés dans les cavernes de stockage), mais aussi sur le gonflement et les pressions de gonflement de la bentonite expansive dans les puits de chauffe, ainsi que sur l'absorption d'eau par la bentonite dans les puits comme dans le matériau de remplissage de la galerie. Ces processus avaient été prévus sur la base de données obtenues en laboratoire et de calculs FEM, compte tenu de la géométrie actuelle.

Les températures enregistrées pour la bentonite et la roche environnante se sont avérées plus basses que les maxima de température que avaient été fixés, mais plus élevées que les valeurs escomptées pour la première période d'essais. Au cours de l'essai, les températures sur les surfaces des corps de chauffe ont chuté, en raison de l'eau emmagasinée par la roche, même dans le puits le plus sec situé dans une roche presque sans disclases.

L'absorption d'eau par la bentonite hautement compactée, dans les puits de chauffe, s'est manifestée par une augmentation constante de la pression de gonflement l'interface roche/bentonite. La pression s'y est assez régulièrement répartie et a atteint une valeur maximale d'environ 10 MPa.

La détermination de la part en eau a confirmé que cette dernière a bien été absorbée par la bentonite, à partir de la roche, même dans les puits les plus secs où le gradient thermique agissant en sens opposé était assez élevé. Dans les puits les plus humides, on est parvenu à une saturation quasi complète; on a également observé un degré de saturation élevé dans le matériau de remplissage de la galerie. Dans les puits de chauffe comme dans la galerie, la pénétration d'humidité s'est avérée régulière le long de la périphérie, ce qu'expliquent en partie les propriétés d'auto-colmatage de la bentonite.

On affirme en conclusion que les processus physiques concernés sont bien compris et que l'état final des matériaux de colmatage dans des conditions de dépôt final peut être prévu avec certitude.

ZUSAMMENFASSUNG

Die Auswertung des Puffer-mass-tests bezog sich vor allem auf die Aufheizung des Bentonit/Gesteinssystems (um warme Behälter in Lagerkavernen zu simulieren), die Quellung und Quelldrücke des sich ausdehnenden Bentonits in den Erhitzerlöchern und die Wasseraufnahme des Bentonits in den Löchern sowie in der Stollenverfüllung. Die Vorhersage dieser Prozesse basierte auf Labordaten und FEM-Berechnungen, unter Berücksichtigung der aktuellen Geometrie.

Die registrierten Temperaturen des Bentonits und des umgebenden Gesteins lagen tiefer als die festgelegten Höchsttemperaturen, aber höher als die erwarteten Werte für die erste Testperiode. Die Temperaturen an den Erhitzeroberflächen sind im Laufe des Tests zurückgegangen, aufgrund der Wasseraufnahme aus dem Gestein; dies geschah auch im trockensten Erhitzerloch, das in beinahe kluftfreiem Fels lag.

Die Wasseraufnahme im hochverdichteten Bentonit in den Erhitzerlöchern manifestierte sich durch eine andauernde Quelldruck-Erhöhung am Bentonit/Gestein-Uebergang. Der Durck war an diesem Uebergang gleichmässig verteilt und erreichte einen Maximalwert von ca. 10 MPa.

Die Ermittlung des Wasseranteils bestätigte, dass Wasser vom Bentonit aus dem Gestein absorbiert wurde, auch in den trockensten Löchern, wo der entgegenwirkende thermische Gradient ziemlich hoch war. In den feuchtesten Löchern wurde fast vollständige Sättigung erreicht. Auch in der Stollenverfüllung wurde ein hoher Sättigungsgrad festgestellt. In den Erhitzerlöchern sowie im Stollen wurde eine gleichmässige Durchfeuchtung entlang der Peripherie gefunden, was zum Teil durch die selbstdichtenden Eigenschaften der Bentonit-Verfüllmaterialien erklärt wird.

Eine allgemeine Schlussfolgerung ist, dass die mitwirkenden physikalischen Prozesse gut verstanden werden und dass der Endzustand der Verfüllmaterialien unter Endlagerungbedingungen mit Sicherheit vorausgesagt werden kann.

CONTENTS

SUMMARY

The general objective of the Buffer Mass Test was to check the function of highly compacted Na bentonite as canister overpack and sand/-bentonite mixtures as tunnel backfill. It involved prediction of the temperatures and swelling pressures and measuring of these quantities. Since they were expected to be functions of the water content it was required to make predictions and conduct measuring also of the uptake and redistribution of water in the buffer materials. Experience shows that recording of water contents by use of moisture sensors is not very accurate, which called for comprehensive sampling of the clay materials for direct determination of the water content at suitable time intervals. These were chosen so as to give information of the rate and uniformity of the moistening in the three "wet" holes no 1, 2 and 5, and in the three "dry" holes no 3, 4 and 6, which required stop of certain tests already after about one year and comprehensive sampling and laboratory testing in connection with these terminations.

The prediction of temperatures was based on FEM calculation and application of laboratory-derived thermal data. It showed that the temperatures at the heater surfaces would not exceed about 80°C at the end of the test period when the heater power was 600 W and about 184°C at 1800 W power, which was also confirmed by the tests. The initial temperatures, soon after the onset of the power, turned out to be higher than expected in most cases but they dropped in the course of the tests, which was explained by temporary drying close to the heaters followed by uptake of water from the rock. This uptake was well manifested by the successively increasing swelling pressures, which were predicted to be 10 MPa at maximum in the "wet" holes. The moisture sensors did not give a reliable picture of the moisture distribution neither in the heater holes, nor in the tunnel backfill.

At the excavation of each heater hole about 2500 samples were taken for the determination of the true water content. The highly compacted bentonite in the "wet" holes had become completely or almost fully saturated after about 2 years, while it showed a moisture gradient and relatively dry conditions close to the heaters in the "dry" holes. The tangential distribution of water at various radial distances turned out to be very uniform, however, which was explained mainly by the ability of dense bentonite to seal off water-bearing fractures. Through this, inflowing water was directed to adjacent, finely fractured rock areas and was thus taken up uniformly by the bentonite. Also, the initial thermally induced redistribution of the original pore water contributed to the uniform wetting. Even in the dry holes complete saturation was obtained in the peripheral part of the bentonite.

It was concluded that the backfill interacted with the rock in much the same way as the heater overpacks. Thus, the largely varying distribution of the inflowing water immediately after the application of the backfill led to local sealing and redistribution to initially dry areas and thereby to a uniform wetting of the backfill. The water pressure at the rock/backfill interface was expected to be increased considerably when the peripheral part of the backfill had been saturated. This stage was reached in about one year but it was not accompanied by any significant piezometric rise. The reason for this was partly that the water was discharged through the rock which had experienced an increased hydraulic conductivity through the blasting and stress redistribution, and partly that practically all the water

that flowed into the tunnel was absorbed by the backfill. Thus, large parts of it turned out to be saturated, the main water-driving mechanism probably being capillary suction due to the low initial water content of the sand/bentonite material.

A general conclusion from the BMT project is that the basic information that was asked for at the planning stage was actually obtained. Thus, the physical processes involved in the moistening and maturation of the buffer materials under repository conditions in crystalline rock are understood in principle and their ultimate physical state and functions can be safely predicted. Also, the preparation and practical applicability of the various buffer materials were amply demonstrated, indicating the feasibility of bentonite-based isolation techniques in general and the KBS 3 concept in particular.

1 TEST PROGRAM

1.1 Heater power and operation time

With 600 W heater power and the applied geometry of the heater/bentonite/rock arrangement in the heater holes, the different hydrological conditions of the rock was expected to yield a large variation in water saturation of the bentonite in the various holes, while the temperature situation was supposed to be only slightly different in them. A primary aim was to run at least one of the "wet" hole experiments for about three years, by which an example of almost complete saturation would be accomplished. This would also illustrate the ultimate physical state of the bentonite in a deposition hole in an actual repository. Hole no 2 was chosen for this purpose (Fig 1.1). Similarly, one of the "dry" hole experiments, the one in no 6, was a long term test which was thought to be representative of the physical state of the bentonite under actual repository conditions for a number of years preceding water saturation. The successive changes in water content under the influence of temperature gradients and with different access to water were illustrated by termination of the remaining heater tests at different times followed by a comprehensive determination of the actual water content distribution.

At a rather late stage of the BMT it was found that the understanding of the physical processes involved in the coupled heat/water flow in the holes could probably be improved by running one of the heaters at a much higher power. This would also give an opportunity to identify possible chemical reactions in the bentonite, such as smectite crystal lattice alterations and cementation. Effects of these kinds require a high degree of water saturation and long reaction time, and hole no 1 was found to be most suitable for such an experiment because it was "wet" and also the last one to be opened. The "hydro-

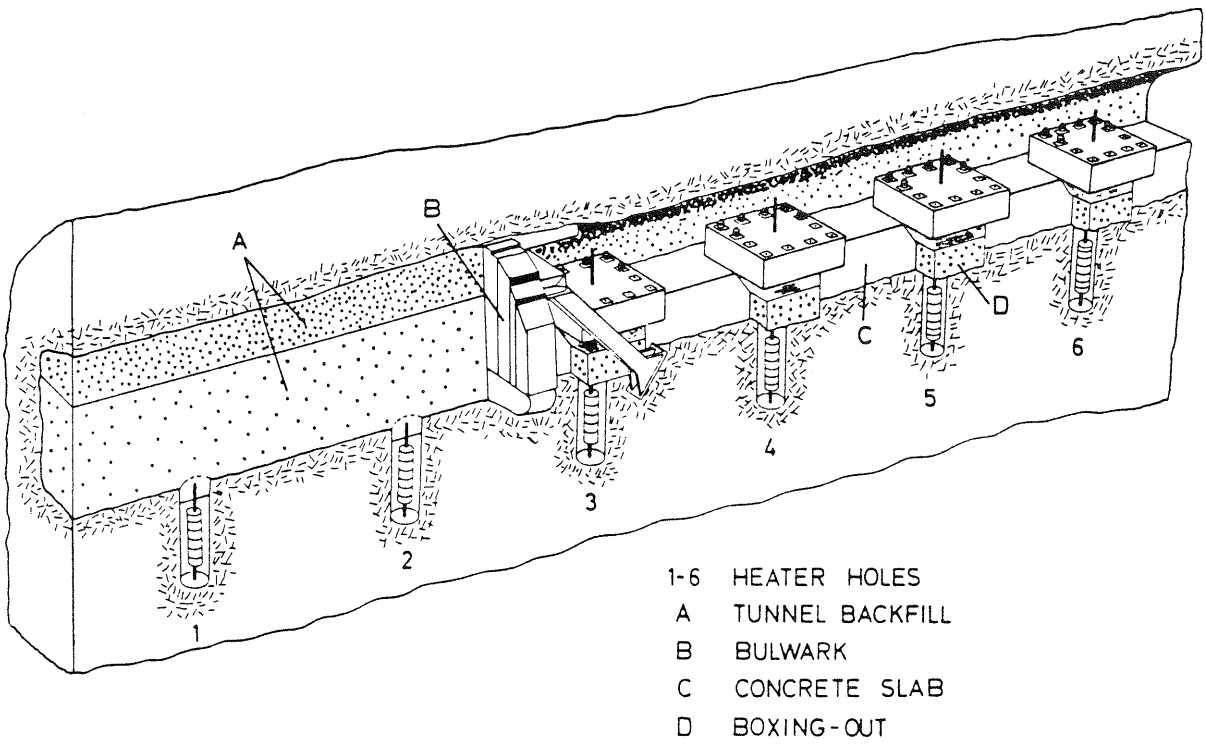

Fig 1.1. The BMT heater hole and tunnel arrangement

thermal" conditions were arranged by increasing the power of heater no 1 from 600 W to 1400 W and running this test for approximately one year. A short term pilot test at 1200-1800 W in hole no 3 preceded the high-power test in hole no 1.

Table 1:1 summarizes the main features of the test program.

Table 1:1. Test data

Site	Heater power, W	Start	Stop	Remark
Heater hole no 1 ("wet")	600	Oct 5, 1981	Mar 20, 1984	
	1400	Mar 20, 1984*	Feb 1, 1985	
Heater hole no 2 ("wet")	600	Oct 7, 1981	Nov 14, 1984	
Heater hole no 3 ("dry")	600	Jan 20, 1982	Apr 12, 1983	
Heater hole no 3 ("dry"; new set of bentonite blocks)	1200	Jun 13, 1983	Jan 17, 1984	
	1800	Jan 17, 1984	May 21, 1984	
Heater hole no 4 ("dry")	600	Jan 20, 1982	Dec 1, 1983	
Heater hole no 5 ("wet")	600	Mar 24, 1982	Jun 7, 1984	
Heater hole no 6 ("dry")	600	Mar 24, 1982	Apr 6, 1984	
Tunnel backfill, completed		Early Dec 1981	Late Nov 1984	Excav of outer half of backfill; inner half excavated in Jan 1985

* Actually, the power was 1800 W in the first three weeks

1.2 Excavation and sampling program

1.2.1 Backfill in boxing-outs

After removal of the tie-rods that anchored the heavy lids to the concrete slab, the backfill was excavated and samples taken for determination of water content and bulk density. The sampling tools for determination of the density were thin-walled cylinders with 50 mm diameter and 50 mm length that were pressed into the mass. 5-10 samples distributed over the approximately 3 m^2 horizontal cross

section of the boxing-out were taken at 3-7 levels, the distance between the sampling levels being larger in the boxing-outs of holes no 5 and 6. Also, about 10 samples were taken in the approximately 75 cm thick backfill that covered the highly compacted bentonite in the heater holes.

A small number of samples was taken for density determination as well.

1.2.2 Tunnel backfill

The tunnel backfill was excavated in 1 m strips, samples being taken for water content determination at 0.5 m - 1 m distance in a checkered pattern over the exposed, steeply oriented surfaces. This frequency was sufficient to yield a clear picture of the variation of the saturation degree. The samples were rather large, 200-500 g, in order to get representative water content values.

1.2.3 Highly compacted bentonite in heater holes

A detailed picture of the water content distribution in the highly compacted bentonite was required, which called for systematic sampling. A very high accuracy in determining the positions of the large number of samples was obtained by putting a steel plate jig with prebored holes on each sampling level (Fig 1.2 - 1.5). These levels coincided with the 15 cm spaced initial joints between the block layers. The sampling was made by use of auger drilling where the degree of wetting of the bentonite was low, and by punching where the bentonite was largely wetted. It was shown that the temperature increase and thus also the evaporation caused by the auger drilling was insignificant. The samples of the very homogeneous clay were small, usually between 20 and 50 g.

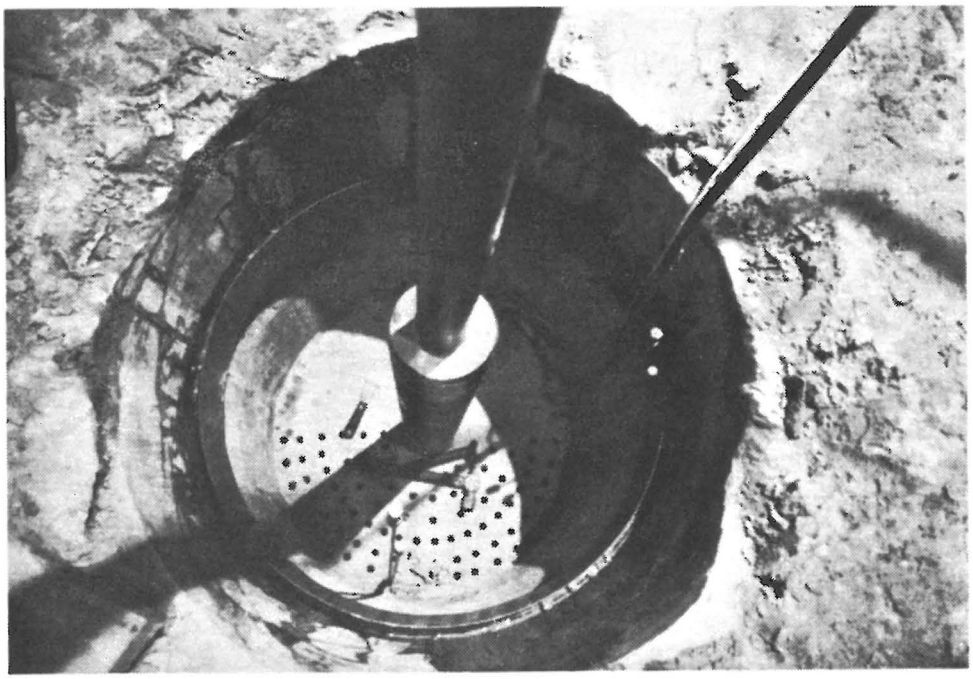

Fig 1.2. Sampling operation. Upper picture shows the steel plate jig. Lower picture illustrates dismantling of heater to give access to the clay for sampling purposes

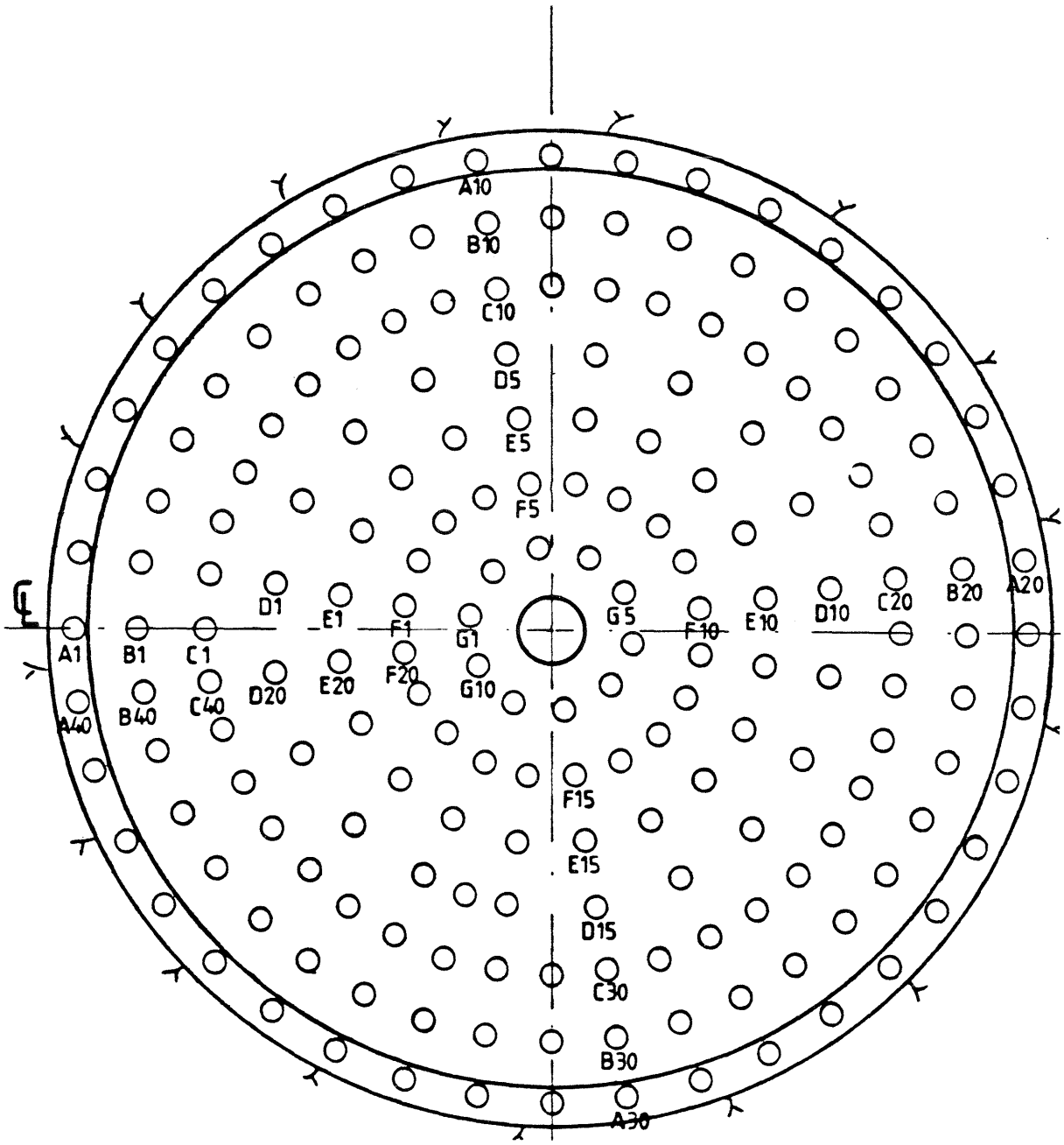

Fig 1.3. Prebored holes in the steel plates used for the sampling operation below the main heater body. Letters and figures refer to the sample coding

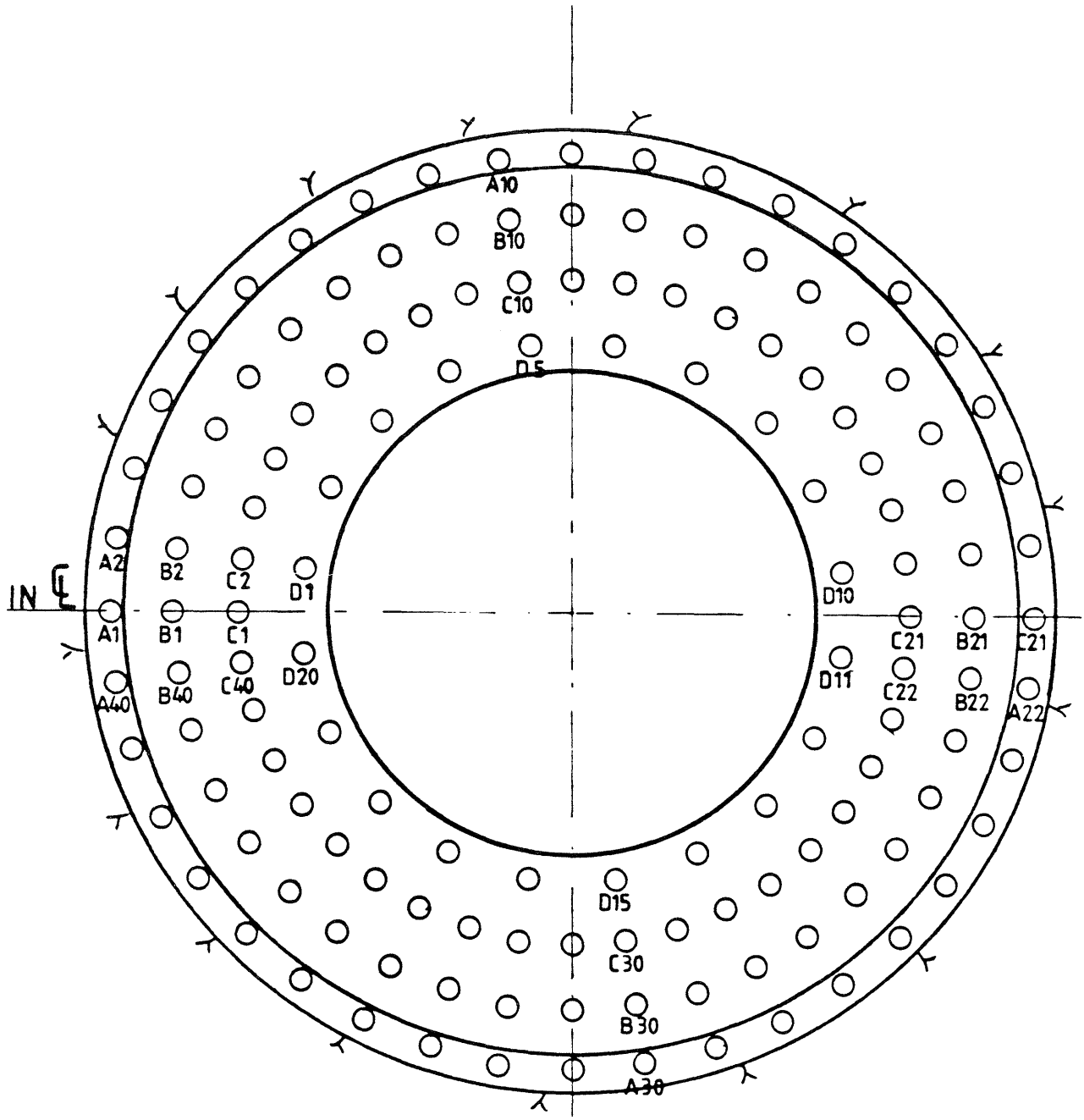

Fig 1.4. Prebored holes in the plates used next to the main heater body

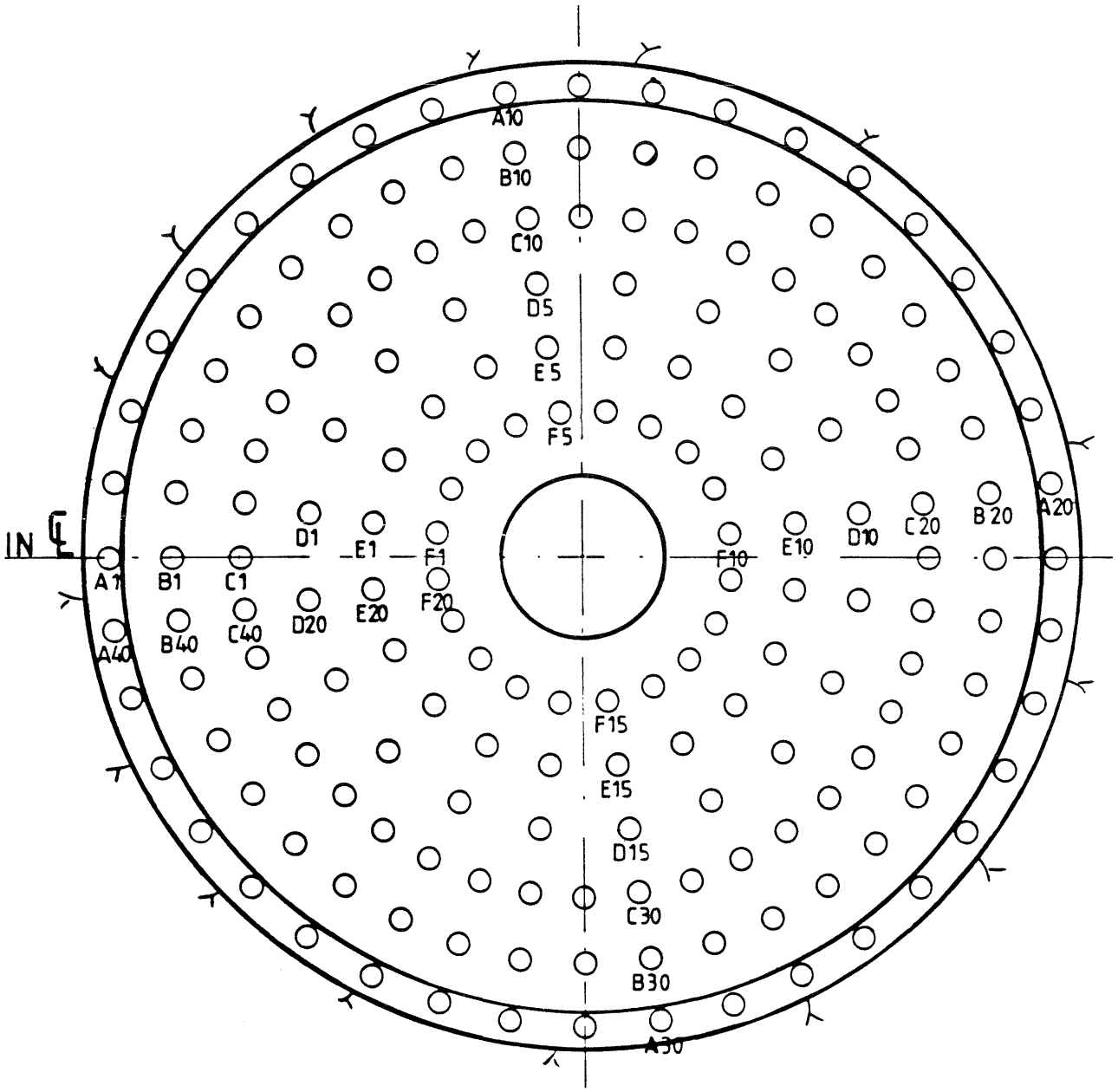

Fig 1.5. Prebored holes in the plates used above the main heater body

Since the number of samples from each heater hole was more than 2000 a rational way of determining the water content was required. For this purpose a semiautomatic Mettler balance was used, which recorded the weight of the wet sample and directly gave the microcomputer-derived water content when weighing the same sample after drying, which took place at 105^{o}C for 1 day, except for the larger sand/bentonite samples. These were usually kept in the oven for a longer period of time.

2 PREDICTIONS AND RESULTS

2.1 General

The Buffer Mass Test was preceded by a number of systematic laboratory tests, which concerned the heat conductivity and the rate and character of the water uptake and associated swelling of various bentonite-based buffer materials (1,2,3,4). It was therefore assumed that the behavior of the clay in heater hole environment could be reasonably well foreseen, but deviations were expected since the boundary conditions at the rock/clay interface could not be reliably simulated in the laboratory.

The heating of the highly compacted bentonite in the heater holes and the magnitude and uniformity of the swelling pressure that this material was expected to exert on the rock, were of primary interest. They are major points in this report.

2.2 Heating of the highly compacted bentonite and the tunnel backfill

2.2.1 Predictions

The complex geometry of the test arrangement in Stripa would call for a 3 D FEM analysis for temperature calculation but considering the uncertainty in thermal parameters and the coupled processes of heat and water migration, a combined 2 D/axisymmetric model was assumed to be satisfactory. The element mesh is shown in Fig 2.1, the boundary conditions representing fixed temperatures, which means that heat can pass through the boundaries without limitation. These conditions yield a slight underestimation of the predicted temperatures during the later part of the test period.

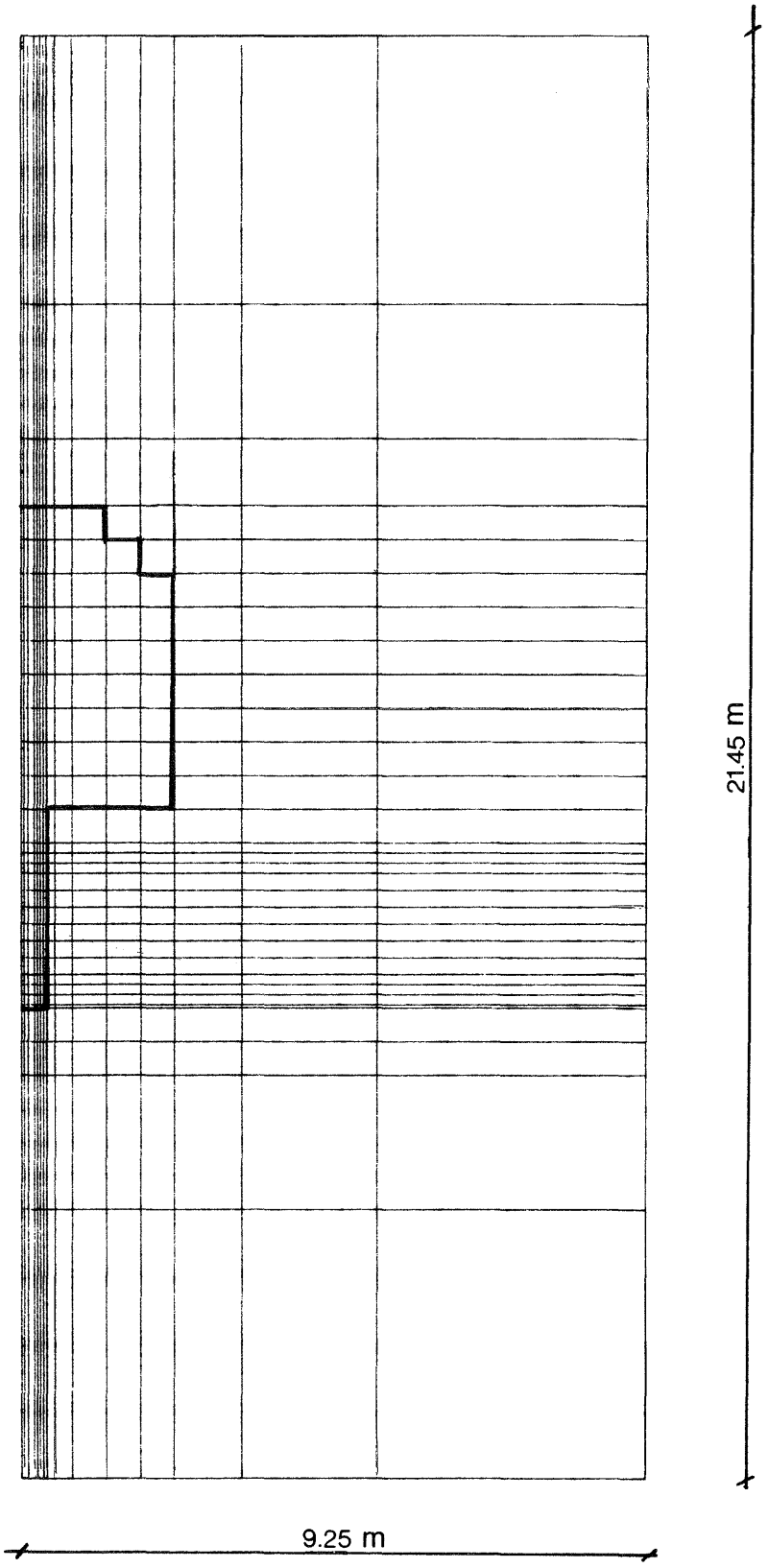

Fig 2.1. The total element mesh used for the heat calculations. The elements are axisymmetric with respect to the vertical axis forming the left, vertical boundary.

The FEM program ENERGY from the CHALMFEM system, available at the Gothenburg Computer Centre, was used for the calculations.

Heater holes no 1, 2 and 5 will be treated as the "wet" group, while holes no 3, 4 and 6 constitute the "dry" group in the subsequent presentation.

2.2.1.1 Heater holes no 1 and 2, 600 W

Holes no 1 and 2 were located in "wet" rock which was expected to lead to rapid water uptake of the bentonite. Yet, a conservative assumption would be that this would not affect the temperature situation in the bentonite until a rather late stage was reached. A first estimation of the temperature field was therefore based on the initial conditions with the original, unaltered water content. The corresponding thermal parameters for the bentonite in holes no 1 and 2 and the tunnel backfill are those given in Table 2:1. The property areas are shown in Fig 2.2.

Table 2:1. Parameters of the components used in the calculation of the heat distribution in heater holes no 1 and 2 and the tunnel backfill

Property area in FEM (cf Fig 2.2)	λ W/m,K	c Ws/kg,K	ρ kg/m^3
1 Heater	59	460	7800
2 Comp bent	1.0	1100	2170
3 Sand/bent	2.2	1400	2150
4 Sand	2.1	1600	2100
5 Rock	3.6	800	2700
6 Slot with water	0.5	4200	1000

The heater was treated as one homogeneous body, the four upper and three lower extra elements representing the casing and basal support,

respectively. The calculated temperature increase after 3.5 years, which is slightly more than the experiments lasted, is demonstrated in Fig 2.3. Fig 2.4 illustrates the predicted temperature increase at different lateral distances from the axes of heaters no 1 and 2. The figures refer to mid-height of the heaters.

The calculations were then repeated for the states of complete water saturation and dry conditions, respectively, the corresponding thermal properties being given in Table 2:2 and 2:3. The latter values refer to material dried at 105°C.

Table 2:2. The parameters used in the heat calculation for completely saturated buffer materials

Property area	λ W/m,K	c Ws/kg,K	ρ kg/m^3
1 Heater	59	460	7800
2 Comp bent	1.4	1600	2100
3 Sand/bent	2.4	1400	2200
4 Sand	2.1	1600	2100
5 Rock	3.6	800	2700

Table 2:3. The parameters used in the heat calculation for dry buffer materials

Property area	λ W/m,K	c Ws/kg,K	ρ kg/m^3
1 Heater	59	460	7800
2 Comp bent	0.39	800	1900
3 Sand/bent	0.39	800	1900
4 Sand	0.29	800	1800
5 Rock	3.6	800	2700

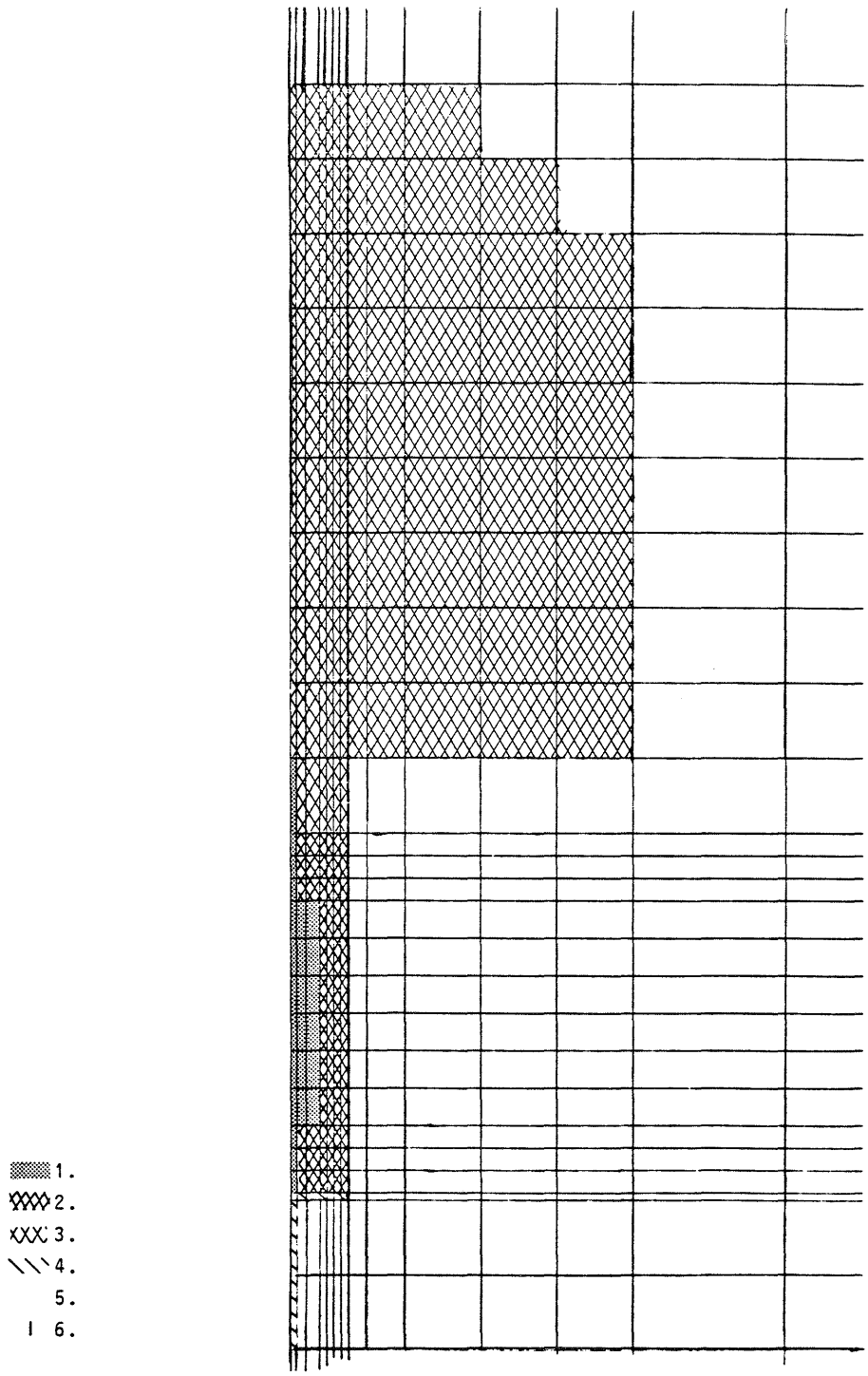

Fig 2.2. Property areas used for holes no 1 and 2:

1. heater	4. sand
2. comp bent	5. rock
3. sand/bent	6. slot

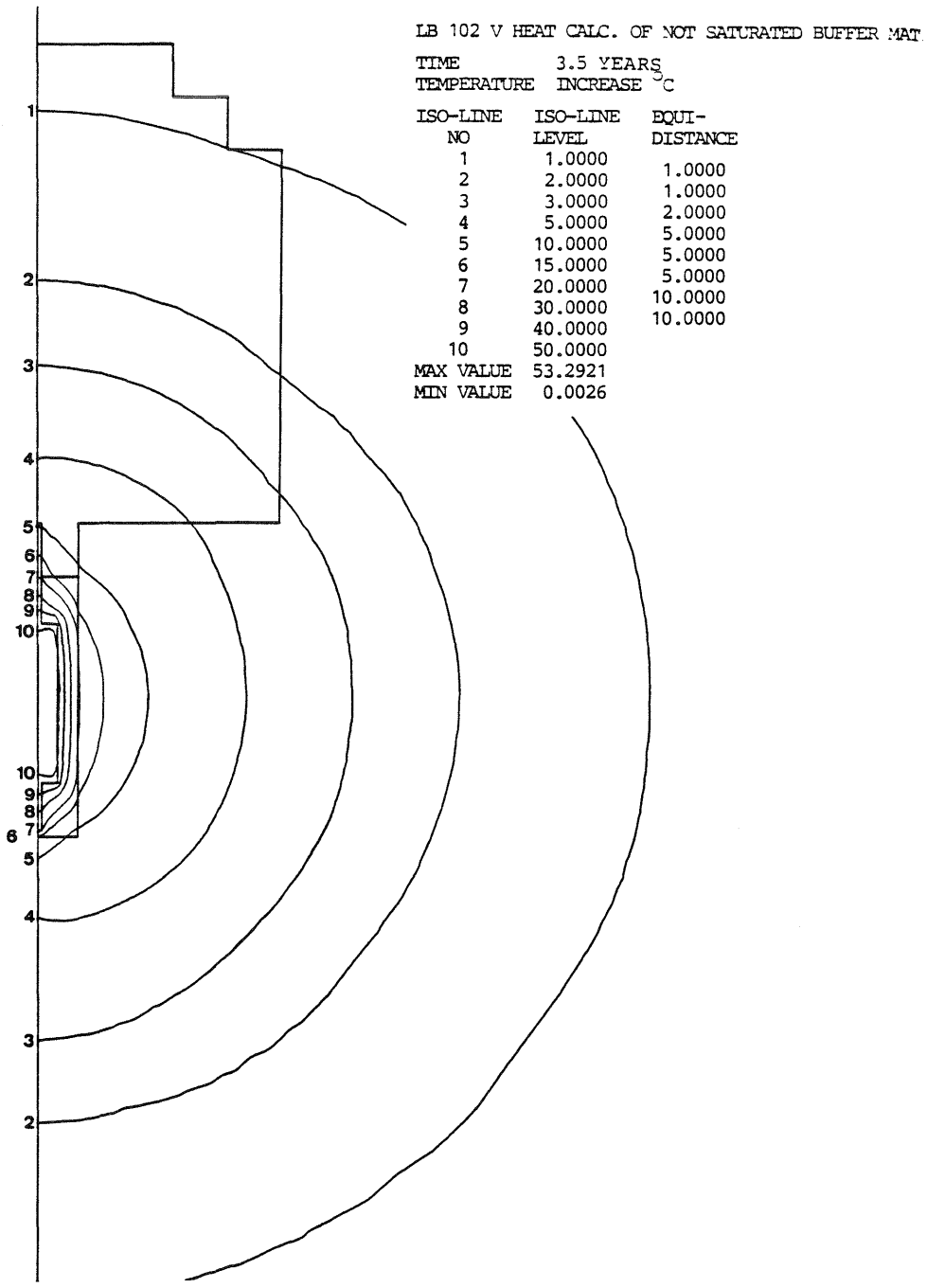

Fig 2.3. Calculated temperature increase around heaters no 1 and 2 after 3.5 years

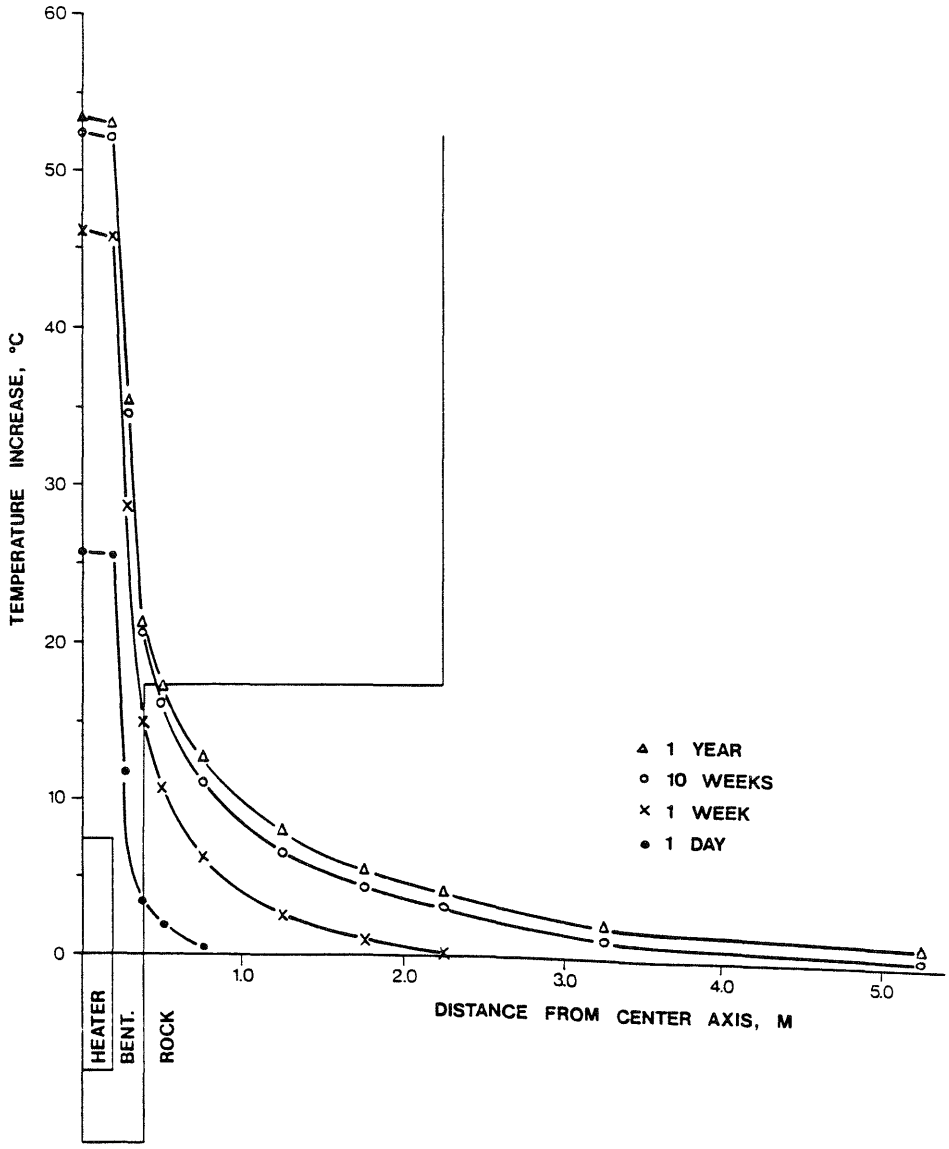

Fig 2.4. The theoretical temperature increase at mid-height of heaters no 1 and 2 as a function of the lateral distance from the heater axis

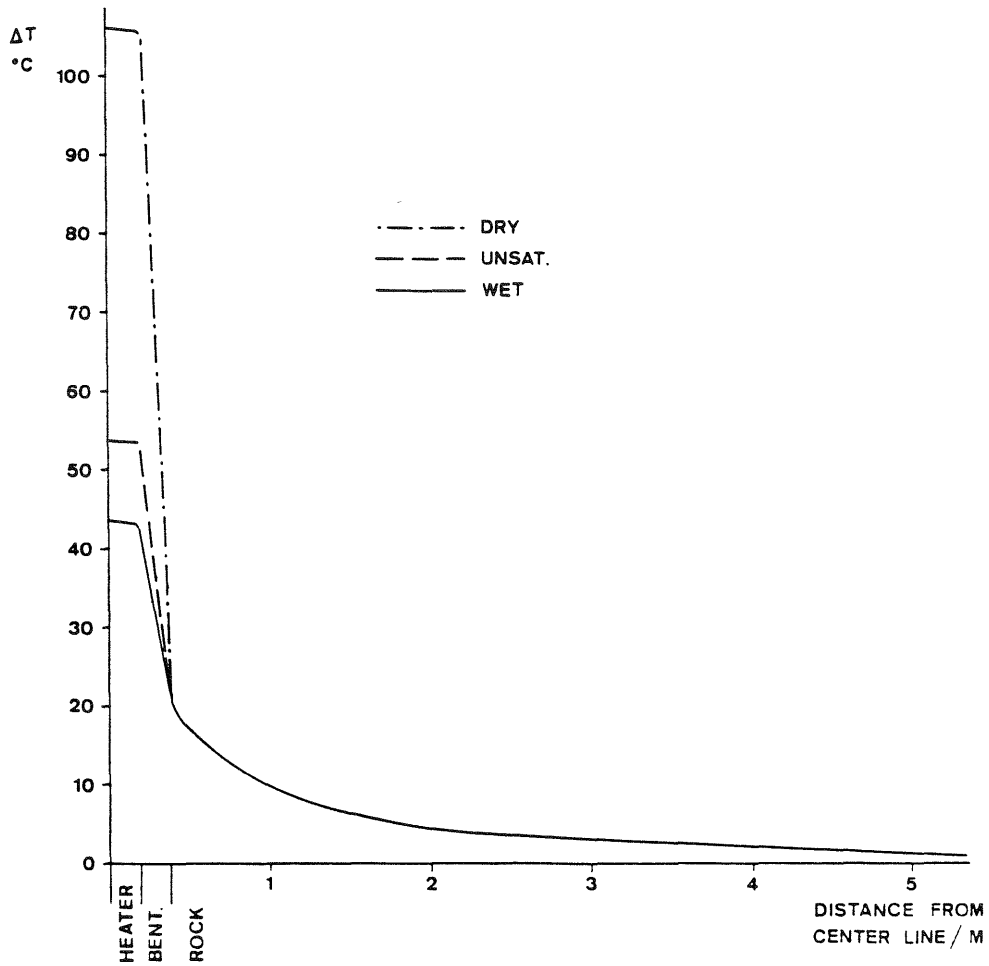

Fig 2.5. Predicted temperature increase at mid-height of heaters no 1 and 2 after 3.5 years. The curves refer to the initial conditions (unsat), and to the two extremes: dry, and completely saturated ("wet")

These analyses showed that additional uptake of water leading to complete saturation would not yield a very significant temperature change while drying would cause a substantial increase in heater surface temperature. The results are given in Fig 2.5 for 3.5 year testing time, referring to mid-height of heaters no 1 and 2, and disregarding the influence of neighboring heaters.

The ambient rock temperature has to be added to the calculated values in order to arrive at the expected net temperatures. The initial rock temperature was 12.5 - 13.0°C which means that if the water content of the bentonite would not be altered in the test, the surface temperature of the heaters at mid-height would be approximately 66°C after about 3 years. The temperature at the rock surface would be about 34°C. If water saturation were reached early in the test the corresponding temperatures would be about 56°C and 34°C, respectively. Drying, on the other hand, would yield a net surface temperature of about 120°C at mid-height of the heater.

These temperatures also need to be corrected with respect to the superposition of the heat flow from the individual heater holes. The resulting expected temperatures for 600 W heater power are shown in Fig 2.6, which demonstrates that the interaction mainly affects the rock located between the holes. The temperature of the bentonite is only increased by 1-2 degrees centigrade during the experiment. When applying higher power, the influence is accordingly stronger.

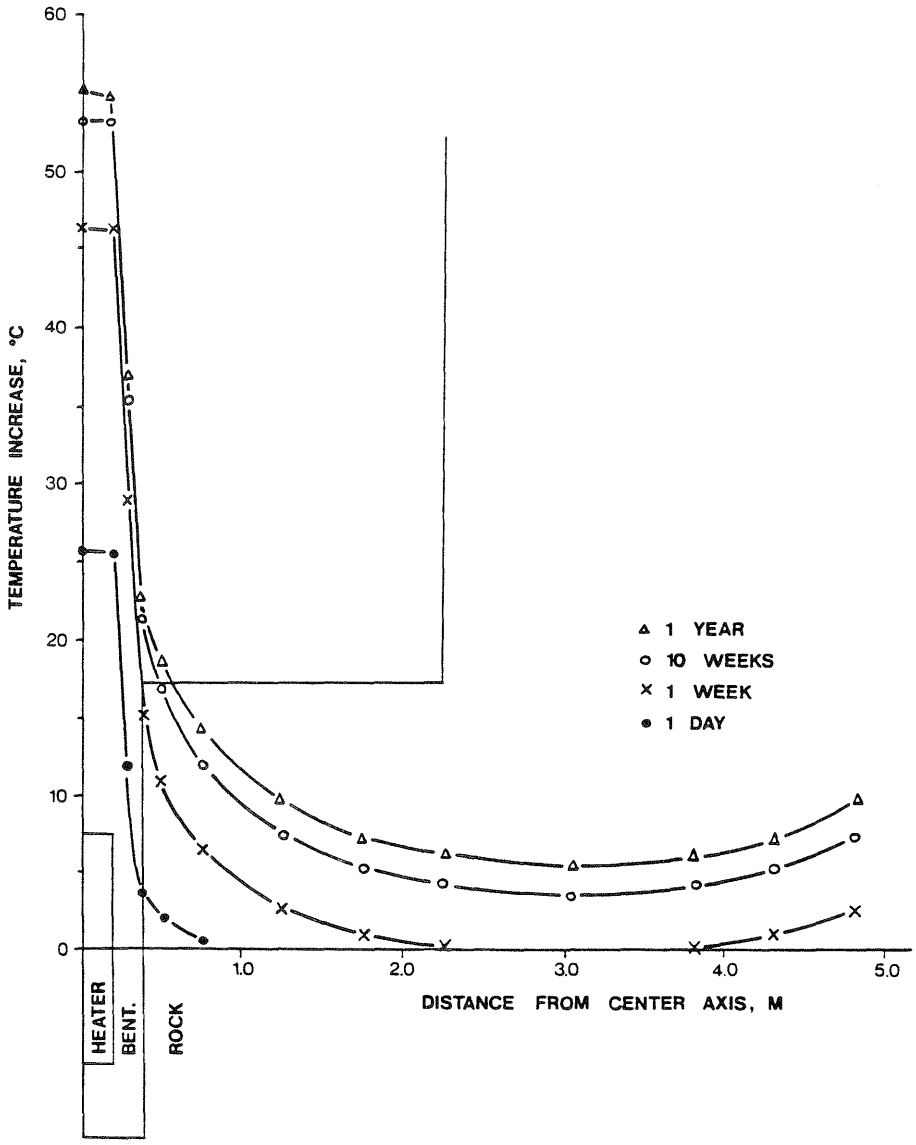

Fig 2.6. Predicted temperature increase calculated by superposition of the temperature fields of two neighboring heater holes

2.2.1.2 Heater hole no 5, 600 W

Heater hole no 5 was located outside the bulwark and covered only by a small volume of sand/bentonite backfill. Thus, the geometry deviated from that of holes no 1 and 2 which required a separate FEM analysis. Using thermal parameters for the initial, unaltered bentonite state according to Table 2:4, the temperature increase after 3.5 years was found to be as shown in Fig 2.7.

Table 2:4. Parameters of the components used in the calculation of the heat distribution in heater hole no 5 and overlying backfill

Property area in FEM	λ W/m,K	c Ws/kg,K	ρ kg/m^3
1 Heater	59	460	7800
2 Comp bent	1.1	1200	2090
3 Sand/bent*	1.5	1200	1950
4 Sand	2.1	1600	2100
5 Rock	3.6	800	2700
6 Concrete	1.8	920	2300
7 Air	0.024	1000	1.29

---

* Lower expected density than in the tunnel

We see that the concrete slab affects the heat distribution and that the temperature is expected to be slightly lower than in holes no 1 and 2. This is explicitely demonstrated by Fig 2.8, which shows the heat distribution in a horizontal plane through mid-height of the heater. This graph, as well as the preceding ones, except Fig 2.6, refer to single heater holes unaffected by the neighboring ones.

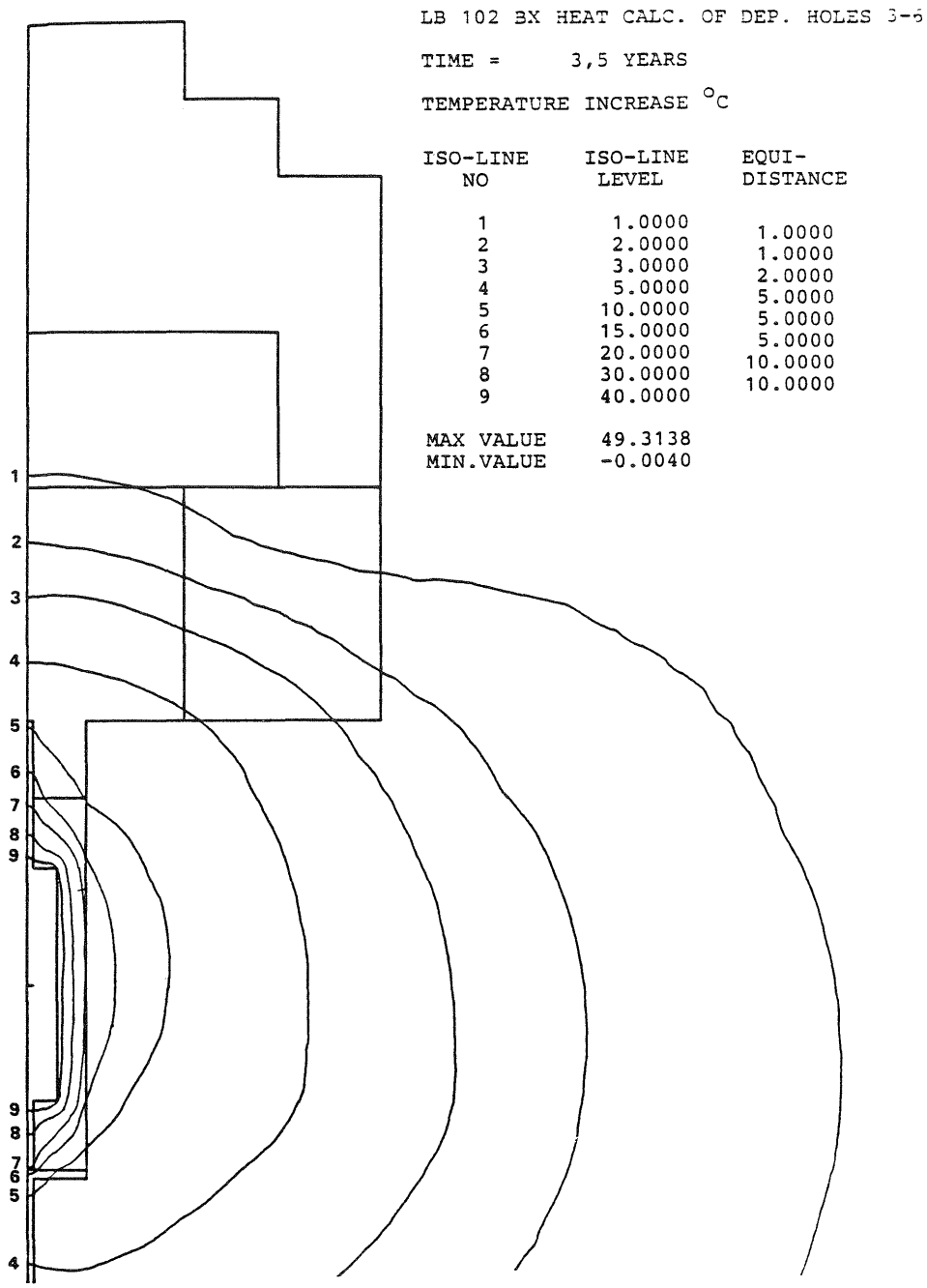

Fig 2.7. Calculated temperature increase around heater no 5 after 3.5 years

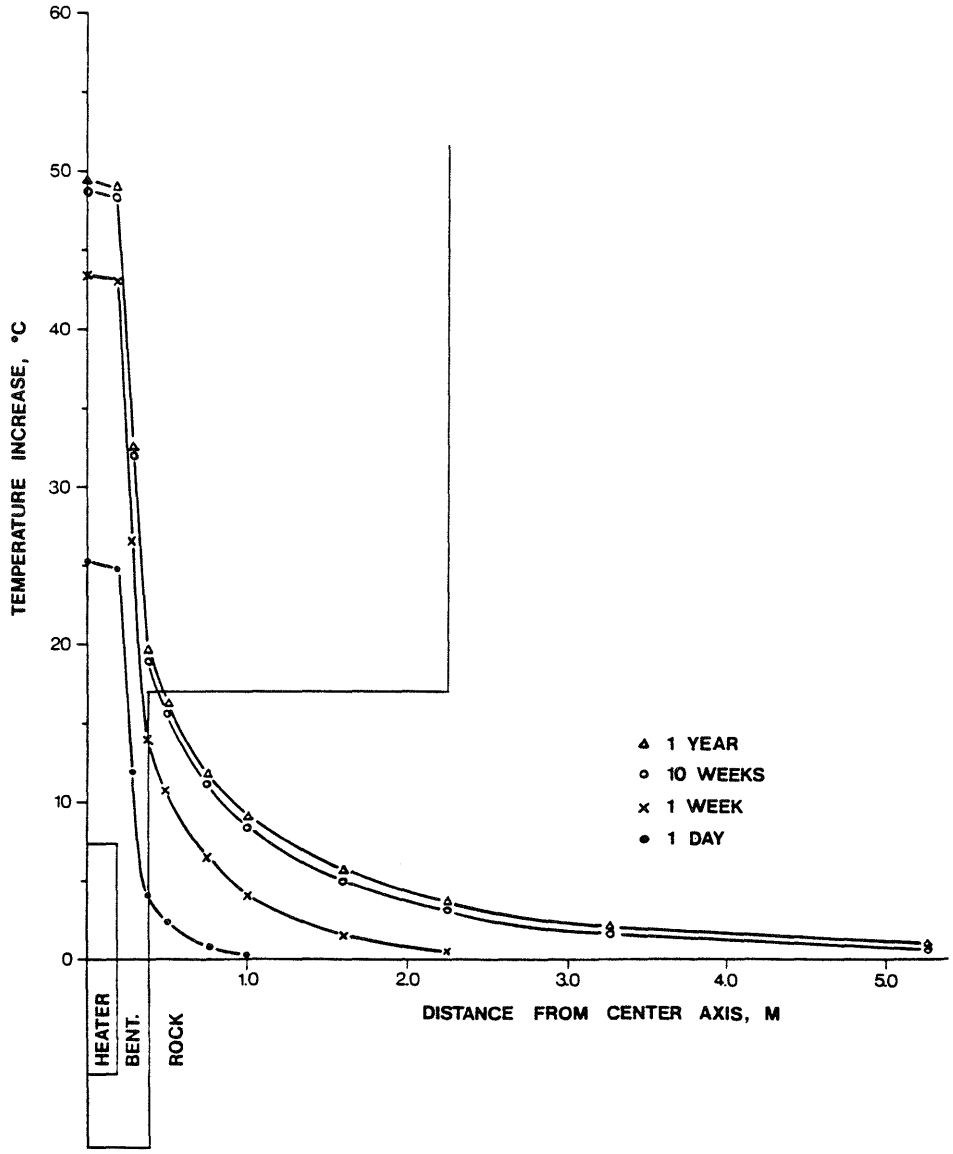

Fig 2.8. The theoretical temperature increase at mid-height of heater no 5 as a function of the lateral distance from the heater axis

2.2.1.3 Heater holes no 3, 4 and 6, 600 W

The highly compacted bentonite in heater holes no 3, 4 and 6 had a slightly higher bulk density than that in the previously discussed holes, another difference being the 3 cm wide slot that separated the bentonite "annulus" from the rock in the presently discussed case (cf Vol I, Chapter 4.1.3.1). This space was filled with air-dry bentonite powder with a much lower heat conductivity than the other backfilling components. The temperature calculations were therefore made by use of a slightly altered element mesh, basically that of hole no 5, to account for the bentonite powder to which the parameter values λ = 0.3 W/m,K and c = 1240 Ws/kg,K (ρ = 1160 kg/m^3) were ascribed. The corresponding figures for the highly compacted bentonite were λ = 1.1 W/m,K and c = 1200 Ws/kg,K for the density 2090 kg/m^3.

Since the 600 W heater tests in holes no 3 and 4 were run only for 15 and 10 months, respectively, the predicted temperature distribution in the early phase is of major interest. Fig 2.9 shows the situation after 10 weeks, while Fig 2.10 demonstrates the status after 1 year. Detailed pictures of the temperature increase at mid-height of the canisters are given in Fig 2.11 and 2.12.

The calculations were also repeated for the states of complete water saturation and dry conditions, respectively, the thermal parameters being those in Table 2:2 and 2:3. For the slot fill the following parameter values were applied: λ = 1.4 W/m,K and c = 1600 Ws/kg, K (ρ = 2100 kg/m^3) at complete saturation, and λ = 0.12 W/m,K and c = 1000 Ws/kg,K (ρ = 1300 kg/m^3 in the dry state. The calculated heater temperatures were found to be slightly higher than those of heater hole no 5, but the difference is insignificant.

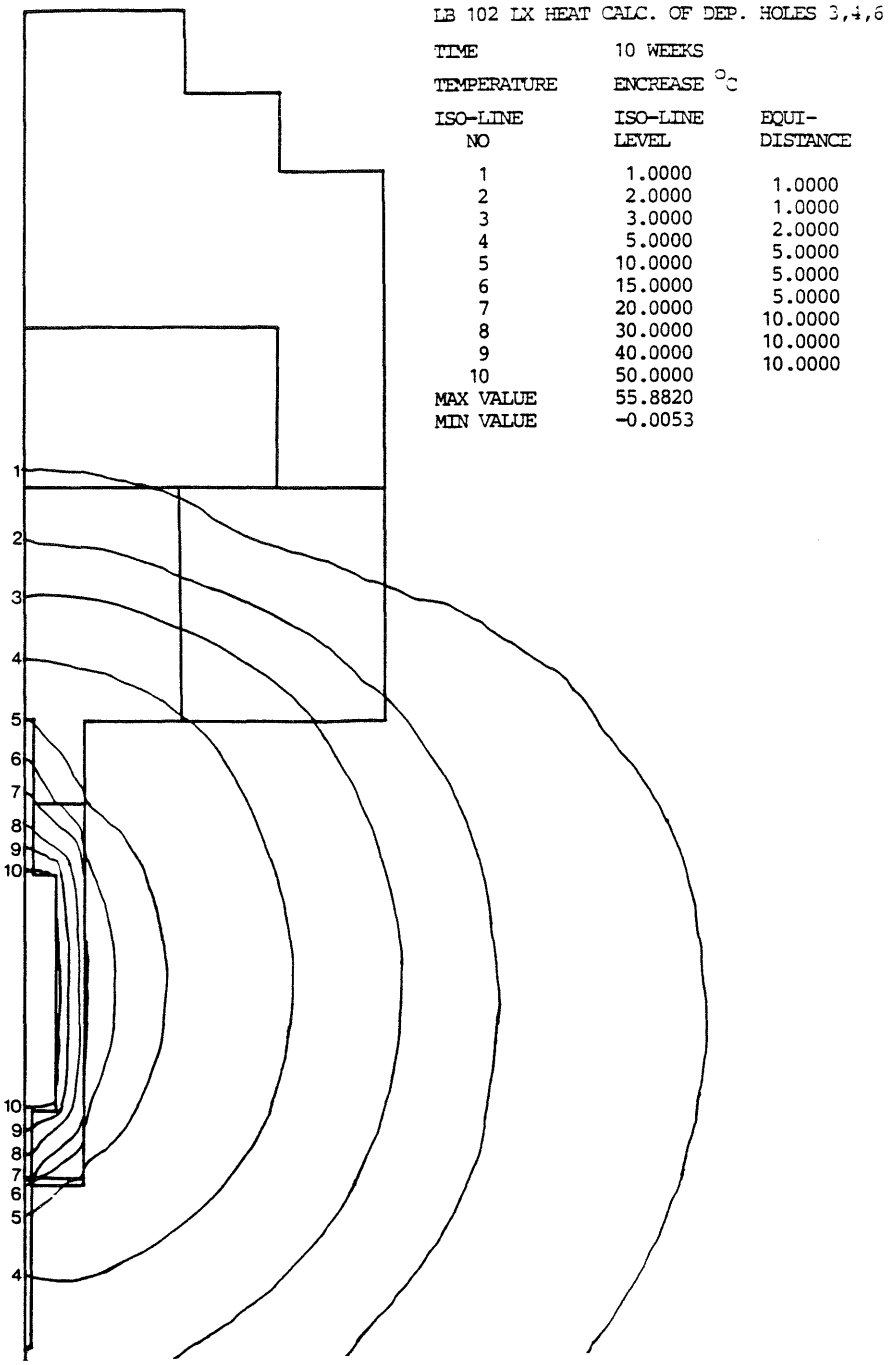

Fig 2.9. Calculated temperature increase around heaters no 3, 4 and after 10 weeks

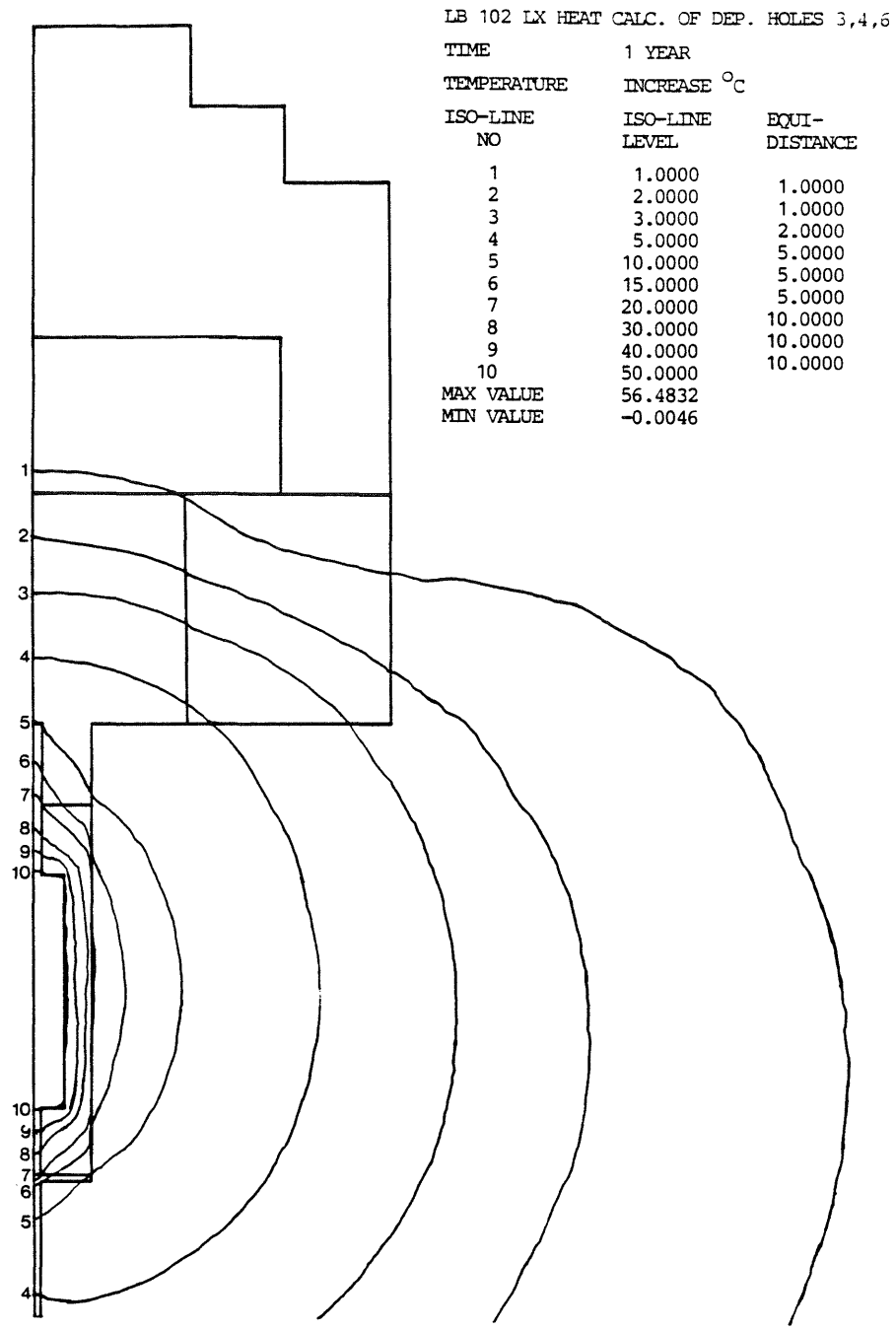

Fig 2.10. Calculated temperature increase around heaters no 3, 4 and 6 after 1 year

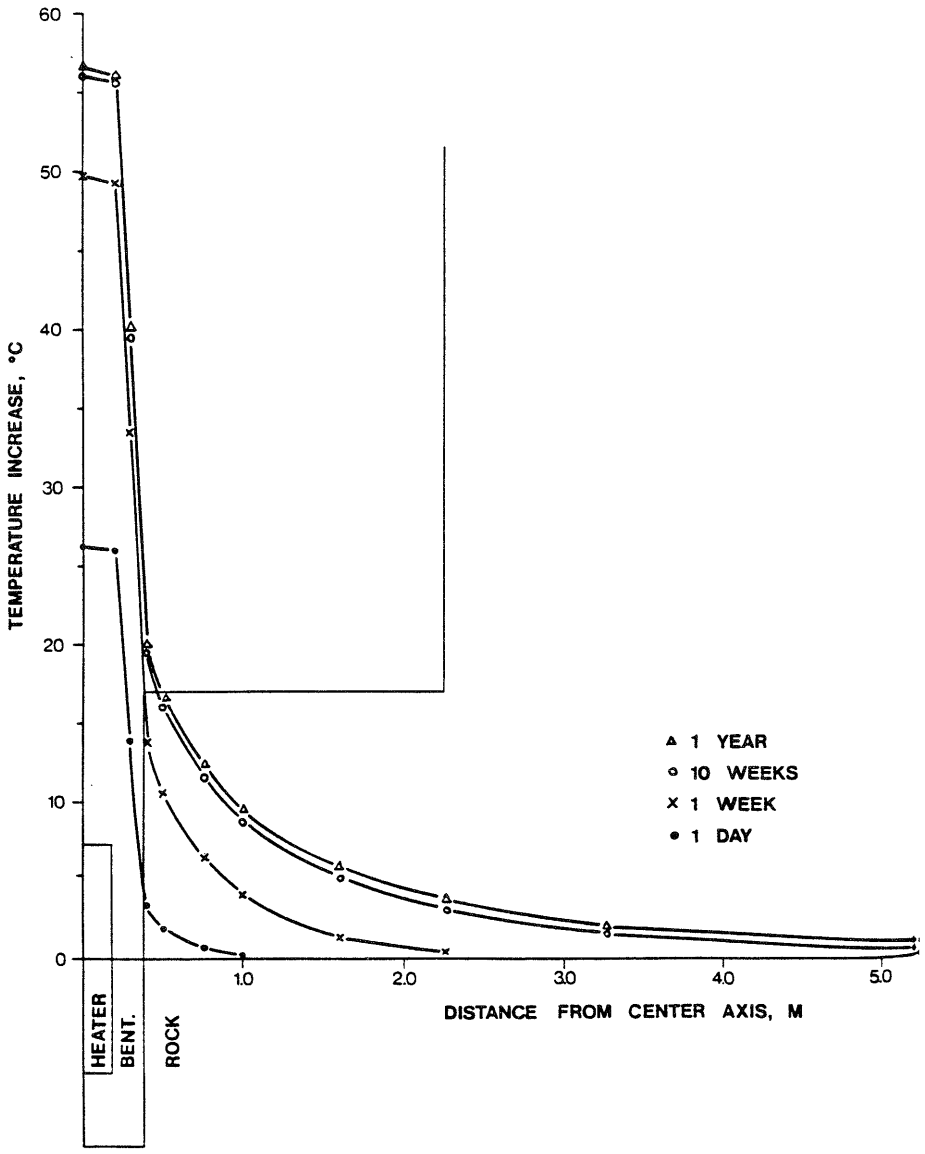

Fig 2.11. The theoretical temperature increase at mid-height of heaters no 3, 4 and 6 as a function of the lateral distance from the heater axis

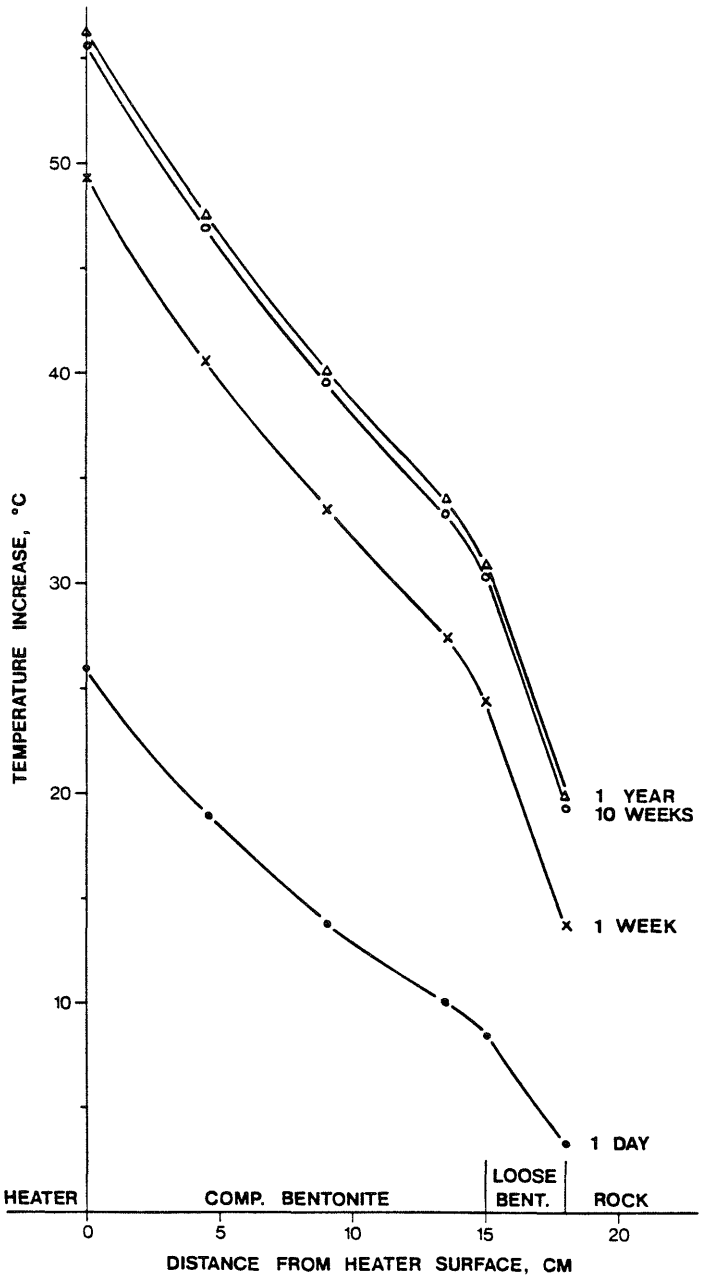

Fig 2.12. Detailed picture of the temperature increase in the bentonite in holes no 3, 4 and 6

2.2.1.4 High power heaters

The temperature increase for any applied power and time can easily be calculated since it is directly proportional to the power if all thermal parameters are assumed to be constant. Such calculations have been made for the power values 1200, 1400 and 1800 W, using the thermal parameters in Table 2:1. The results are reported in Table 2:5.

A separate study was conducted for an increased power with particular respect to the influence of the heat conductivity, which was assumed to be significantly affected by the temperature and by water redistribution due to higher temperature gradients (2). Thus, for 1200 W power and using slightly different thermal parameters, the time-dependent temperature development at mid-height of the heaters was found to be as shown in Figs 2.13-2.15 for the three assumed heat conductivities 0.5, 0.75 and 0.9 W/m,K of the dense bentonite. These values were assumed to represent averages for the bentonite located between the heater and the rock after possible pore water redistribution caused by the thermal gradient. Two of the diagrams, which give the net temperature, i.e. the sum of the temperature increase and the original temperature which was assumed to be 10°C here, cover a short time period only. The temperature conditions after 10 weeks is obtained by adding 3.3°C to the value for 28 days (2).

This study shows that the heat conductivity of the bentonite is of profound importance for the heater surface temperature, while the temperature at the bentonite/rock interface is much less affected.

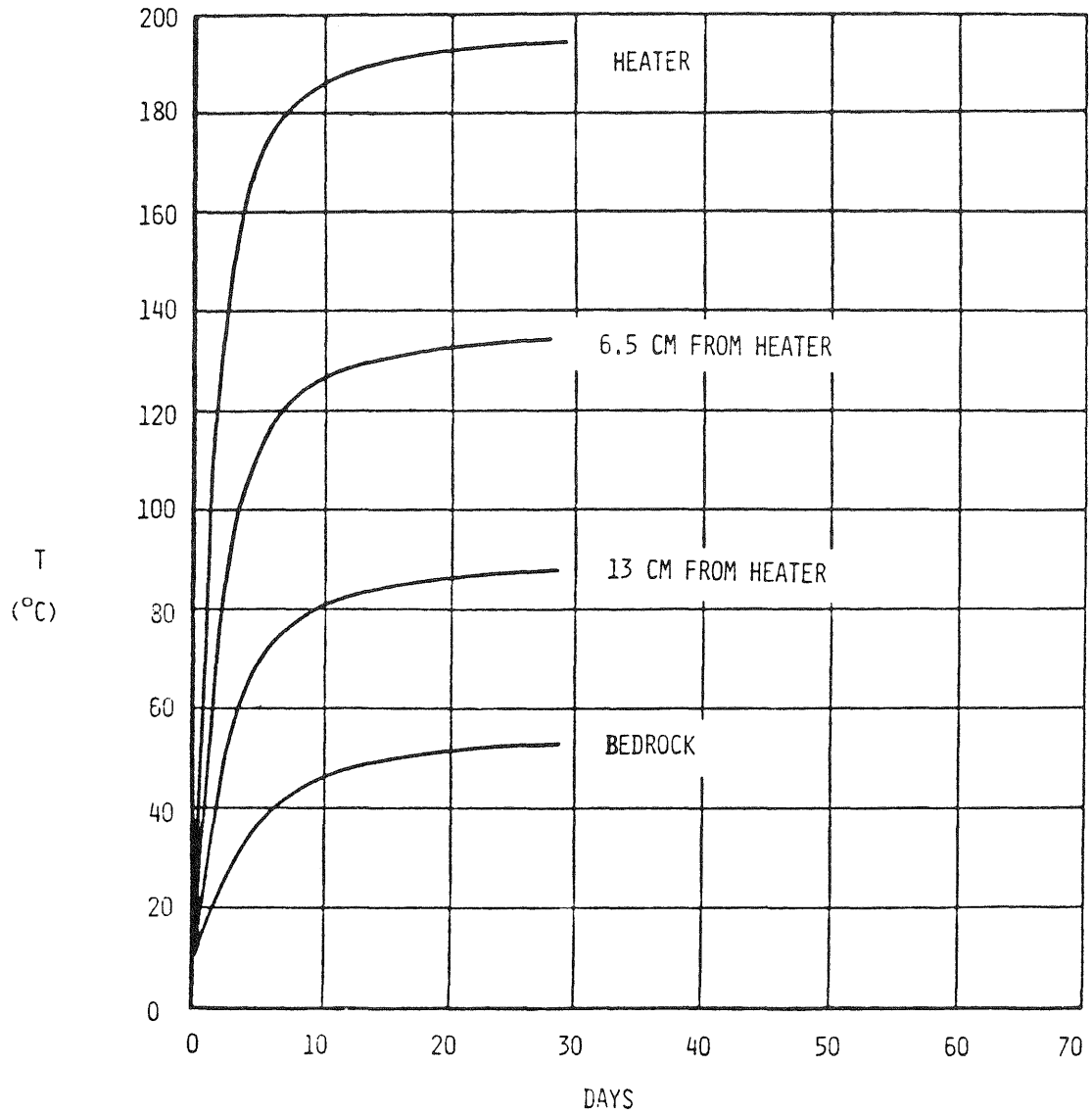

Fig 2.13. Calculated temperatures at mid-height of 1200 W heater. Heat conductivity of the bentonite 0.5 W/m,K

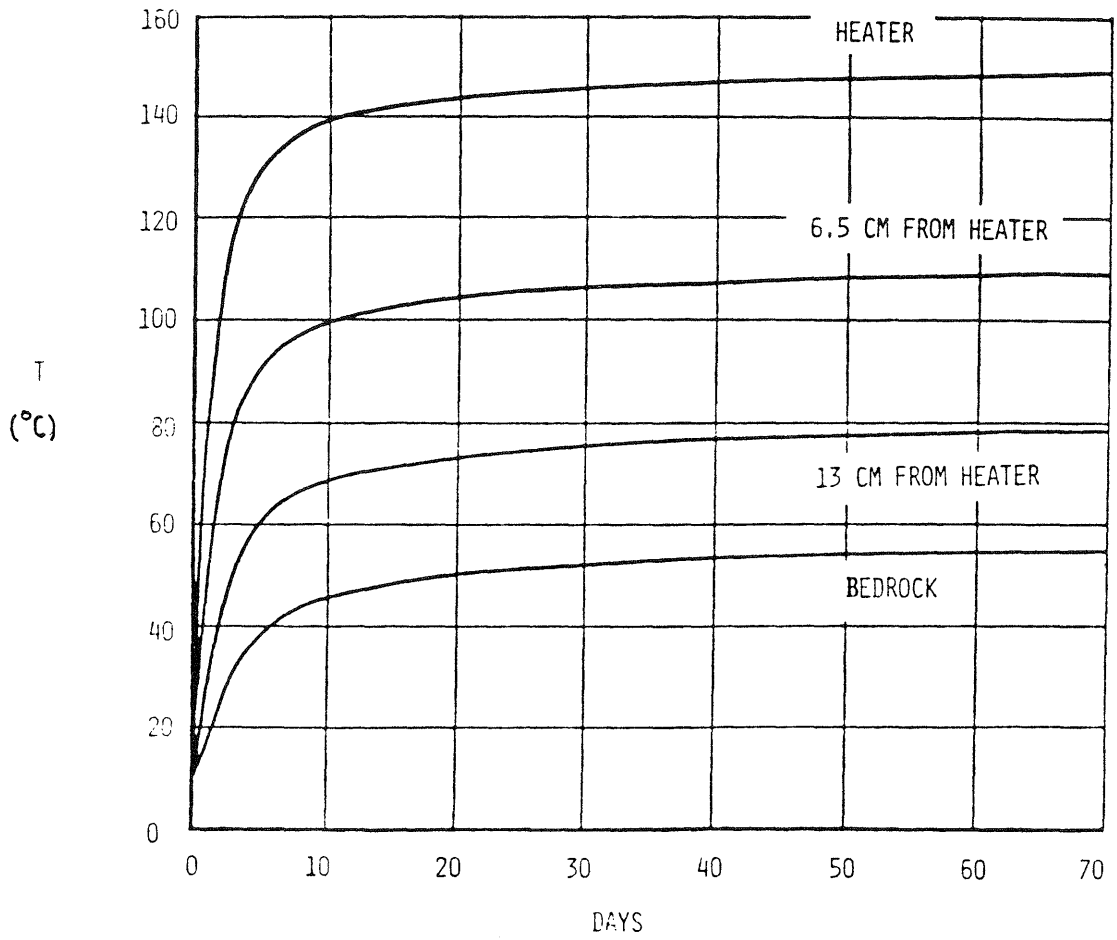

Fig 2.14. Calculated temperatures at mid-height of 1200 W heater. Heat conductivity of the bentonite 0.75 W/m,K

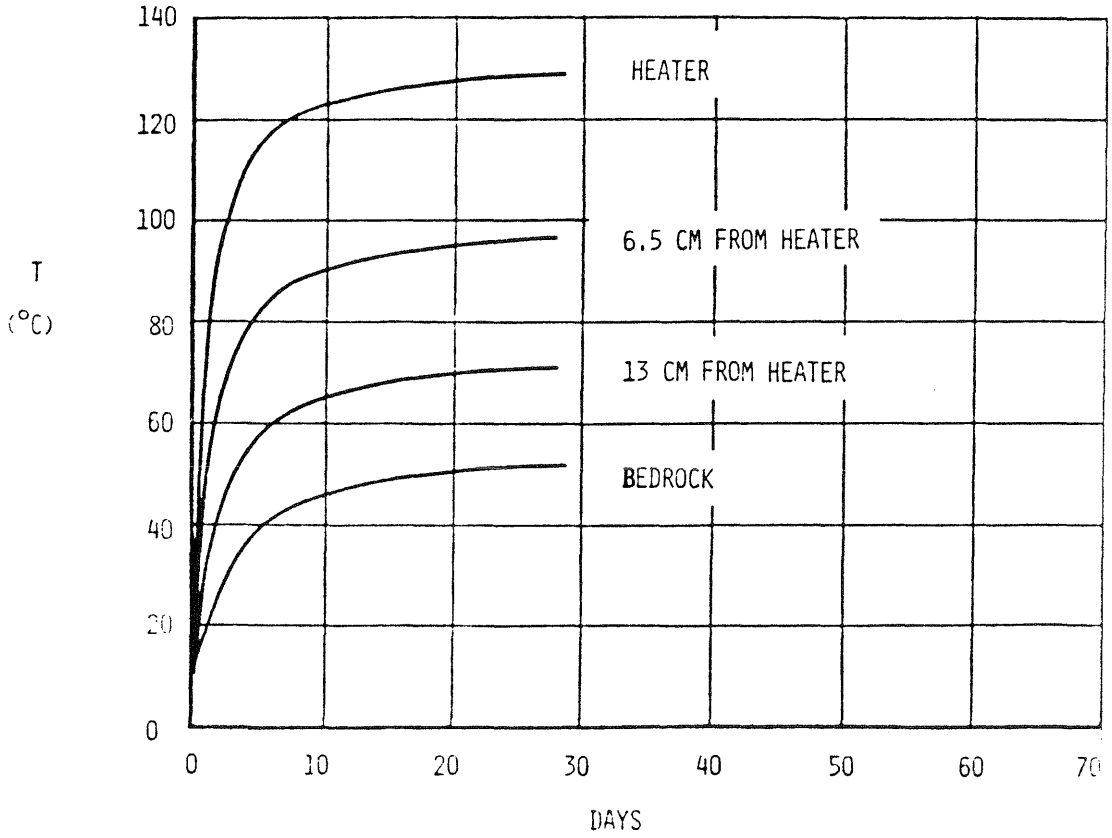

Fig 2.15. Calculated temperatures at mid-height of 1200 W heater. Heat conductivity of the bentonite 0.9 W/m,K

2.2.1.5 Comments and conclusions

The accuracy of the temperature calculations depends on a number of uncertainties and approximations, the major ones being:

1 The correctness of the applied heat conductivities and capacities. Thus, 10 % deviation from the assumed heat conductivity of the bentonite results in a temperature change of as much as 3°C

2 In practice, the heat flow will be a complex transient process because the bentonite undergoes changes with respect to the water content. At least in the "wet" holes no 1, 2 and 5 this is expected to lead to a successive increase of the heat conductivity by more than 20-30 %. This suggests that the predicted values may be overestimated by as much as 5-10°C

3 The small air gap between the heater and the bentonite blocks due to the imperfect fitting was not considered. This gap is expected to increase the surface temperature of the heater at an early stage, while it should be of no practical importance at a late stage of the water uptake when the swelling is expected to improve the contact between the heater and the bentonite

4 Approximations with respect to the nature of the FEM calculation method and assumed boundary conditions.

For the sake of simplicity and clarity in comparing predicted and recorded temperatures in the heater holes, a selection of characteristic temperatures has been made. These are preferably those at mid-height of the heaters as summarized in Table 2:5. For the 600 W tests, the values represent the sum of the ambient temperature 13°C and the calculated temperature increase, assuming that the initial thermal properties of the components are constant and considering also the influence of neighboring heaters. For increased powers proportionality between power and temperature has been assumed.

Table 2:5. Predicted temperatures in °C at mid-height heaters

Heater hole no	Power W	Time after power onset	Heater surface	Rock/bent interface	Remark
1	600	1 week	59	27	
	600	10 weeks	65	33	
	600	1 year	67	34	
	600	2.4 years	68	36	
	1400	0.9 years	138	62	Test terminated after 3.3 years
2	600	1 week	59	27	
	600	10 weeks	65	33	
	600	1 year	68	35	
	600	3.1 years	75	42	Test terminated after 3.1 years
3	600	1 week	62	27	
	600	10 weeks	70	33	
	600	1 year	71	35	
	600	1.3 years	71	35	Test terminated after 1.3 years
	1200	1 week	115	43	New set of bentonite blocks, ambient rock temperature 16°C
	1200	10 weeks	127	54	
	1200	0.6 years	128	55	
	1800	1 week	177	69	
	1800	10 weeks	183	74	
	1800	0.3 years	184	74	Test terminated after 0.9 years

Table 2:5 (continued)

Heater hole no	Power W	Time after power onset	Heater surface	Rock/bent interface	Remark
4	600	1 week	62	27	
	600	10 weeks	69	32	
	600	0.9 years	71	34	Test terminated after 0.9 years
5	600	1 week	56	27	
	600	10 weeks	62	32	
	600	1 year	64	34	
	600	2.2 years	64	34	Test terminated after 2.2 years
6	600	1 week	62	27	
	600	10 weeks	69	32	
	600	1 year	70	34	
	600	2.1 years	71	35	Test terminated after 2.1 years

As to the heating of the sand/bentonite backfill the temperature increase is expected to be very moderate. Assuming the initial temperature to be 13°C the calculated temperature at 1 m above the tunnel floor and 1 m below the tunnel crown right over heaters no 1 and 2 is given by Table 2:6. The temperature at these sites are taken as characteristic in the comparison between predicted and recorded values.

Table 2:6. Predicted temperatures in °C in the tunnel backfill. Ambient temperature 13°C

Time	1 m from tunnel floor		1 m from tunnel crown	
	Above heater no 1*	Above heater no 2	Above heater no 1*	Above heater no 2
1 year	18	18	14	14
2.4 years	20	22	15	16
3.1 years	25	22	16	16

* Power increased to 1400 W after 2.4 years

2.2.2 Results

The determination of the heat distribution was conducted with only a few breakdowns of individual gauges and the build-up of the temperature fields has therefore been recorded in detail throughout the field experiment. This offers an excellent possibility of checking the predictions.

2.2.2.1 Heater holes no 1 and 2, 600 W

The temperature rose rapidly and symmetrically in the highly compacted bentonite at the power onset. As suggested by the preceding calculations, the large majority of the temperature increase took place in the first few weeks. This is shown by Figs 2.16 - 2.19 which give the recorded temperatures after 1 week and the temperature change from 1 to 10 weeks. The temperature situation at the termination of the tests is demonstrated by Figs 2.20 and 2.21 and it is immediately seen that in both holes there was a significant drop in heater surface temperature in the time interval from 10 weeks after test start to the end of the individual test periods. This finding is important since it demonstrates that the water uptake leads to a fairly rapid, significant increase in heat conductivity of the bentonite, at least in rather fractured and water-bearing rock. The temperature distribution shows that the water uptake must have been very uniform.

The temperature gradient in the tests was found to be in the range of 1.5 - 2.5°C per cm radial distance close to the heater to 1.0-1.5°C per cm close to the rock. This is in perfect agreement with the premises, as is also the observation that the maximum bentonite temperature at the applied geometry and power was well below 90°C, which has been taken as a maximum safe temperature for the KBS 3 concept.

The difference between the predicted "characteristic" values given in Table 2:5 and the actually recorded ones is fairly small as seen by comparing these values and those in Table 2:7 except for the first few weeks when the air-filled space between the bentonite and the heater had not yet been affected by the swelling pressure of the peripheral, saturated bentonite. As will be shown later the recorded value for 2.4 years represents a largely water-saturated state, while the values for 10 weeks is representative of an almost unchanged average water content of the bentonite located between the heater and the rock. If the thermal parameters for complete saturation (Table 2:2) are applied, the net temperature 3.1 years after the start of heater no 2 should be 65°C at the heater surface. This is in reasonable agreement with the actually recorded temperature in hole no 2.

Table 2:7. Temperatures in °C at mid-height heater in holes no 1 and 2

Heater hole no	Power	Time after power onset	Heater* surface	Rock/bentonite* interface
1	600	1 week	66/59	32/27
	600	10 weeks	70/65	33/33
	600	1 year	65/67	34/34
	600	2.4 years	65/68	35/36
2	600	1 week	70/59	29/27
	600	10 weeks	66/65	34/33
	600	1 year	64/68	36/35
	600	3.1 years	60/75	38/42

---

* First value is the maximum recorded one, the second is cited from Table 2:5 (prediction)

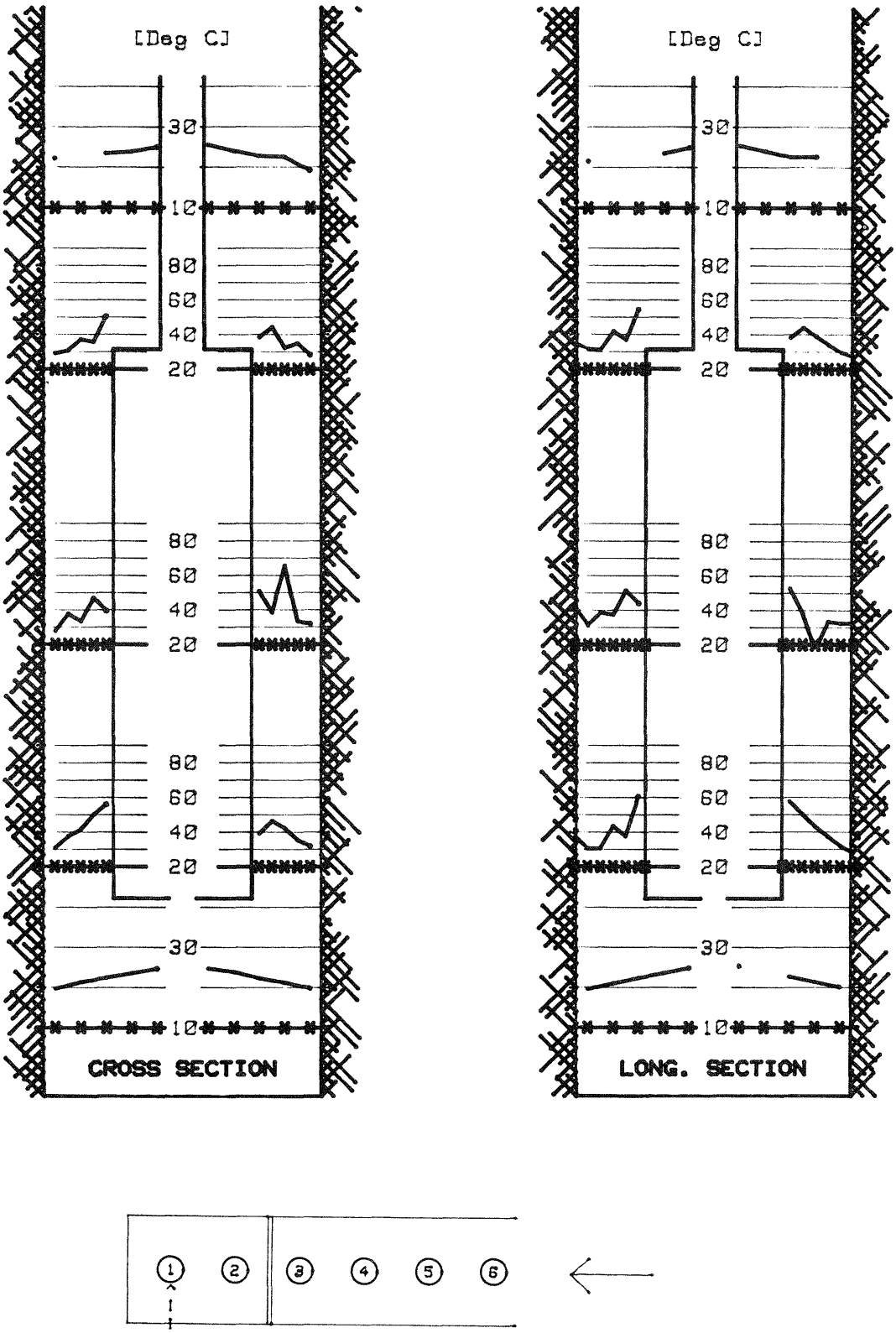

Fig 2.16. Recorded bentonite temperatures in heater hole no 1, 1 week after onset of 600 W power. Notice the irregular curves which are due to incomplete block contacts and initial vapor migration

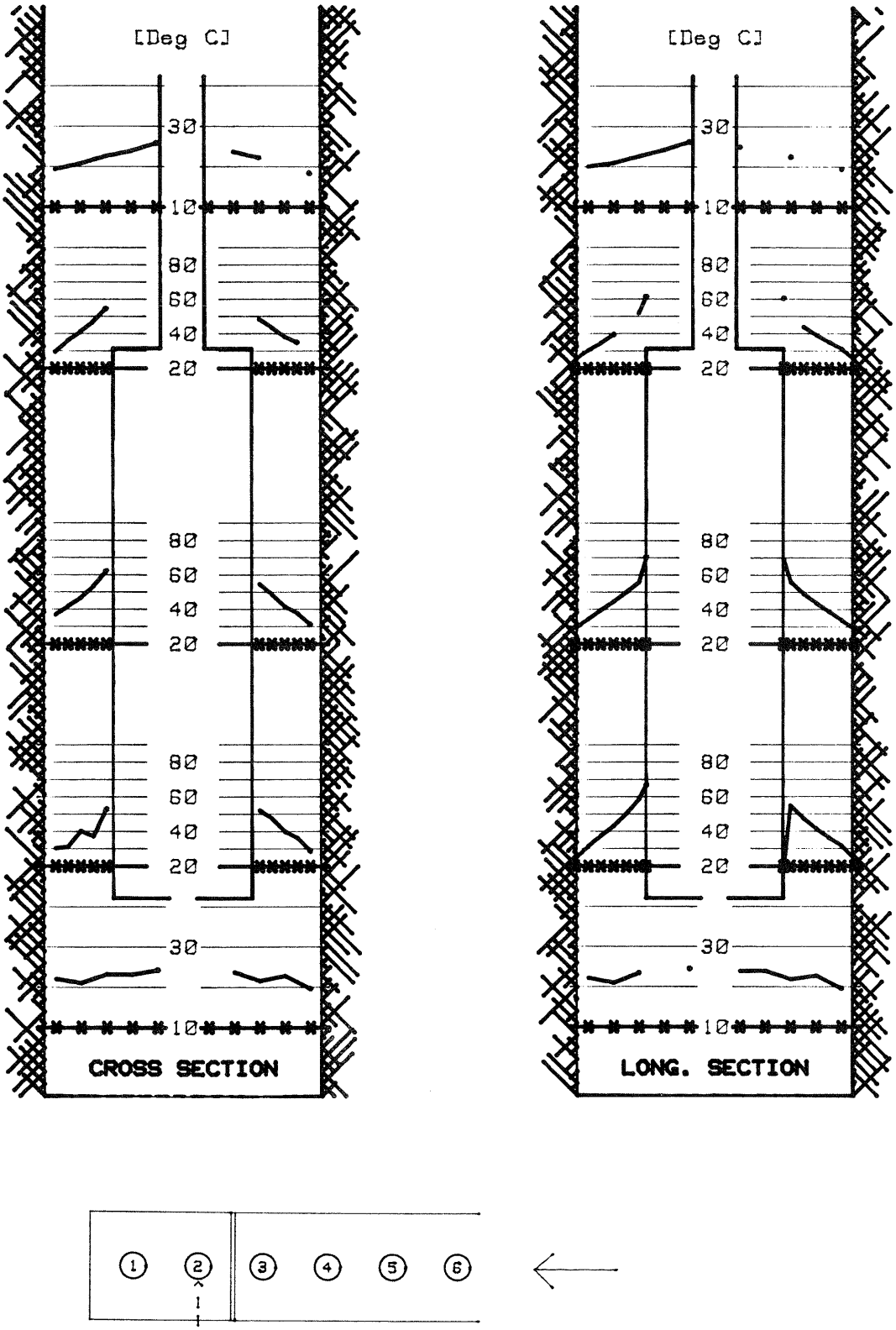

Fig 2.17. Recorded bentonite temperatures in heater hole no 2, 1 week after onset of 600 W power

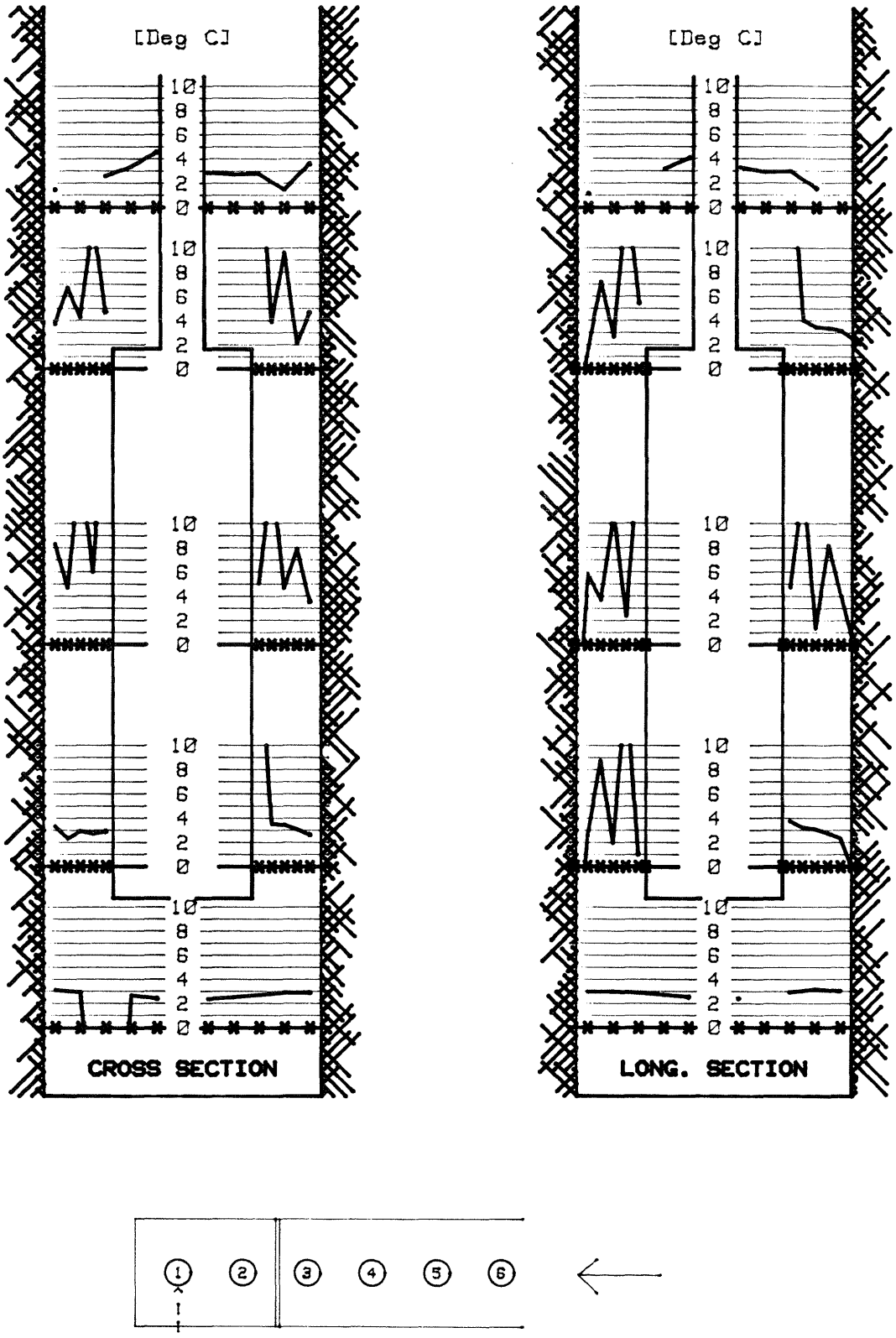

Fig 2.18. Change in temperature in the period 1-10 weeks after the start of the 600 W test in heater hole no 1

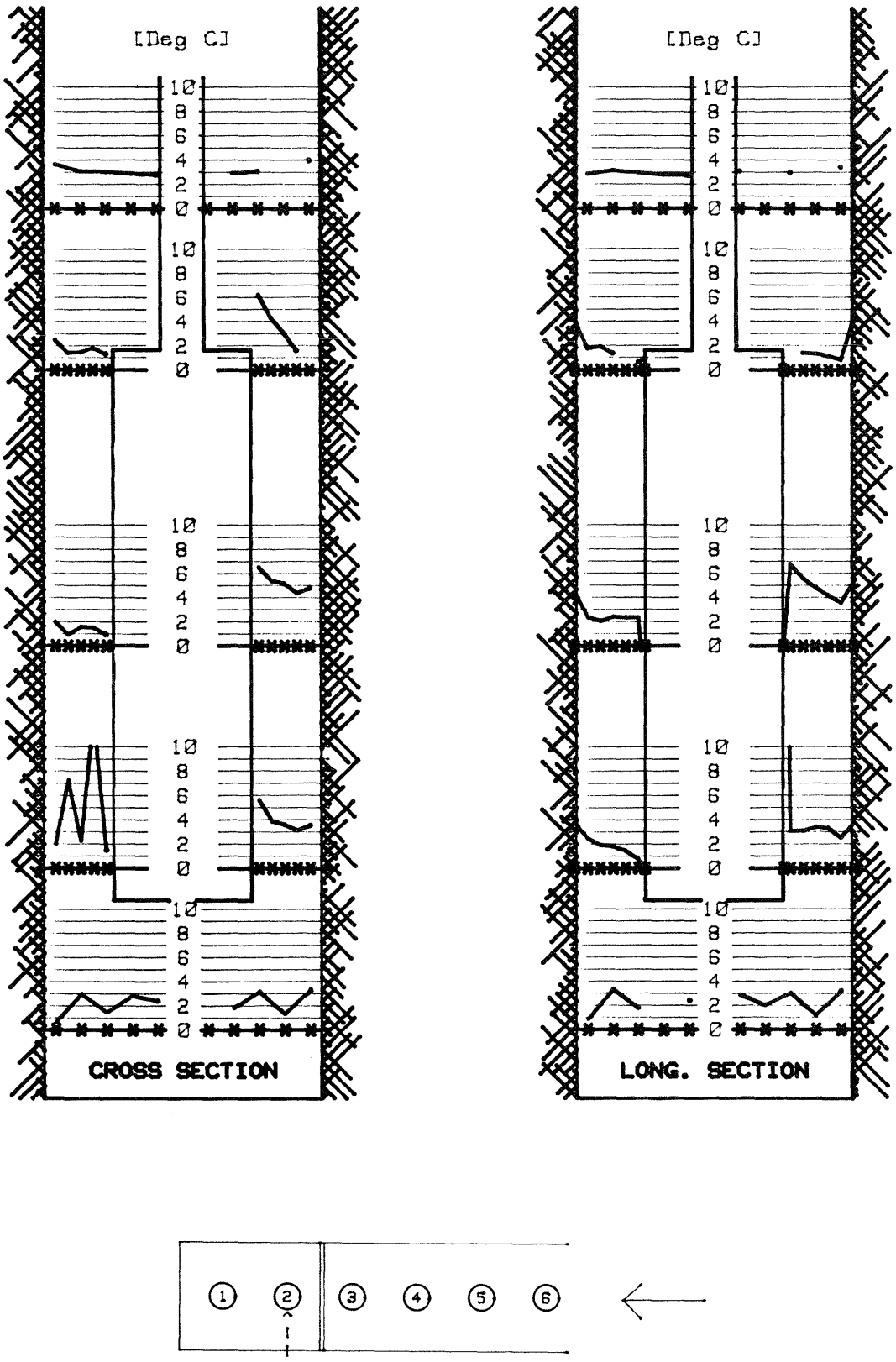

Fig 2.19. Change in temperature in the period 1-10 weeks after the start of the 600 W test in heater hole no 2

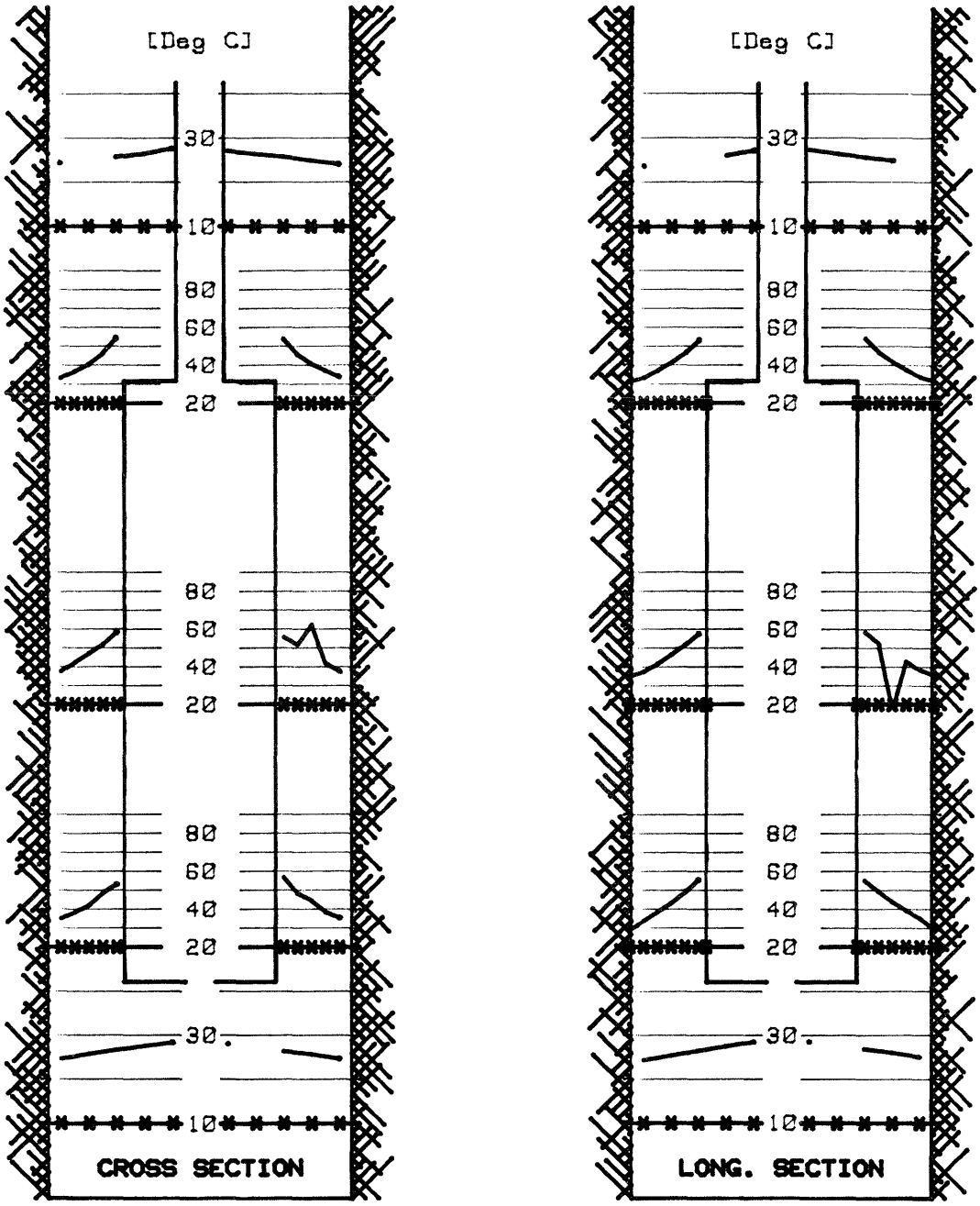

Fig 2.20. Temperature distribution in heater hole no 1 immediately before the power increase from 600 to 1400 W 2.4 years after the test start. Notice the smooth curve shape except for two erratics

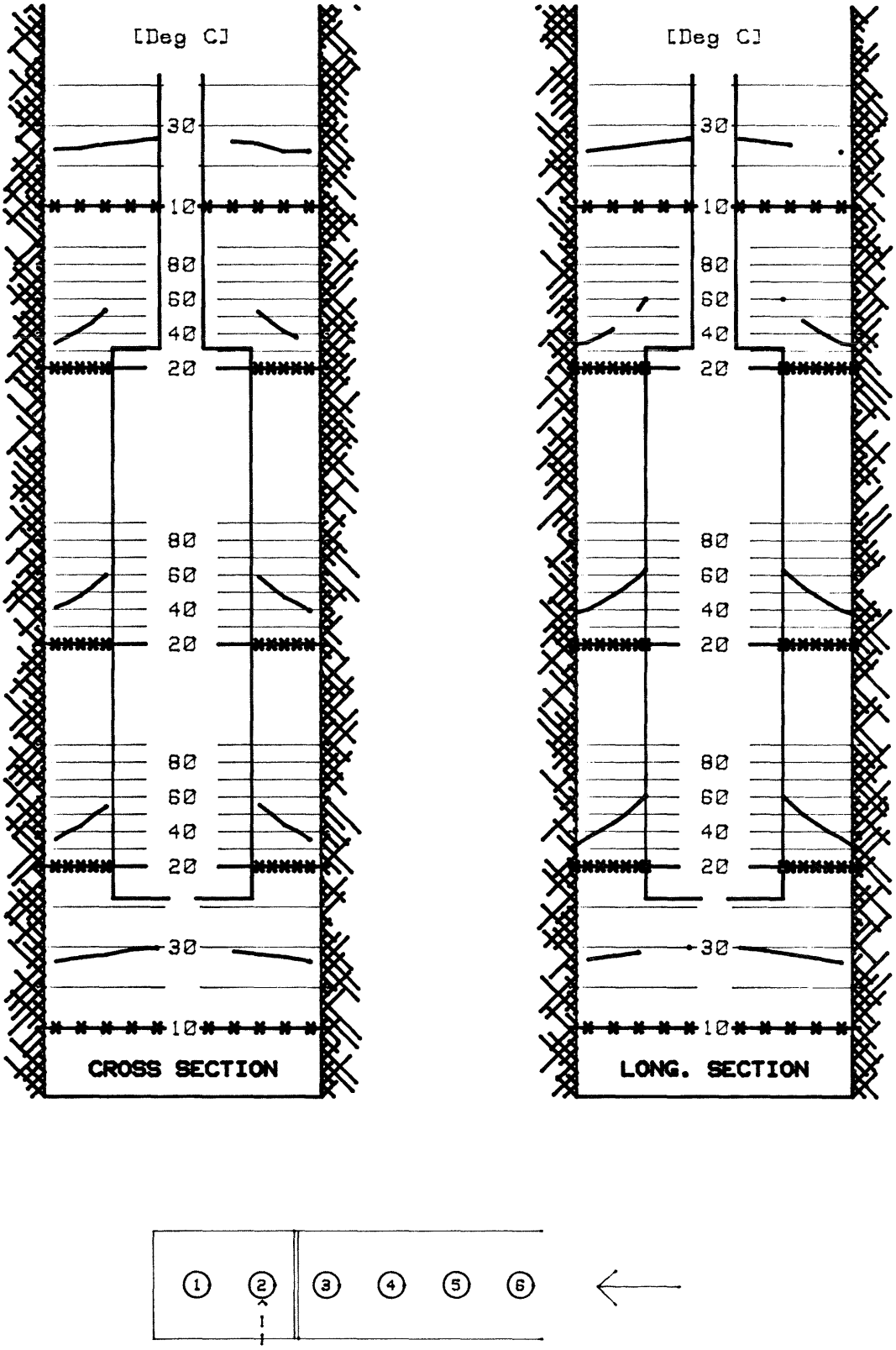

Fig 2.21. Temperature distribution in heater hole no 2 at the termination of the 600 W test 3.1 years after the test start

2.2.2.2 Heater hole no 1, 1400 W

The power increase from 600 to 1400 W yielded a fast "symmetric" temperature increase which led to a heater temperature that was significantly lower than predicted. The temperature distribution at the termination of the test, i.e. 0.9 years after the power increase is shown in Fig 2.22. We see that the temperature at mid-height of the heater at the heater/bentonite interface rose to about 127°C and to about 71°C at the bentonite/rock interface, while the predicted values were 138°C and 62°C, respectively. The temperature differences indicate an efficient heat transfer to the rock due to water uptake in the bentonite.

A good agreement with the recorded temperatures is obtained if the average heat conductivity of the bentonite is taken as 1.2 W/m,K which is actually close to the value of saturated bentonite given in Table 2:2. As will be shown later, the slightly dry conditions close to the heater and the complete saturation of the outer part of the bentonite in fact imply different heat conductivities in these zones, 1.2 W/m,K being a reasonable average.

2.2.2.3 Heater hole no 5, 600 W

The temperature development in hole no 5 was similar to that in holes no 1 and 2, but contrary to the predictions, the temperatures were higher in hole no 5 in the first 10 weeks. After about 1 year holes no 1 and 2 showed higher values, the difference being very slight, however. The agreement between predicted (Table 2:5) and observed "characteristic" temperatures is very good after slightly more than 1 year as demonstrated by Table 2:8. The initial high surface temperature is due to the air-filled space between the bentonite and the heater as in the case of holes no 1 and 2. The same conditions prevailed in the "dry" holes as well.

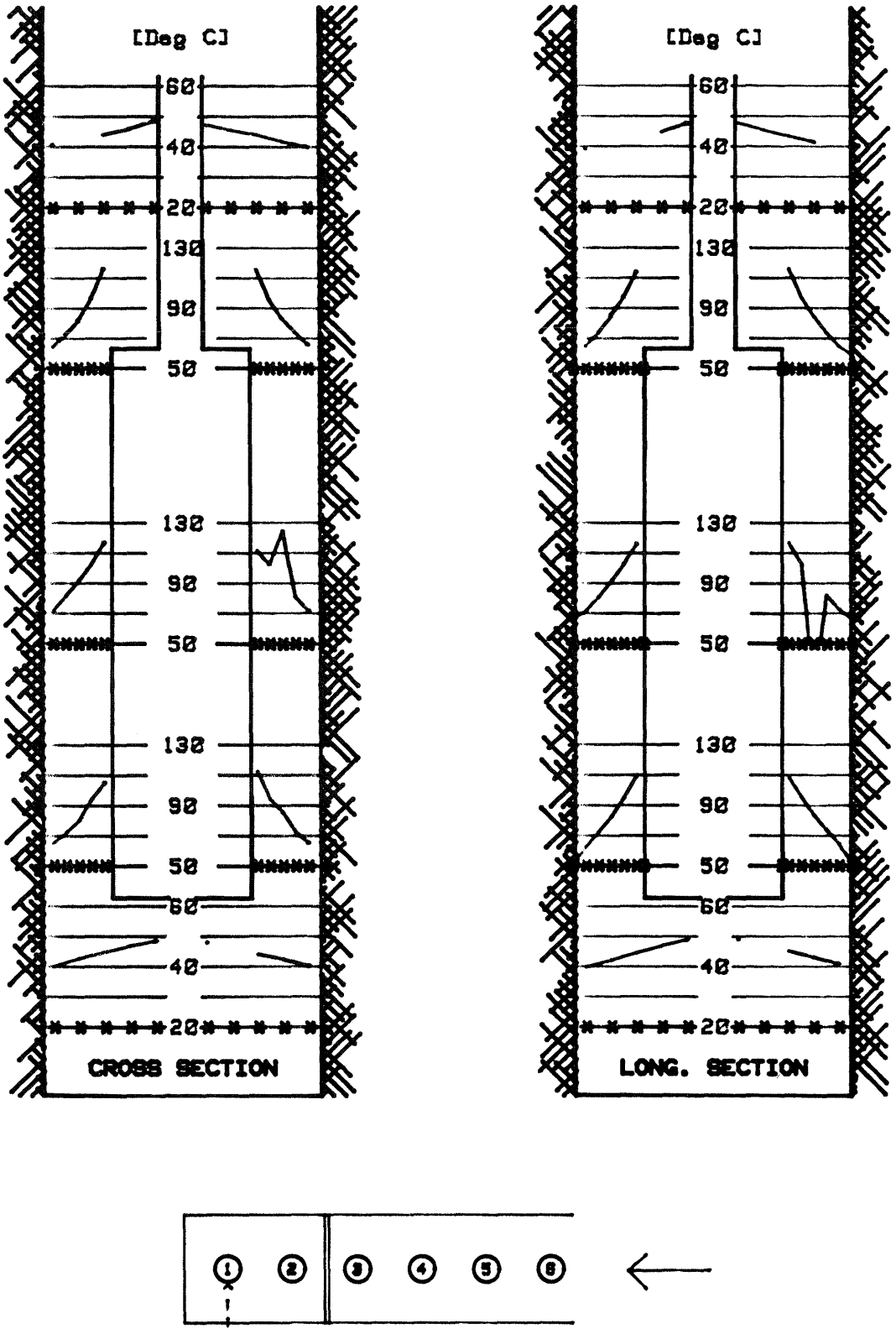

Fig 2.22. Temperature distribution in heater hole no 1 at the termination of the 1400 W test 0.9 years after the test start

Table 2:8. Temperatures in °C at mid-height heater in hole no 5, 600 W

Time after power onset	Heater* surface	Rock/bentonite interface*
1 week	70/56	30/27
10 weeks	70/62	32/32
1 year	66/64	33/34
2.2 years	63/64	34/34

* First value is the recorded one, the second is cited from Table 2:5 (predictions)

2.2.2.4 **Heater holes no 3, 4 and 6, 600 W**

As suggested by the predictions the temperature became higher in the three "dry" holes than in the "wet" holes no 1, 2 and 3. The same pattern of a rapid "symmetric" build-up of temperature fields was observed, the situation at the termination of the individual tests being shown in Figs 2.23 - 2.25.

The test in the "driest" hole no 6 is of particular interest since it represents conditions which will be met with in actual repositories. Here, the temperature should be higher than in the other holes but a successive drop in heater surface temperature is still probable as a consequence of the expected water uptake. This is evidenced by Fig 2.26, which demonstrates the change in temperature from 1 year after power onset to the termination of the test 2.1 years later.

As in the preceding discussion of heater holes no 1, 2 and 5, we will compare the predicted "characteristic" temperatures specified in Table 2:5 with the actual ones. They are both reported in Table 2:9 from which it is concluded that the differences are insignificant for the rock/bentonite interface as in holes no 1, 2 and 5. For the heater surface it is fairly high on the other hand, the main reason being drying and cracking of the bentonite blocks close to these heaters.

Table 2:9. Temperatures in °C at mid-height heater in holes no 3, 4 and 6

Heater hole no	Power W	Time after power onset	Heater* surface	Rock/bentonite interface*
3	600	1 week	78/62	28/27
	600	10 weeks	81/70	33/33
	600	1 year	79/71	33/35
4	600	1 week	76/62	26/27
	600	10 weeks	80/69	32/32
	600	0.9 years	81/71	33/34
6	600	1 week	78/62	30/27
	600	10 weeks	83/69	34/32
	600	1 year	84/70	35/34
	600	2.1 years	81/71	35/35

---

* First value is the recorded one, the second is cited from Table 2:5 (predictions)

2.2.2.5 Heater hole no 3, 1200 - 1800 W

The test in heater hole no 3 served as a pilot study for the planned high-power test in hole no 1. The test ran for 0.6 years at a power of 1200 W and at 1800 W for another 0.3 years.

The 1200 W test gave lower temperatures than expected, the situation immediately before the subsequent power increase to 1800 W being the one shown in Fig 2.27. As in the case of the 1400 W test in hole no 1, an attempt was made to evaluate an equivalent heat conductivity of the bentonite to yield the observed heater surface temperature. The result is given in Fig 2.28, according to which there is a reasonable agreement between recorded and calculated temperatures if we assume three bentonite zones with different heat conductivities. In practice, a successive change in thermal parameters in the radial direction in the bentonite is of course more plausible. The choice of heat conductivities requires a comment; the central zone represents the original state of the bentonite while the peripheral zone was assumed to be extraordinarily conductive. The inner zone was given a heat

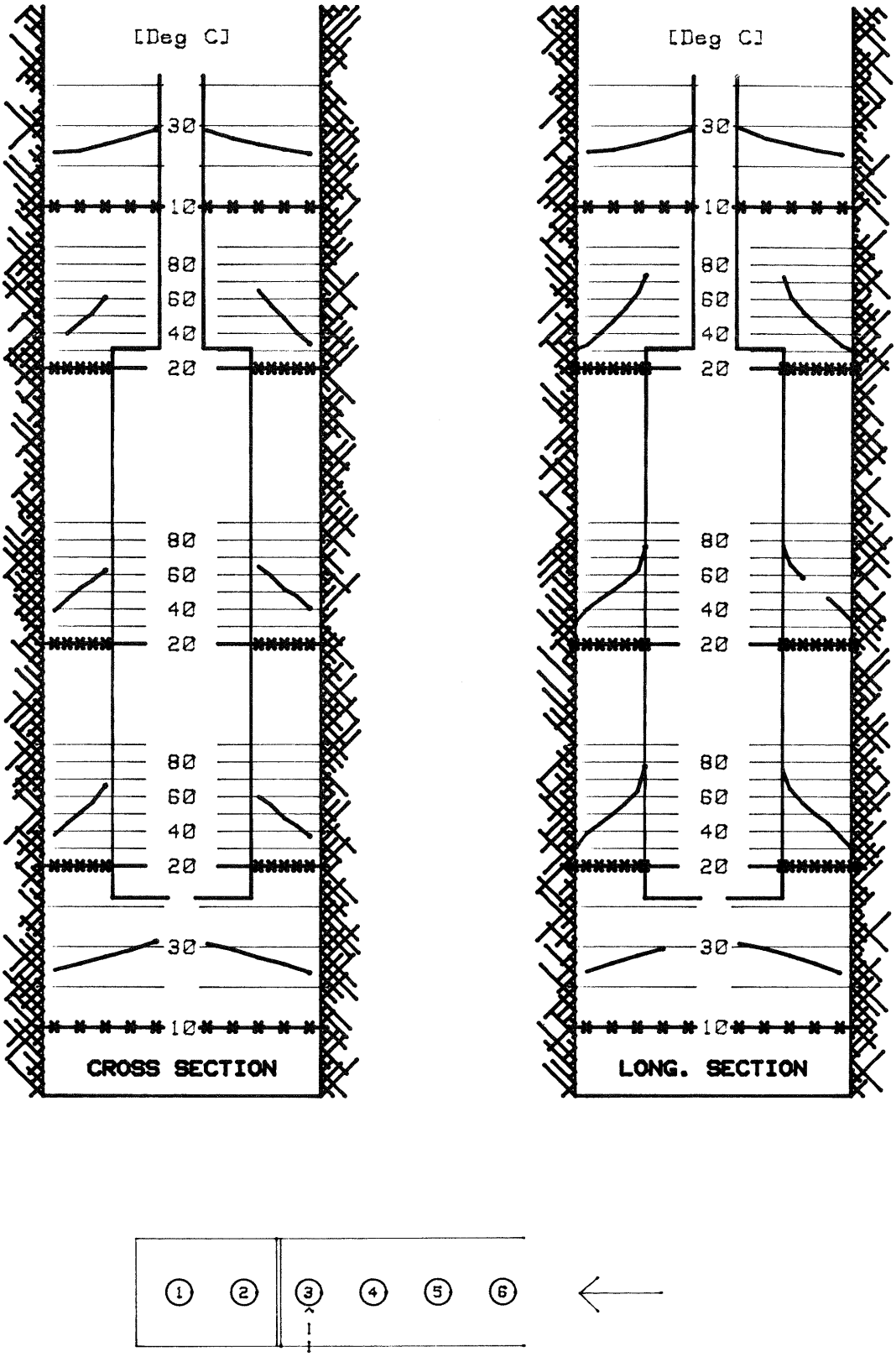

Fig 2.23. Temperature distribution in heater hole no 3 at the termination of the 600 W test 1.3 years after the test start

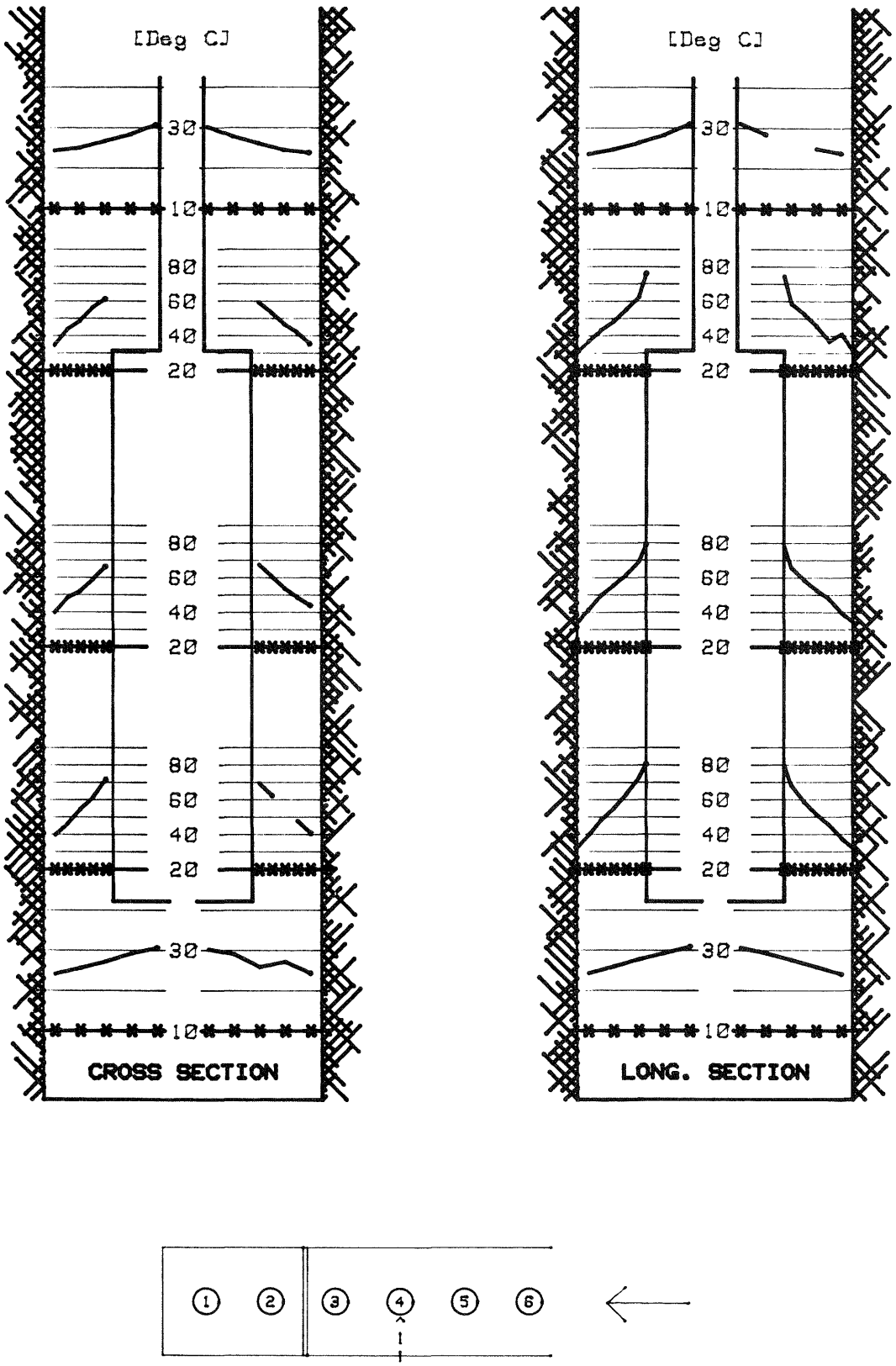

Fig 2.24. Temperature distribution in heater hole no 4 at the termination of the 600 W test 0.9 years after the test start

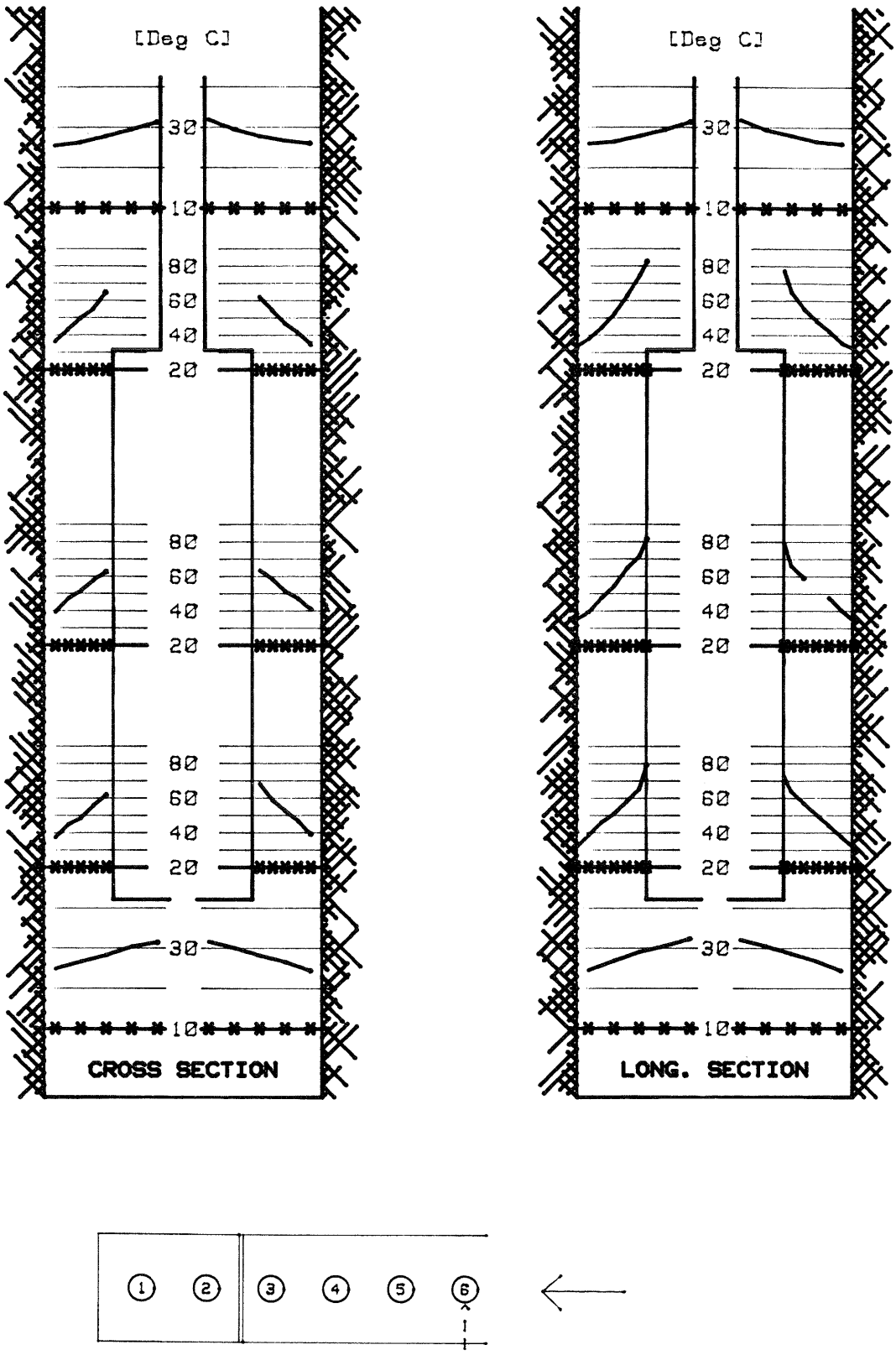

Fig 2.25. Temperature distribution in heater hole no 6 at the termination of the 600 W test 2.1 years after the test start

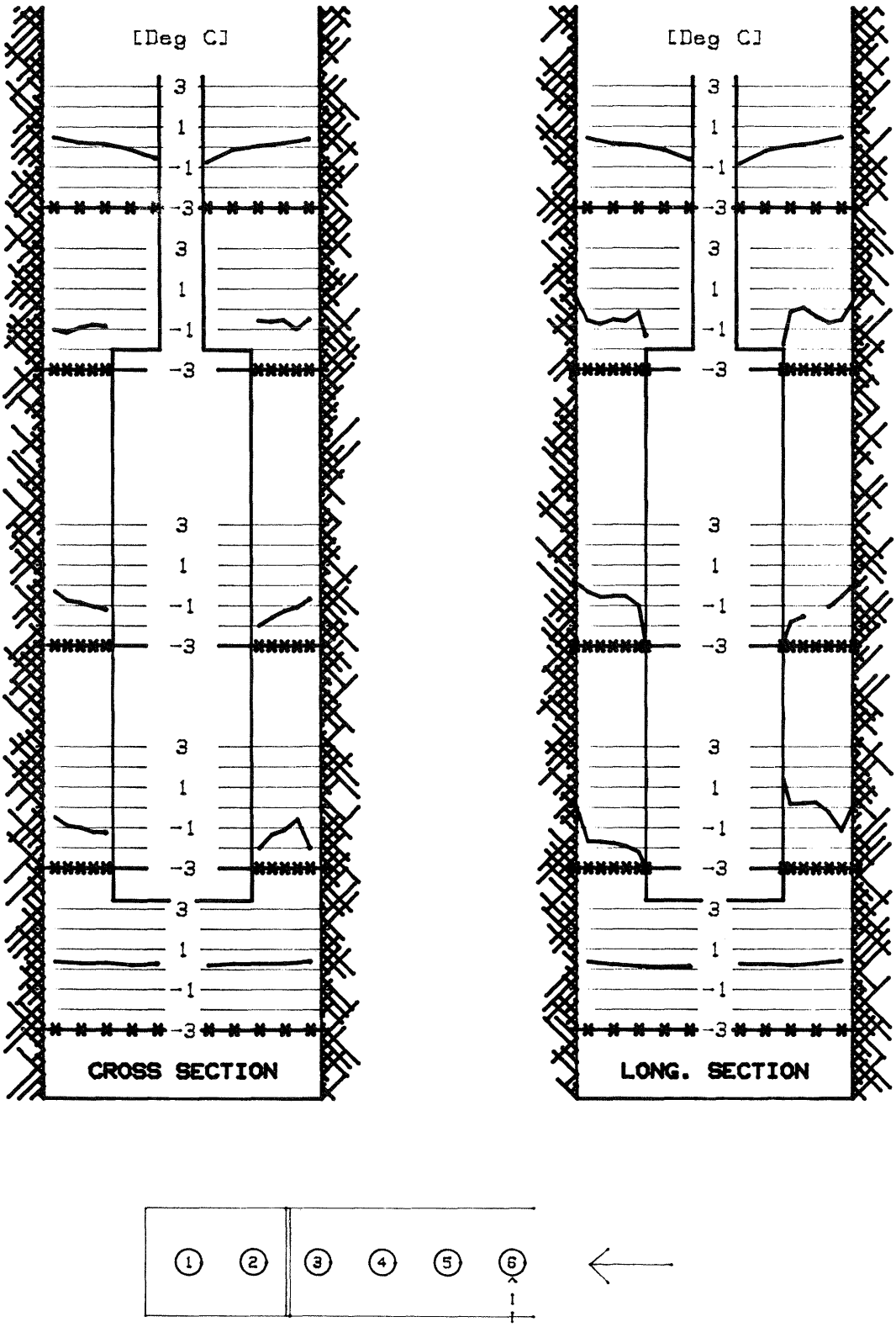

Fig 2.26. Change in temperature in the period 1-2.1 years after the start of the 600 W test in heater hole no 6

conductivity representing approximately the average of the initial λ-value and the one for bentonite dried at 105°C.

The 1800 W test (cf Fig 2.29) confirmed the conclusion from the 1200 and 1400 W tests that the predicted temperatures for the high-power tests were too high. Table 2:10 offers a comparison between the predicted "characteristic" temperatures given in Table 2:5 and the actual ones.

Table 2:10. Temperatures in °C at mid-height heater in holes no 3, 1200-1800 W

Power W	Time after power onset	Heater* surface	Rock/bentonite interface*
1200	1 week	115/115	48/43
1200	10 weeks	123/127	56/54
1200	0.6 years	123/128	57/55
1800	1 week	168/177	73/69
1800	10 weeks	172/183	76/74
1800	0.3 years	172**/184	76/74

* First value is the recorded one, the second is cited from Table 2:5 (predicted)
** From 10 weeks to 0.3 years there was an actual drop in temperature by 0.2°C

2.2.2.6 Tunnel backfill, boxing-outs

The heating of the sand/bentonite backfills occurred at a slightly slower rate than predicted (cf Table 2:11), the main reason probably being that the heat conductivity of the lower part of the backfill increased due to water uptake from the rock. A possible additional explanation may be that cooling of the rather fractured tunnel floor took place through groundwater percolation. Such effects, and the less homogeneous state of the sand/bentonite backfill in the upper part of the heater holes and in the boxing-outs, make the temperature recording in these materials rather irrelevant. We confine ourselves here to conclude that the temperatures at mid-height of the boxing-outs were of the same order of magnitude as the predicted ones (cf Fig 2.9).

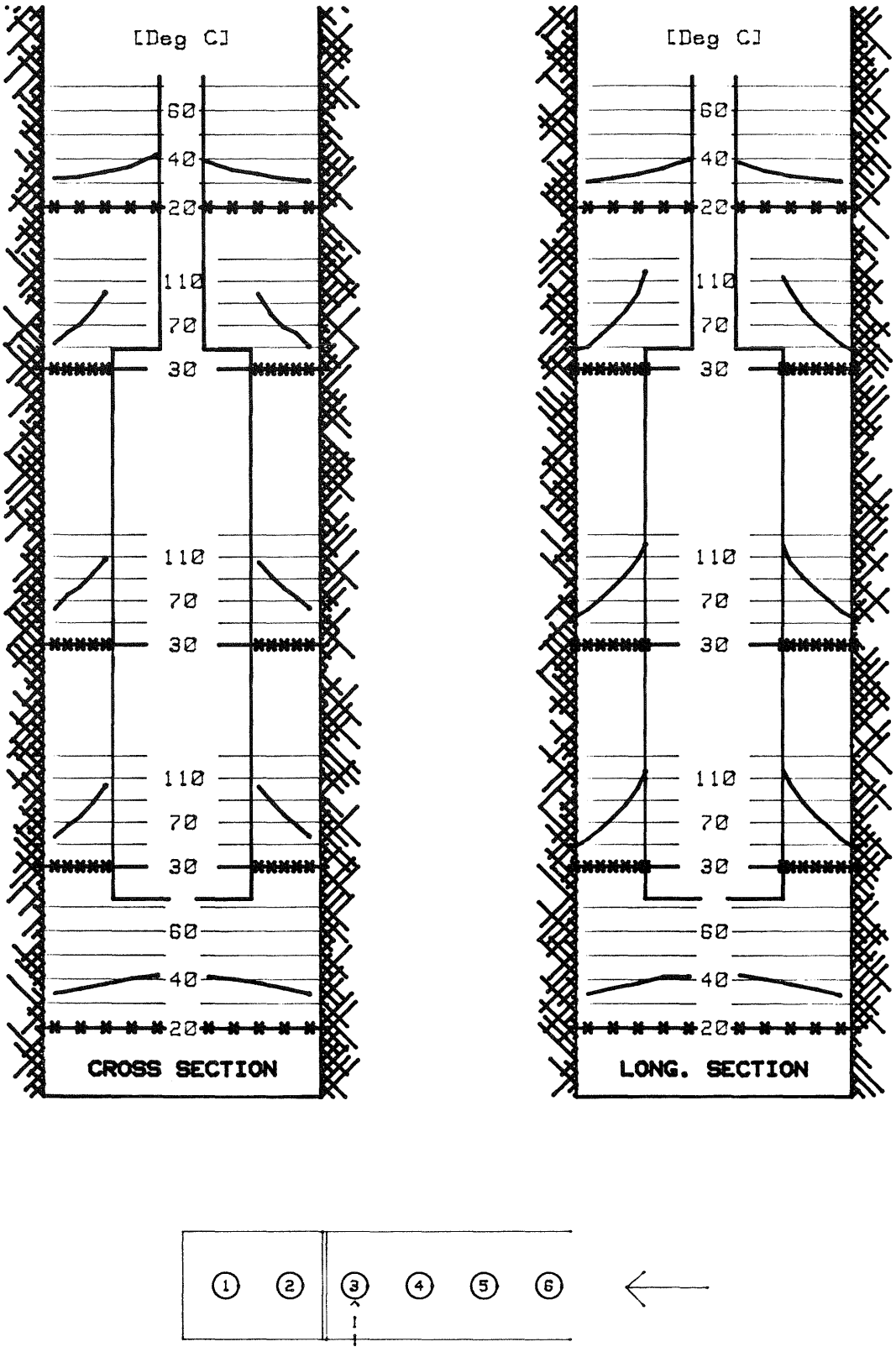

Fig 2.27. Temperature distribution in heater hole no 3 0.6 years after the start of the 1200 W test

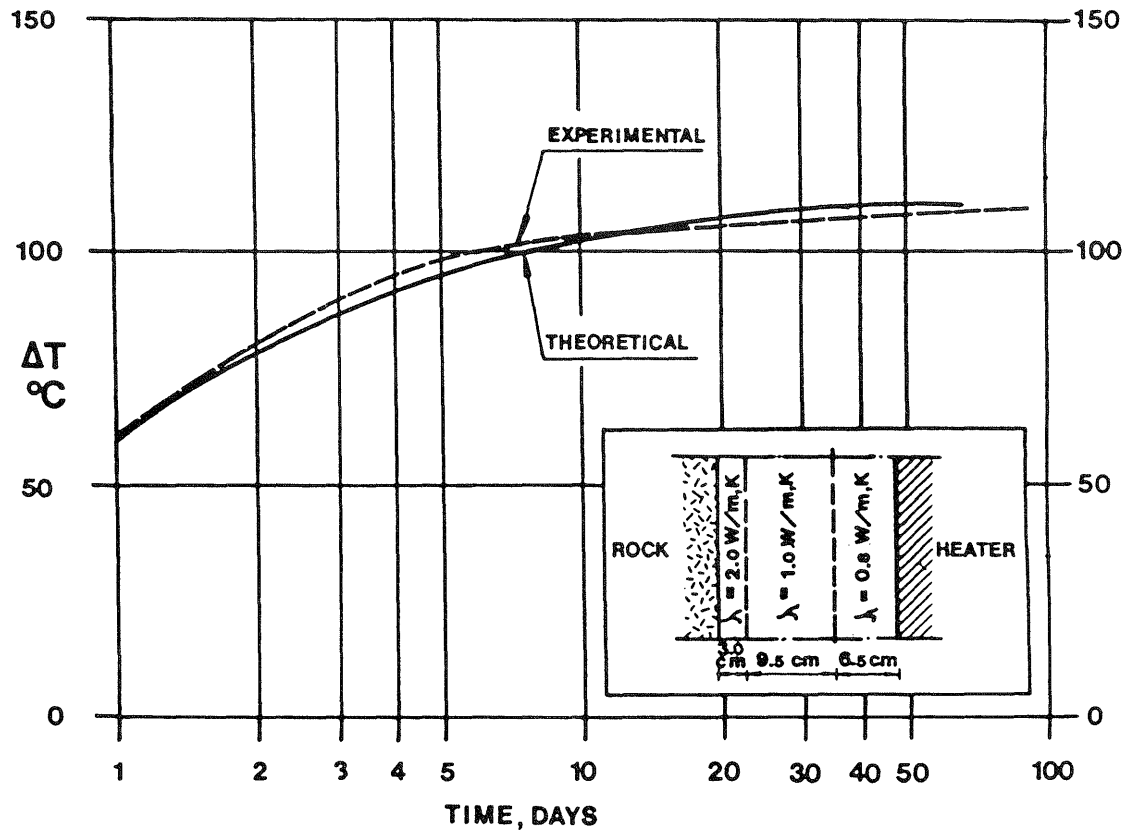

Fig 2.28. Recorded and calculated temperature increase T at mid-height of the heater in hole no 3, 1200 W test

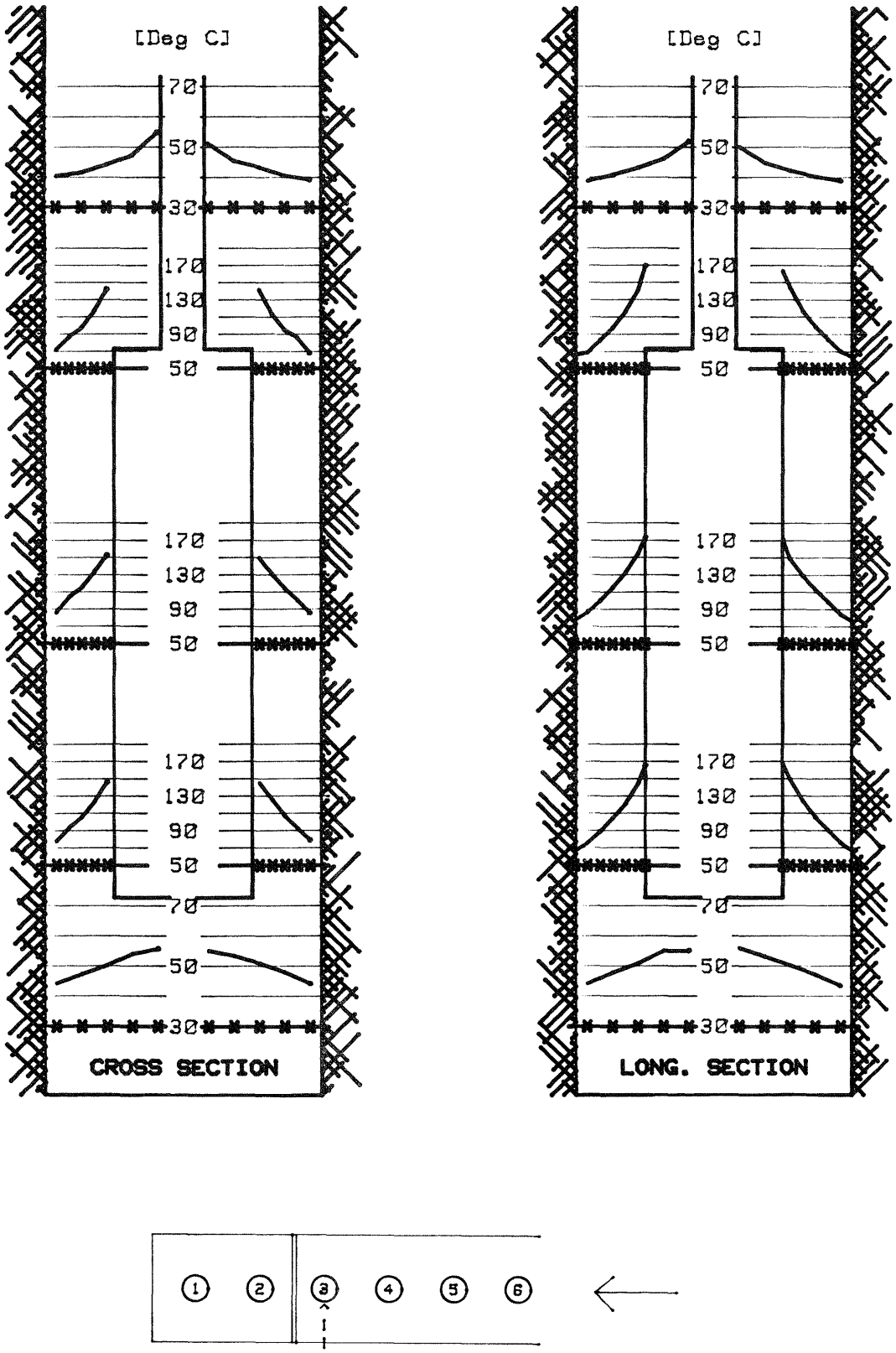

Fig 2.29. Temperature distribution in heater hole no 3 0.3 years after the start of the 1800 W test

Table 2:11. Temperatures* in ^{o}C in the tunnel backfill

Time	1 m from tunnel floor		1 m from tunnel crown	
	Above heater no 1	Above heater no 2	Above heater no 1	Above heater no 2
1 year	15.3/18	17.3/18	12.5/14	12.8/14
2.4 years	16.1/20	18.2/22	12.8/15	13.5/16
3.0 years	23.0/25	19.0/22	14.5/16	13.8/16

---

* First value is the recorded one, the second is cited from Table 2:6 (predicted)

2.2.2.7 Rock

The temperature recording in boreholes in the vicinity of heater hole no 5 showed a fair agreement with the predictions. The expected and recorded values of a number of representative gauges are given in Table 2:12.

Table 2:12. Rock temperatures* in cross section through heater hole no 5

Distance from heater, m	Level** (z-coord)	Time after onset of heater 1 week	1 year
1	338.6	17.5/17.0	21.9/22.5
	339.7	15.6/15.0	19.6/20.0
2	338.6	14.7/14.0	17.9/18.0
	339.7	14.1/13.5	17.4/17.5
3 (Betw hole no 5 and 6)	338.6	14.7/13.0	17.8/17.0
	339.7	14.0/13.0	17.5/17.0

---

* First value is the recorded one, the second is the predicted temperature

** z = 338.6 is appr. mid-height heater, z = 339.7 is appr. base of the heater hole

At half the distance between heater holes no 5 and 6, which both operated at 600 W power, the predicted temperatures after 1 year at the levels corresponding to the base and mid-height of the heaters

were almost identical with the recorded ones. The values for 1 week at mid-distance between holes no 5 and 6 are higher than predicted but this is due to the fact that the initial ambient rock temperature was about 14°C here rather than the assumed 13°C. As expected, the overlap of the individual temperature fields of neighboring heaters only produced insignificant heating of the rock located between the holes.

2.2.3 Conclusions and remarks

The main conclusions from the heat investigation are:

1 Even in very poorly water-bearing rock, the bentonite temperature will not exceed 90°C with 600 W power at the applied geometry

2 The predicted and actually recorded bentonite temperatures in the "wet" heater holes and the surrounding rock are in reasonable agreement in the 600 W tests except for the first stage. The agreement is less good and non-conservative for the holes in poorly water-bearing rock although it is successively improved with increasing time after the test start. The discrepancy points to overestimation of the heat conductivity in the predictions, for which drying of the bentonite close to the heater seems to be responsible. The actual reason for this is probably the development of fractures initiated by the drying, and expanded by the swelling pressure that was transferred from the peripheral wet zone via the cracked inner zone to the heaters. The phenomenon was actually observed at the excavation of holes no 3, 4 and 6 and must have occurred temporarily also in the "wet" holes. A more accurate way of predicting the temperature distribution would be to ascribe different heat conductivities to different radial zones instead of applying an average λ-value. Since the deviation from the predicted temperatures is less than about 10 % and the duration of the period of "over-heating" should be a few years only, the laboratory-derived thermal parameters are still sufficiently accurate for practical use.

3 The predicted temperatures of the highly compacted bentonite in the high-power tests are significantly higher than the recorded ones. This was probably caused by two effects which are related to the high temperature. One is that the heat conductivity per se increases with the temperature, the other that heat is transferred through vapor flow more effectively than at low temperatures. The latter mechanism is expected to be effective when a large part of the water is vaporized and the open pores in vicinity of the heater become continuous.

2.3 Swelling pressures in the heater holes and tunnel backfill

2.3.1 Predictions

2.3.1.1 General aspects

The swelling pressure p_s in the heater holes was expected to be a function of the rate of water uptake and of the compression of the overlying sand/bentonite backfill. The maximum p_s-value was predicted on the basis of the calculated net bulk density of the highly compacted bentonite at full saturation, taking the swelling to fill the heater holes and to displace the overlying backfill into consideration.

Radial swelling to fill the holes and subsequent homogenization of the clay would give the theoretical net bulk density ρ_m= 2.1 t/m^3, which corresponds to p_s=20 MPa at 70°C according to Volume I, Table 4:4. More recent considerations indicate that the pressure would rather be in the range of 10-20 MPa [cf. (5), p. 68] with a probable average value of 16-18 MPa.

The compression of the overlying backfill caused by the swelling pressure of the highly compacted bentonite was estimated by assuming that shear forces along the rock/bentonite interface become mobilized and that the displacement proceeds until vertical force equilibrium at full saturation is developed of the swelling power on the one hand and the counteracting wall friction and reaction pressure of the compressed backfill on the other. This yields the swelling pressure distribution shown in Fig 2.30, and taking the friction angle as 30° the resulting, final displacement of the interface between the highly compacted bentonite and the overlying backfill will be 6 cm in the tunnel and 4 cm in the boxing-outs. The corresponding p_{s_a} -value should be 2.5-3 MPa for heater holes no 1 and 2 and 5 MPa for the

smaller. The z-value, i.e. the depth to which vertical expansion of the dense bentonite was expected to take place, was estimated at 0.5 m, which corresponds to the upper end of the heaters. The pressure distribution in calculating the compression of the backfill was assumed to be that in Fig 2.31. Zone 3 was missing in the case of the backfill confined in the boxing-outs.

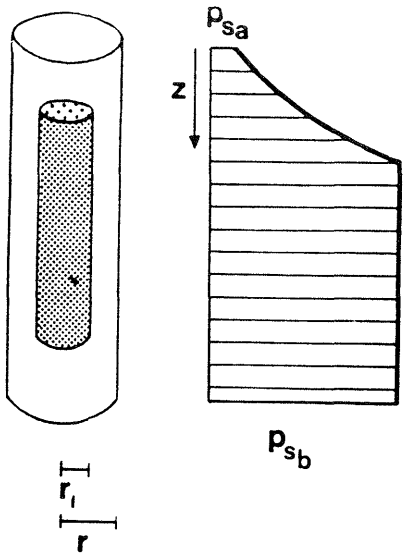

Fig 2.30. Schematic picture of heater hole with assumed swelling pressure distribution. Z is the distance from the upper end of the highly compacted bentonite

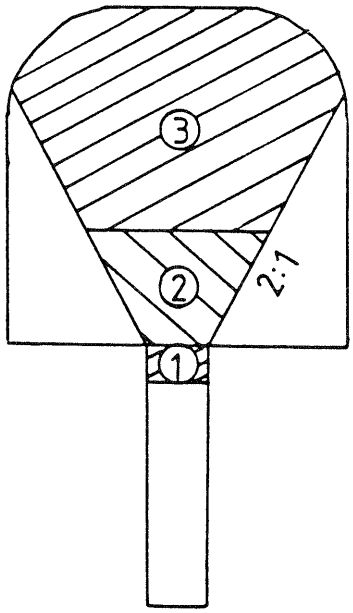

Fig 2.31. Stress distribution pattern and subdivision of the backfill for calculation of the displacement of the interface between the highly compacted bentonite and the overlying backfill

The calculation was extended to cover also the possible long-term effect of zero friction at the bentonite/rock interface. Such a condition is expected as a result of creep processes and of the redistribution of water and solid matter that yields a successively improved homogeneity throughout the bentonite. Fig 2.32 shows the general resulting relationship between the swelling pressure and the displacement of the interface between the highly compacted bentonite and the overlying backfill.

In the course of the field experiment in Stripa, laboratory tests were conducted to determine the relationship between the water uptake and the swelling pressure of confined, initially non-saturated highly compacted bentonite (6). This study indicated that the swelling

pressure is a linear function of the degree of saturation, which suggested that a relevant prediction of swelling pressures in the Buffer Mass Test required an estimation of the rate and degree of uniformity of the water uptake.

The swelling pressure p_{sb} below the upper zone was assumed to be slightly lower than the figure 16-18 MPa since 100 % saturation was not expected, not even in the wettest holes. Thus, the maximum swelling pressure was assumed to be about 10 MPa in the heater holes.

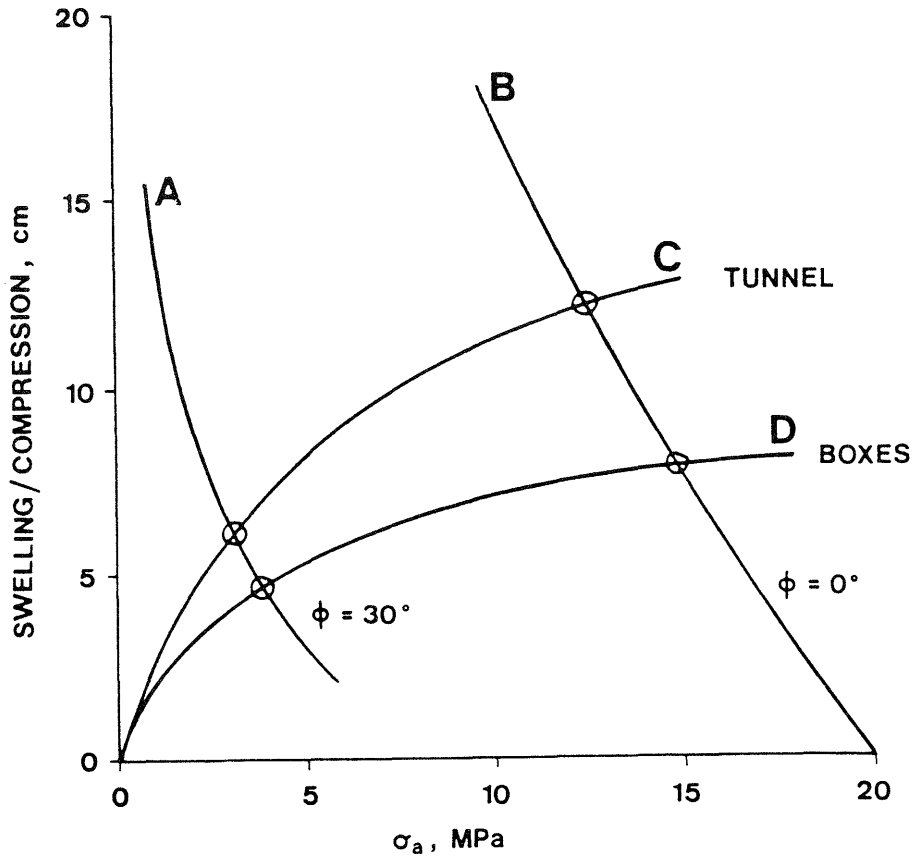

Fig 2.32. Swelling pressure σ_a versus displacement of the interface between the compacted bentonite and the overlying backfill at 0 and 30^0 wall friction angles. Curves A) and B) show the influence of the expansion of compacted bentonite on the swelling pressure while curves C) and D) show the influence of the swelling pressure on the compression of the sand/bentonite.

2.3.1.2 Water uptake

The exact physical nature of the water uptake in bentonite is not known. However, laboratory tests have shown that the water uptake under isothermal conditions can be approximated as a diffusion process with water content gradients as driving forces (3). The differential equation will thus be:

$$\frac{\delta w}{\delta t} = D \nabla^2 w$$

where w = water content
t = time
D = "diffusion coefficient"

The rate of water migration and distribution was determined by using the finite element method as in the case of the heat flow analyses. The main difficulty in predicting the moistening was the lack of empirical data concerning the diffusion process and the limited information of the exact nature of water transfer from the rock to the strongly water-absorbing clay. Thus, it was not known initially if water was going to enter the bentonite only from a few wide joints and fractures or whether it would migrate through a large number of narrow fissures, in which case it should be available all over the bentonite/rock interface. Because of these uncertainties no particular water distribution pattern was ascribed to the individual heater holes or to the tunnel. Instead, a number of characteristic cases were considered to make it possible to estimate the time required to reach various degrees of saturation and corresponding swelling pressures. Knowing the actual water distribution at the termination of the tests it would also be possible to identify the major mechanisms of water transfer from rock to bentonite.

2.3.1.3 FEM analyses of water uptake for estimation of swelling pressures

The tunnel and heater holes were considered separately, plane elements being used for the tunnel and axi-symmetric ones for the holes. The element mesh patterns are shown in Figs 2.33 and 2.34. The hydraulic interaction between the bentonite and the rock was simulated by ascribing a constant water content equal to that at full saturation to the nodes of the mesh where water transfer was allowed for, i.e. at the fracture openings or fissured zones. This model requires that there is enough water available at these water inlets, which means that the capacity of the rock to give off water must be at least as high as the capacity of the buffer material to absorb water.

Heater holes

The water uptake calculations for the heater holes were made by using the FEM programme FEMTEMP II, while the calculations for the tunnel were made using the program ENERGY. Both originate from the CHALMFEM system which is available at the Gothenburg Computer Centre.

The laboratory-derived diffusion coefficient $D = 4 \times 10^{-10}$ m^2/s was used in all the calculations. The theoretical, ultimate water content corresponding to 100 % saturation would be 20 % in the confined bentonite while its initial water content in deposition holes no 1 , 2 and 5 was 13 % and 10 % in the other three holes. As shown earlier in the text a displacement of the interface between the highly compacted bentonite and the overlying backfill is expected, the associated change in density at the interface at full saturation of the bentonite being a drop from 2.1 t/m^3 to about 1.9 t/m^3. This corresponds to an increase of the water content from about 20 % to approximately 35 %, provided that the displacement is 6 cm as predicted for the two inner holes.

Three cases, all assuming an initial water content of 13 %, were considered, the first one implying that water is available over the entire boundary. Fig 2.35 shows the water content versus the distance from the heater at different times after onset of the water uptake. Practically complete water saturation, i.e. $S_r \geq 95$ %, is expected after about 2 years under the given conditions.

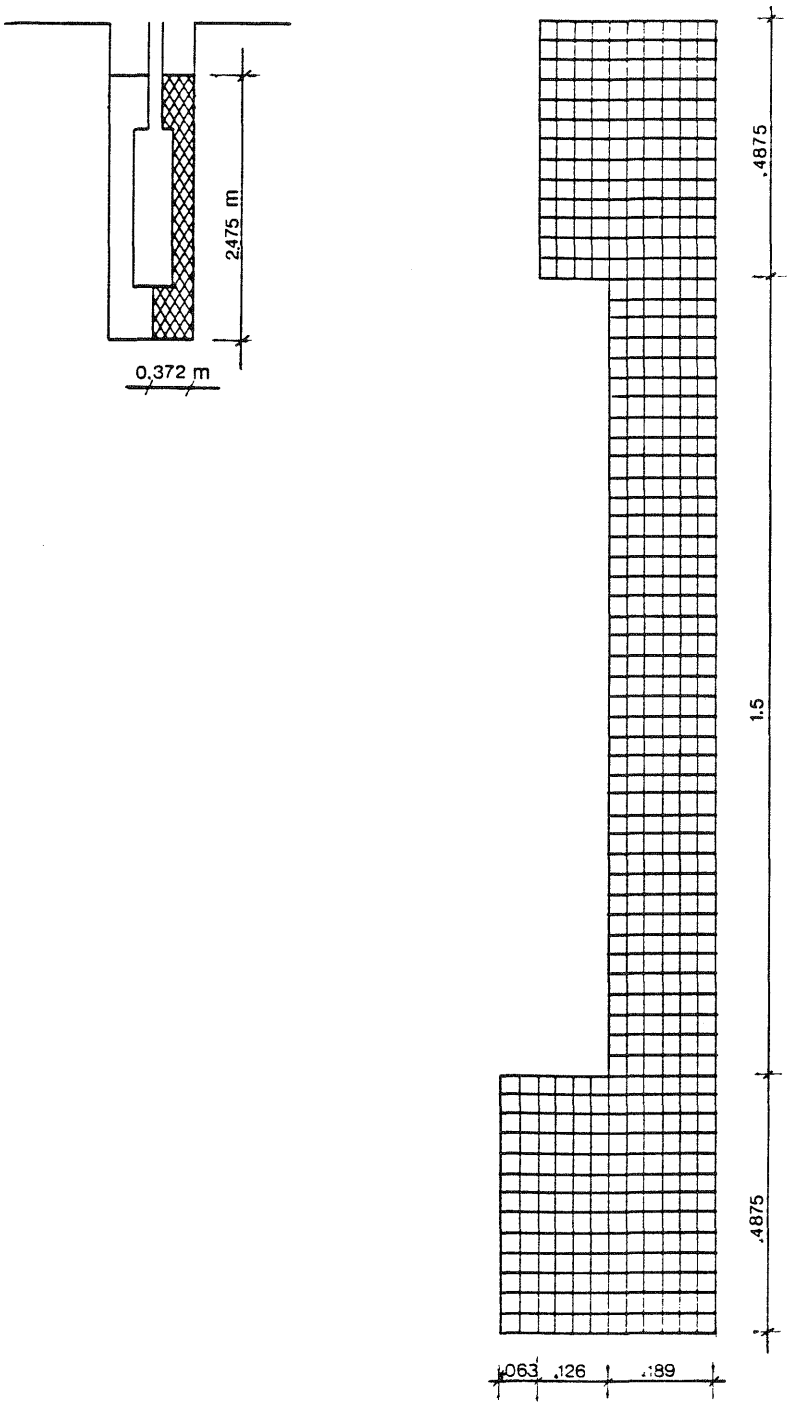

Fig 2.33. Axi-symmetric element mesh of the compacted bentonite in the heater holes

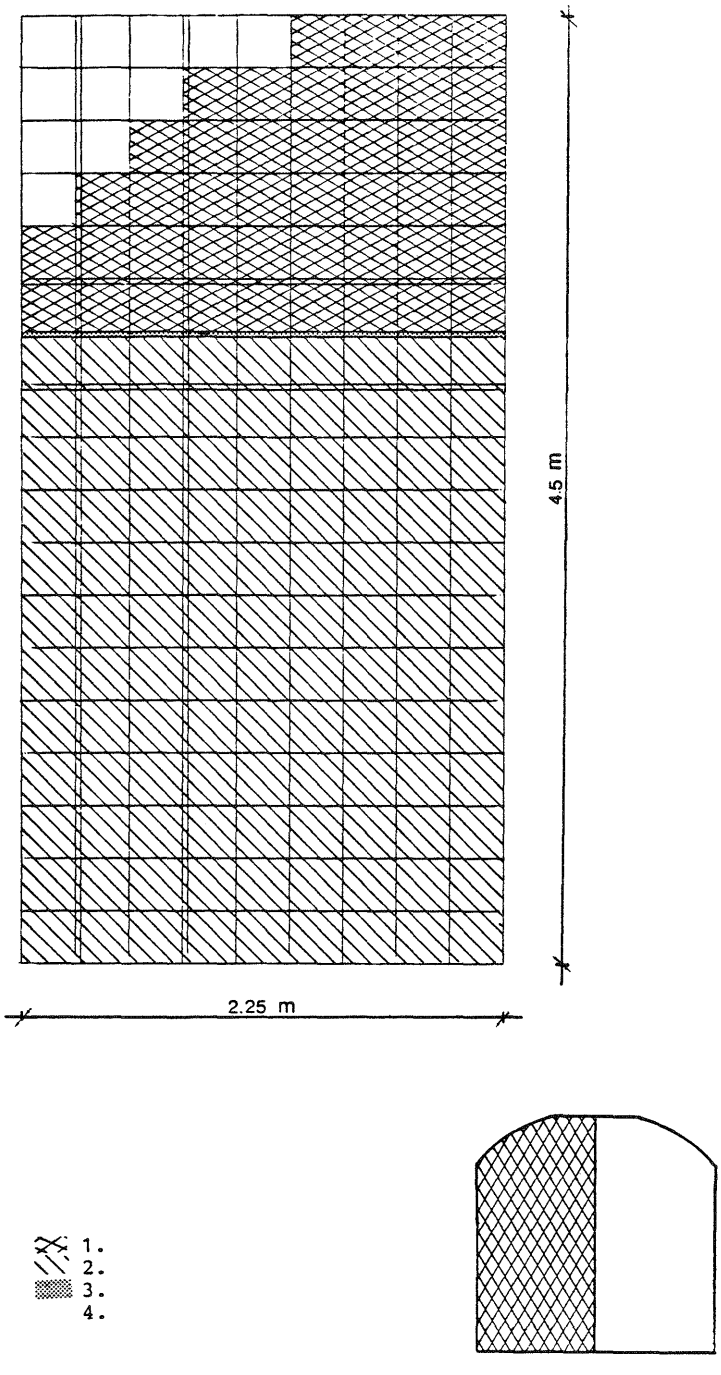

Fig 2.34. Property areas of the tunnel element mesh
1 blown sand/bentonite
2 compacted sand/bentonite
3 contact zone
4 rock

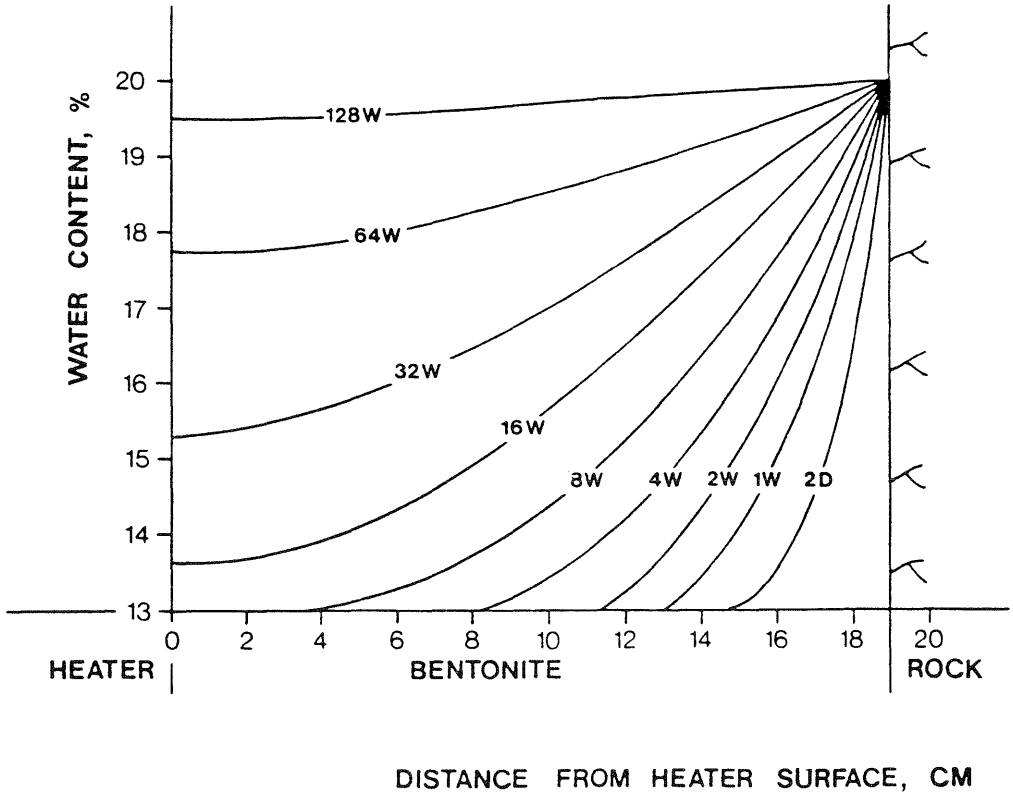

Fig 2.35. The diffusion-type water uptake and distribution at mid-height heaters at uniform access to water over the rock surface. Isothermal conditions. D represents days, and W weeks

This case of uniform access to water over the entire periphery of the hole should be perfectly valid at the beginning of the tests in holes no 1, 2 and 5 because of the water-filled slot between the bentonite and the rock. Here, the moistening of the rock was predicted to take place with simultaneous rapid swelling and build-up of a uniformly distributed swelling pressure. Later, the geometry of the water-bearing structures would become decisive of the uptake rate and thus of the magnitude and distribution of the swelling pressure. A reasonable prediction concerning holes no 1, 2 and 5 was therefore that a uniform pressure of 1-3 MPa was expected to be built up in the first few months, after which further water uptake would lead to a p_{s_a} -value of 3 MPa and a p_{s_b} -value of 10 MPa in about 2 years, implying that water would still be available over the entire rock/bentonite interface.

The second case implied that water would be available only in one water-bearing zone of fractured rock. The zone was assumed to be perpendicular to the axis of the heater hole and to have a vertical extension of 3.75 cm (one element). The calculated water content after 2 months and 4.5 years, respectively, is shown in Figs 2.36 and 2.37, which demonstrate that this fracture-poor rock model yields an extremely slow moistening. Thus, after 2 months only insignificant amounts of water would be absorbed, causing a local swelling pressure of a few MPa at maximum. Complete saturation would require about 450 years. It should be mentioned that if the fractured zone is replaced by one single joint or fracture with a typical aperture of 0.1 - 0.5 mm, the process would be even slower.

The third case was characterized by a rather fractured rock of the type represented by heater holes no 1, 2 and 5. The model implies that water is available at the top and base of the hole and at a few zones of fractured rock. Figs 2.38 and 2.39 illustrate the moistening after 2 months and 4.5 years, respectively. Complete saturation will require about 20 years but already after 4.5 years all parts of the bentonite have reacted and produce swelling pressures ranging between 3 and 10 MPa. After 2-3 years, the swelling pressure ranges between about 1 and 10 MPa, the highest value being developed at the base of the hole. This case as well as the previous one and various versions of these two water-deficient models would theoretically be applicable to any of the heater holes except for the first few months of water uptake in holes no 1, 2 and 5 as pointed out earlier in the text.

Tunnel backfill

As to the tunnel backfill the input data for the FEM calculation are given in Table 2:12. The diffusion coefficients of the buffer materials were derived from laboratory studies, while that of the

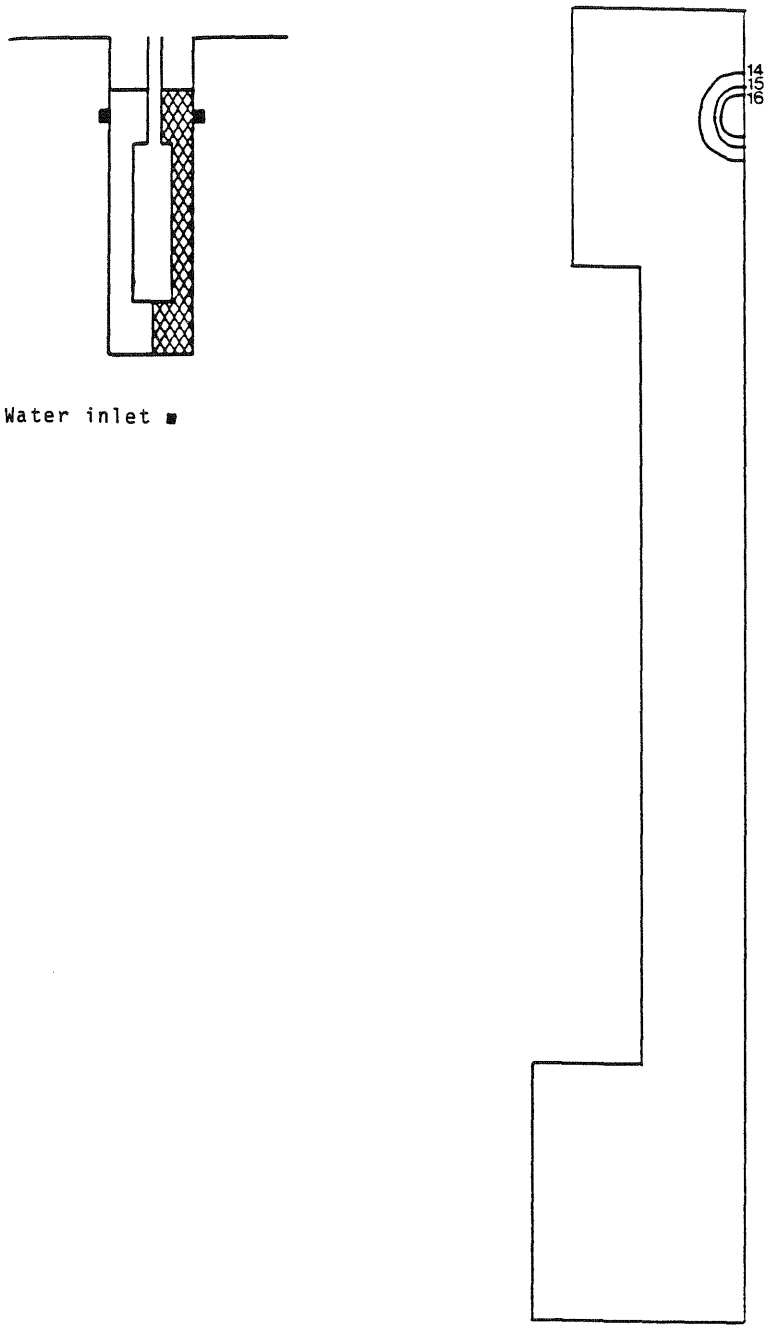

Fig 2.36. Water content distribution in percent 2 months after the beginning of the water uptake from a single water-bearing zone. Isothermal conditions

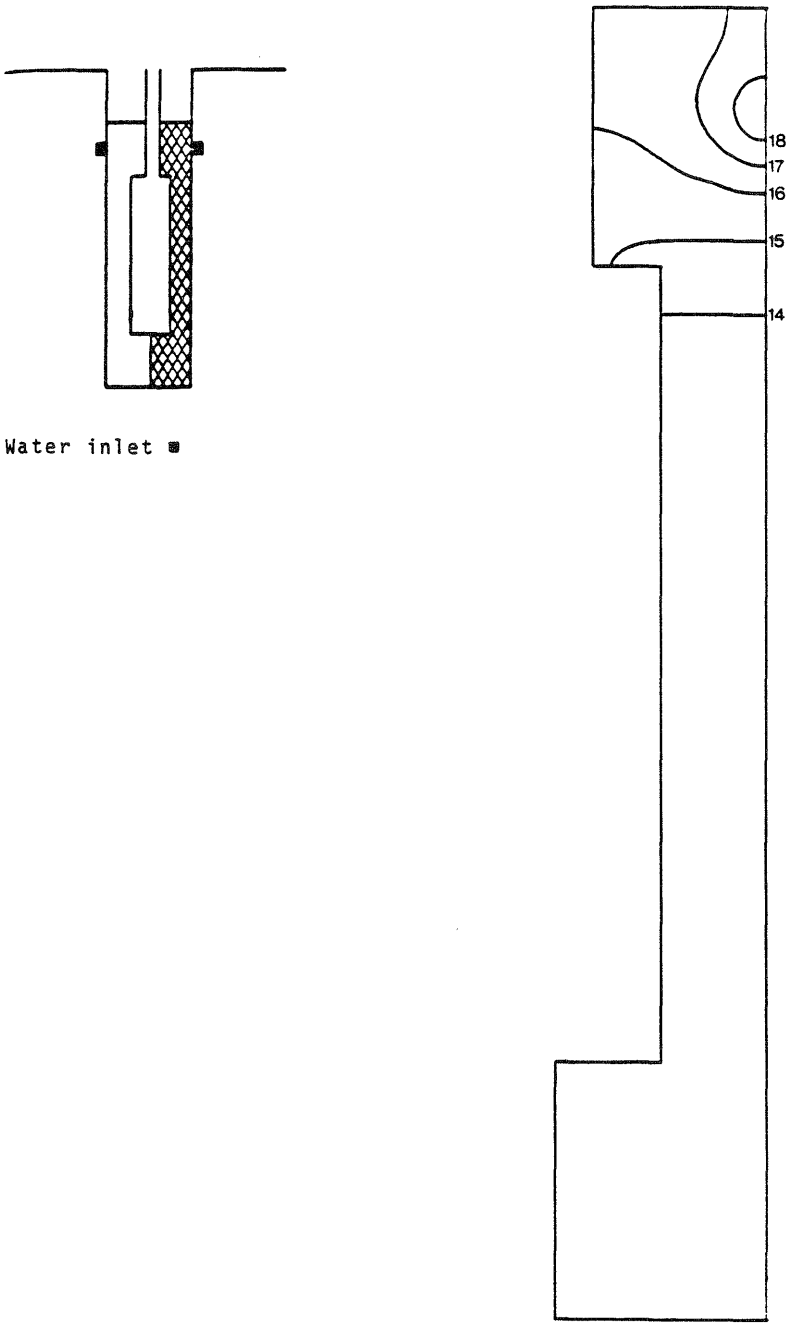

Fig 2.37. Water content distribution in percent 4.5 years after the beginning of the water uptake from a single water-bearing zone. Isothermal conditions

contact zone between the upper backfill with 20 % bentonite and the lower with 10 % bentonite had to be chosen so as to eliminate false, computer-generated water uptake in the lower part to more than 100 % water content.

Table 2:13. Parameters of the components used for the prediction of the water uptake; w_o = initial water content w_s = water content at saturation

Property area		D m^2/s	w_o %	w_s %
1	sand/bent 80/20	$1.0 \cdot 10^{-8}$	15	36
2	sand/bent 90/10	$1.0 \cdot 10^{-8}$	10	17
3	contact zone	$1.0 \cdot 10^{-10}$	15	36
4	rock	$1.0 \cdot 10^{-50}$	-	-

The same difficulty appeared in the prediction of water uptake in the tunnel as in the case of the heater holes. Thus, the number and distribution of water-bearing structures were largely unknown. Still, considering the water migration as a diffusion process and disregarding the influence of thermal gradients, a number of hydrological cases were analyzed for correlation with the results of the water content determination at the termination of the test, rather than to predict the moistening and the associated swelling pressures.

Two basic cases were analyzed in detail, the first one implying unlimited access to water over the entire rock/backfill interface. Fig 2.40 shows the result of the FEM calculation for 10 weeks after the beginning of the water uptake. We see that the water content of the backfill has increased within a distance of somewhat less than 1 m from the rock/backfill interface, while this distance has increased to about 1.5 m after 1 year according to the same model (Fig 2.41). Slightly more than 5 years after the test start, practically all of the backfill should be saturated (Fig 2.42) and the swelling pressure

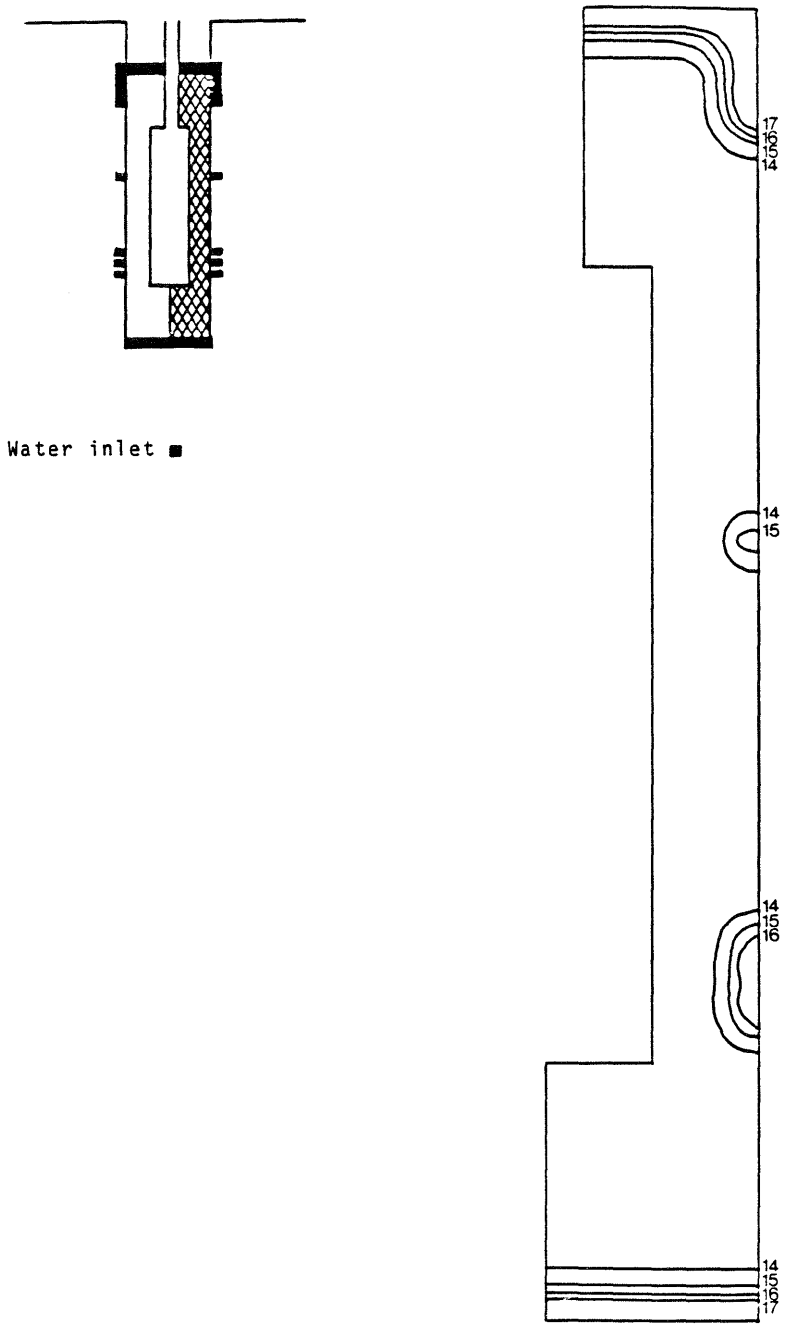

Fig 2.38. Water content distribution in percent 2 months after the beginning of the water uptake in rock with several water-bearing zones. Isothermal conditions

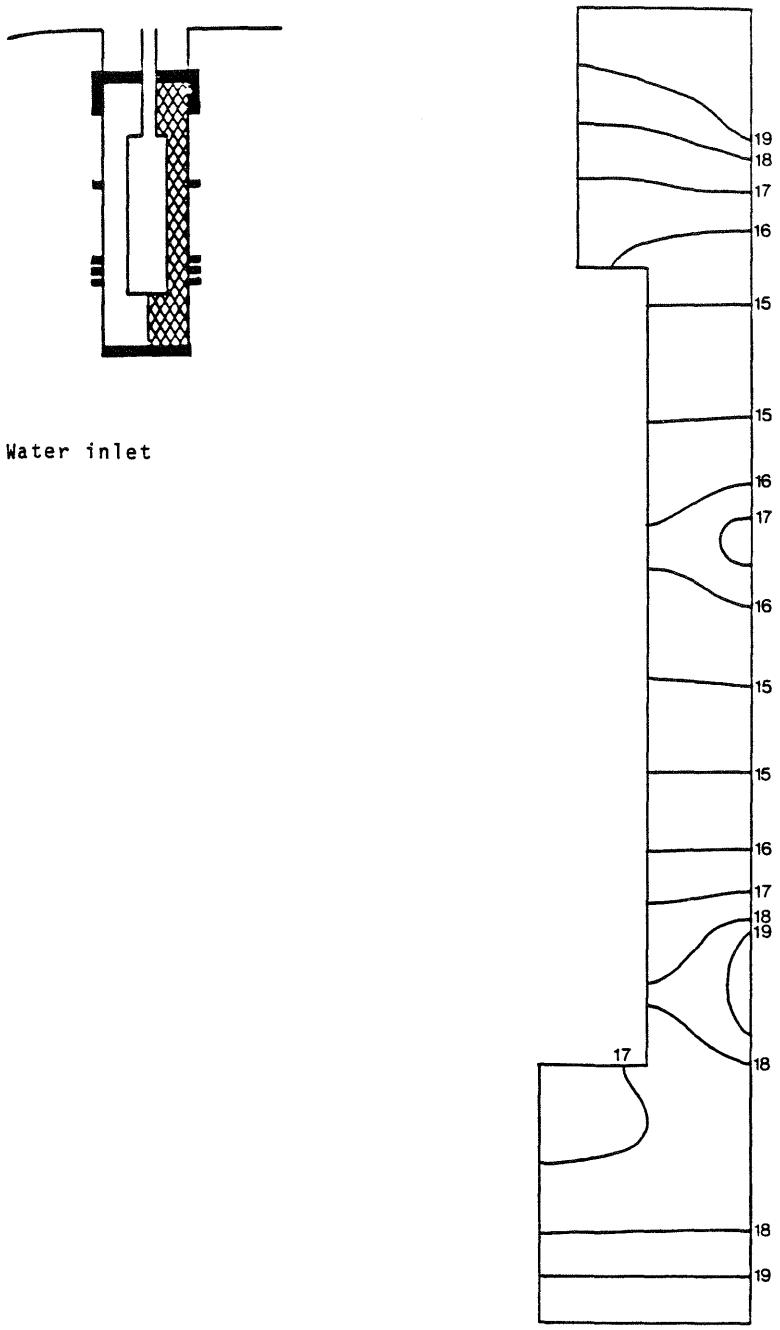

Fig 2.39. Water content distribution in percent 4.5 years after the beginning of the water uptake in rock with several water-bearing zones. Isothermal conditions

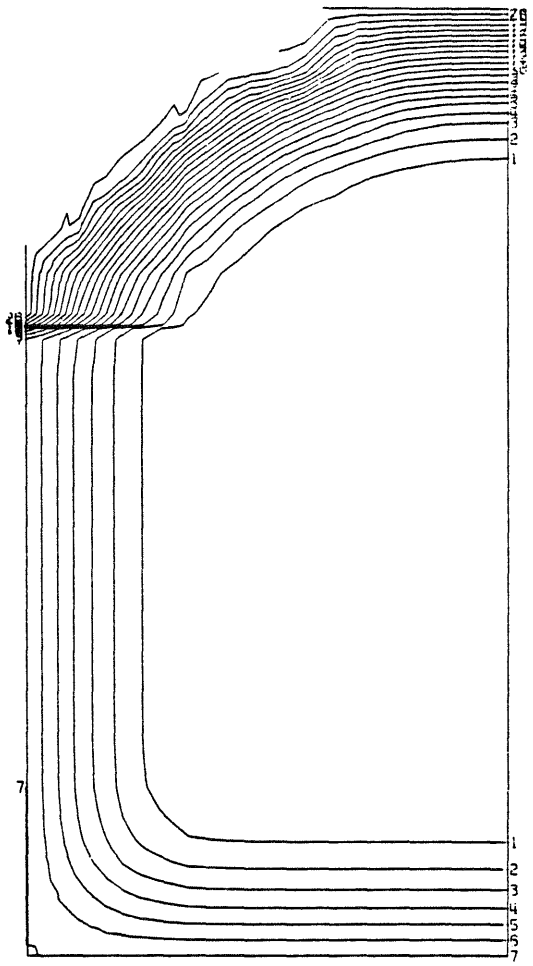

LB 150A WATER UPTAKE IN TUNNEL IN %

TIME ~10 WEEKS

ISO-LINE NO	ISO-LINE LEVEL	EQUI-DISTANCE
1	1.0000	1.0000
20	20.0000	

MAX VALUE 20.9369
MIN VALUE -0.0011

Fig 2.40. Water content increase in the tunnel after 10 weeks. Water available from the entire rock surface. Isothermal conditions

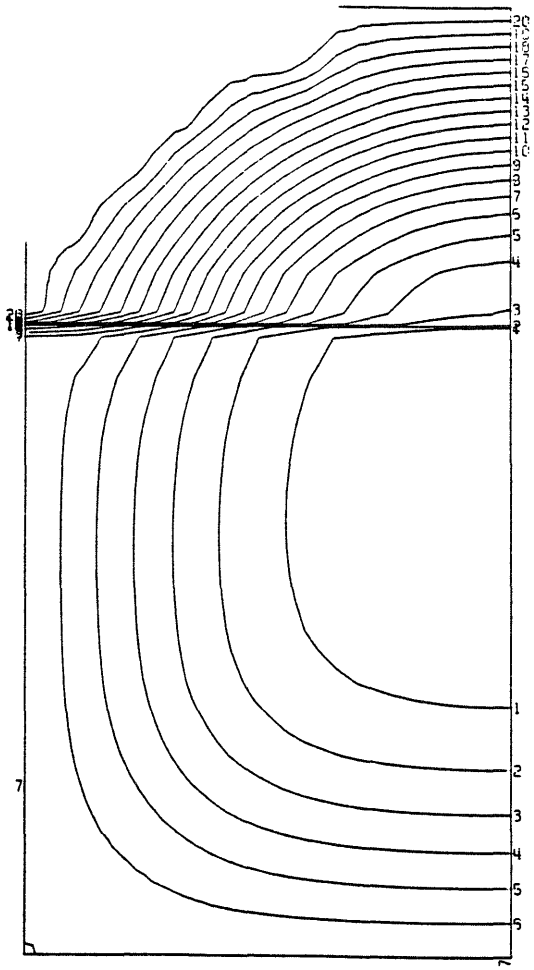

LB 150A WATER UPTAKE IN TUNNEL IN %

TIME ~1 YEAR

ISO-LINE NO	ISO-LINE LEVEL	EQUI-DISTANCE
1	1.0000	1.0000
20	20.0000	

MAX VALUE 20.9830
MIN VALUE -0.0011

Fig 2.41. Water content increase in the tunnel after 1 year. Water available from the entire rock surface. Isothermal conditions

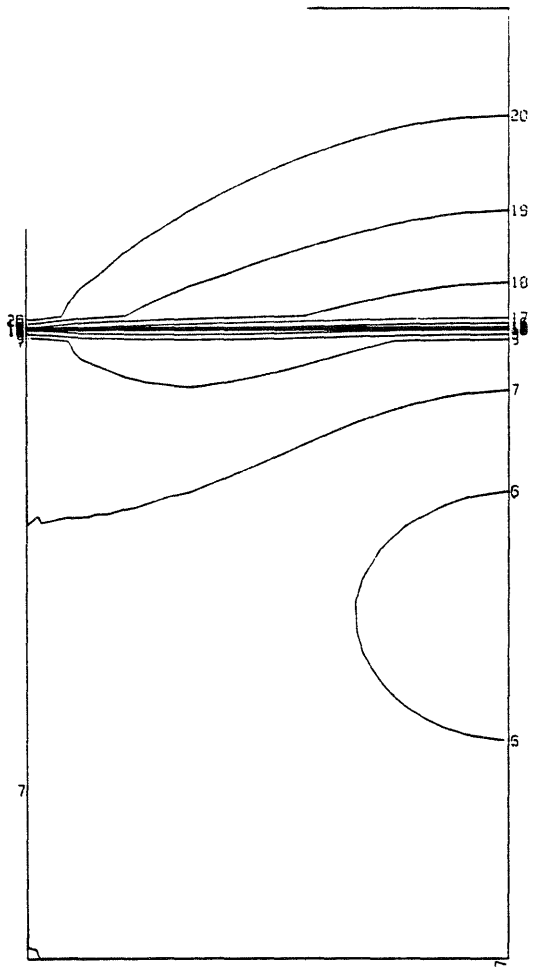

LB 150A WATER UPTAKE IN TUNNEL IN %

TIME ~5.3 YEARS

ISO-LINE NO	ISO-LINE LEVEL	EQUI-DISTANCE
1	1.0000	1.0000
20	20.0000	

MAX VALUE 20.9963
MIN VALUE -0-0011

Fig 2.42. Water content increase in the tunnel after 5.3 years. Water available from the entire rock surface. Isothermal conditions

should then be almost fully developed. According to the laboratory-derived data (cf. Volume I, Chapter 4.1.4.5) this pressure, which refers to complete saturation, is expected to be of the order of 0.05-0.15 MPa for the lower backfill and about 0.05-0.1 MPa for the less dense upper backfill with a higher content of bentonite. Slightly lower values are expected after about 3 years, which was the actual duration of the backfill test.

The second case implies access to water from four approximately 1.7 m wide zones as well as in five 25 cm wide ones, the location of these zones being taken rather arbitrarily. Fig 2.43 illustrates the geometry of these hydraulically active zones and the calculated increase in water content after 10 months. The corresponding increase after 4.7 years is shown in Fig 2.44. We see that large parts of the lower backfill would still not be saturated at the rock boundary after almost five years, indicating that the swelling pressure would vary from a few tens of kilopascals to 0.15 MPa over the rock/backfill interface at the end of the Buffer Mass Test. After one to two years the swelling pressure would only be detectable locally. In the upper backfill, on the other hand, it would be almost uniformly distributed already after about one year with the given geometry. The magnitude of this pressure is expected to be less than 0.05 MPa in this period of time.

The two considered cases yield theoretical water uptake rates that are illustrated in Fig 2.45 for the backfill with 10 % bentonite. The curve "water available" corresponds to the inflow rate from the rock that was deduced on the basis of the LBL "Macropermeability Test" as well as on the BMT field determinations. As pointed out earlier (Volume I, Chapter 3.5.2.1) the inflow rate was probably almost twice as high, which means that the water uptake according to the upper curve would not exceed the ability of the rock to release water.

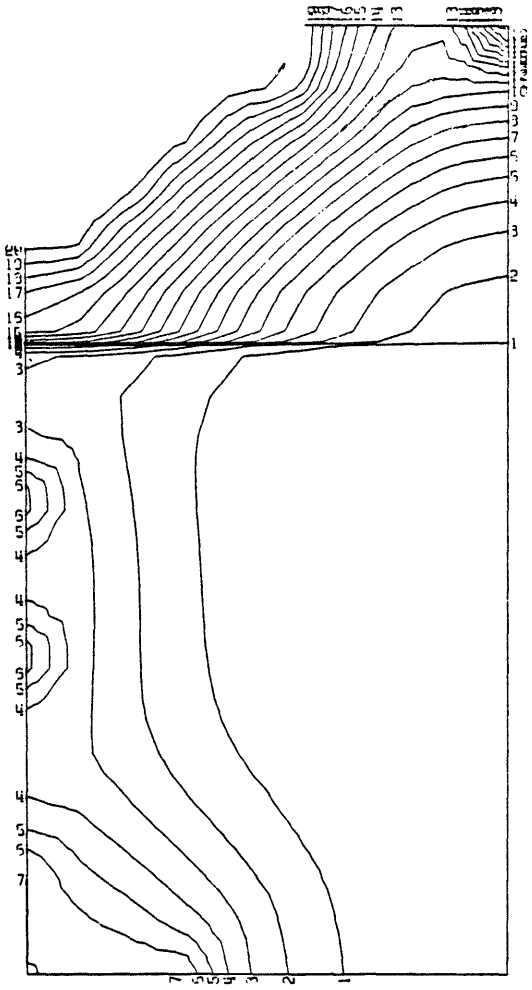

LB 150A WATER UPTAKE IN TUNNEL IN %

TIME ~314 DAYS

ISO-LINE NO	ISO-LINE LEVEL	EQUI-DISTANCE
1	1.0000	1.0000
20	20.0000	

MAX VALUE 20.9761
MIN VALUE -0.0011

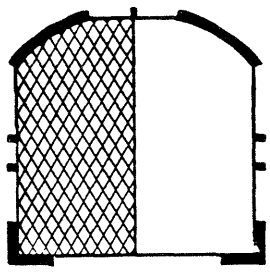

Fig 2.43. Water content increase in the tunnel after 10 months. Black zones in the schematic section represent water inlets

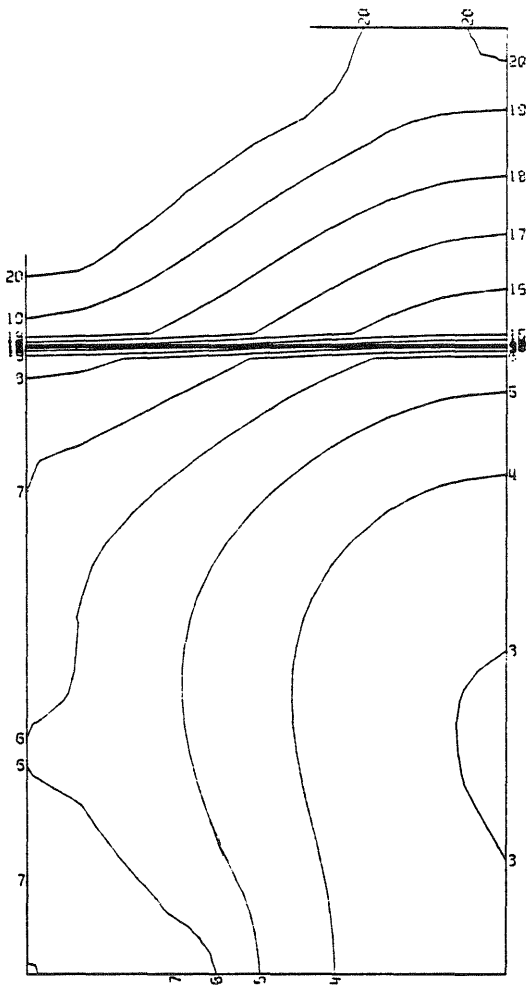

LB 150A WATER UPTAKE IN TUNNEL IN %

TIME ~4.7 YEARS

ISO-LINE NO	ISO-LINE LEVEL	EQUI-DISTANCE
1	1.0000	1.0000
20	20.0000	

MAX VALUE 20.9941
MIN VALUE -0.0011

Fig 2.44. Water content increase in the tunnel after 4.7 years. Water available as in Fig 2.43

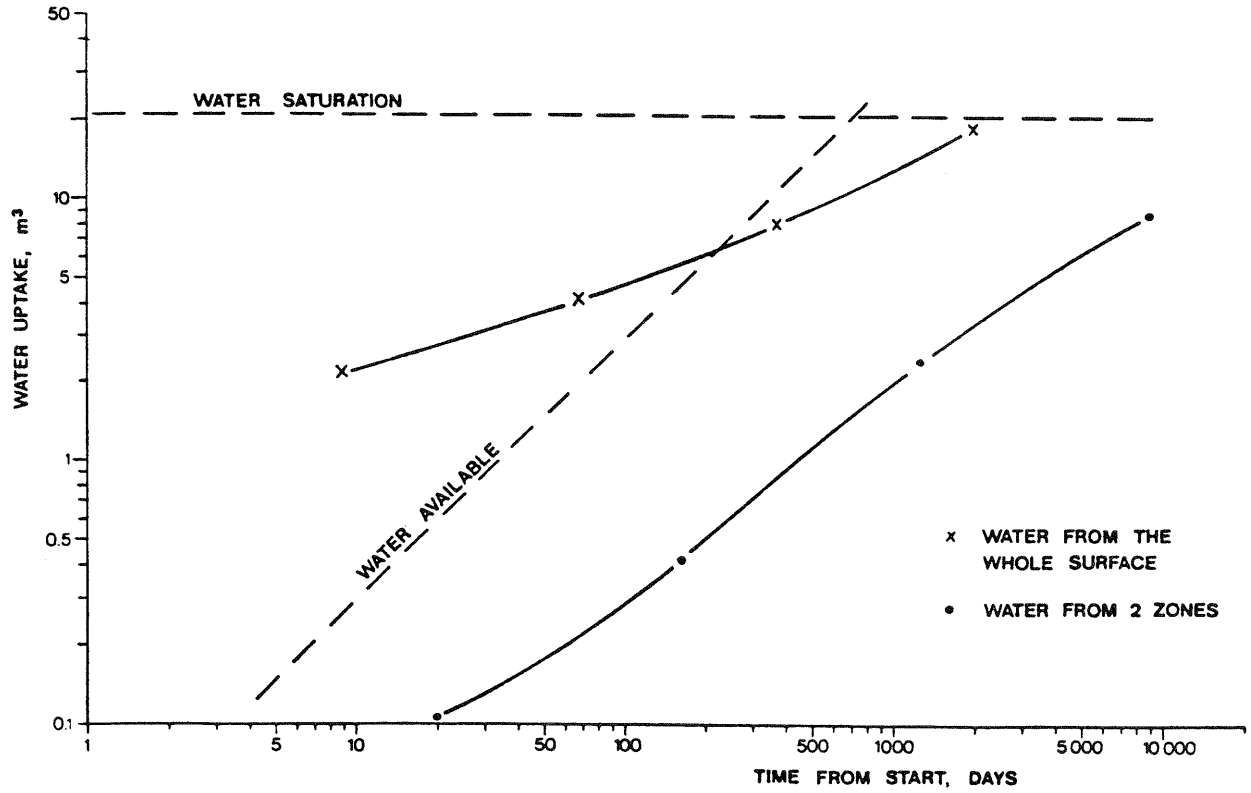

Fig 2.45. Predicted amount of water taken up by the 10/90 buffer material in the tunnel

The influence of the distribution and discharge capacity of the water-bearing zones in the rock is amply demonstrated by the second case considered in the preceding text. This matter was identified as one of major importance and an attempt was made to calculate the rate of water uptake in backfill with 10 percent bentonite as a function of the aperture of a contacting water-bearing rock zone or fracture. The result is illustrated by the finding that the required time for absorption of one and the same amount of water by the backfill is doubled when the aperture is reduced from 2.5 to 0.25 mm.

2.3.2 Results

The swelling pressures were evaluated as the difference between total pressures determined by use of Gloetzl cells, and the separately measured water pressures. The large majority of the cells worked well in the first year, while the number of cell failures increased considerably later in the test. The recording system needed to be adjusted and components replaced a few times but in general the system worked satisfactorily and yielded the required data.

Since the water heads were usually low in relation to the swelling pressures, the first-mentioned are neglected in the presentation of the results from the heater hole tests. As to the tunnel backfill the water and swelling pressures were of the same order of magnitude and the water pressure situation therefore needs consideration. The matter will be discussed in detail in Chapter 2.4.

As in the preceding chapters, holes no 1, 2 and 5 form the "wet" group which is discussed first.

2.3.2.1 Heater hole no 1, 600 and 1400 W

The wet conditions in holes no 1 and 2 and particularly the initial state with a water-filled slot, suggested a rather rapid development of a uniform swelling pressure. This turned out to be the case as shown by the diagram in Fig 2.46. Thus, the swelling pressure over the central 1.5 m high part of the hole (cells no 5, 6, 7, 8, 9, 10) increased almost linearly and at approximately the same rate, the swelling pressure ranging between 5 and 6.5 MPa 2.4 years after the start of the 600 W test. In the same period of time, the pressure at the base of the hole (cell no 1) went up to 3 MPa, of which about 0.7 MPa refers to water pressure. Unfortunately, this swelling pressure reading is inadequate because of incorrect gauge mounting.

The uniform pressure build-up over the central part of the hole also in the later phase of the 600 W period must have been caused by a very uniform water uptake. This means that the location and water-bearing capacity of individual joints and fractures were of minor importance. The degree of water saturation that corresponds to the measured swelling pressures, at the end of the 600 W period was estimated at 70-80 %. An interesting observation is that the swelling pressure at the interface between the highly compacted bentonite and the overlying, compressible backfill is almost exactly the predicted value at a high degree of saturation and after expansion to yield force equilibrium (cf. Chapter 2.3.1.1).

The power was increased to 1400 W* after 29 months which increased the pressure by 0.5-1 MPa in the lower part of the hole (cells no 5, 6, 8 and 9) while it caused a slight drop in the upper, less temperature-affected part of the hole (cells no 7 and 10). The increment took place in about 2 months time and was partly due to the thermal sensitivity of the pressure cells and partly to the temperature-induced expansion of the bentonite and heater. The intrinsic drop in swelling pressure of bentonite at increased temperature probably had a dominant effect in the slightly expanded, upper part of the bentonite which would explain the observed slight reduction of the pressure.

After a few months the pressure development in the lower part of the hole tended to proceed along curves which were more or less prallel to the virgin curves. The true maximum swelling pressure at the termination of the test is estimated at about 8 MPa.

---

* Actually, the power was increased to 1800 W in a three week period but had to be kept at 1400 W for the rest of the test period due to breakdown of one heater element.

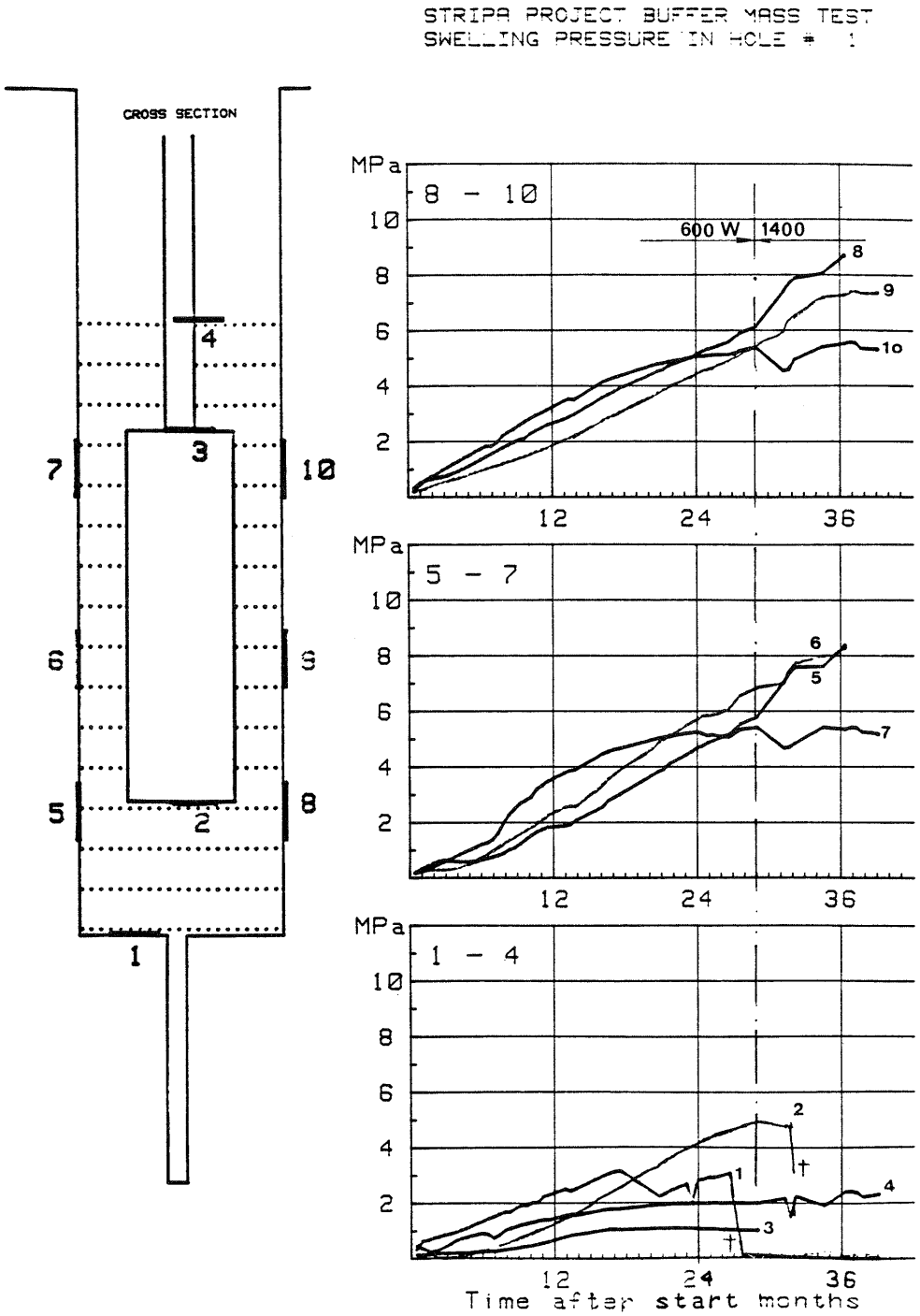

Fig 2.46. Recorded swelling pressures in heater hole no 1 (600 and 1400 W)

2.3.2.2 Heater hole no 2, 600 W

Fig 2.47 illustrates the development of swelling pressures in the wettest heater hole in the Buffer Mass Test. As expected the pressures were quite considerable and indicate a very high degree of water saturation. The reactions of the three cells located in the central part of the hole which survived until the termination of the test (cell no 5, 8 and 9) followed practically the same path throughout the test and yielded a maximum value of 10.2-11 MPa. Taking temperature effects and the water pressure of about 0.5 MPa into consideration, the true maximum swelling pressure was about 10 MPa, which was the predicted value. The drop in pressure that started after about 36 months was caused by the excavation of the overlying backfill in the hole. Cell no 6 exhibited a somewhat faster pressure build-up than the other, centrally located gauges, the pressure difference between this cell and cell no 9 on the same level being about 1.5 MPa at maximum. The pressure difference may be explained by cell deficiency as indicated by the unexpected breakdown at the moderate pressure 7.7 MPa.

Cells no 7 and 10 yielded lower pressures than the cells located deeper down in the hole. This is logically explained by the expected tendency of the top part of the bentonite overpack to swell as indicated by the low recorded pressure 2 MPa (cell no 4) at the interface between the highly compacted bentonite and the overlying, compressible sand/bentonite backfill. It is interesting to notice that the pressure at this interface and the time/stress path are almost identical in heater holes no 1 and 2. This turned out to be the case also for the wet hole no 5, which suggests that the sand/bentonite served as a major water source in the wet holes.

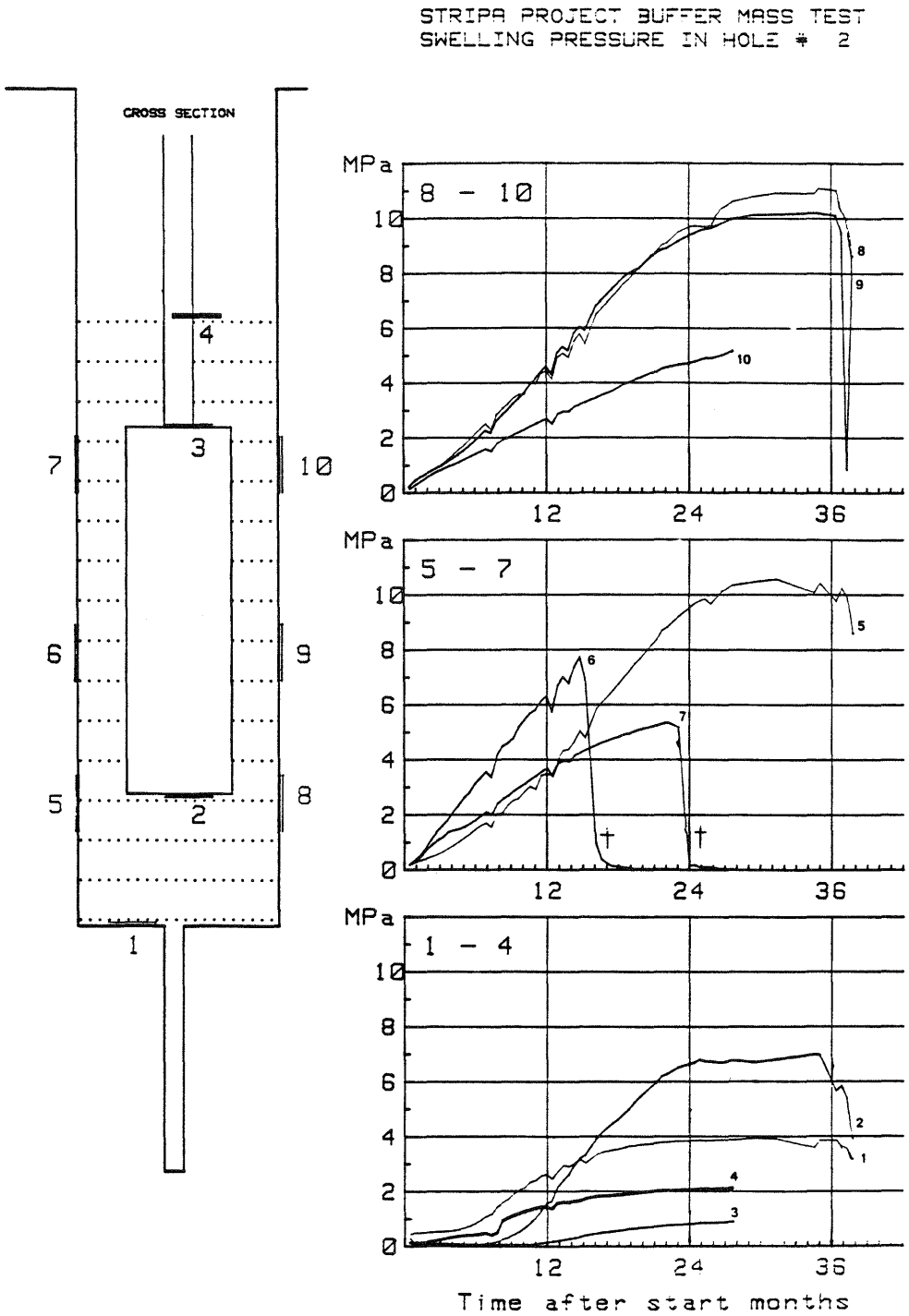

Fig 2.47. Recorded swelling pressures in heater hole no 2 (600 W)

2.3.2.3 Heater hole no 5, 600 W

Hole no 5 had a relatively high water inflow before the bentonite was applied and a rather rapid and uniform development of swelling pressures was expected. However, as demonstrated by the recordings (Fig 2.48) the pressure build-up was significantly slower than in holes no 1 and 2 which is attributed to the less wet conditions in hole no 5. Thus, the maximum pressure 5 MPa was reached late in the test in the lower part of the hole (cell no 5), the average rate of water uptake being approximately 50 % of that in holes no 1 and 2. The scattering is fairly small as in the other wet holes.

The fact that cells no 5 and 8 show a somewhat faster wetting of the lower part of the bentonite column, indicates that the base of the hole served as a major water source.

It was assumed that the swelling produced at the interface between the highly compacted bentonite and the overlying backfill would be transferred to the boxing-out and superimposed on the swelling pressure of the backfill acting on the lid. No change in the tie-rod stresses could be identified, however, which indicates that the first-mentioned pressure (about 2 MPa in cell no 4) was completely balanced by friction at the rock/backfill interface in the heater hole.

2.3.2.4 Heater hole no 3, 600 and 1200/1800 W

The water inflow measurements in this hole prior to the application of the first bentonite block set for the 600 W test indicated rather dry conditions and the development of swelling pressures also turned out to be slow as demonstrated by Fig 2.49. It is quite obvious, however, that pressure reactions appeared at a rate and uniformity that excludes the applicability of water uptake models implying only

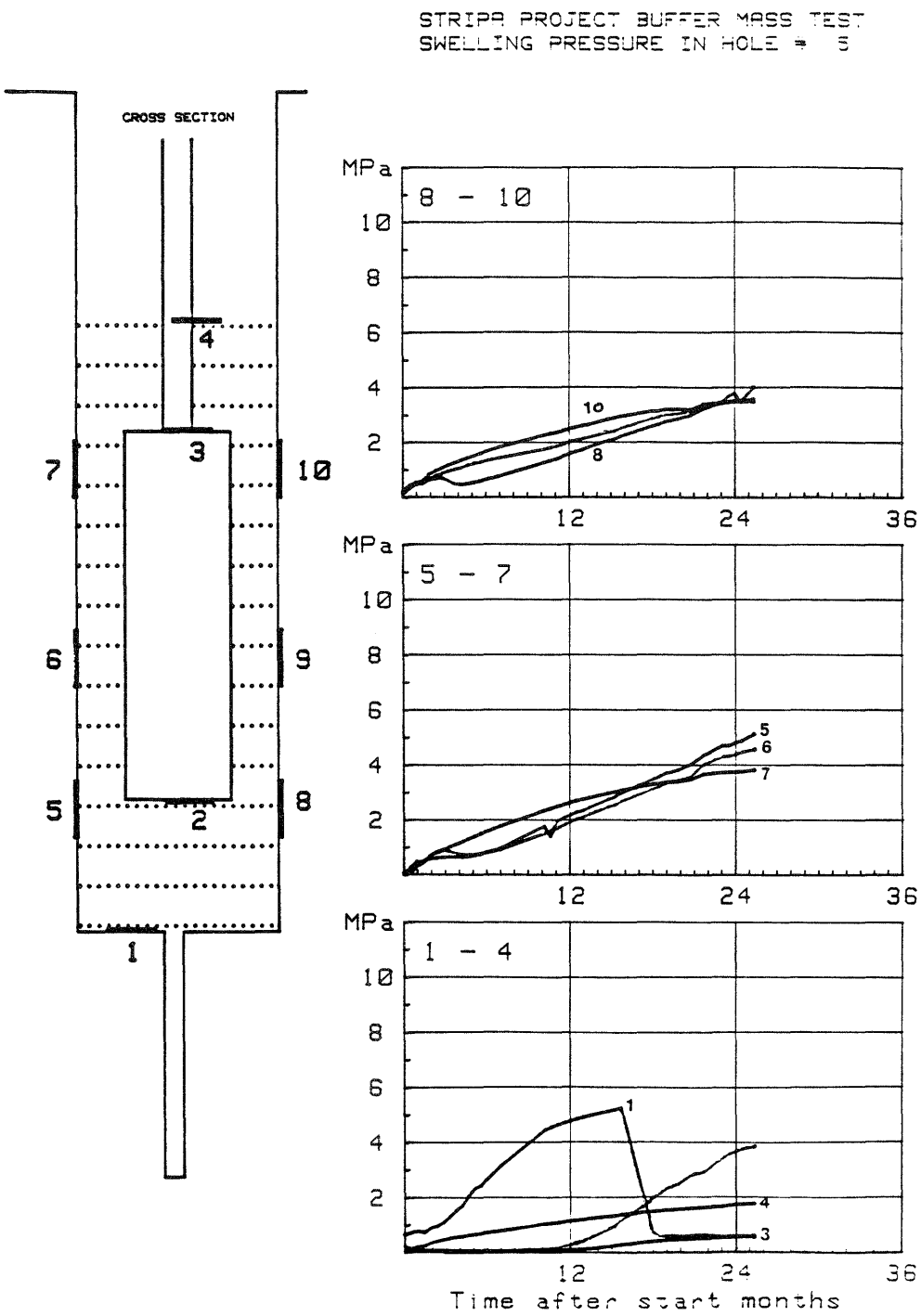

Fig 2.48. Recorded swelling pressures in heater hole no 5 (600 W)

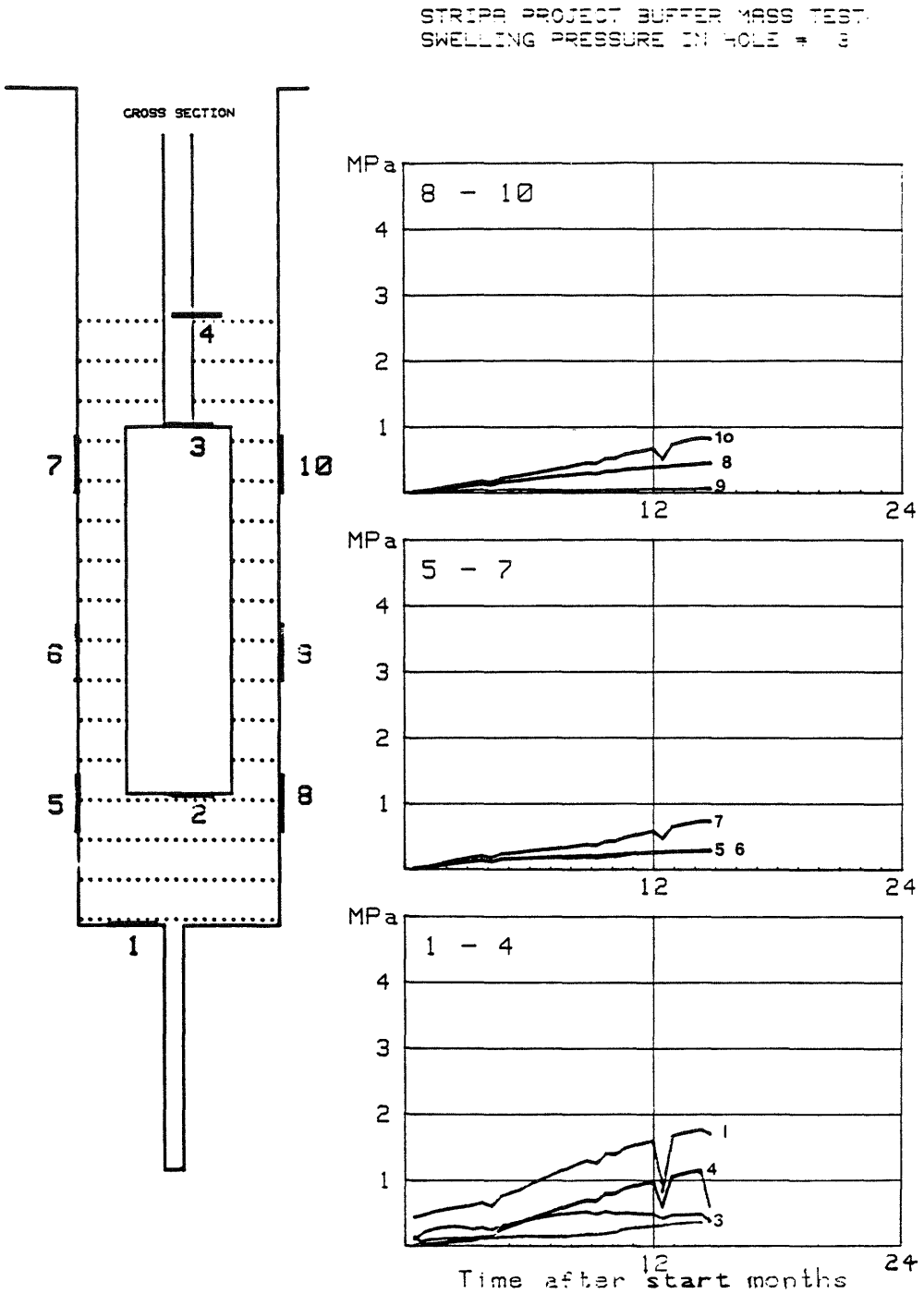

Fig 2.49. Recorded swelling pressures in heater hole no 3 (600 W)

water migration from a few discrete water-bearing zones (Figs 2.36 and 2.38). Thus, it was concluded that water must have entered the bentonite relatively uniformly over the rock/bentonite interface in the hole.

The maximum pressure recorded in hole no 3 in the 15 month test period at 600 W power was 2 MPa at the top of the heater (cell no 7 and 10), which shows that the fractured tunnel floor and the sand/-bentonite backfill in the upper part of the hole acted as major water sources.

The subsequent test at 1200 and 1800 W power showed a more rapid development of swelling pressures than in the 600 W power test (Fig 2.50). The maximum recorded value at the end of the 1200 W power test, about 7 months after test start, was 6 MPa at the base of the heater hole (cell no 1). Fairly high pressures also appeared at the lower end of the heater, i.e. 2-4 MPa (cells no 2, 5 and 8), while the value was only about 1 MPa at the bentonite/rock interface higher up in the hole (cells no 7 and 10). Unfortunately, the cell at the interface between the highly compacted bentonite and the overlying sand/bentonite backfill broke down and no conclusions could be drawn as to the water uptake from the upper end of the hole until the excavation took place. It demonstrated that the moistening in the upper part of the heater hole was also more rapid in the high-power test, indicating an increased access to water in the surrounding rock in the course of the BMT study. It should be noticed that cells no 6 and 10 were malfunctioning after about 10 months probably due to the high temperature.

The power increase from 1200 to 1800 W after about 7 months had an obvious effect on the recorded pressures. They increased about 0.5-1 MPa at the rock/bentonite interface in the lower part of the hole

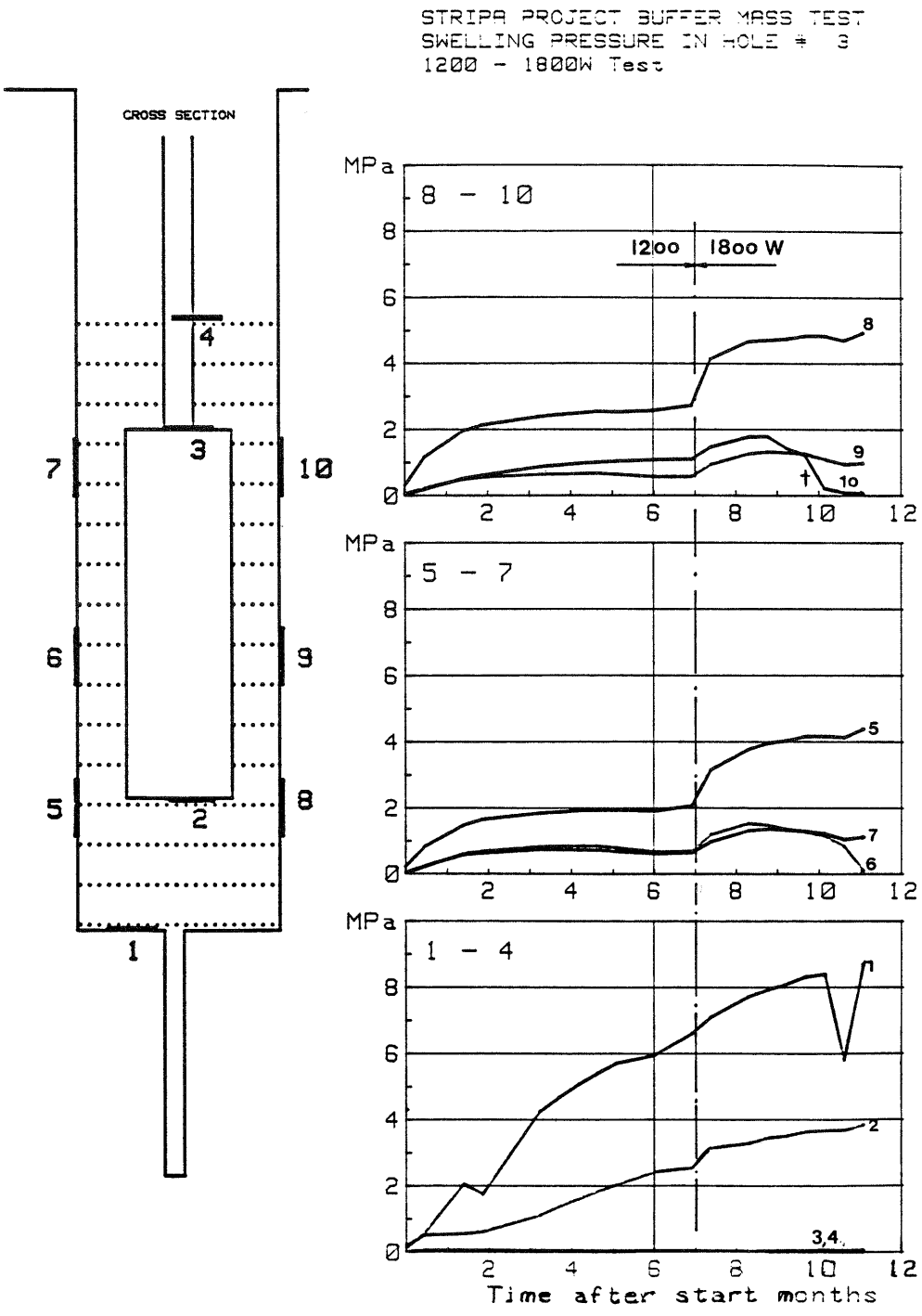

Fig 2.50. Recorded swelling pressures in heater hole no 3 (1200 and 1800 W)

(cells no 1, 5 and 8), which was partly due to the thermal sensitivity of the pressure gauges and partly to the temperature-induced expansion of the heater and the bentonite.

2.3.2.5 Heater hole no 4

The hydrological conditions in heater hole no 4 were concluded to be similar in holes no 3 and 4, which suggested a slow development of swelling pressures also in hole no 4. This was evidenced by the measurements as demonstrated by Fig 2.51.

The maximum pressure in hole no 4 at the end of the 10 month test period was 0.8 MPa (cell no 4) at the interface between the highly compacted bentonite and the overlying sand/bentonite backfill. This backfill and probably also the richly water-bearing rock at the upper part of the hole served as the main water source. The base of the hole was also furnished with much water emanating from the old LBL hole R9 as demonstrated by the pressure curves representing cells no 1 and 2. The water pressure here was higher than 600 kPa in the last 6 months and this pressure therefore gave the largest contribution to the recorded total pressures.

Although the pressures over the larger part of the rock/bentonite interface were not very significant they indicate a slight, uniformly distributed uptake of water at this interface. Since the pressure build-up seemed to cease after about half a year, it was concluded that the major part of the pressure-producing moistening originated from an internal heat-induced internal redistribution of water. As shown later in the report this turned out to be the case.

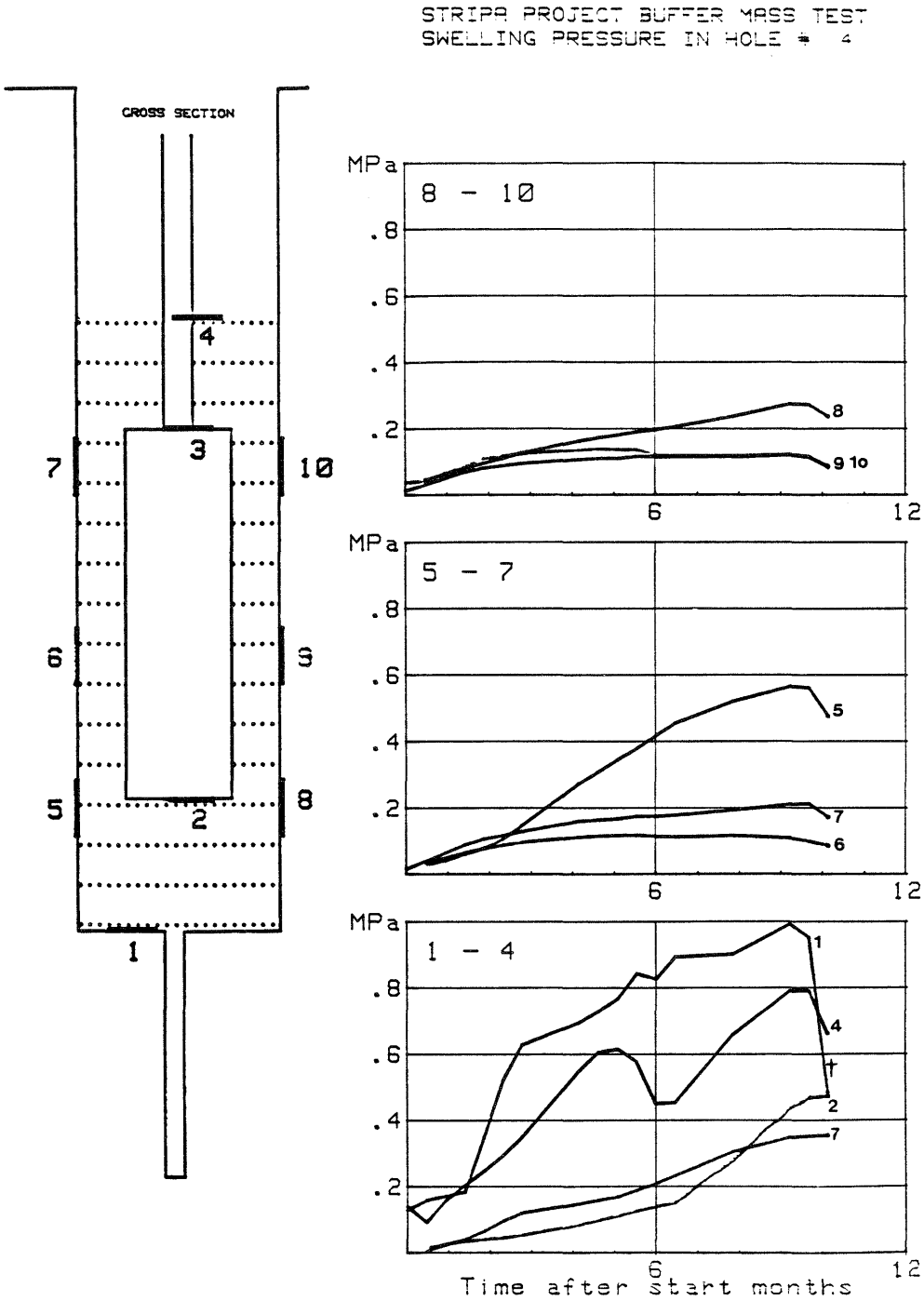

Fig 2.51. Recorded swelling pressures in heater hole no 4 (600 W)

2.3.2.6 Heater hole no 6

This hole had the smallest water inflow in the hydrological test that preceded the application of the bentonite in the six holes and the swelling pressure recording also showed a rather slow pressure build-up. It was approximately as fast as in holes no 3 and 4, however, and proceeded at an almost constant rate in the first two years indicating a uniform distribution of the water uptake from the rock (cf. Fig 2.52). The average rate of pressure increase was about one tenth of that in hole no 2.

As in the other heater holes the fractured tunnel floor and the sand/bentonite backfill in the upper part of the hole must have served as effective water sources, as concluded from the fact that cell no 4 gave a pressure value of almost 1 MPa at the termination of the test.

2.3.2.7 Tunnel backfill

It was assumed at the planning of the test that the very high water pressures in the rock measured a few meters from the tunnel periphery would be transferred to the tunnel/backfill interface in the course of the saturation of the peripheral parts of the tunnel backfill. This called for cells suited for pressures up to about 2 MPa. The accuracy of the recorded pressure reactions of such cells is about 80 kPa (cf. Volume I, Chapter 4.3.3.1) and since the fully developed swelling pressure of the tunnel backfill was not expected to exceed about 150-200 kPa, no precise information of the latter pressure was expected. The matter will be discussed in connection with the reporting of piezometric heads in the tunnel.

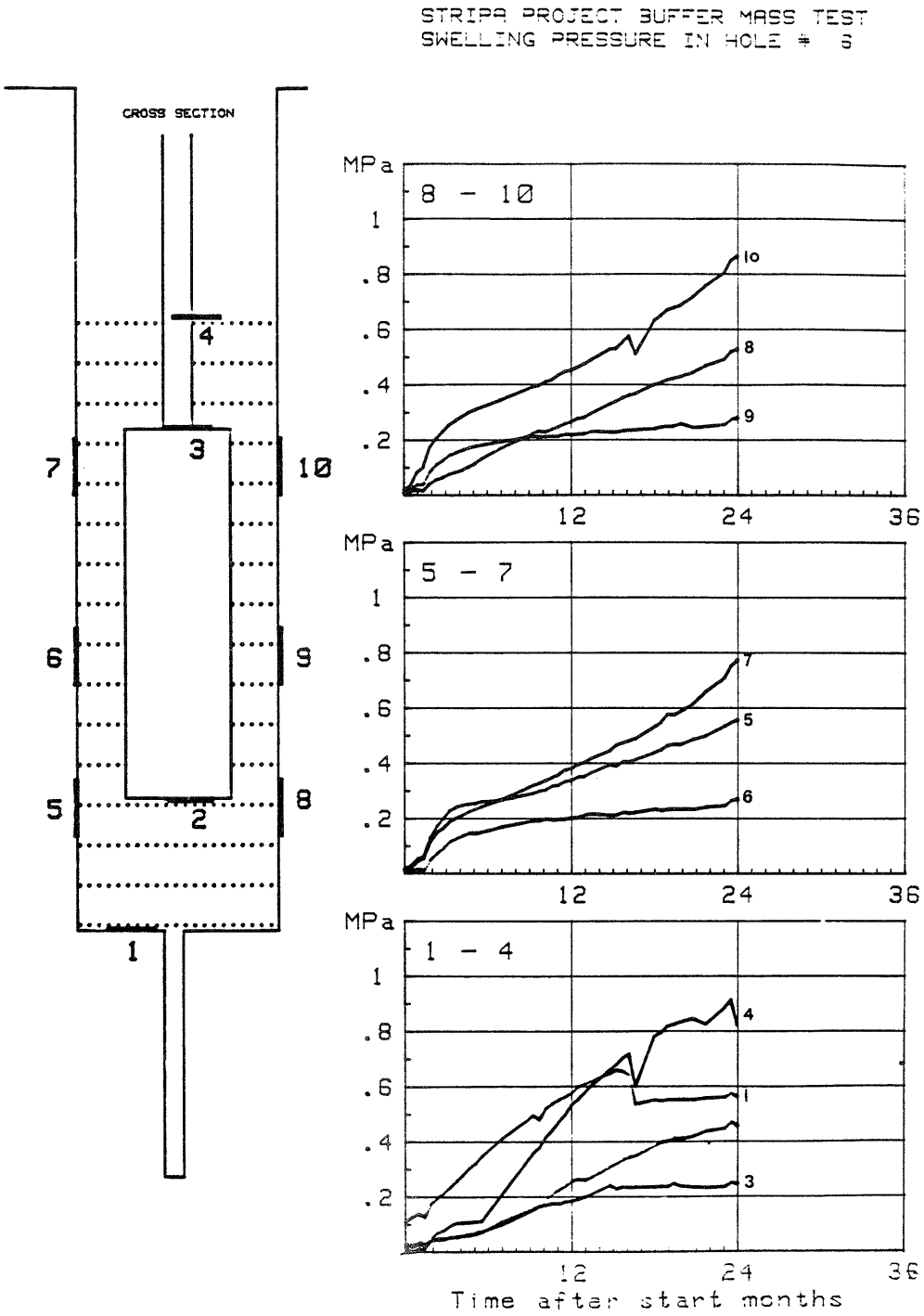

Fig 2.52. Recorded swelling pressures in heater hole no 6 (600 W)

2.3.3 Conclusion and remarks

The main conclusions from the determination of swelling pressures are the following:

1 The maximum recorded swelling pressure in the wettest heater hole agreed with the predicted value, i.e. 10 MPa

2 The vertical expansion of the upper part of the dense bentonite overpack resulted in a reduction of the swelling pressure at its upper boundary to slightly less than the expected value. The model of wall friction used in the prediction thus applies in short term tests

3 The swelling pressure appeared to be relatively uniformly developed over the rock/bentonite interface in all the holes. In one of them (no 4 , 600 W test) the pressure became constant after about half a year which indicates that the pressure may partly have resulted from an internal redistribution of pore water caused by thermal gradients. In all the other holes the steady, fairly uniform pressure increase points to a successive, uniformly distributed water uptake and this disqualifies models of the type represented by Figs 2.36 and 2.38 which imply discrete water sources

4 The sand/bentonite backfill in the upper part of the heater holes, and the fractured rock forming the tunnel floor acted as main water sources in the moistening of the highly compacted bentonite

5 Although it is concluded that the distribution and frequency of water-bearing structural features does not significantly affect the uniformity of the pressure build-up, the flow capacity of these features seems to be a determinant of the rate of water uptake. This called for a detailed study of the water uptake process in the buffer materials and of the hydrologic interaction of the rock and the buffers.

2.4 Water pressures in heater holes and tunnel

2.4.1 Predictions

Determination of the water pressure at the various rock/buffer interfaces was required for the evaluation of the effective pressure, which is equivalent to the swelling pressure. Also, the piezometric heads needed to be known for the understanding of the hydrological interaction of rock and buffer materials.

No actual predictions were made but it was expected that the high water pressures recorded in the "Macropermeability Test" would be rather rapidly transferred to the rock/buffer interface and later to the pore water of the buffers in the tunnel and in most heater holes as a result of the increasing degree of saturation. The matter is of considerable interest since such hydraulic conditions could cause flow at the interface in the axial direction of the tunnel whereby erosion and redistribution of fines in the backfill could take place and pervious passages possibly be formed.

2.4.2 Results

2.4.2.1 Heater holes

The piezometers at the base of the heater holes reacted soon after the application of the bentonite/heater units as is illustrated by Table 2:14.

Table 2:14. Piezometric heads at the base of the heater holes (kPa)

Time after start of heater no 1	1	2	3	4	5	6
2 months	710	490	-	-	-	-
5 "	750	500	30	220	300	30
0.7 "	760	495	20	645	500	10
1 year	700	430	15	630	620	15
1.5 "	775	520	20	-	490	10
2 "	780	540	-	-	485	15
2.5 "	785	500	15	-	460	0
2.8 "	660	455	20	-	-	10
3 "	745	485	-	-	-	-

The table shows that the pressures were in the range of 500-800 kPa at the base of holes no 1, 2, 4 and 5 over the major part of each heater test. This proves that the high piezometric heads which prevailed at a rather small distance from the tunnel periphery at the start of the Buffer Mass Test were largely preserved during the test. It is concluded, however, that such pressures were not operative at the base of hole no 6, while there is a suspicion that the piezometer in hole no 3 failed early in the test and that the water pressure was underestimated here. This idea is supported by the observation that the maximum total pressures appeared at the base of the hole.

An interesting observation is that the piezometric heads occasionally varied by as much as 110-120 kPa in holes no 1 and 2 in the course of the test. These changes were not related to filling or excavation operations in neighboring holes but clearly mirrored drainage activities in remote test areas, thus indicating hydrological interaction over long distances in the mine. In the other holes altered conditions in the close vicinity caused the recorded pressure changes. Thus, the pressure drop from 620 kPa to 490 kPa in hole no 5 in the time interval 1-1.5 years after the start of heater no 1 is logically explained by the excavation of the nearby hole no 4, which was left open thereafter.

Water pressures could also be measured by manometers at the interface between the tunnel floor and the concrete slab outside the bulwark but no pressures appeared here. This indicates that seepage took place along this interface and through the fractured, pervious tunnel floor so that no piezometric heads could be built up here.

2.4.2.2 Tunnel

The water pressures in the tunnel floor below the backfilled tunnel were found to be insignificant. Here, piezometers located in shallow boreholes at the lower corners of two tunnel sections (Vol I, Figs 4.40, 4.41, 4.44, 4.45) showed only a slow increase of the water pressures from the date of completion of the backfilling in December 1981 to its removal three years later (Fig 2.53). This diagram exhibits a similar influence on the recorded pressures by draining operations in remote test areas as demonstrated by Table 2:14. The general trend is a flattening of the curve set, however, which suggests that activities like removal of packers in the borehole N1 in the SGU area or excavation of rock for the 3D migration experiment were not of major importance for the local piezometric conditions in the BMT area. Instead, the various operations in the BMT project probably had a much stronger influence, such as the emptying of the four outer

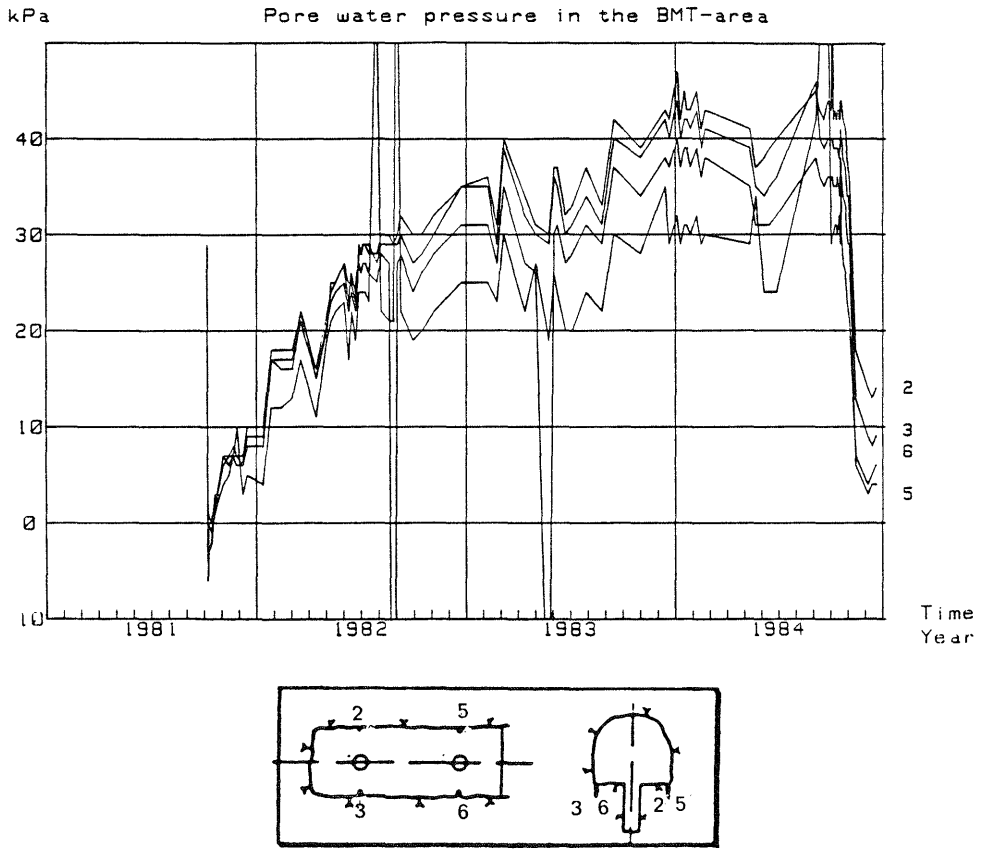

Fig 2.53. Piezometric heads in the tunnel floor inside the bulwark

heater holes no 3, 4, 5 and 6. Thus, the promising pressure increase in 1981 and 1982 turned into a pressure drop in late 1982 when hole no 4 was excavated and another one in early 1983, i.e. when hole no 3 was excavated and kept open until the fall the same year. This hole was then reloaded with a new set of bentonite blocks for the high-temperature test by which the draining effect was counteracted. Consequently, the pressures began to rise again and a rather steep increase was recorded at the beginning of 1984 but this trend turned into a significant pressure drop in spring the same year when hole no 3 was again excavated. The correlation between the observed pressure drop and the excavation and filling operations in hole no 3, implies that the tunnel floor is rather richly fractured where this hole is located. This is amply evidenced by the fracture mapping in this hole (cf. Vol I, Fig 3.6) which shows the presence of several subhorizontal and steeply oriented water-bearing fractures here as well as in the tunnel floor north of the bulwark.

As mentioned earlier in the text it was assumed in the planning of the BMT that the high rock water pressures that were recorded in the LBL study would be transferred to the rock/backfill interface as soon as the water saturation of the adjacent backfill became significant. However, the pressures were low not only at the tunnel floor but also at the rest of the tunnel periphery and after three years the pressures at the rock/backfill interface did not exceed 50 kPa. This discrepancy is particularly obvious if we take the expected swelling pressure of the tunnel backfill into consideration; it should actually be of the same order of magnitude. The matter requires a renewed analysis of the water pressure recordings, and we will start here by considering the piezometric levels given by the old LBL gauges.

The gauges in the five radially oriented LBL holes that are located in the inner part of the tunnel (R1, R2, R3, R4 and R5, cf. Vol I,

Fig 3.1) and in the second set of holes located in the cross section through heater hole no 4 (R6, R7, R8 and R10) gave recordings that are summarized in Table 2:15.

Table 2:15. LBL gauge recordings in kPa

Time after completion of tunnel backfilling		Inner set					Outer set			
		R1	R2	R3	R4	R5	R6	R7	R8	R10
1 week	(Dec 1981	1700	1700	1400	1450	1300	1500	-	130	20
1 month	(Jan 1982)	1600	1700	1450	1100	1300	1500	1300	100	25
0.5 years	(May 1982)	1600	1700	1450	1200	1450	1600	1300	160	160
1 year	(Dec 1982)	1700	1650	1400	1100	1400	1600	1300	240	280
1.5 years	(Jun 1983)	1700	1700	1450	1200	1400	1600	1300	160	280
1.8 years	(Oct 1983)	1700	1700	1450	1100	1400	1600	1300	160	360
2.0 years	(Dec 1983)	1700	1700	1450	1100	1400	1600	1300	160	200
2.8 years	(Aug 1984)	1600	1600	1400	1000	1300	1500	1200	160	160

These values demonstrate that the hydraulic regime of the rock at a distance of more than 3-5 m from the BMT tunnel remained largely unchanged throughout the test period with the exception of holes no R8 and R10. With the limited present knowledge of the hydrologically important rock structures in the area it is not clear why R10 should react on filling and excavation activities in the heater holes. However, the recorded pressures seem to be related to the operations in heater holes no 3 and 4, the maximum value being associated with the application of the second set of bentonite blocks in hole no 3 in summer 1983, and the minimum being observed at the start of the entire test. The pressure drop after about 2 years is logically explained by the excavation of heater hole no 4.

Further information of the rock water pressures was offered by the BAT piezometers that were inserted in the tunnel walls and which gave information about the piezometric situation close to the rock/back-

fill interface (Fig 2.54). This figure also shows the Ø56 mm DbH2 hole which is parallel to the tunnel axis and which is equipped with three filters connected to manometers. The distance between this hole and the tunnel wall is approximately 1 m.

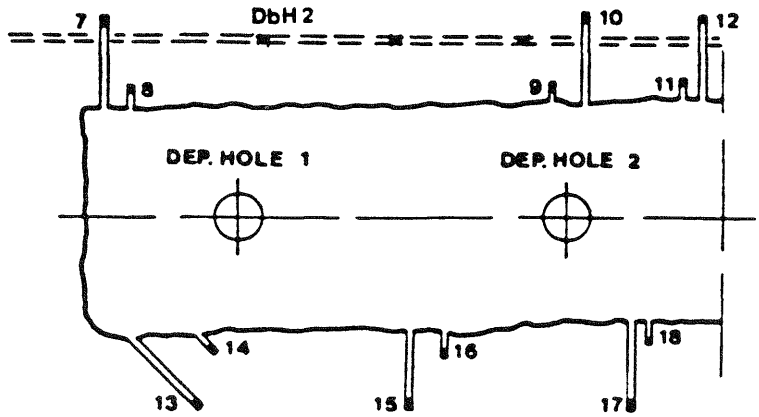

Fig 2.54. BAT gauge positions. The cylindrical gauges were all slightly dipping into the rock (cf. Volume I, Chapter 4.3.5.3

The BAT gauges which only reached 0.1-0.2 m into the rock (i.e. no 8, 9, 11, 14, 16, 18) yielded low values. Thus, at the end of the test the pressures ranged from about 10 to 35 kPa. The gauges with their tips located at 0.8-1.1 m distance from the rock/backfill interface (e.g. no 7, 10, 12, 13, 15 and 17) showed considerably higher values in the last year, the pressures being in the range of 105 to 290 kPa just before the termination of test. The water pressure in the DbH2 borehole soon came in equilibrium with the pressure regime in the rock. It was constantly about 500-700 kPa in the last year.

The pressures became higher at the inner end of the drift than closer to the bulkhead in the course of the test which shows that a pressure gradient was built up in the axial direction of the drift (Fig 2.55). This indicates a successively increased outward water flow through the shallow rock from the inner end of the backfilled tunnel towards the open part. The appearance of an increased axial water outflow instead of the expected build-up of high water pressures at the rock/backfill interface suggests that the hydraulic conductivity of the rock at this interface is substantially higher in the axial direction than in the radial one. This matter will be discussed later in the report.

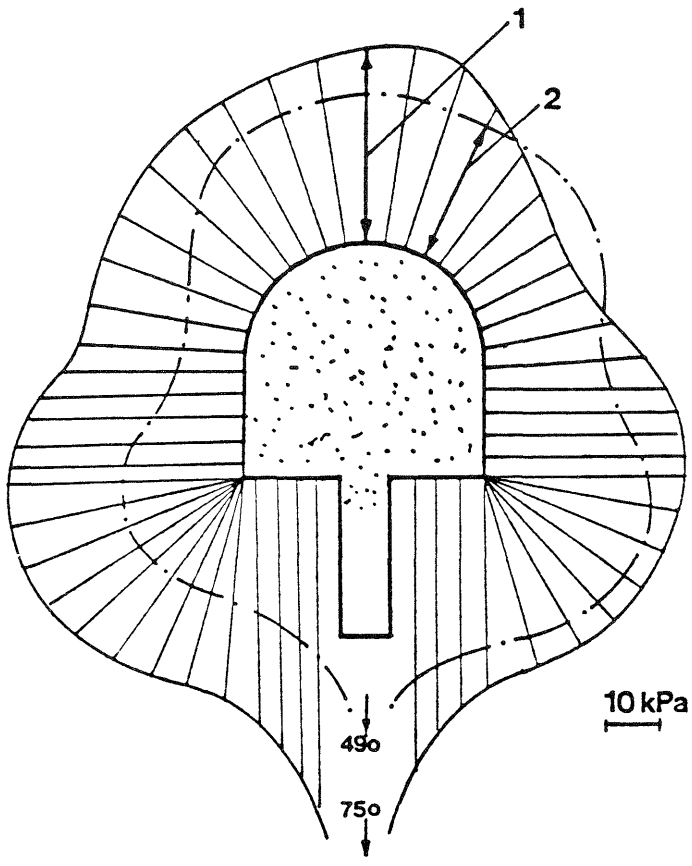

Fig 2.55. Pressure contours at the rock/backfill interface at sections through heater holes no 1 and 2 in late summer 1984. The full line represents the section through hole no 1, while the broken line represents the section through hole no 2. Figures at the base of the diagrams represent pressures at the base of the heater holes

2.4.3 Conclusions and remarks

The major conclusions as to the measurement of water pressures are the following:

1 The water pressure at the lower end of all the heater holes, except the "dry" no 6 and possibly also no 3, rose quickly to several hundred kilopascals soon after the application of the bentonite-enveloped heaters. In the upper part of all the holes the water pressure at the rock/bentonite interface did not exceed about 50 kPa.

The pressure conditions at the base of the holes implied that more water flowed towards the hole than the bentonite could absorb. In the low-pressure holes the bentonite was fed with less water by the rock than it could absorb. It is assumed that if these holes had been packer-sealed at their base and had not contained bentonite, much higher water pressures would have evolved.

2 The maximum recorded pressure 50 kPa at the interface between the tunnel backfill and the rock is approximately equal to the lower limit of the swelling pressure of the backfill. Since the large majority of the peripheral part of the backfill should be water saturated after about three years this swelling pressure must then have been developed. This implies that practically no water pressures at all existed at the rock /backfill interface, which can be explained in two ways. One is that the water uptake in the backfill was much more rapid than expected meaning that the ability of the backfill to absorb water was higher than the capacity of the rock to give off water. The other possibility is that the water overpressure that was expected to be generated when the peripheral part of the backfill became saturated was released by an increased leakage through the shallow, fractured rock from the inner end towards the open part of the tunnel. The matter will be settled by considering the water uptake processes that are reported in the subsequent chapter.

2.5 Water uptake and redistribution in the buffer materials

2.5.1 Predictions

The predicted rate and distribution of the water migration from the rock into the bentonite were presented in Chapter 2.3. These predictions only served to give a first approximation of the pressure build-up under certain specified hydrological conditions. The influence of temperature gradients of the order of 1-2^{o}C per cm was therefore omitted in these calculations although it was realized from

literature surveys and from pilot laboratory tests that such gradients certainly affect the water distribution pattern in soils.

2.5.2 Results

2.5.2.1 General

It was hoped that the signals from the more than 500 moisture sensors would give valuable information about the successive changes in water content in the heater holes and the tunnel backfill but the very limited experience from moisture recording using these gauges suggested that the measurements would rather give a qualitative measure of the moisture changes than quantitative data. Thus, sampling and direct water content determination at the termination of each test were considered to be necessary to obtain reliable water content values.

2.5.2.2 Moisture sensor reactions

Heater hole no 1, 600 and 1400 W

The moisture sensors reacted in agreement with the expectations. Thus, the gauges signalled a rapid increase of the water content close to the rock in the first weeks already and this increase proceeded throughout the first year. Figs 2.56 and 2.57 illustrate the water content situation 0.8 and 2 years after the start of the 600 W test in hole no 1, while Fig 2.58 shows the distribution at the termination of the subsequent 1400 W test in this hole. Certain gauges showed very erratic signals that are not consistent with the uniform build-up of the swelling pressures. If these extremes are disregarded it is concluded that the bentonite had taken up water also close to the heater and should have a saturation degree of 80-90 % at the end of the 600 W test about 2.1 years after the start. Only slight changes seem to be caused by the higher power.

Heater hole no 2, 600 W

The very wet conditions in this hole are manifested by the rapidly increasing water content as demonstrated by Figs 2.59. The reactions appeared approximately as fast as in hole no 1 and the same irregular signals were observed here as in hole no 1. The signal pattern at the end of the test (Fig 2.60) gave a completely false picture of the saturation progress as demonstrated by the swelling pressures and the water content determination of samples taken after the test.

Heater hole no 5, 600 W

The rate and uniformity of the water uptake in this hole, as indicated by the recordings, were similar to those in holes no 1 and 2. As in the case of these holes irregular reactions were noticed but as indicated by the uniform development of temperature fields and swelling pressures, the average degree of saturation should have been about 90 % at the termination of the test, the vicinity of the heater probably being somewhat drier (Fig 2.61).

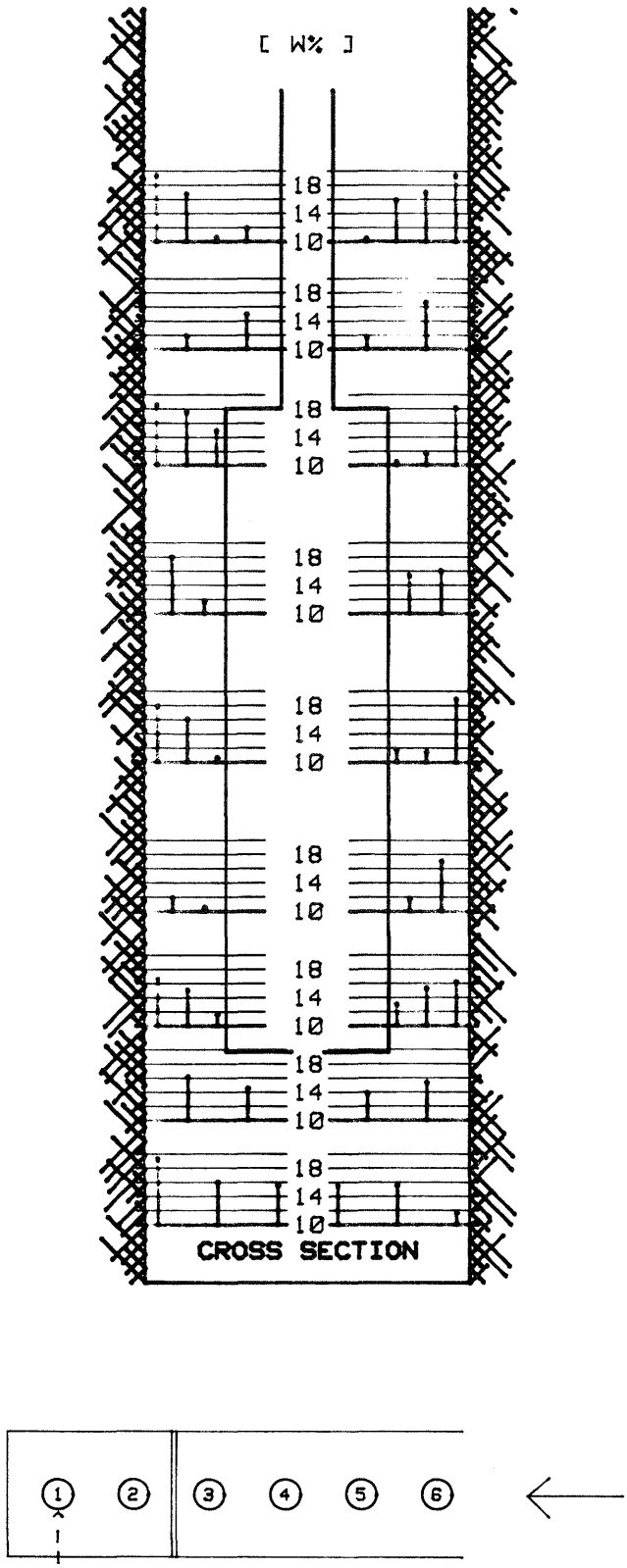

Fig 2.56. Recorded water contents in heater hole no 1 (600 W) 0.8 years after test start

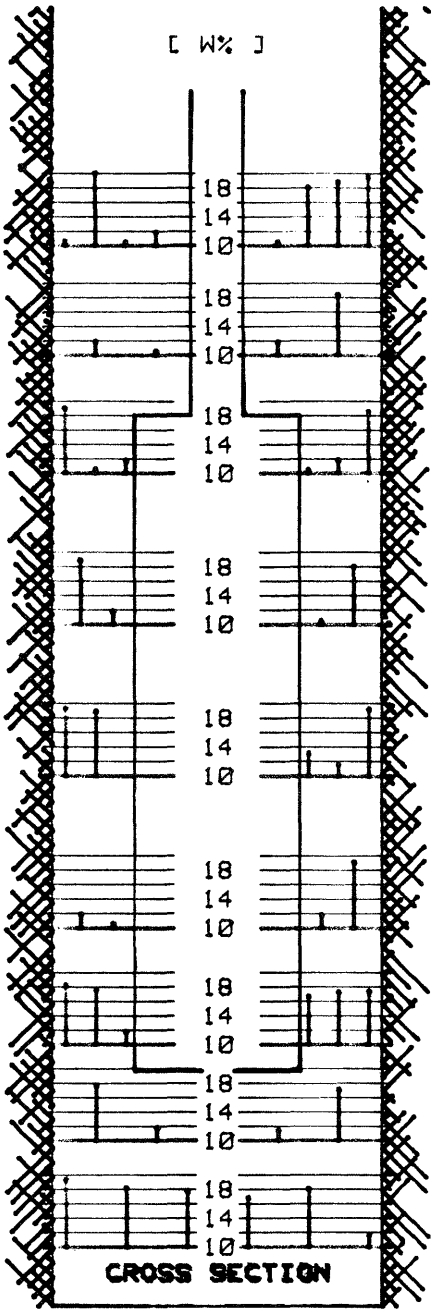

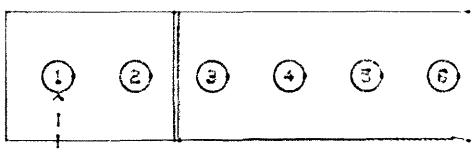

Fig 2.57. Recorded water contents in heater hole no 1 (600 W) 2 years after test start

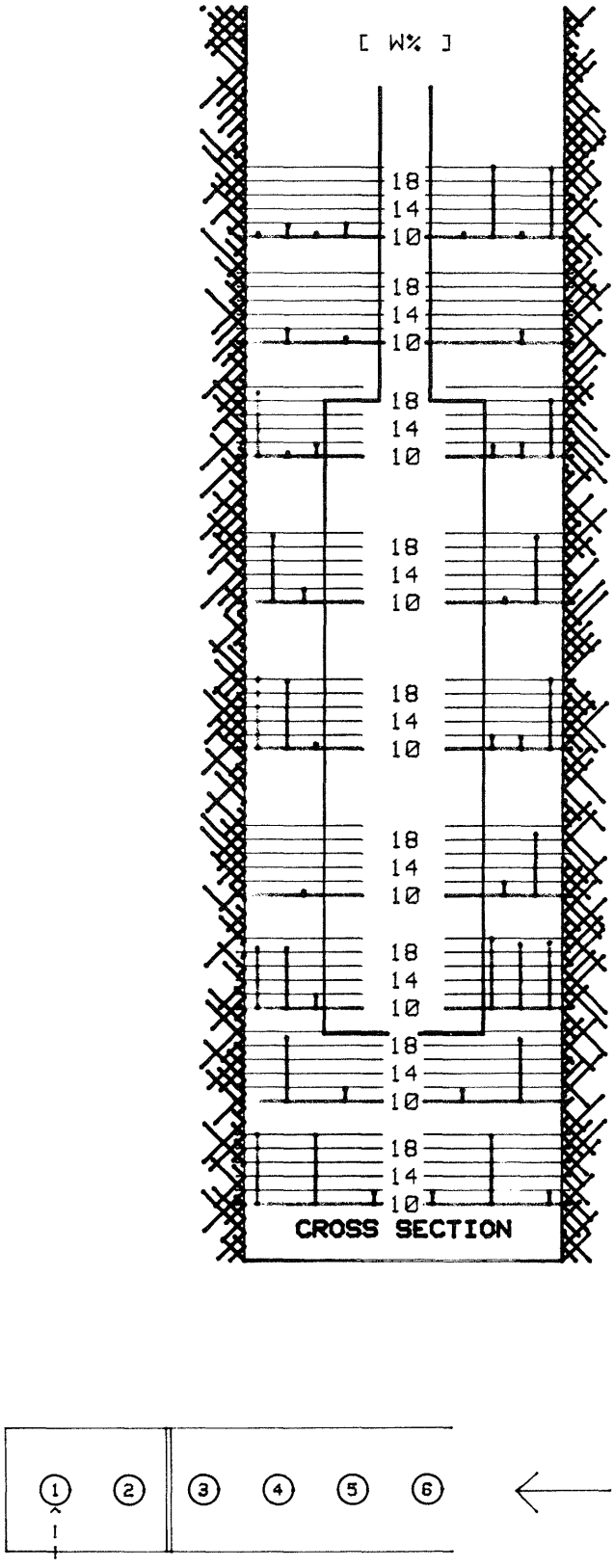

Fig 2.58. Recorded water contents in heater hole no 1 (1400 W) at the termination of this test

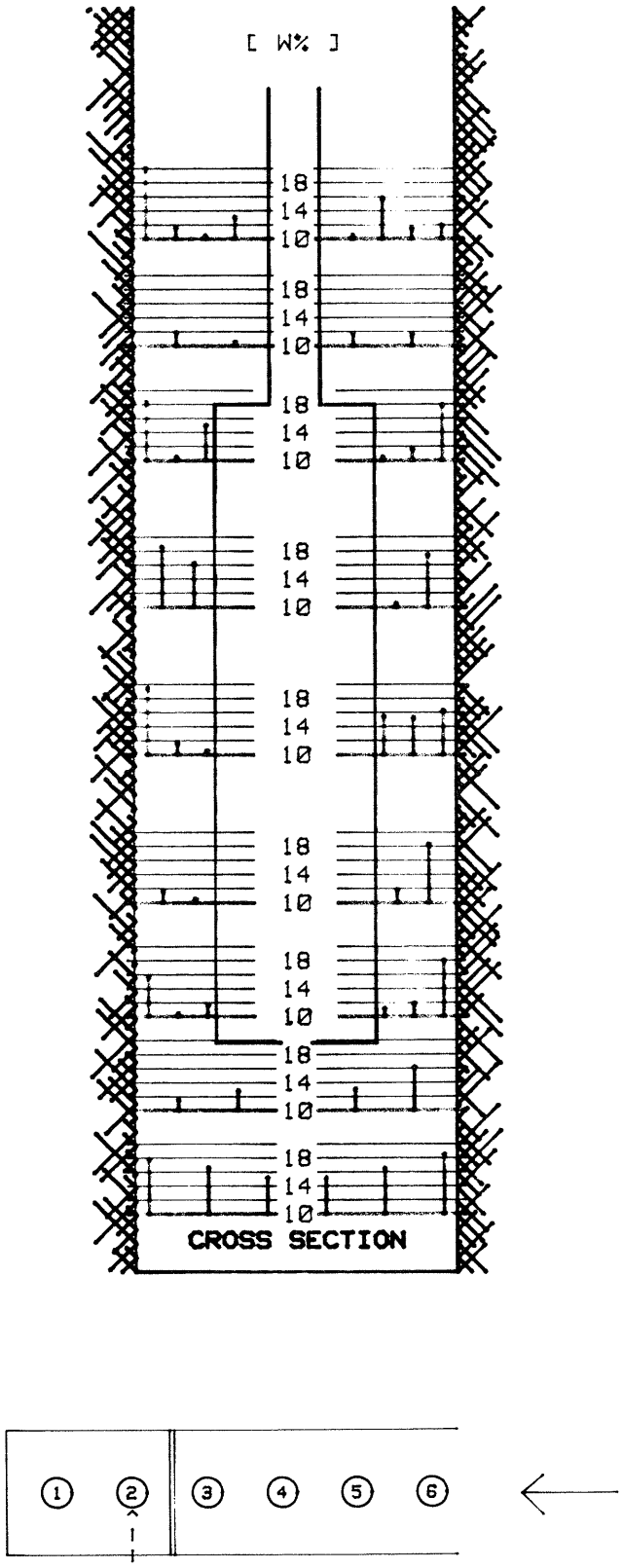

Fig 2.59. Recorded water contents in heater hole no 2 after 0.8 years

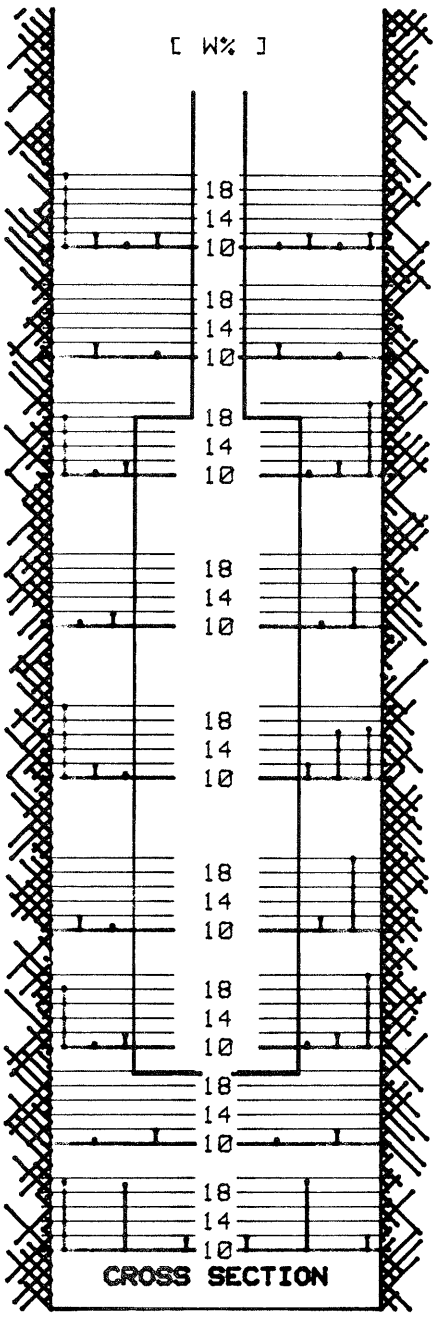

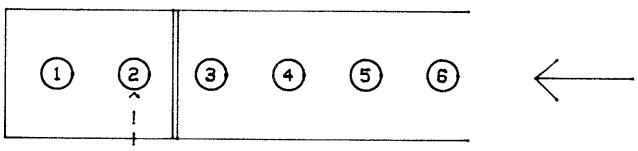

Fig 2.60. Recorded water contents in heater hole no 2 at the termination of the test

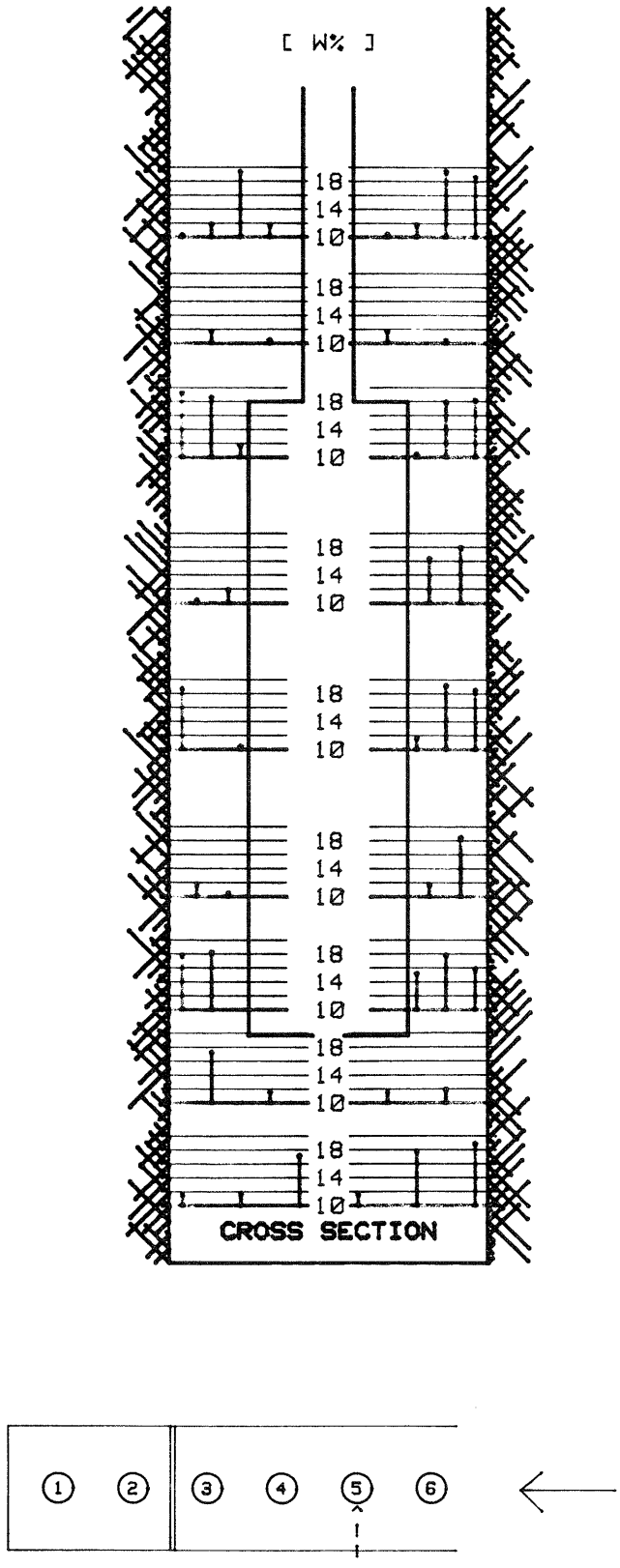

Fig 2.61. Recorded water contents in heater hole no 5 (600 W) at the termination of the test

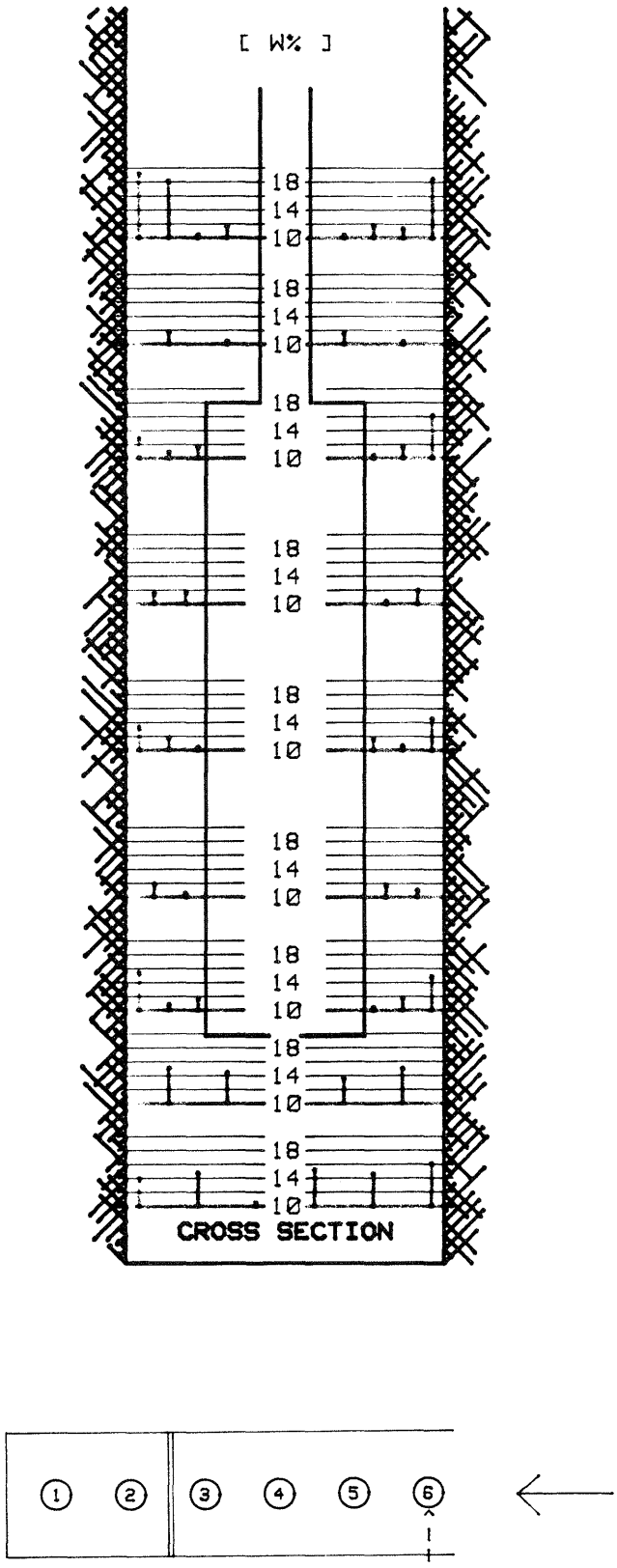

Fig 2.62. Recorded water contents in heater hole no 6 (600 W) at the termination of the test

Heater holes no 3, 4 and 6, 600 W

The moisture gauges that were located close to the rock in these holes reacted very soon after power onset as in the "wet" holes. After a few months the tendency of the water content to increase was no longer obvious and it ceased long before the termination of the tests. Fig 2.62 serves as a representative illustration of the recorded values at the end of the tests in holes no 3, 4 and 6.

Heater hole no 3, 1200 and 1800 W

The moisture readings were not considered to be relevant since the sensors had not been calibrated for the actual high temperatures.

Tunnel backfill

The gauges inserted in the backfill did not give a clear picture of the water uptake and redistribution. The accuracy of the recordings was not sufficient to evaluate them in terms of water content percentages, the main reason probably being the low degree of microstructural homogeneity of clay/sand mixtures compacted in situ. However, the general trend of wetting of the backfill could be estimated by identifying those sensors which consistently showed an increased voltage signal. This gave diagrams of the kind shown in Figs 2.63 and 2.64, which roughly illustrated the successive moistening of the backfill. The conclusion was drawn that the water content of the peripheral part began to increase soon after the sealing of the bulwark. After slightly less than one year moistening had occurred to about 1 m distance from the rock/backfill interface all around the periphery, and after two years only a central portion with approximately 1 m height and 1-1.5 m width seemed to be unaffected by the water uptake. After 2.5 years practically all the gauges indicated an increased

water content. Actually, a large number of centrally located sensors initially signalled decreasing water content values, which was taken as an indication of insufficient accuracy of the gauges. It is possible, however, that this effect is real and that it was caused by a slightly higher bulk density of the bentonite/sand material applied in the gauges than that of the surrounding backfill. Such a difference would yield slight swelling of the first-mentioned material on wetting by which a lower signal would be generated.

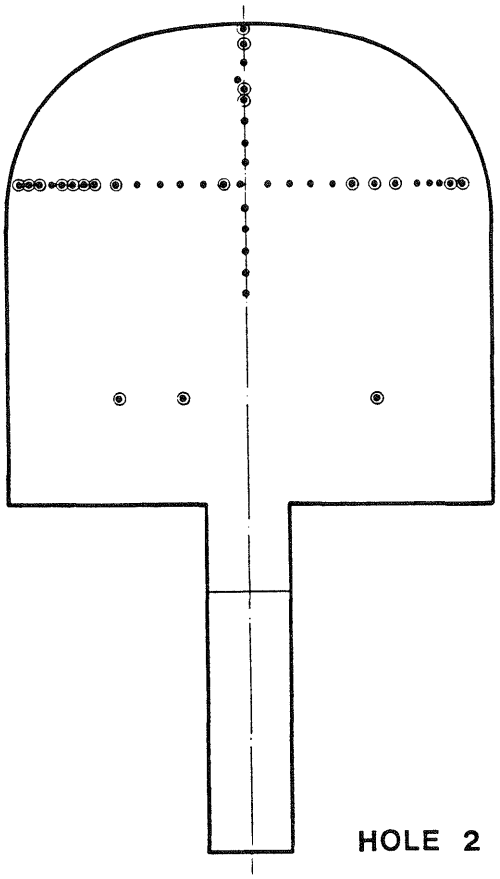

Fig 2.63. Distribution of activated moisture sensors in the cross section through heater hole no 2, 1.5 years after the sealing of the bulwark

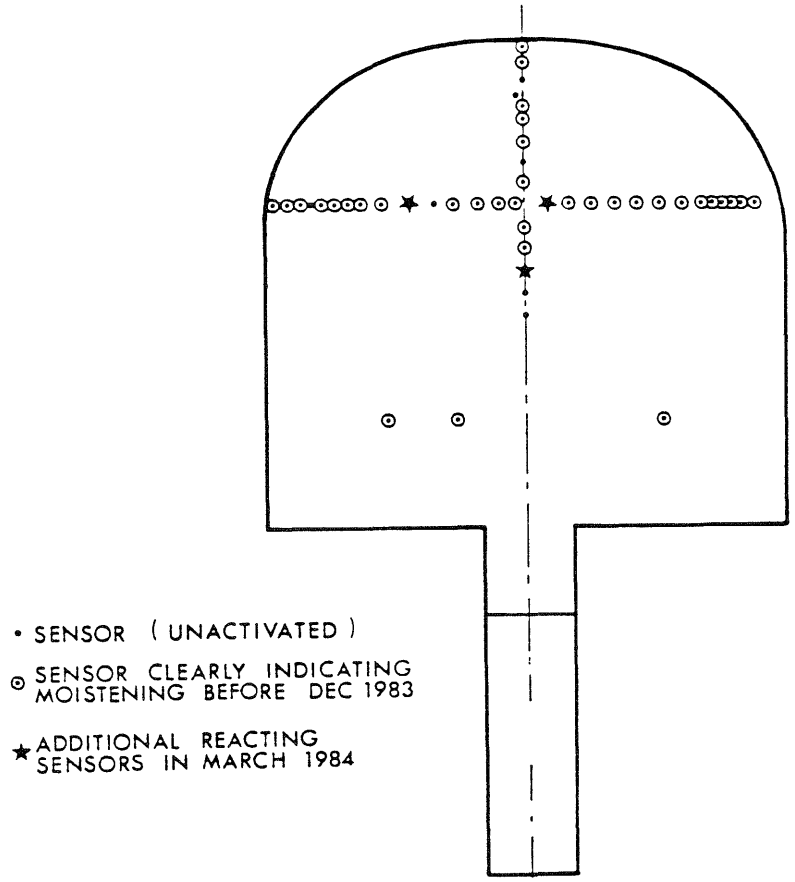

Fig 2.64. Distribution of activated moisture sensors in the cross section through heater hole no 2, 2.3 years after the sealing of the bulwark

2.5.2.3 Sampling

Heater hole no 1, 600 and 1400 W

The water content determination of samples taken in hole no 1 in connection with the excavation after the termination of the 1400 W test, showed that the average degree of saturation was 90-95 %. Even close to the heater the average water content was found to be about 19 % which corresponds to slightly less than 90 % saturation. This demonstrates that the thermal gradient and higher temperatures at the heater surface had not prevented water from being absorbed to almost complete saturation throughout the bentonite annulus. It also shows that the power increase from 600 to 1400 W had not driven water from the vicinity of the heater. The water content at any radial distance from the heater was very uniformly distributed in the bentonite as demonstrated by the three figures 2.65, 2.66 and 2.67.

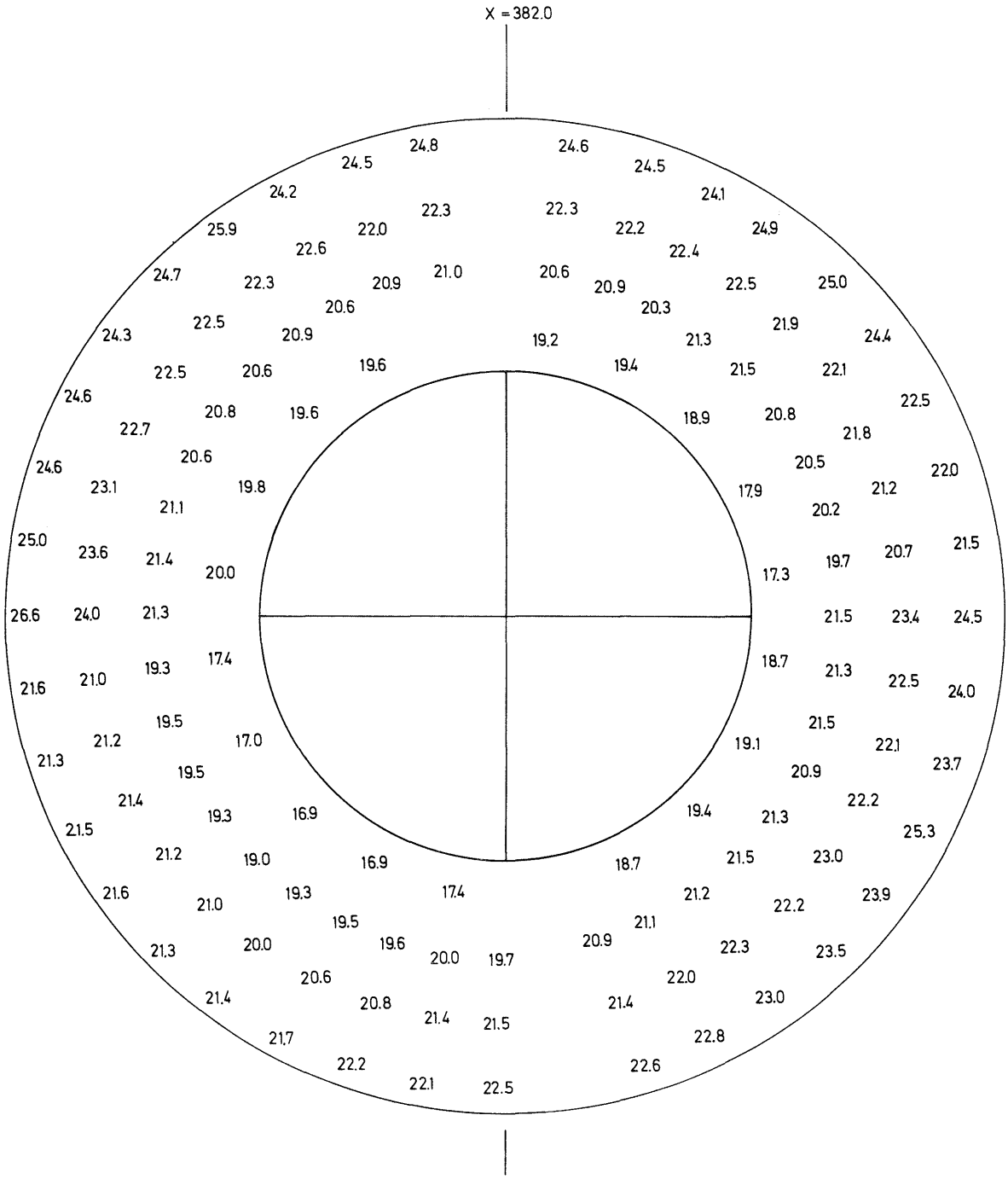

Fig 2.65. Distribution of water contents in the highly compacted bentonite at the upper end of the heater in hole no 1 (1400 W)

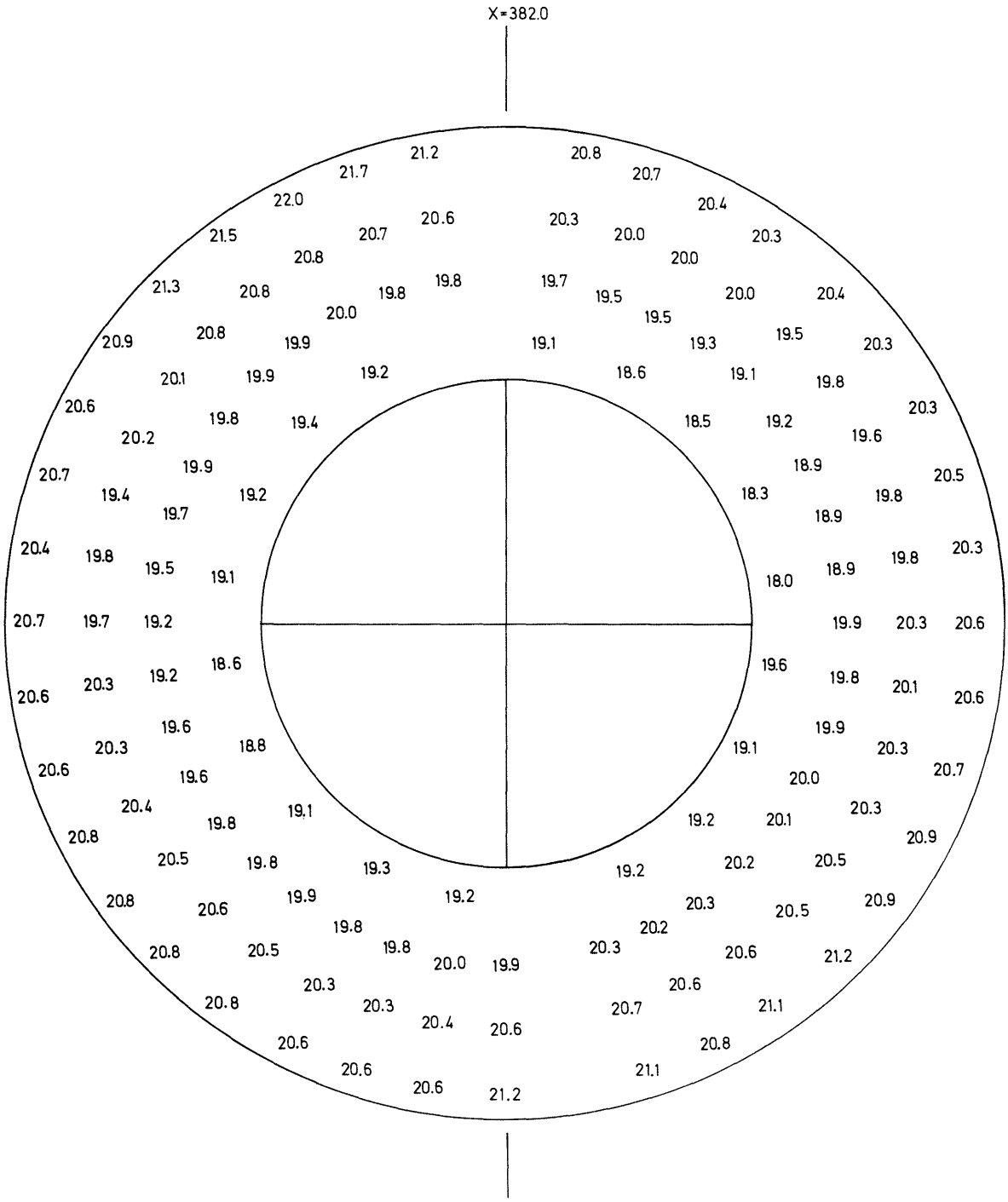

Fig 2.66. Distribution of water contents in the highly compacted bentonite at mid-height of the heater in hole no 1 (1400 W)

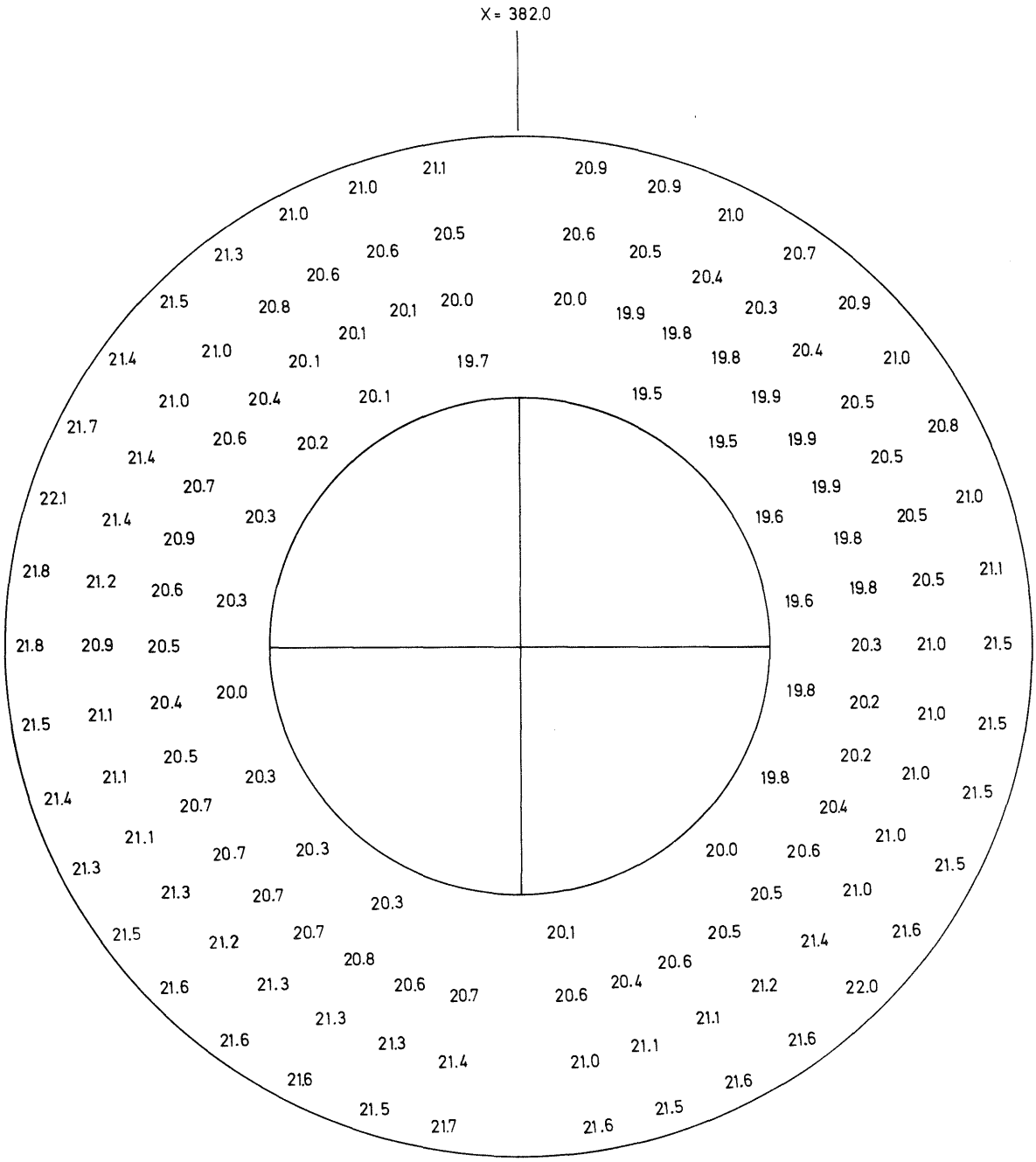

Fig 2.67. Distribution of water contents in the highly compacted bentonite at the lower end of the heater in hole no 1 (1400 W)

Fig 2.68 shows "isomoistures" for a vertical section through the hole, the curves being based on the arithmetric means of all measured values for each individual radial distance from the heater. This diagram demonstrates that the maximum water content at full saturation is slightly higher than 20 % at the rock/bentonite interface in the central and lower parts of the hole, while the uppermost part of the bentonite showed water content values of as much as 35 % indicating swelling of this part. The swelling was manifested also by a measured upward displacement of 5 cm of the interface between the highly compacted bentonite and the overlying backfill. This displacement was slightly concave upwards, the minimum elevation being found at the central casing.

A couple of very important observations were made in the course of the sampling, one being that the original joints between the blocks could no longer be identified although the blocks were more easily fractured along them than in other directions. It was also found that the contact was perfectly tight between the heater and the bentonite and between the rock and the bentonite (cf. Fig 2.69). At the first-mentioned interface the teflon coating was partly disrupted by which direct contact between aluminum and bentonite was established. Local corrosion of the aluminum was observed.

Heater holes no 2 and 5, 600 W

The sampling in hole no 2 showed that the water content ranged between 20 and 22 % in the entire bentonite mass except for the upper 30 cm where slightly higher values were recorded. The maximum value was about 35 %, which is explained by swelling as in the case of hole no 1. The upward movement of the upper boundary of the highly compacted bentonite was almost identical to that in hole no 1.

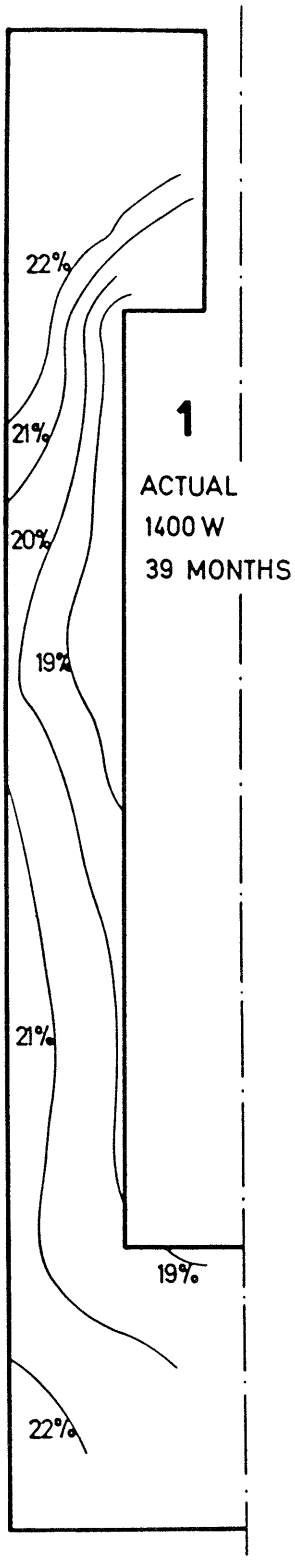

Fig 2.68. "Isomoistures" in heater hole no 1 at the termination of the 1400 W test

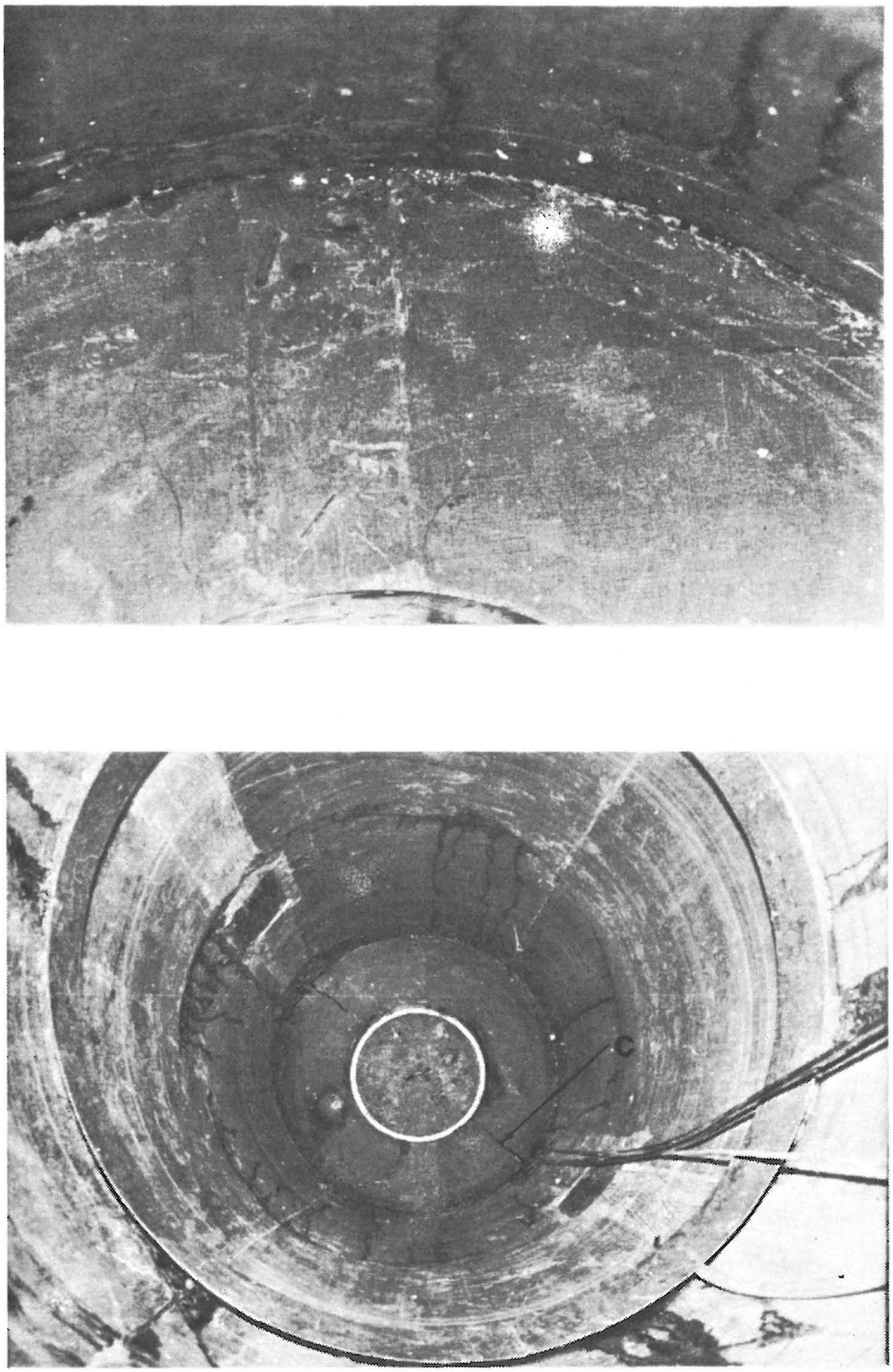

Fig 2.69. The appearance of the bentonite in heater hole no 1 at the excavation slightly more than 3 years after the start (1400 W). Notice the tight contact between bentonite and rock and the absence of open joints in the bentonite. The black lines denoted "C" in the lower picture are cables from moisture sensors

The conditions in hole no 5 were very similar to those in holes no 1 and 2. Thus, a very high degree of saturation was attained in all of the highly compacted bentonite except for the vicinity of the heater at its lower end (Fig 2.70). Even here, however, the water content was as high as 16-18 % and it is expected that full saturation had been reached if the test had been run for another year or slightly more than that. We thus see that the hydration power of the very dense sodium bentonite was sufficiently strong to overcome the drying effect of the warm heater.

Heater hole no 3, 600 W

The comprehensive sampling for water content determination showed that the moistening was remarkably uniform in the peripheral 5 cm wide zone, i.e. the initially powder-filled slot and the outermost part of the highly compacted bentonite. The water content of this zone ranged between 18 and 22 %, which indicates almost complete water saturation. The initially very soft filling of bentonite powder had been effectively consolidated by the swelling pressure exerted by the highly compacted bentonite and the two materials thus appeared as one, homogeneous substance.

Figs 2.71-2.73 shows the variation in water content of the bentonite in horizontal cross sections at the upper and lower ends of the heater, and at its mid-height. These diagrams demonstrate that the water content was uniformly distributed in the respective bentonite "annulus", which in turn explains the observed uniform build-up of temperature fields and swelling pressures.

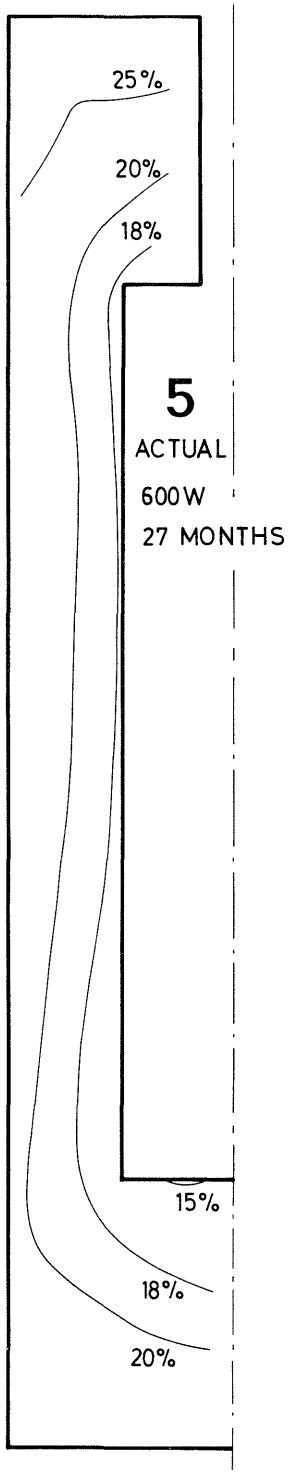

Fig 2.70. "Isomoistures" in heater hole no 5 at the termination of the 600 W test about 27 months after the start

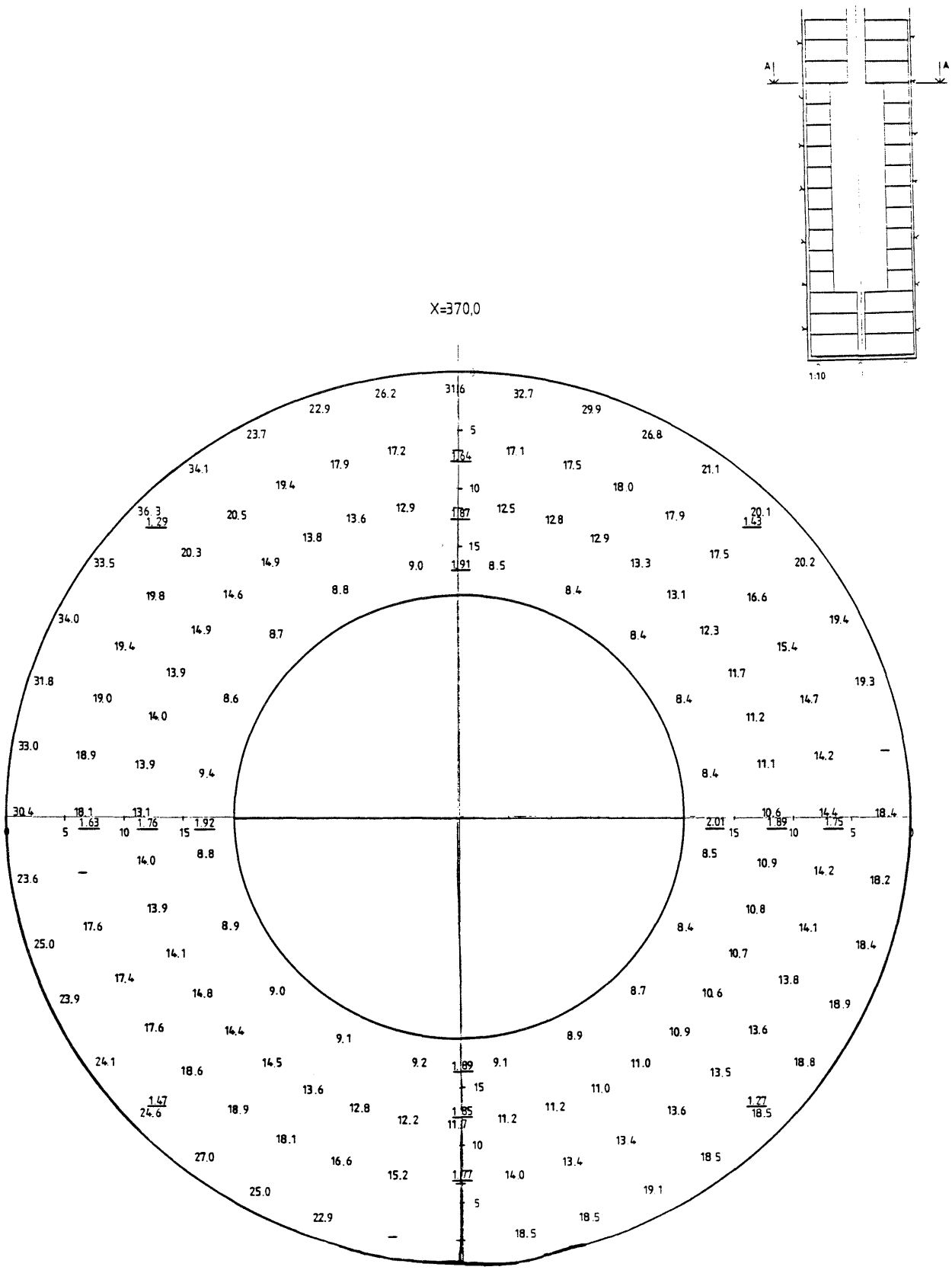

Fig 2.71. Water content distribution at the upper end of heater no 3 at the end of the 15 month test (600 W)

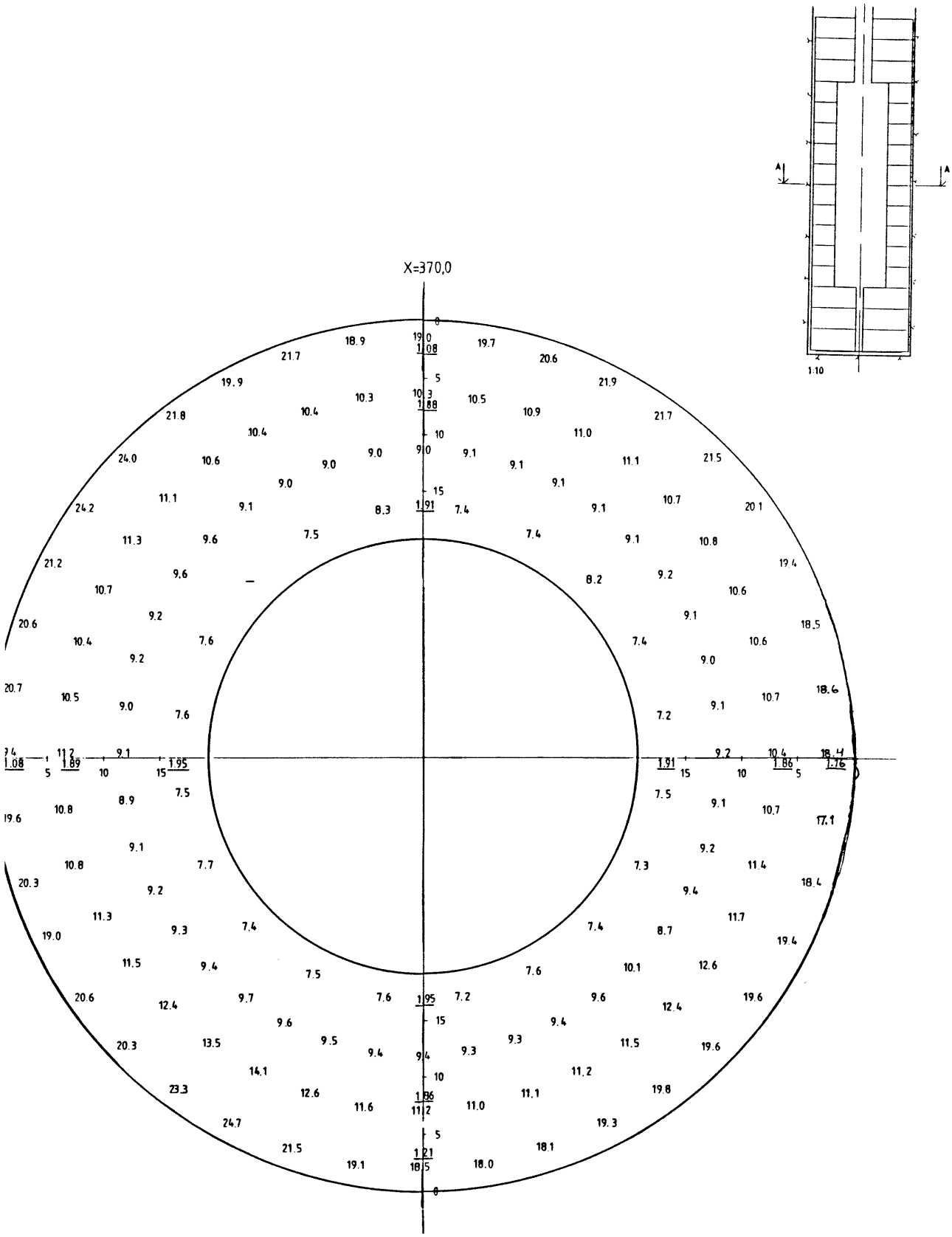

Fig 2.72. Water content distribution at mid-height of heater no 3 at the end of the 15 month test (600 W)

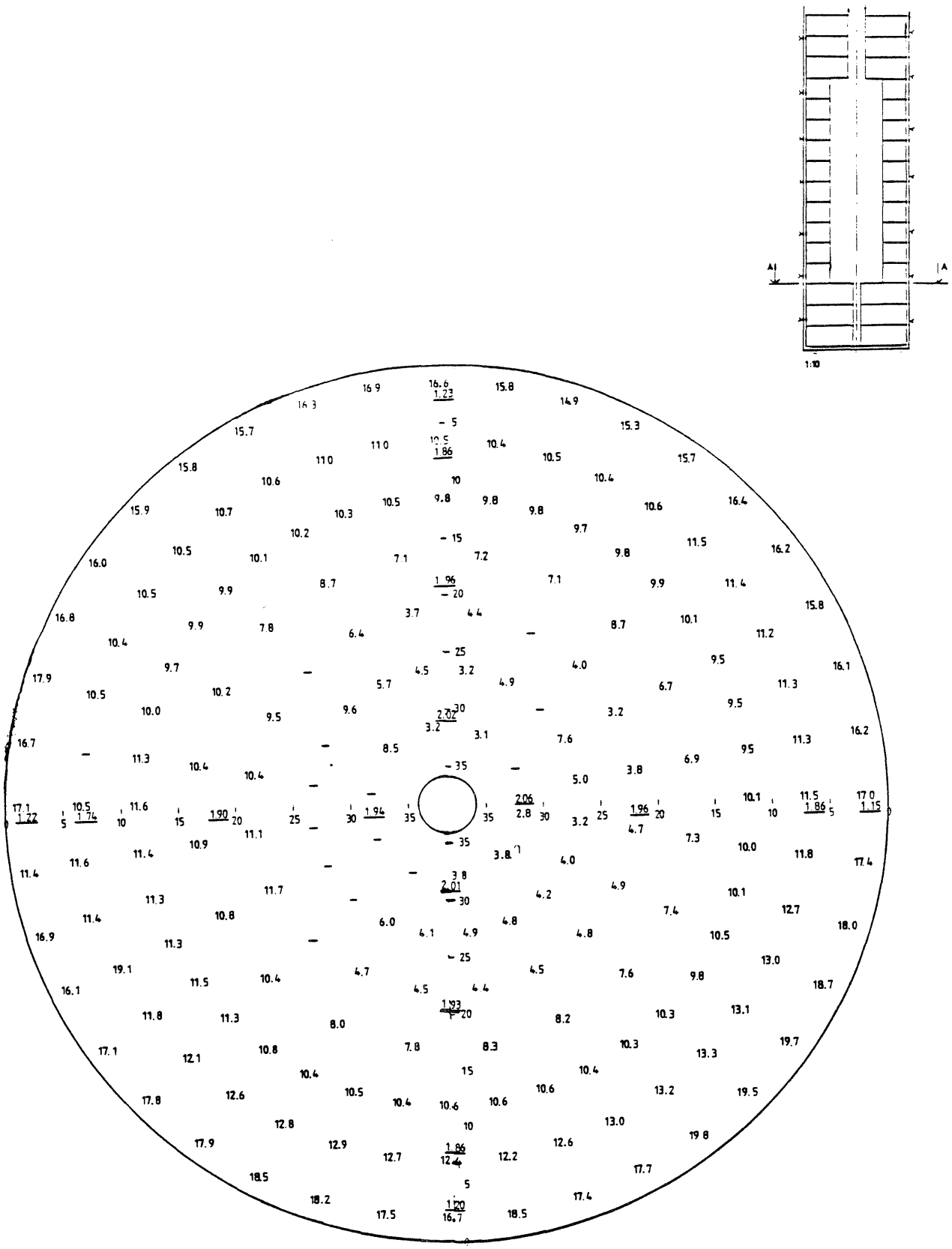

Fig 2.73. Water content distribution at the lower end of heater no 3 at the end of the 15 month test (600 W)

The evaluation of the water content determination showed that the 8 bentonite zones specified in Fig 2.74 had experienced an increased water content, except for the inner, lower part. Here, we notice a net reduction of the amount of pore water due to the "drying" effect of the heater but as shown by Fig 2.72 the reduction in water content is actually confined to the inner half of the bentonite annulus. The net water uptake of the heater-embedding bentonite was found to be 26 liters.

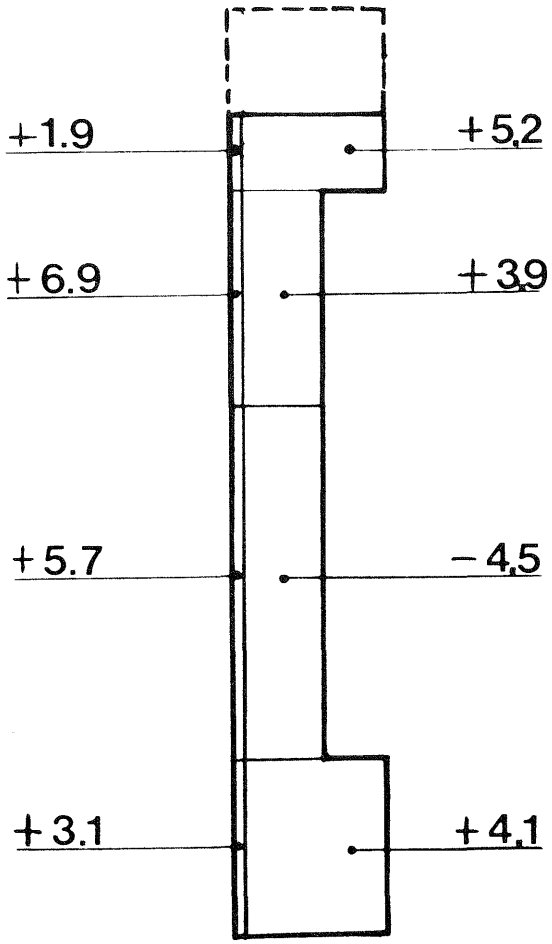

Fig 2.74. Changes in average amounts of pore water, expressed in liters, in 8 characteristic bentonite zones at the end of the 15 month test in hole no 3. The thin, peripheral zones have a lateral thickness of 5 cm.

Fig 2.75 shows the average radial distribution of water over two horizontal cross sections. It demonstrates that there is a slight moisture gradient in the axial direction in the larger part of the bentonite column. This is expected to induce a successive vertical migration of moisture towards the horizontal plane through the center of the heater. The wet conditions in the upper and lower parts of the bentonite overpack clearly illustrate that the major water sources were the tunnel floor and overlying sand/bentonite backfill, and the lower end of the hole, respectively.

The average water content distribution in "isomoisture" plotting is shown in Fig 2.76.

Heater hole no 3, 1200/1800 W

The 9 months long high-power test in hole 3 yielded a similar water content distribution pattern as in the preceding 600 W test (cf. Fig 2.77).

The difference in water content, as indicated by comparing Figs 2.76 and 2.77, clearly shows that more water was absorbed over the entire length of the bentonite overpack in the high-power test, despite the fact that the latter test ran for only half the time used for the 600 W power test. This is a very significant finding since it clearly shows that the temperature gradient and absolute temperatures do not have a major influence on the rate and distribution of the water uptake. It is concluded that more water must have been available in the high-power test than in the earlier test, which is compatible with the conclusion that the water outflow from the inner part of the tunnel increased in the course of the BMT and that most of this water was discharged through the tunnel floor.

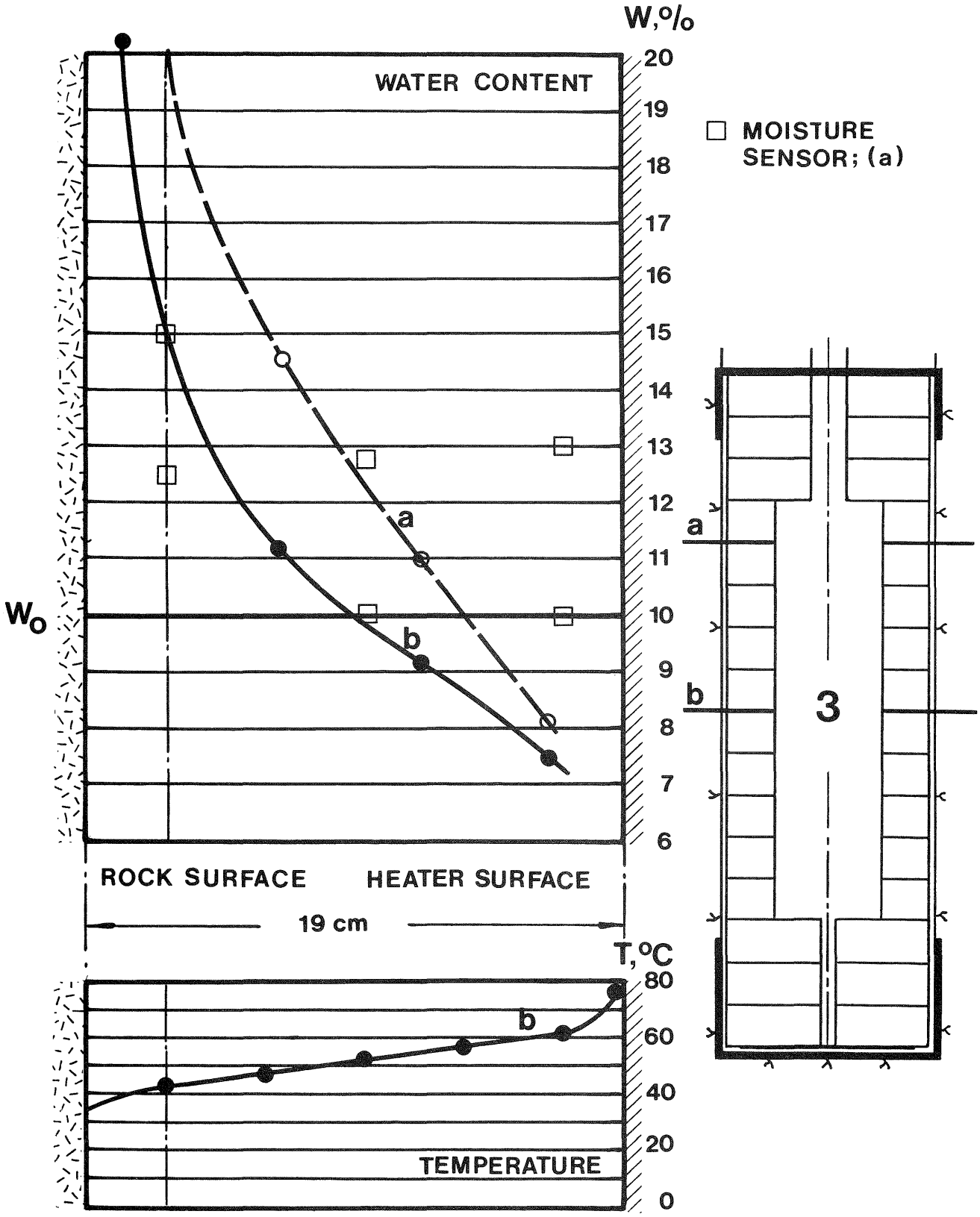

Fig 2.75. Water content and temperature distributions in two cross sections (a and b) at the end of the 15 month 600 W test in hole no 3. W_o is the original water content

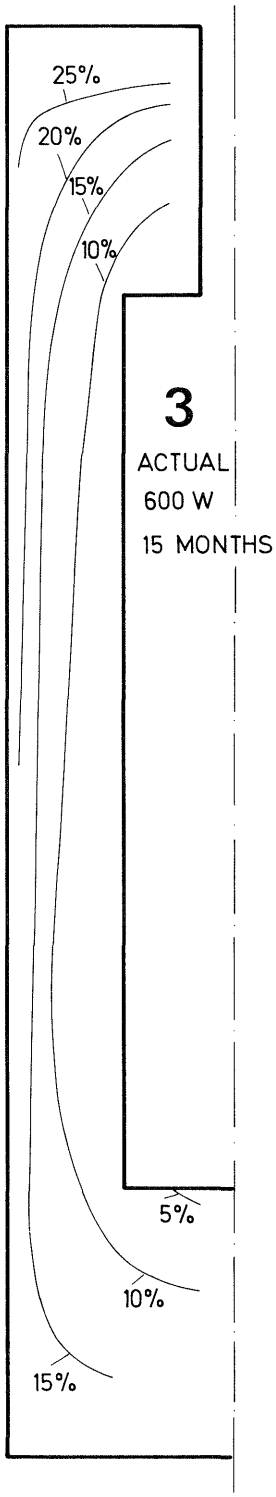

Fig 2.76. "Isomoistures" in heater hole no 3 at the termination of the 600 W test about 15 months after the start

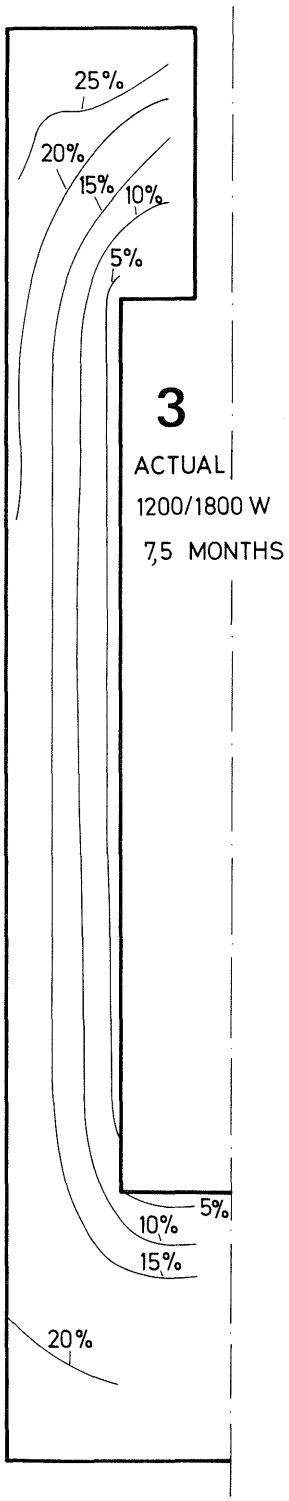

Fig 2.77. "Isomoistures" in heater hole no 3 at the termination of the 7.5 month test at 1200/1800 W

Heater hole no 4, 600 W

The excavation and associated sampling which took place about 10 months after the test start showed the same uniform distribution of the water in the peripheral zone as in hole no 3. Except for the close proximity of the earthing wire, which served as an efficient water conductor and produced strong local wetting, the peripheral zone had a water content that ranged between 16 and 19 %. The distribution turned out to be much the same as that observed in hole no 3, although less water had been taken up by the bentonite (Fig 2.78). The total uptake turned out to be 22 liters in 10 months, which is

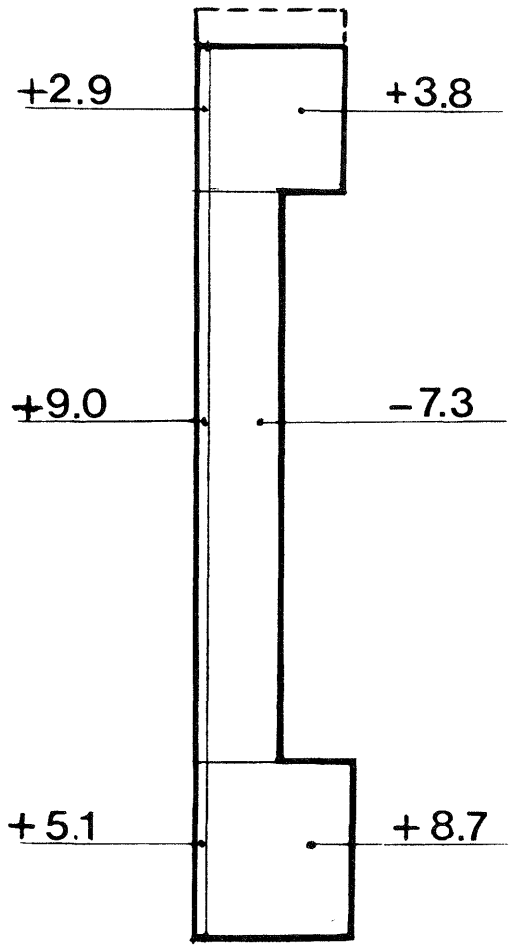

Fig 2.78. Changes in average amounts of pore water, expressed in liters, in 8 characteristic bentonite zones at the end of the 10 month test in hole no 4 (600 W). The thin, peripheral zones have a lateral thickness of 5 cm.

in reasonable agreement with the 26 liter inflow in the 15 months long 600 W test in hole no 3. The wetting of the upper and lower ends of the bentonite overpack was undoubtedly caused by the supply of water offered by the richly water-bearing, fractured tunnel floor, and the LBL hole no 9 which ends at the base of this heater hole. This hole was packer-sealed but clearly leaked water through the base of the heater hole.

Fig 2.79 shows the average radial distribution of the water content at the same levels as in Fig 2.74. In contrast to the distribution shown in the latter diagram, which represents the conditions at the termination of the test in hole no 3, the distribution obtained for hole no 4 shows no moisture gradient in the vertical direction. Thus, practically all the water uptake in the peripheral zone at mid-height of the heater originated from lateral migration of water while only 1.7 liters (9.0-7.3 liters) stem from the rock. The water loss in the inner part of the bentonite annulus was caused by the outward heat-induced transfer of moisture and probably also by evaporation of some water close to the heater along the shaft.

The average water content distribution in "isomoisture" plotting is shown in Fig 2.80.

Heater hole no 6, 600 W

The actual water content distribution in hole no 6 after the approximately 2 years long test period was similar to that in the somewhat shorter 600 W test in hole no 3, except for the lower part of hole no 6, which was considerably wetter (Fig 2.81). It is clear, therefore, that there was a net water uptake in the bentonite with the exception of the 6-8 cm thick annulus close to the heater. This bentonite zone experienced a reduction of the water content from the initial value 10 % to values ranging from 7 to 10 %.

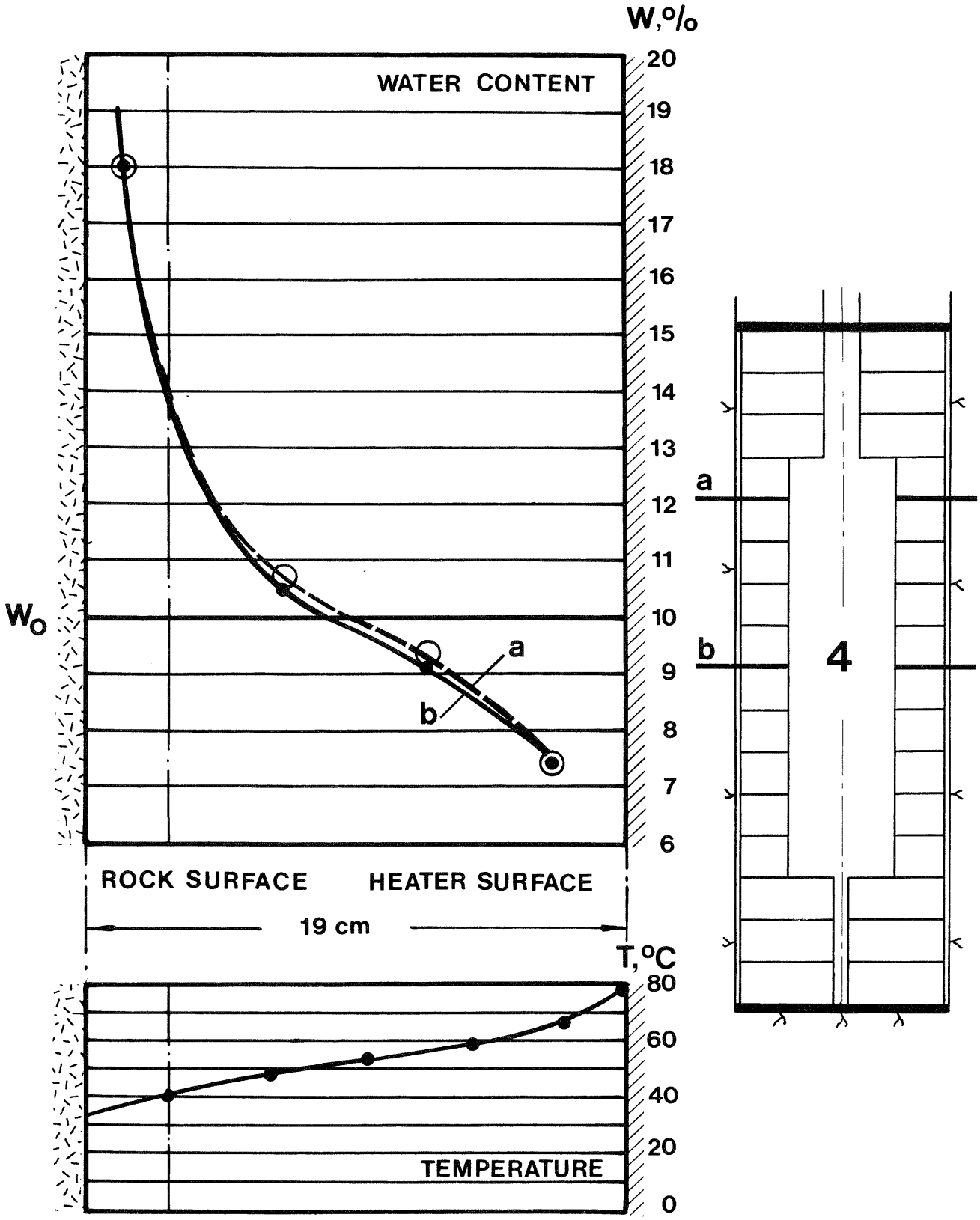

Fig 2.79. Water content and temperature distributions in two cross sections (a and b) at the end of the 10 month 600 W test in hole no 4

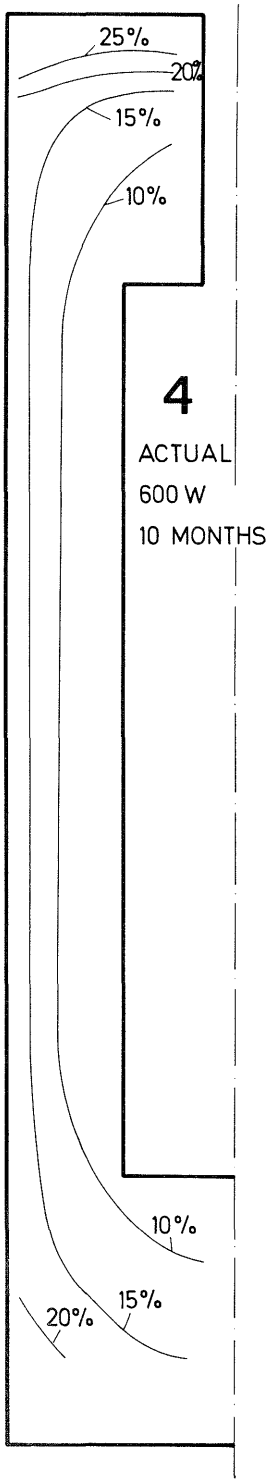

Fig 2.80. "Isomoistures" in heater hole no 4 at the termination of the 600 W test about 10 months after the start

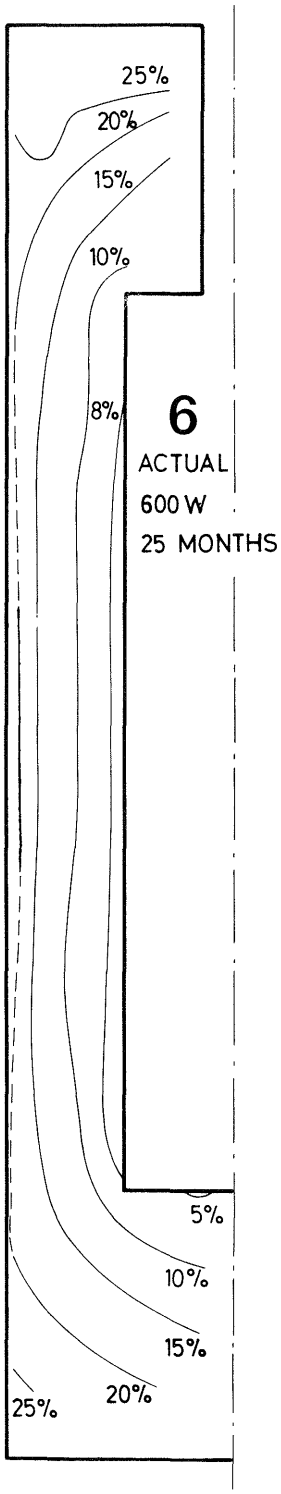

Fig 2.81. "Isomoistures" in heater hole no 6 at the termination of the 600 W test about 25 months after the start

Since the surface temperature of the entire heater dropped in the last year while the swelling pressures increased over the entire length of the hole in the same period of time, it is concluded that the water uptake continued in the form of a largely uniform, slow migration of water from the rock into the bentonite. The water uptake was obviously considerably smaller in this hole than in hole no 3 during the much shorter high-power test which is explained by the much lower hydraulic conductivity or discharge capacity of the rock surrounding hole no 6.

Tunnel backfill

The contradictory and rather strange moisture sensor signals that were received from the tunnel backfill called for a direct determination of the conditions through sampling after about one year. This involved cutting of two holes in the steel components of the bulwark and driving of two steel tube casings with an outer diameter of 100 mm in which almost continuous sampling was made parallel to the penetration. One of the tubes was almost 6 m long and directed upwards for sampling all the way to the tunnel roof, while the second, 3 m long one dipped slightly and gave samples to within a distance of about 0.5 m from the western tunnel wall. Fig 2.82 shows the location of the tubes and the water content distribution, indicating complete saturation of the upper backfill next to the rock and a water content increase from 15 % to 17-20 % to about 0.3 m distance from the rock/backfill interface. The casing was also used for TV-inspection of the conditions at the tunnel crown and this investigation gave evidence of a tight contact between the rock and the backfill. Thus, the backfill had not settled and no free water flowed into the casing at the inspection.

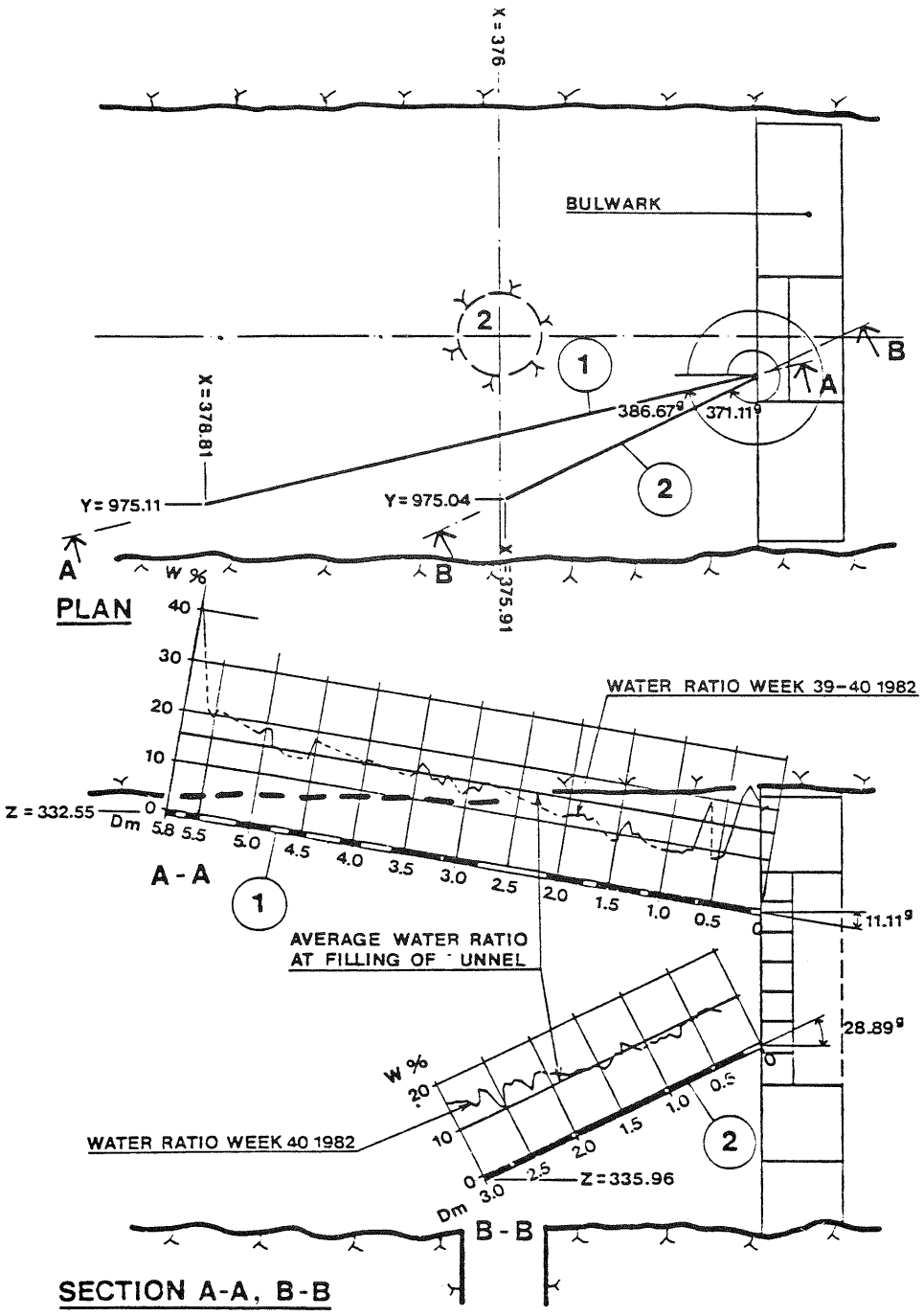

Fig 2.82. Sampling in the backfill 10 months after the closure of the backfilled tunnel section

The moistening at the lower part of the western wall was even more obvious. Thus, the water content had increased from the initial value 10 % to 13-17 % to about 1 m from the rock/backfill interface.

The moistening of the backfill at the tunnel crown was found to be much slower than predicted if the model implying equal and unlimited access to water over the entire rock surface would apply. The water uptake at the lower part of the tunnel wall, on the other hand, was close to the predictions using the same model. At that stage, i.e. after about 1 year, it was not possible to draw conclusions concerning the access to water from the confining rock, or how this water was distributed. It was clear, however, that the availability of water at the tunnel crown was limited, which was in agreement also with the absence of water pressures in this region.

The excavation of the tunnel backfill, which started in November/December 1984, i.e. almost exactly 3 years after its application, gave a very clear picture of the physical state of the material as illustrated by Figs 2.83 - 2.85. It appeared that the lower, about 3 m thick bentonite-poor mass was completely saturated with the exception of small local zones. The upper part of the backfill, which had a bentonite content of 20 % and had been blown in place, was saturated to approximately 0.5 m distance from the tunnel roof and to about 1-1.5 m from the rock at its base. The average degree of saturation of the entire backfill was slightly less than 90 %, the water uptake being about 33 m^3. This amount is almost twice the inflow measured before the backfilling took place which shows that the applied technique for determination of water inflow by using air-driers yields a considerable underestimation of the inflow. It is also concluded that the rapid and strong water absorption by the backfill took care of practically all the water that flowed from the

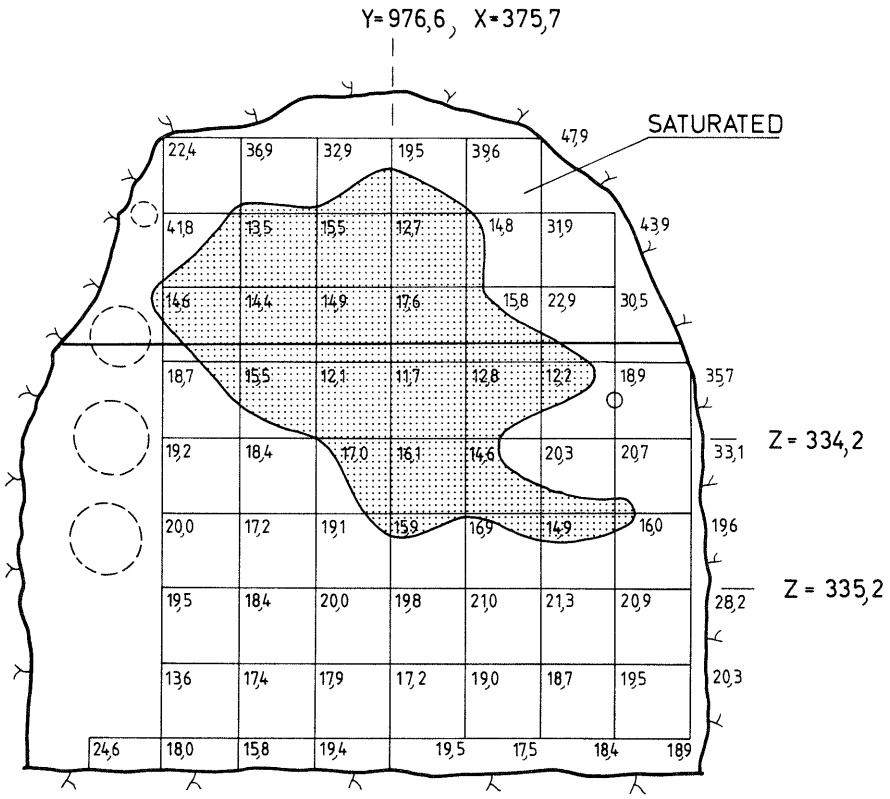

Fig 2.83. Water content distribution approximately 1 m from the bulwark. Dotted area is non-saturated

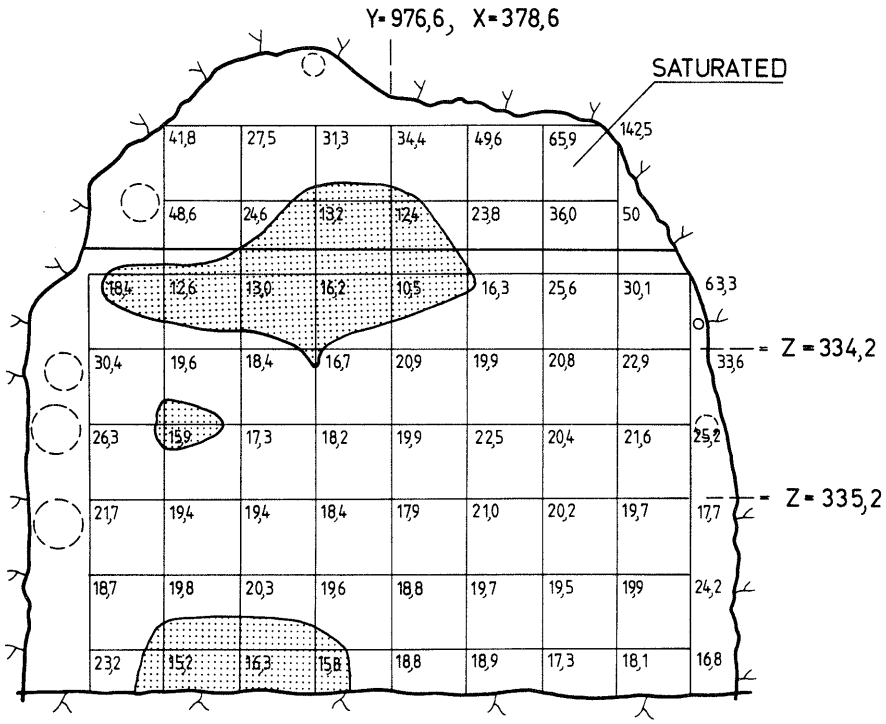

Fig 2.84. Water content distribution in the cross section at half-distance between heater holes no 1 and 2. Dotted area is non-saturated

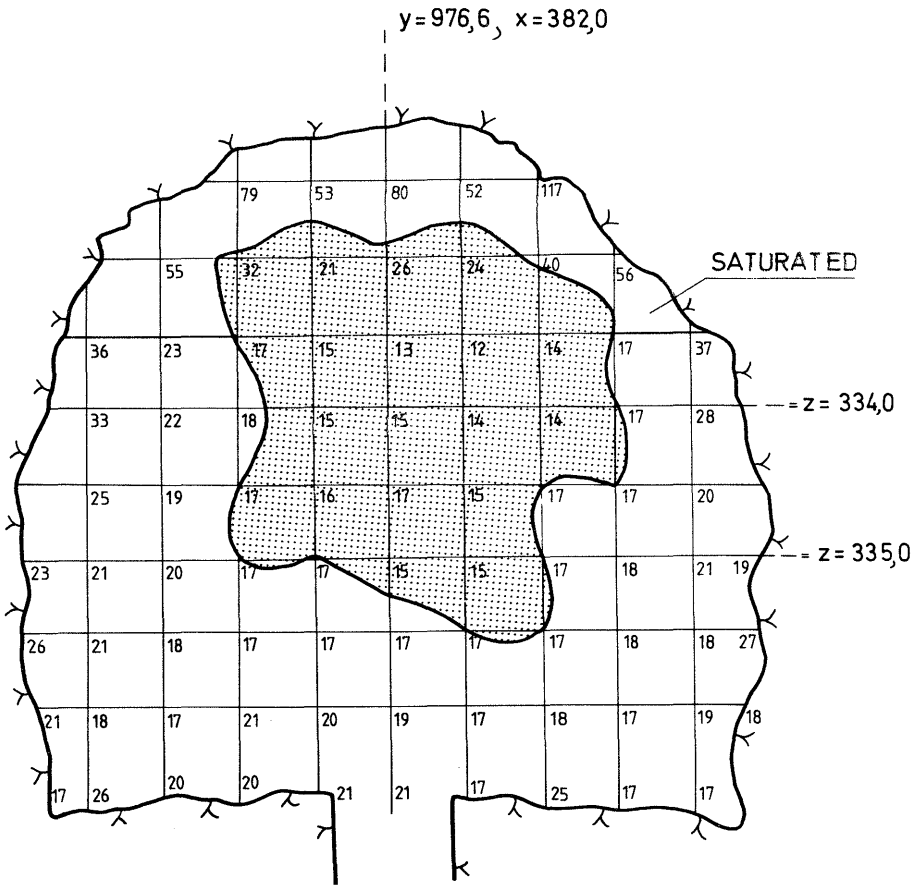

Fig 2.85. Water content distribution in the cross section through heater hole no 1

rock. This fits well with the observed low rate by which piezometric heads were built up at the rock/backfill interface in the tunnel.

It should be noticed that the moisture sensors obviously gave a rather correct picture of the moistening of the tunnel backfill. Thus, the early reaction of the lower three gauges clearly indicated rapid water uptake in the bentonite-poor backfill, while the late-appearing signals in the uppermost part of the blown-in backfill predicted the actual, very slow water uptake.

2.5.3 Conclusions and remarks

The main conclusions concerning the water uptake in the buffer materials are:

1 Initially, there was a heat-induced redistribution of the original water content through which partial drying took place close to the heaters, while water was accumulated close to the rock. This yielded water saturation at the latter site, by which swelling pressures began to appear.

2 Where much water was available in the heater holes, the bentonite took up water at a rate and uniformity which fits with the hydrological model that predicts uniform access to water all over the periphery of the holes, and with the assumption that the water migration is a diffusion process. The distribution and character of visible joints and fractures in the rock did not seem to be of any importance for the uniformity of the moistening process.

3 In holes with insignificant water inflow, the initial, heat-induced moisture redistribution was successively altered by wetting which appears to be very slow in rock with no visible water-bearing discontinuities. This suggests that no net loss of water takes place as long as the absolute heater surface temperature is lower than about 130°C, provided that the upper end of the heater hole is effectively sealed so that no evaporation can take place. Also in "dry" holes the water uptake from rock with a few discontinuities results in a uniform but very slow moistening.

4 In blasted tunnels the fractured floor clearly serves as a major water source for the wetting of the dense bentonite. It also seems as if the base of a few meter deep hole offers substantial amounts of water. The reason for this is that the lower end of such holes extends to a depth where the rock water pressures are high, and that stress concentrations due to geometrical discontinuities ("corners") and drilling operations generate fractures and fissures which increase the hydraulic conductivity of the rock.

5 The moistening of the tunnel backfill took place very uniformly around the tunnel periphery, which shows that the distribution and water-bearing capacity of discrete fractures or sets of fractures are not very important for the distribution of the water uptake.

6 The process of saturation appeared to fit with the one predicted on the basis of uniform access to water at the tunnel periphery, assuming that the migration mechanism is one of diffusion, at least in the initial phase. At later stages the uptake rate may be faster than simple diffusion implies.

The pores of the non-saturated central part of the backfill may have contained slightly compressed air which originated from the initially non-saturated voids of the backfill and that was pushed ahead of the migrating water. In a repository, this air would be dissolved when the water pressure increases, by which complete saturation is ultimately attained.

2.6 Physical processes

2.6.1 General

It is obvious from the preceding text that there was a fairly good agreement between the predictions and the recording of the practically important processes. Thus, the temperatures and swelling pressures were of the expected order of magnitude. Some findings were surprising, however, particularly the very uniformly distributed water migration from the rock into the bentonite also in those heater holes where only a few discrete water-bearing joints or fractures had been identified. Also, it appeared strange that the initial heat-induced redistribution of the original water content was altered to an almost uniform and complete wetting in certain holes, despite the counteracting thermally driven moisture migration. Another surprise was the strong and uniform water uptake by the bentonite-poor part of the tunnel backfill despite the large variation in water inflow from the rock. These conditions can only be explained by considering the detailed physical processes involved in the uptake and redistribution of water in the buffer materials as outlined in this chapter.

2.6.2 Isothermal water uptake in bentonite

2.6.2.1 Microstructural features of highly compacted bentonite

The microstructural constitution of the air-dry bentonite powder used for production of compacted blocks and for the mixing with ballast materials to produce the backfill, is a key to the understanding of the wetting process. The air-dry powder consists of aggregates with aligned, face-to-face grouped smectite flakes with only one interlamellar hydrate layer at a relative humidity of 40-60 %. This corresponds to approximately 10 % water content of the MX-80 bentonite clay. When the powder is compacted under a pressure of about 100 MPa, as in the case of the BMT blocks, the aggregates are forced together

and form a coherent mass with a rather isotropic microstructure and a degree of water saturation which is about 50-60 %. Air is enclosed in larger voids, i.e. pores with an average diameter of about 0.1-50 um, while smaller openings between aggregates and all the interlamellar space are fully hydrated. When water is taken up by this non-saturated, very hydrophilic substance, the number of hydrate layers between the smectite lamellae increases to 2 or 3, while the corresponding theoretical bulk density will be in the approximate range of 2.2 to 1.9 t/m^3 at full saturation. Thus, the wetting yields an improved degree of homogeneity by causing a redistribution of the solid phase that tends to expand small voids at the expense of large ones (Fig 2.86). Still, however, fairly large and more or less continuous passages exist as demonstrated by the micrographs in Fig 2.87.

2.6.2.2 The wetting process in highly compacted bentonite

The exact nature of the water migration and hydration is not fully understood but available information on the physical status of smectite-adsorbed water suggests a strong coupling between the basal planes of the flaky crystals and water molecules, particularly when the exchangeable cations are monovalent (7). Thus, one-layer hydrates in Na-montmorillonite, i.e. the presently investigated clay type, seem to consist of water molecules arranged in a strained, ice-like configuration with strong bonds formed with the oxygens of the silicate surface. Various investigations indicate that the mineral-induced water structure extends over more than 10 Ångström units from the basal planes, and that the strong hydration potential is primarily due to crystal/water interaction through hydrogen and London - van der Waals bonds, and not to osmotic effects when the number of hydrate layers is as small as 3 to 4 (8). The strong hydration means that water molecules are transferred to the sites of strongest ad-

sorption. If there are two adjacent interlamellar hydrates, one of them holding one layer of water molecules and the other three layers, water molecules therefore migrate from the thicker layer to the thinner in a "crystallization"-like fashion. The main consequence of this is that bentonite has an ability to self-heal and become homogeneous and that water is absorbed by "suction".

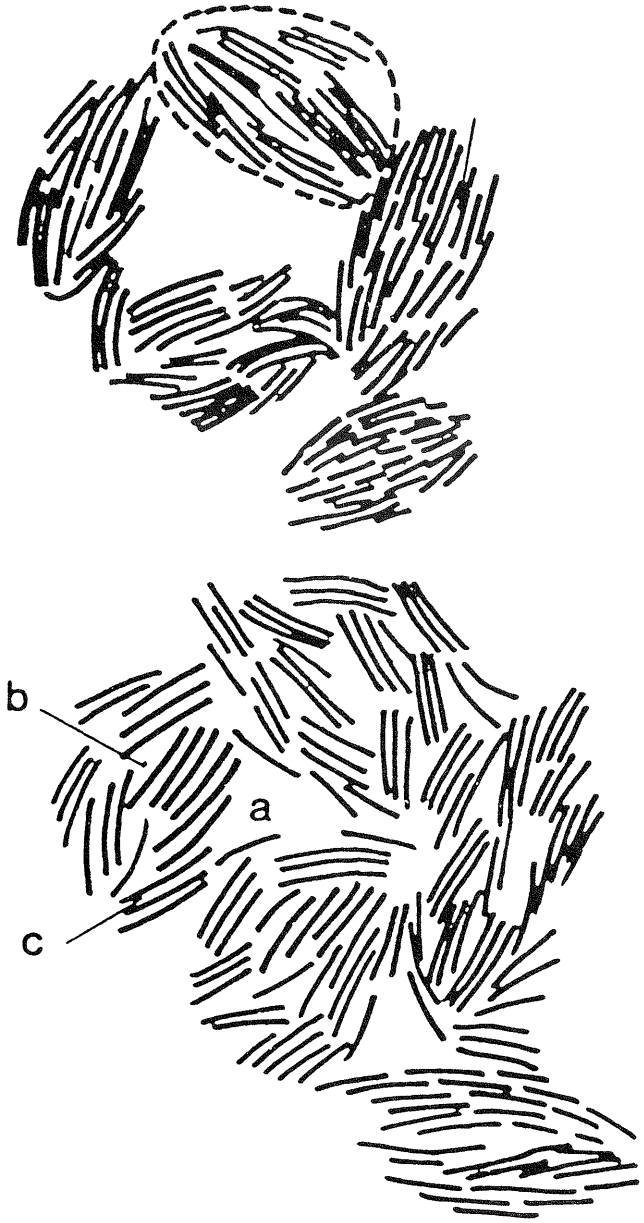

Fig 2.86. Microstructural arrangement of smectite flakes in MX-80 clay. Upper picture: freshly compacted powder. Lower picture: ultimate equilibrium state with largely uniform interparticle distance. a) Large void ($\geq$ 10 μm), b) small void (<10 μm), c) Intra-aggregate inter-lamellar) space

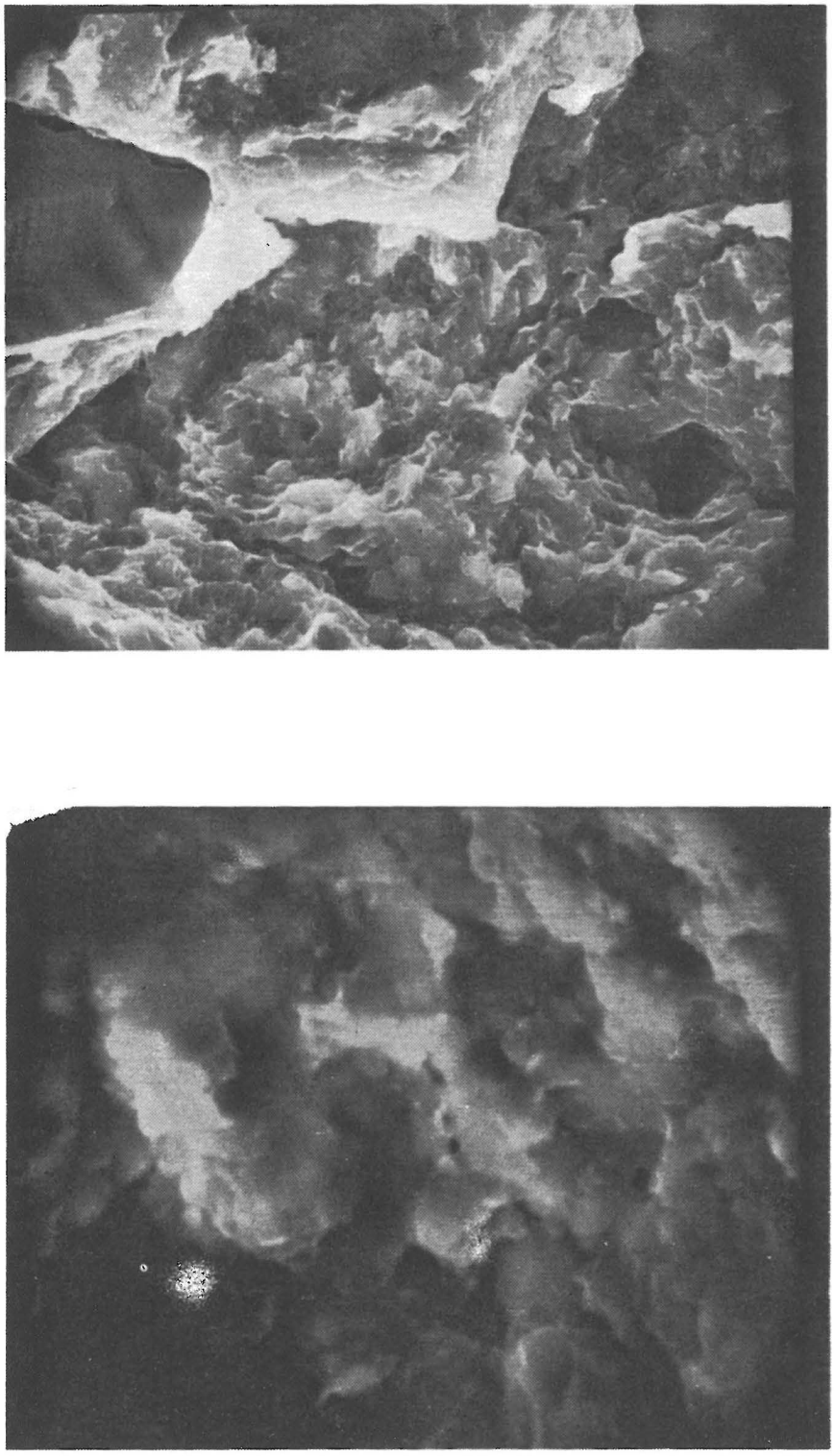

Fig 2.87. Scanning micrographs of freeze-dried MX-80 bentonite. The samples were 1 year old, saturated Na clay. In the left part of the upper picture a fractured calcite crystal is seen. Magnification 1500x

The air that is trapped in isolated voids in highly compacted bentonite will be compressed when water is absorbed by the clay if swelling is prevented. It is dissolved in the water and can leave the saturated clay by diffusion, which explains why the degree of saturation of dense bentonite in swelling pressure oedometers becomes almost 100 % even if no air outlets have been arranged.

The rate of water uptake is largely determined by surface diffusion mechanisms. However, it also seems to be affected by more or less continuous, larger interaggregate voids which act as capillaries and in which water is primarily sucked up when the clay is exposed to an external water source. It is secondarily redistributed into smaller voids and is finally available for interlamellar hydration. This initial capillary uptake is probably insignificant at bulk densities exceeding about 2 t/m^3 but it is assumed to be of great importance when the bulk density is less than 1.5-1.8 t/m^3.

The very high capillary and hydration-related suction, which is of the same order of magnitude as the swelling pressure /with reversed sign, cf.(9)/ implies that saturation cannot be accelerated by applying an external water pressure unless it is very high.

2.6.2.3 Microstructural features of bentonite/ballast mixtures, water uptake in the tunnel backfill

With a properly graded ballast material only 5-10 % bentonite (by weight) is needed to fill up the voids between the ballast grains (Fig 2.87). If the mixing is made at optimum water content the bentonite component becomes very wet by which the ballast grains easily slip into a close layering. The degree of saturation can thereby become as high as 80 % and in this state the air-filled voids are very small and separated from each other. In the BMT case the voids were water-filled to about 60 % and air-filled systems of continuous

passages were consequently numerous. They must have operated as effective conductors in the initial rapid water uptake through capillary action and then served as water sources for the subsequent saturation of smaller, adjacent voids. This suggests that the water uptake rate was exceptionally rapid in the BMT backfills and that it was much less dependent on the piezometric heads at the rock/backfill interface than on the availability of water for suction at this interface.

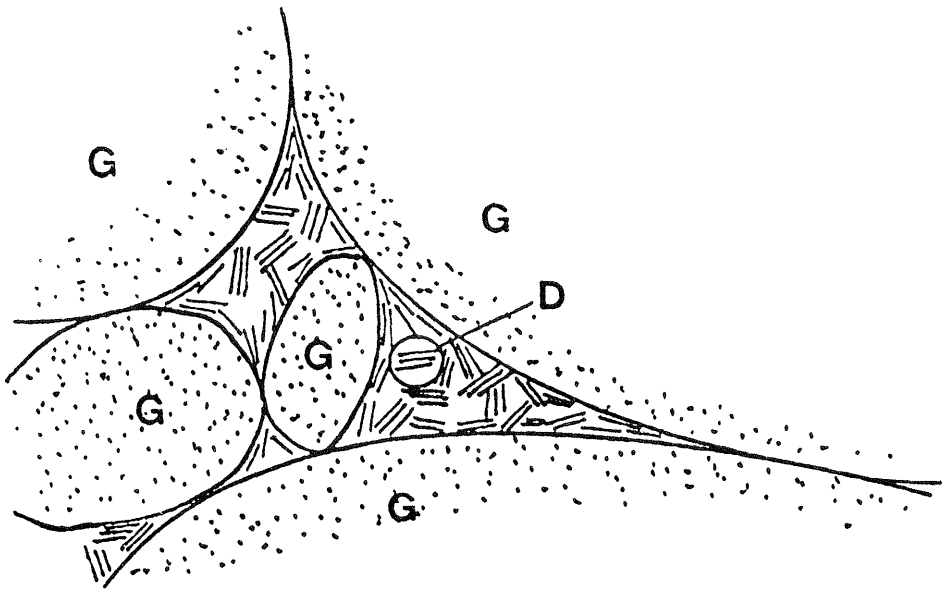

Fig 2.88. Schematic particle arrangement in a meager bentonite/ ballast mixture

The low density of the bentonite gel in the voids of the ballast matrix is not expected to produce significant compression of trapped air and isolated bubbles are therefore expected to be preserved until the piezometric heads become high. Since the initial degree of saturation was low in the BMT backfills, the air could probably be moved fairly easily by penetrating water that was driven by capillary forces as mentioned earlier. This would yield a central air-filled, largely non-saturated zone in the tunnel just as the one that was recognized in the field test. The fact that the upper, blown-in

backfill was less saturated than the lower part is actually also in agreement with this model. Thus, the complete absence of water pressures at the tunnel crown in the course of the test tells us that very little water was available for capillary suction from the rock, while the piezometric heads at the lower parts of the tunnel walls and at the floor, however small, indicate that a sufficient amount of water was discharged from the rock here to allow for rapid wetting of the backfill.

2.6.3 Water uptake in highly compacted bentonite in the presence of thermal gradients

2.6.3.1 General aspects of water migration caused by thermal gradients

Moisture migration in non-saturated soils exposed to thermal gradients is a classical problem in agriculture. There are several theories based on thermodynamics that have been developed for the description and prediction of such migration, but the lack of laboratory-derived parameters and experimentally demonstrated validity on the microscopic level mean that they cannot be applied without the use of empirical coefficients. It is also clear that the physical models that have been derived on this basis all concern rather soft, usually clay-poor soils with very moderate suction power.

Most investigators have claimed that the major mechanism of water transport under the influence of a temperature gradient is that of water vapor diffusion (10). In a closed system the condensation of diffused water vapor within the coldest region will create a moisture gradient and therefore also a pressure gradient within the liquid, from cold to warmer regions in opposition to vapor movement, whereby an equilibrium condition with a water content gradient is established. A slightly different approach was early made by some well

established soil physicists from the USA and USSR /Winterkorn, Derjaguin, Lebedev etc, cf. (11)/ who stated that moisture migration is basically a film transport phenomenon. As explained earlier, the flow is due to unbalanced tangential surface forces which cause slippage along the soil particle surfaces and as a result, water moves in the films, the different film thickness giving rise to a gradient in surface forces.

The flow, expressed for uniaxial migration of water, can be put as:

$$q = C_1 \cdot \frac{\Delta\Psi}{\Delta x} \cdot A_e \qquad (1)$$

where C_1 = constant

$\frac{\Delta\Psi}{\Delta x}$ = moisture content potential

A_e = effective pore section area

Considering the particular physical state of the pore water in dense smectites and their characteristic microstructural features it is clear that the effective pore section area should be understood as the part of a cross section that consists of the second and third and possibly fourth hydrate layers that are adsorbed on the basal planes of the smectite crystallites. Since this fraction is a function of the water content as well as of the degree of saturation, A_e represents a rather ill-defined average value.

Increased temperatures lead to stronger thermal vibrations and a drop in adsorption energy and consequently also a decrease in activation energy for migration. This results in a vaporization of a certain fraction of the adsorbed water in a closed system. In the presence of thermal gradients, the major effect is a film movement due to the change in adsorption energy that is related to the temperature change. This flow has been termed "thermo-capillary" flow, the average rate of which can be expressed as:

$$v = C_2 \cdot \frac{\Delta T}{\Delta x} \qquad (2)$$

where C_2 = constant

$\frac{\Delta T}{\Delta x}$ = thermal gradient

If the film concept applies, meaning that all water molecules migrate along mineral surfaces, the effective pore section area is the same both for water moving due to water content gradients and for "thermo-capillary" flow. At equilibrium we would then have:

$$\frac{\Delta \Psi}{\Delta x} = k_1 \cdot \frac{\Delta T}{\Delta x} \qquad (3)$$

or

$$\frac{\Delta w}{\Delta x} = k_2 \frac{\Delta T}{\Delta x} \qquad (4)$$

where k_1 and k_2 = coefficients

w = water content

T = temperature in centigrades ($T > 0^oC$)

It can be concluded from this that for non-saturated soils with constant total amounts of water and solid constituents, there may be a characteristic relationship between the temperature gradient and the water content gradient. Theoretically, the same reasoning can be applied also if water migration in gaseous form is assumed to be caused by the thermal gradient but this requires that the effective pore section area for vapor movement is the same as that for film transport. This can only be the case for low degrees of saturation.

A number of laboratory tests with confined samples of MX-80 bentonite with an original water content of about 10 % were conducted in Luleå a few years ago and they yielded an approximate gradient ratio k_2 of about 0.002. This implies that a thermal gradient of 2.0^oC per cm would produce a water content gradient of 0.4 % per cm provided that mass preservation holds. If this coefficient is applied to the "dry" heater holes (no 3, 4 and 6), where the thermal gradient at mid-

height of the heaters was about 2.0°C per cm and where insignificant amounts of water were taken up in the entire test periods, we would expect to have a water content difference of about 6 percent units from the heater surface to a distance of 10-15 cm from this surface. This is very close to what was actually observed in the tests in the "dry" holes as shown by the k_2-values in Figs 2.89 - 2.91.

2.6.3.2 Tracer tests

At the preparation of the heater test in the "wet" hole no 5 in early 1982, hairpin-shaped, finely porous filters were arranged vertically at the rock/bentonite interface as well as close to the heater (cf. Volume I, Chapter 4.29). The filters were originally intended for diffusion tests, but were instead used for identifying the major physical processes associated with the thermal gradients. For this purpose the outer filters were filled with Methylene Blue solution (200 ppm) and the inner ones with hydrogen sulphide gas.* No pressure was used in either case. The main idea was that the dye, which is known to have a very low diffusion rate and to move mainly with flowing water through wider clay pores, was expected not to be transported from the filter if the degree of saturation and homogeneity were high during the testing. The hydrogen sulphide gas, on the other hand, was expected to be dragged from the filter by water vapor flowing from the warm heater and producing blackish sulphide compounds by reacting with the iron content of the bentonite, thus indicating the existence of continuous non-saturated pores close to the heater. If, unexpectedly, a high degree of saturation would be at hand here, blackening would still take place through diffusion of dissolved hydrogen sulphide, which has a diffusion coefficient of

---

* The gas indicator was suggested by Professor Ingemar Grenthe, Royal institute of Technology, Stockholm, Sweden

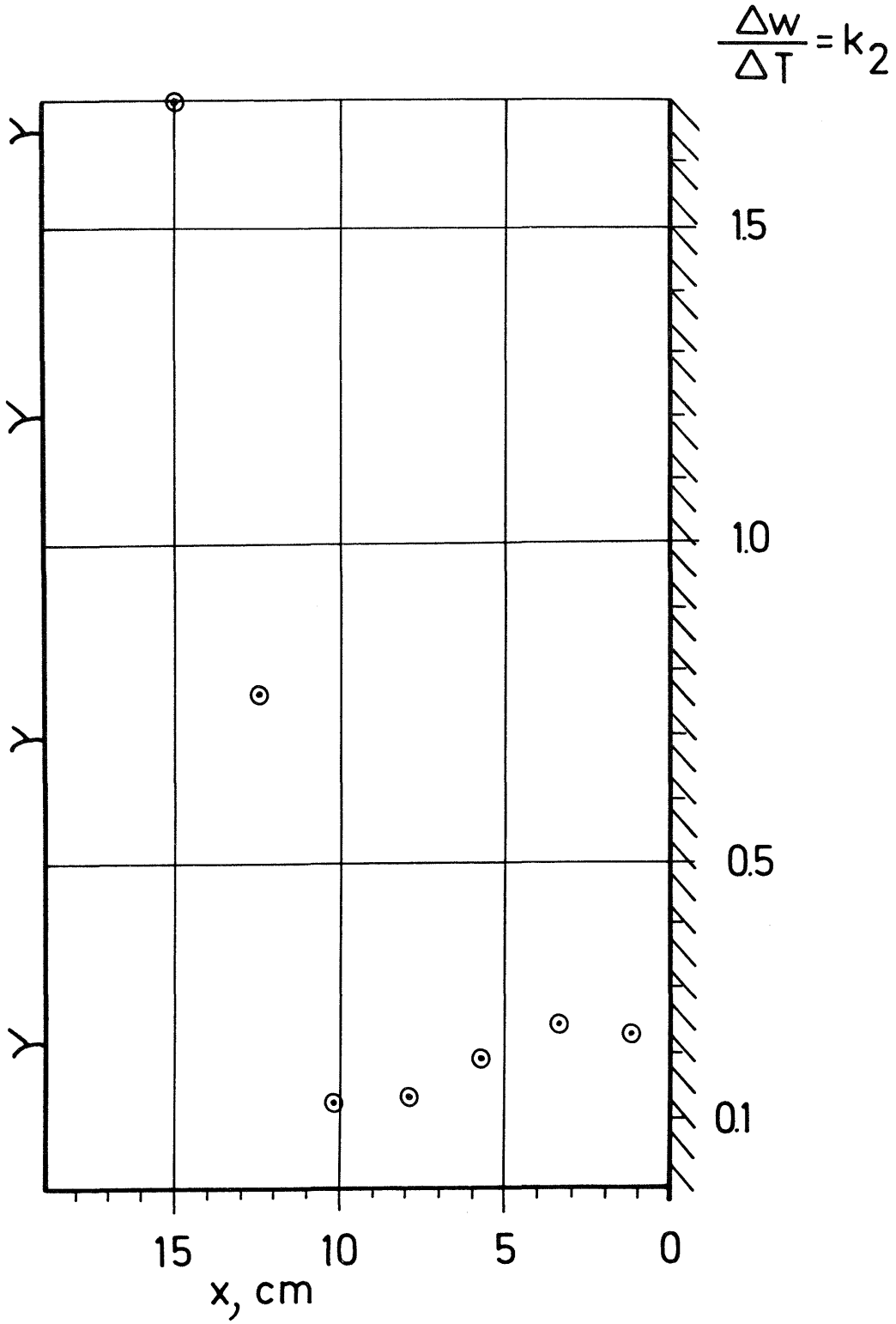

Fig 2.89. Moisture/temperature ratio (k_2) in hole no 4 at various distance x from the heater at the end of the 10 month test. Mid-height of the 600 W heater

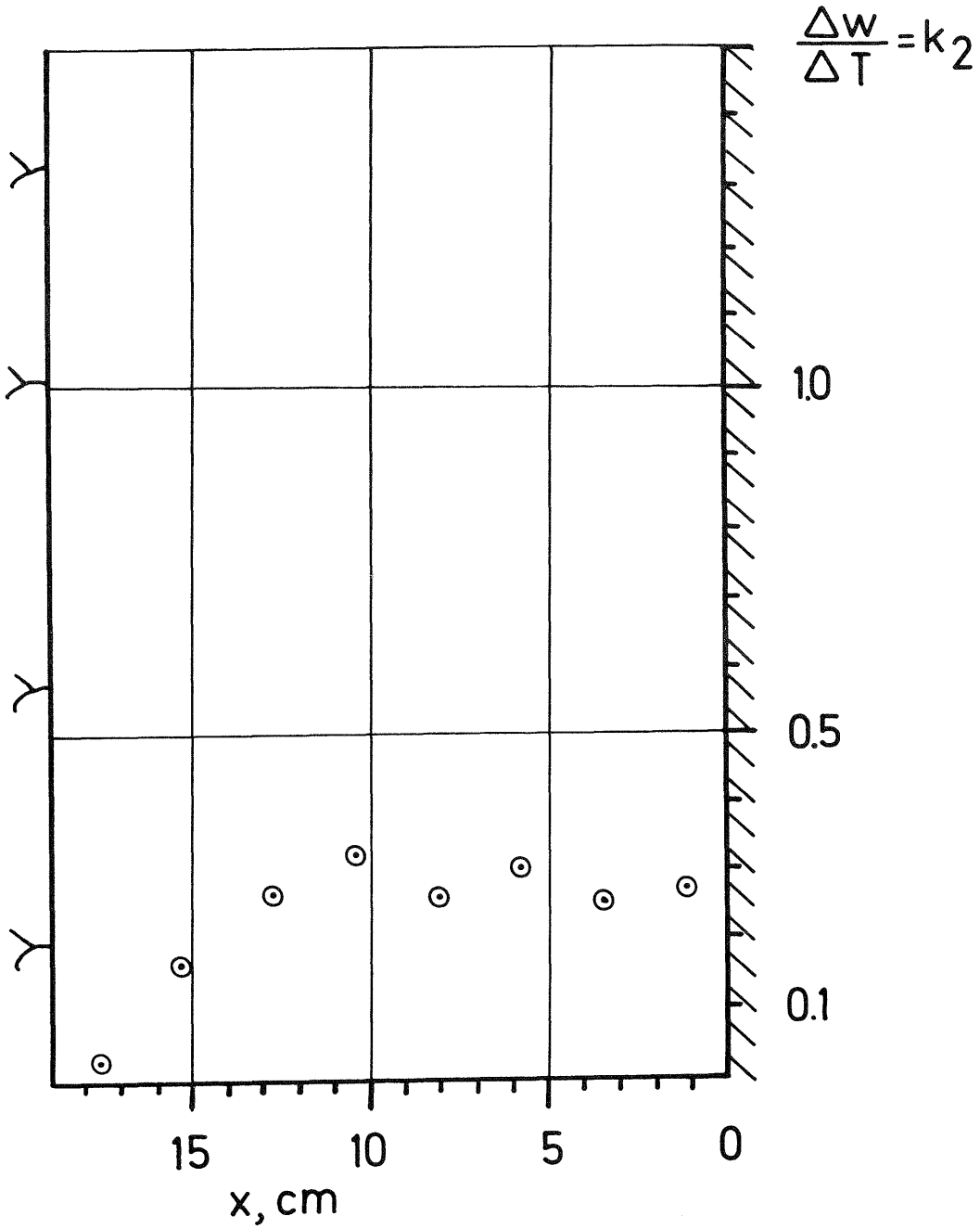

Fig 2.90. Moisture/temperature ratio (k_2) in hole no 3 at various distance x from the heater at the end of the 8 month, high temperature test. Upper edge of the 1800 W heater

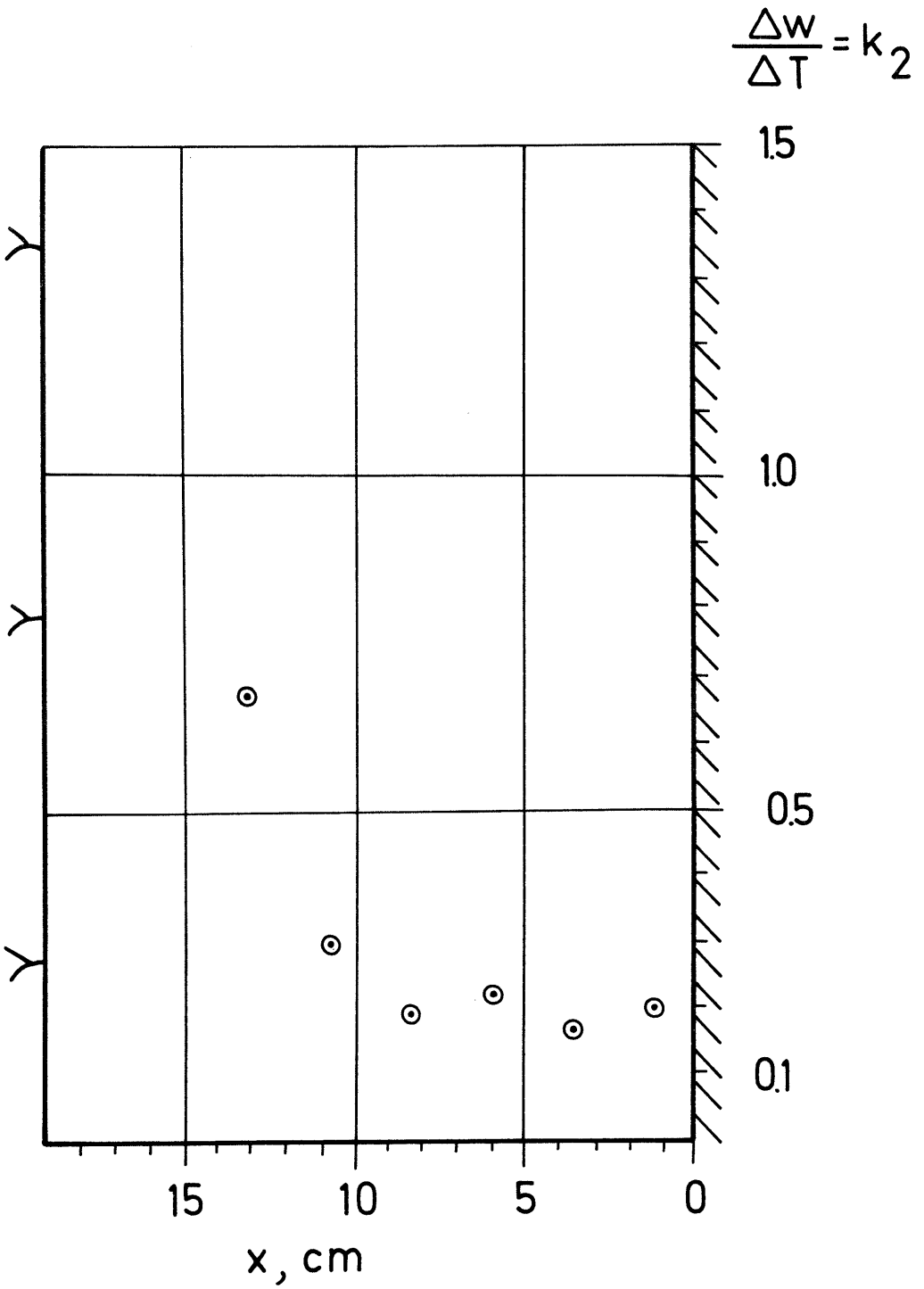

Fig 2.91. Moisture/temperature ratio (k_2) in hole no 6 at various distance x from the heater at the end of the 25 month test. Mid-height of the 600 W heater

about 9×10^{-12} m^2/s (12), but the coloring of the reaction zone should then typically be very weak at the front and strong at the filters. This is in contrast with the gas reaction process which was expected to yield a uniform blackening with a rather sharp front where the pores were no longer continuous.

At the excavation of hole no 5, it was found that the tracer tests using hydrogen sulphide and methylene blue had given very valuable information. The dye, which is known to move readily with flowing pore water in larger voids in structurally heterogeneous clay but to migrate extremely slowly by diffusion in dense clays as most high molecular weight dyes (13), was found to be present only in and very close to the filters at the rock/bentonite interface (Fig 2.92). This confirms that the bentonite had already matured and self-healed the original joints between the blocks at the onset of the tracer test 5 months before the excavation took place.

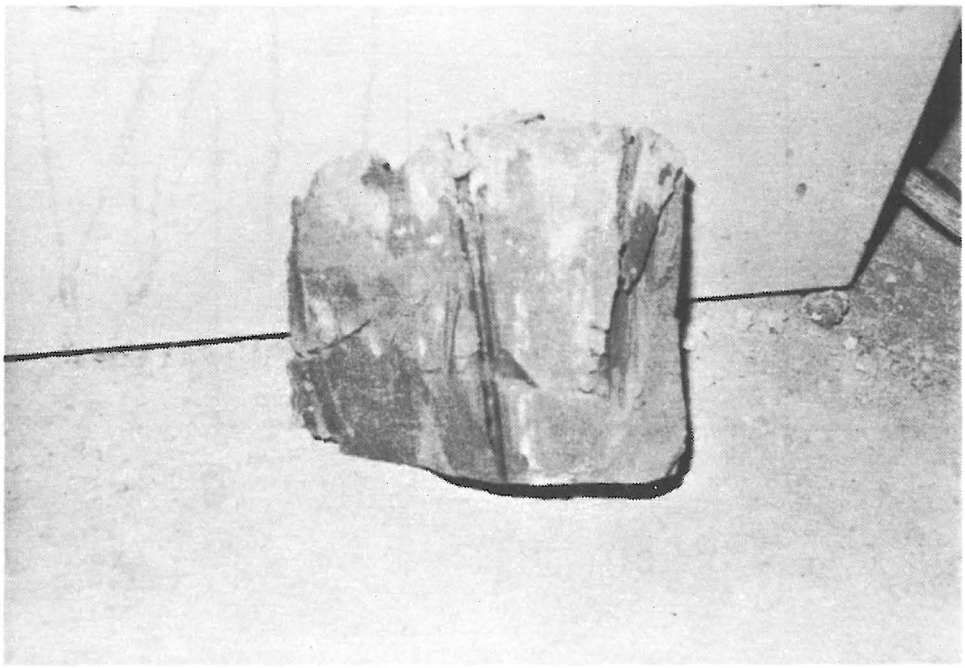

Fig 2.92. Appearance of contact between filters and bentonite close to the rock at the excavation of hole no 5. The dye had not entered the bentonite to more than a few millimeters

The hydrogen sulphide gas that was introduced in the filters close to the heater, reacted with the bentonite exactly as expected, i.e. by forming blackish iron sulphide with the iron content of the bentonite. The black zone extended radially about 1.5-3 cm from the filters over the lower half of the heater and to about 6 cm from the heater at its upper part. The blackening was rather uniform over the reaction zone extending from the filters, which suggested that the reactive gas did not migrate by diffusion. Instead, the hypothesis appeared to be confirmed that the gas moved with vaporized pore water in the continuous cyclic vaporization/condensation water movement induced by the thermal gradient in the non-saturated bentonite close to the heater (Fig 2.93). However, the reaction zone had a larger extension at the upper part of the heater which is not in agreement with the moisture distribution in Fig 2.70 if vapor transport would be a true mechanism. Since this figure clearly shows that the degree of saturation was actually much too high to offer continuous passageways for vapor transport, it is still probable that diffusion in water contributed to the migration of the hydrogen sulphide.

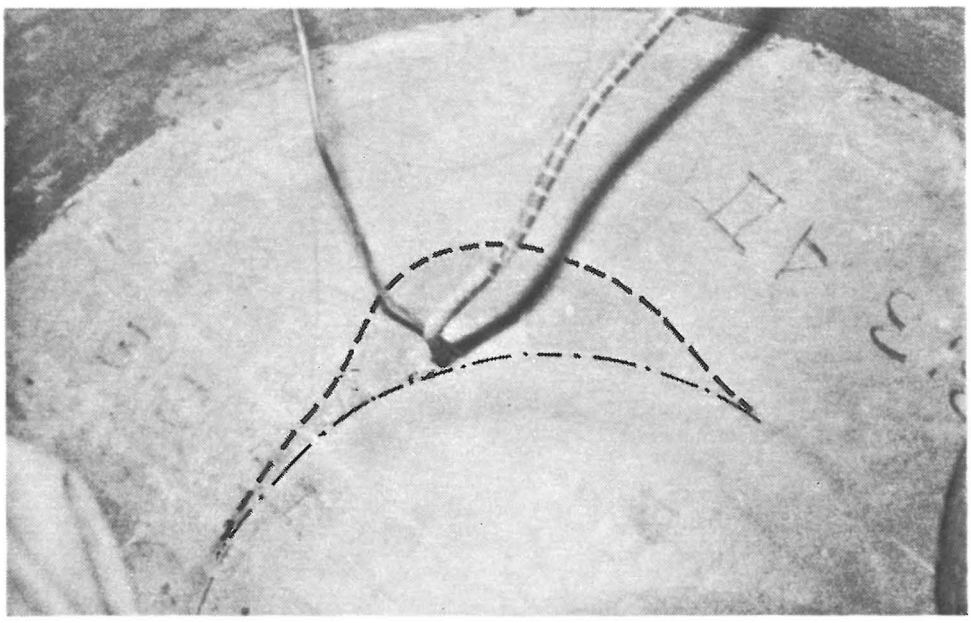

Fig 2.93. Iron sulphide zone close to the heater. The "down the hole" photo was taken at the excavation of the bentonite, the level corresponding to the lower end of the heater

Cyclic water movement could possibly result in salt accumulation close to the heater, or more generally, at the surface of a canister in its deposition hole. To check whether this had occurred in hole no 5, the amount of soluble sodium chloride wad determined in samples located as shown in Fig 2.93. The analysis did not give evidence of this process, as demonstrated by Table 2:16, which supports the assumption that the extension of a possible zone of vaporization/ condensation must have been very small. It should be noticed that the rather high salt content stems for the natural bentonite and not from the Stripa groundwater.

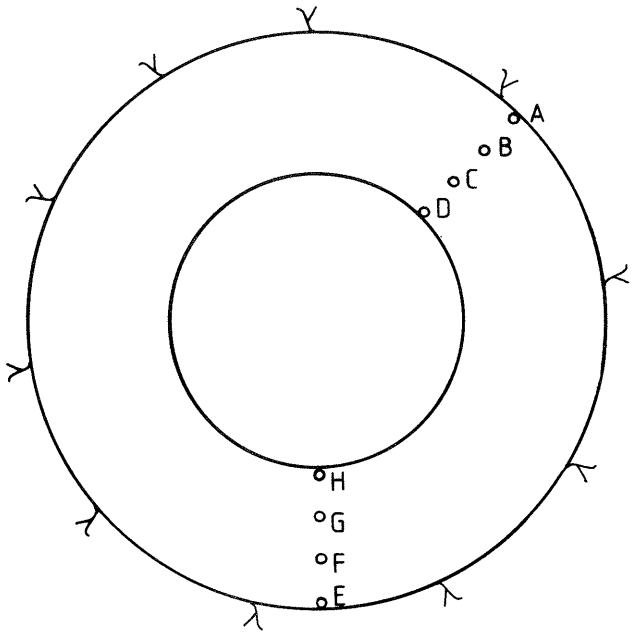

Fig 2.94. Location of samples used for salt determination in heater hole no 5

Table 2:16. Salt distribution as a function of the distance from the surface of the heater in hole no 5

Code	Distance from heater surface, cm	Total amounts of Na %	Cl ppm
D	1.5	2.5	200
C	6.8	2.4	150
B	12.1	2.6	150
A	17.5	2.5	150
H	1.5	2.6	150
G	6.8	2.6	100
F	12.1	2.6	100
E	17.5	2.5	150

2.6.3.3 Water migration as interpreted from the "high temperature" test

At the application of the second set of bentonite blocks in hole no 3 special measures were taken to prevent evaporation and loss of water through passages along the heater shaft, which was assumed to have contributed to the low water contents of the bentonite close to the heater in the preceding 600 W test. For this purpose the shaft was surrounded by tightly fitting collars. Also, the bentonite was equipped with Vaisala HMP 19 UT gauges for measuring the relative humidity at different distances from the rock at mid-height of the heater. These sensors yield a signal which is primarily a function of the moisture content in the air that is contained in the porous filter tips, and which is transformed into digital RH readings.

The RH-measurement was applied in order to obtain indirect information about the amount of adsorbed water. Thus, preceding laboratory investigations (2) had indicated that there is a unique relationship

between this amount and the relative humidity, and that it is only slightly affected by the temperature (Table 2:17).

Table 2:17. Approximate relationship between the water content (w) and the ambient relative humidity (RH) for smectite rich Na saturated clay (after Knutsson)

RH %	w %
7	3
15	5
25	7
35	8
50	10
65	12
75	15

The RH-recordings are plotted in Table 2:18, which also gives the temperature at the bentonite/rock interface and at the heater surface at mid-height of the heater. In addition, the swelling pressure recordings are presented in the last two columns. The temperature of the clay at the gauge located 7 cm from the rock was 70°C as an average, while it was approximately 90°C at the gauge that was situated 12 cm from the rock.

Table 2:18. Recordings of the relative humidity, temperature and swelling pressure at mid-height of the heater in hole no 3, 1200 W

Recordings at mid-height of the heater in hole no 3, 1200 W power, att different times after test start

Time	Temp* heater	Temp* rock	Rh 1 cm fr rock	RH 7 cm fr rock	RH 12 cm fr rock	Gloetzl press west	Gloetzl press east
weeks	°C	°C	%	%	%	kPa	kPa
0	15.0	14.0	60	54.0	54.0	0	0
2	119.9	52.1	82	63.0	64.0	62	110
4	121.6	54.6	82	59.0	57.0	286	286
6	122.1	55.5	85	54.5	54.5	590	466
8	122.4	56.0	90	53.0	54.0	648	499
10	122.7	56.5	95	53.0	54.0	792	600
12	122.9	56.8	96	53.0	54.5	817	631
14	123.2	57.2	98	54.0	55.5	836	644

---

* Northern set of thermocouples (towards heater no 2)

It is obvious from the Gloetzl cell reactions that the bentonite close to the rock took up water early in the test and continued to do so. The pressure actually increased much faster than in the 600 W test, which is due partly to the increased access to water in the high-power test, partly to the smaller width of the slot with the porous bentonite, and partly to a more intense thermally induced moisture transfer from the interior. The narrow slot reached a high degree of water saturation soon after test start and initiated rapid swelling of the adjacent highly compacted bentonite.

The RH gauges reacted logically: the initial increase in relative humidity of the two central gauges is simply related to vaporization with the moisture still retained in the pores, while the subsequent

drop was largely due to the temperature rise. The outer gauge signalled a continuous increase in water content due to water inflow from the rock and - after a while - also through moisture transfer from the interior. The fact that the two central gauges showed practically the same value despite the different temperatures demonstrates that there were different amounts of water in vapor form and, specifically, a higher vapor pressure at 12 cm distance from the rock than at 5 cm distance. It is concluded from this that the pores in the outer 12 cm clay annulus were not continuous and did therefore not serve as passages for long-range vapor flow. This is consistent also with the water content value that can be derived from Table 2:17. Thus, we find for an RH value that slightly exceeds 50 % that the water content should be at least 10 %, which implies 50-60 % water saturation and isolated air-filled voids. The actual water content in the outer 12 cm thick annulus was found to be even higher than this value (cf Fig 2.77) despite the fact that the power was raised to 1800 W in a late phase before the excavation took place.

The observations made in the course of the "high temperature" test are of fundamental importance for the understanding of the main features of the water migration. Thus, they indicate that the suction power of very dense Na-rich smectite is sufficiently strong to yield water uptake even when counteracting thermal gradients of more than $3^{o}C$ per centimeter are applied. A necessary prerequisite is of course that water is available for uptake by the bentonite from the surrounding rock.

2.6.3.4 Distribution of water migration over the rock/bentonite interface in the heater holes

The remarkably uniform water uptake in the bentonite over the larger part of the rock/bentonite interface in the heater holes is explained

by the swelling potential of the bentonite, and by the hydraulic conductivity not only of fractures and fissures in the rock but also of the crystal matrix. Laboratory tests as well as theoretical considerations (14) have shown that highly compacted bentonite is able to penetrate joints and fractures in the rock (cf. Fig 2.95). The rate of penetration and the depth that can be reached by expanding Na bentonite is a function of the bulk density of the bentonite and of the chemical composition of the water as well as of the aperture of the discontinuity.

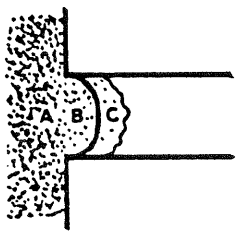

Fig 2.95. Schematic picture of observed zones in wider slots. A very stiff bentonite, B fairly stiff region, C very soft region

The minimum aperture of fractures into which bentonite can penetrate with a significant rate to form a relatively stiff filling is approximately 0.1 mm, the approximate rate of penetration being illustrated by Table 2:19.

These data represent measured penetration depths in systematic laboratory investigations using MX-80 bentonite and distilled water (14). The tests confirmed that the process is very much retarded following approximately a log time law.

Table 2:19. Measured penetration depth of bentonite expanding into slots in Stripa granite. Laboratory tests (14)

Aperture mm	Time months	Filling with stiff consistency (1.5-1.7 t/m^3), mm	Soft front mm	Remark
1.5	3	23	20	Nat fracture
1	2	10	30	Plane slot
0.5	3	7	15	"
0.4	3	5	10-15	"
0.3	3	4	10	"
0.2	3	3	10	"
0.1	3	2	10	"

The fracture logging of the rock exposed in the heater holes showed that 2-10 potentially water-bearing joints or fractures intersected each hole (Volume I, Chapter 3.4.2.3, Figs 3.4 to 3.9). At least one fracture in each hole had a visible aperture of about 1 mm, which must have been effectively sealed by penetrating bentonite within a few months, according to the laboratory study. This was also found to be the case as demonstrated by Fig 2.96; all fractures with visible apertures were actually sealed with bentonite that had an estimated bulk density of at least 1.5 t/m^3. The major natural inclined fractures with an aperture of about 0.5 mm in the "wet" holes had been filled with dense bentonite to a depth of 5-10 mm in 2 to 3 years, which is in reasonable agreement with the laboratory-derived values.

This self-sealing process must have had a significant effect on the distribution of water in the rock. Thus, while the initial flow towards the holes probably took place in a few discrete, wider rock discontinuities, the water was successively directed to fractures with a smaller aperture, and in the late phase most of the water may

have entered only through the fine capillaries formed by the fissures and incomplete mineral contacts in the crystal matrix. This matrix has been found to have an average hydraulic conductivity in the order of 10^{-13} - $5 \cdot 10^{-13}$ m/s (15), which is actually about the same as the conductivity of the water saturated, highly compacted bentonite. The inflow into the holes through this low-permeable matrix required considerable hydraulic gradients which may have been offered by water overpressures in the rock or by suction produced by the bentonite. We will see here that both are possible.

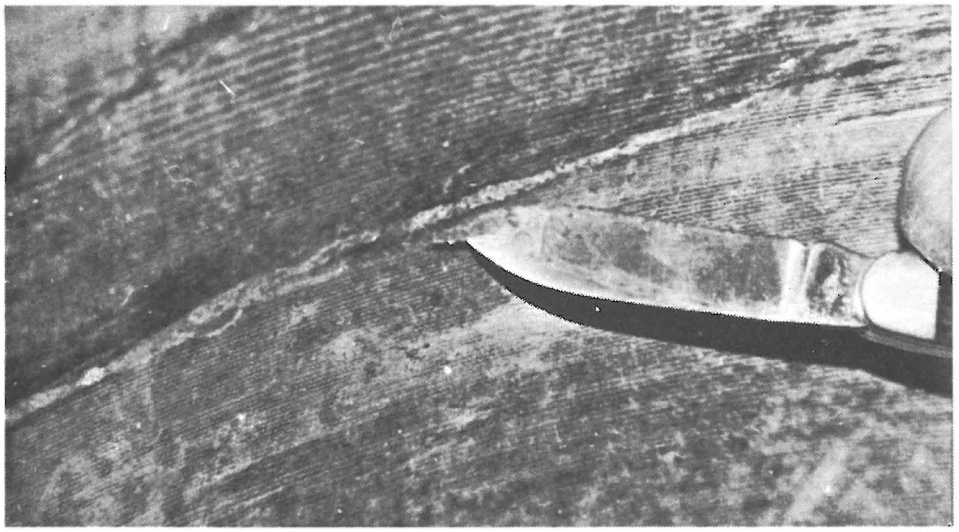

Fig 2.96. Bentonite-filled fracture in the rock wall

Considering first the case of rock water overpressure we can assume the crystal matrix to be approximated as a homogeneous porous medium, which offers a way of estimating the radial inflow into the heater holes by applying simple potential theory (cf. Fig 2.97):

$$q = \frac{k \cdot 2 \pi b(h_2 - h_1)}{\ln (r_2/r_1)}$$

where q = volumetric water flow rate into the infinitely long opening

k = coefficient of hydraulic conductivity

r_1 and r_2 = radial distances from the hole axis to the first and second water head measuring points

h_1 and h_2 = pressures at distances r_1 and r_2, respectively

b = length in axial direction of inflow

This flow equation is valid for steady flow conditions, which puts certain restrictions to its use. As to the pressure heads, the LBL gauges constantly yielded a h_2 -value of 80-130 m water head at r_2 = 10 m, while h_1 was considerably lower and slowly increasing. A reasonable and conservative assumption is that h_1 was 10 m at r_1 = 1 m during the first year of operation for all the BMT heater holes.

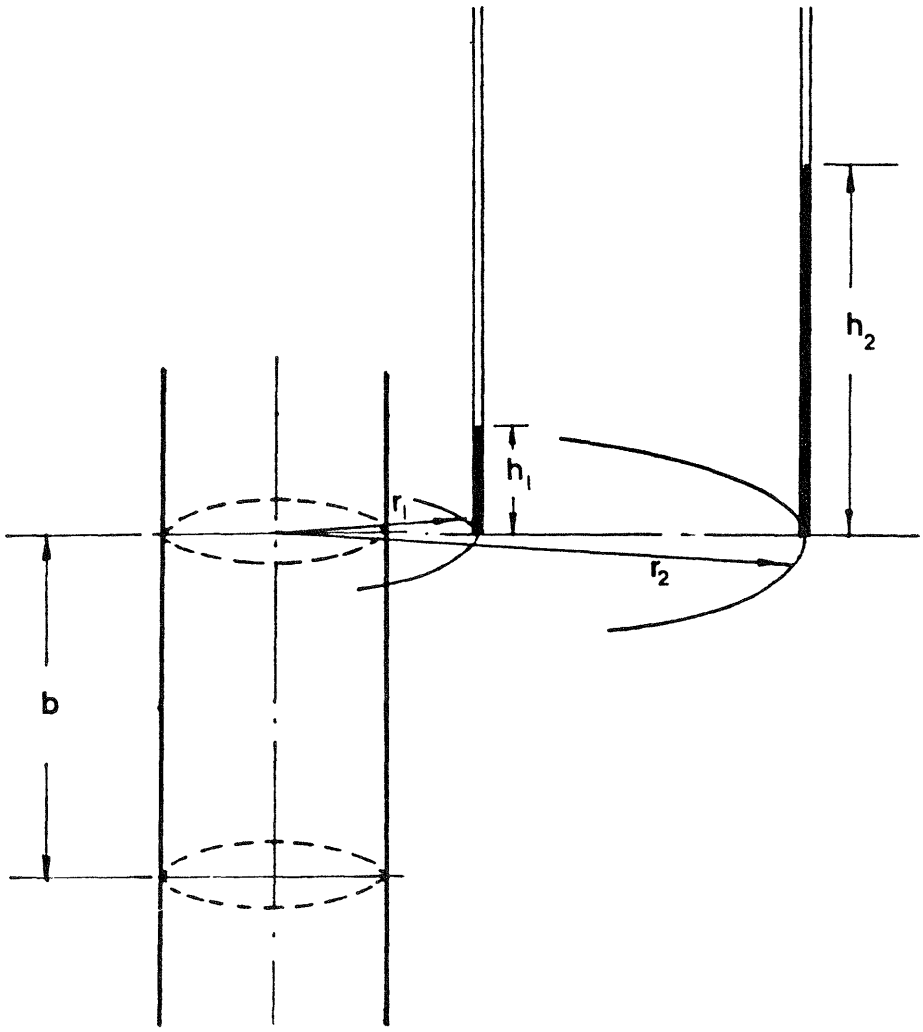

Fig 2.97. Flow conditions in porous medium with long cylindrical hole

If the respective values are introduced in the formula, and using the average of the conductivity values, we arrive at a radial, uniformly distributed inflow of about 6 ml/day over the 1 m high zone of fracture-poor rock in hole no 3, and about 9 ml/day over the corresponding 1.5 m high zone in hole no 4. In the first 15 months of the test in hole no 3, the inflow would be about 1.8 liter, which is very near to the recorded net water uptake in the fracture-poor part of hole no 3. In hole no 4 the corresponding theoretical figure for 10 months is also about 1.8 liters, which is almost exactly the recorded uptake. If the degree of fissuring is taken three to five times higher and the estimated inflow correspondingly higher, the conditions may be representative of those at holes no 1, 2 and 5. Actually the sum of the corresponding inflow over the 1.5 m high central zone and the initial amount of water in the open slots of the "wet" heater holes would roughly correspond to the amount of water that was taken up in these holes during the respective test. These calculations show that the water flow capacity of the rock was the controlling factor of the water uptake and not the absorbing capacity of the bentonite. It is concluded from this that the external piezometric heads were sufficient to produce the required hydraulic gradient. Theoretically, however, the suction power of the bentonite would also be able to bring in the corresponding amounts of water. In the latter case negative pore pressures would have resulted and they may actually also have existed in the finest water passages.

2.6.3.5 Distribution of water migration over the rock/backfill interface in the tunnel

The rather similar moisture distribution patterns in all the 11 investigated cross sections that were observed in spite of the very obvious variation in water bearing capacity of the rock, suggests a water redistribution pattern similar to that of the rock around the

heater holes. Thus, water initially flowing from the two zones in the western wall which gave off much water in the inflow study (x = 376-378, and x = 381-382, respectively) probably produced local swelling and sealing, by which water was directed to those parts of the tunnel periphery which represented permeable zones of the second order. This process, although producing a very heterogeneous moistening of the backfill in the initial stage, may later have yielded a very uniform access to water over the entire rock/backfill interface. This would fit well with the observed moisture distribution.

The assumed major water uptake mechanism in the fill, i.e. capillary suction, may have produced negative pore water pressures also in many fractures, wich served as flow paths. It is estimated that joints and fractures with a smaller aperture than about 0.01 mm did hardly contribute to the wetting of the backfill and since passages in the range of 0.01-0.1 mm have a very low discharge capacity it is assumed that only discontinuities with an aperture exceeding 0.1 mm, i.e. visible joints and fractures, contributed substantially to the water feeding of the backfill.

2.6.4 Mechanical interaction of swelling bentonite and rock in heater holes

2.6.4.1 Displacement of the interface between the highly compacted bentonite and the overlying sand/bentonite

The copper coin arrays that were put on the top of the upper bentonite block layer in the holes gave information about the upheaval of the top surface at the excavation. It amounted to slightly more than 5 cm in holes no 2, 3, 5 and 6, while it was 7 cm in hole no 1, where the test was of longest duration. These values are in good agreement with the predictions (cf. p. 58). In the 10 months long test in hole no 4 it was approximately 4 cm, which indicates that the rate of heave was approximately the same in all the holes and that the rich

access to water at the fractured tunnel floor gave equal opportunity to water uptake. This is compatible with the water content distributions in the upper block layers in the holes, and with the observed swelling pressure distribution.

In holes no 2 and 5 the heave was slightly higher at the rock than at the heater shaft. This bowl-shape may indicate that the rock acted as the major water source through subhorizontal fractures located close to the upper boundary of the highly compacted bentonite. In the other holes, the sand/bentonite backfill being water-fed from the uppermost part of the tunnel floor, may have contributed more to the wetting of the dense bentonite.

2.6.4.2 Rock displacements around heater no 5*

The expected measurable effect on the rock in heater hole test no 5 was a thermally induced upward expansion, and a superimposed uplift due to axial lifting forces caused by the swelling of the upper part of the bentonite overpack.

The moderate heating of the rock was expected to give small deformations only, and the accuracy of the measurements therefore had to be high. A conservative estimate based on the instrument data, repeated calibrations, temperature compensation, and observed reproducibility, yielded the net accuracy 10 μm/m of individual measurements.

The results of the investigation are compiled in Fig 2.98. The major part of the strain was developed in the first month, i.e. in the period during which most of the heating took place. The vertical strain at about 1 m below the base of the heater hole was zero, while it was approximately 50×10^{-6} about 0.5 m below the tunnel floor.

---

* Results reported by Bengt Leijon, Div of Rock Mechanics, University of Luleå, Sweden

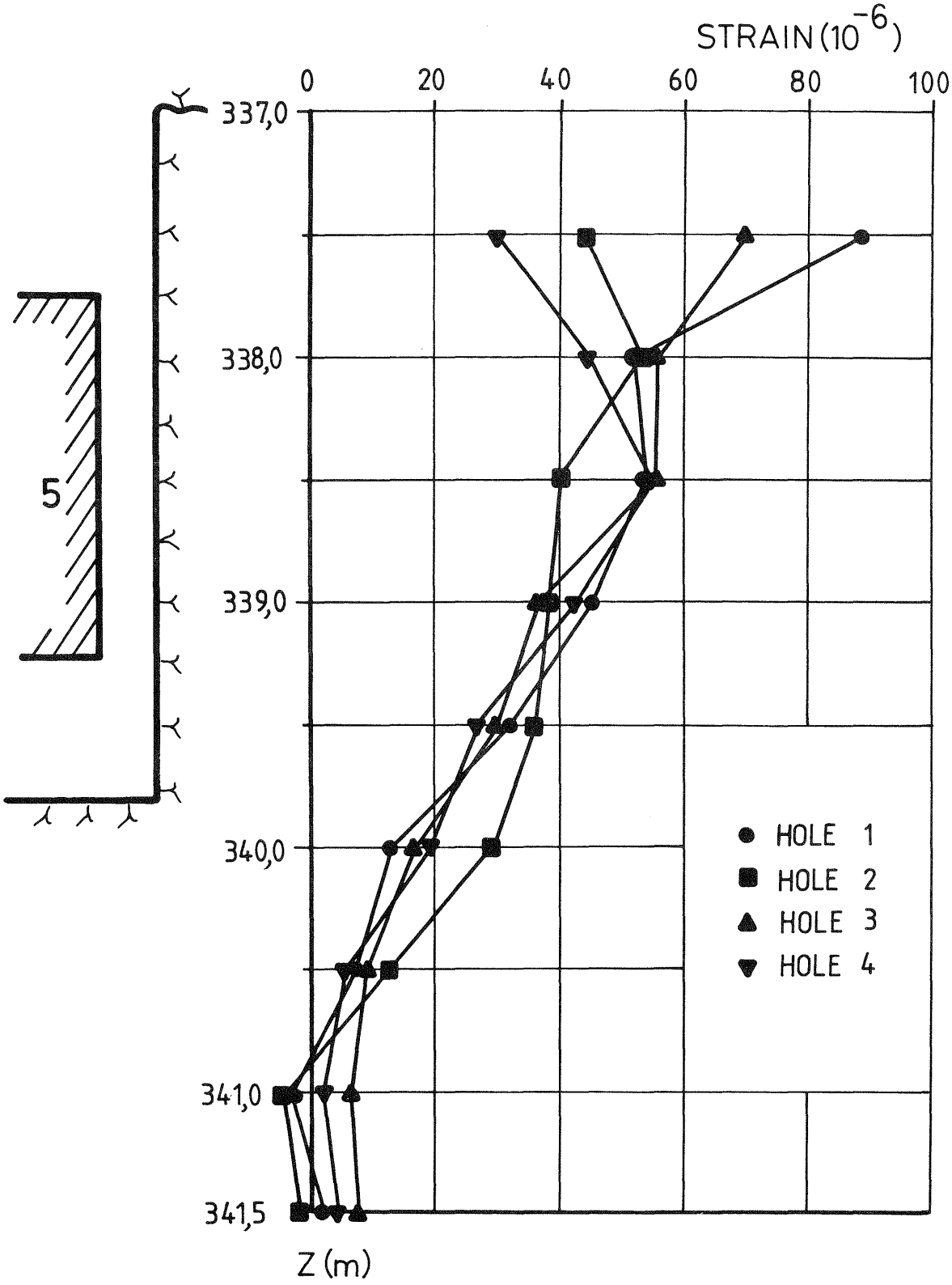

Fig 2.98. Vertical strain in the rock surrounding heater hole no 5 as a function of depth. The data represent the average of 4 readings in 2 years

The accumulated vertical displacement of the tunnel floor varied between 0.13 and 0.18 mm in the holes, the average heave being 0.15 mm.

After the development of the initial heat-induced rock deformations essentially no additional strain was recorded. The rather uniform strain profiles indicate that the joints and fractures did not affect the thermal expansion. Thus, the expected discontinuous deformation on heating and on build-up of swelling pressures that was assumed to be due to the steeply inclined open fracture (Fig 2.99) intersecting the hole, was not observed.

The lack of influence of the vertical drag forces on the aperture of the large subhorizontal fracture which reaches down to about z = 337.6 in the upper part of the hole is not readily explained. It is possible that some of the vertical expansion took place at such an early stage that its effect on the rock could not be distinguished from the thermal influence. An additional explanation may be that the induced strain was in the same order of magnitude as the accuracy of the measurements, i.e. about 10 μm. The Kovari installation did not reach up to the top of the tunnel floor and the possible heave due to increased fracture apertures in the uppermost part of the rock forming this floor could therefore not be determined. However, ocular inspection showed no obvious sign of any expansion of this kind.

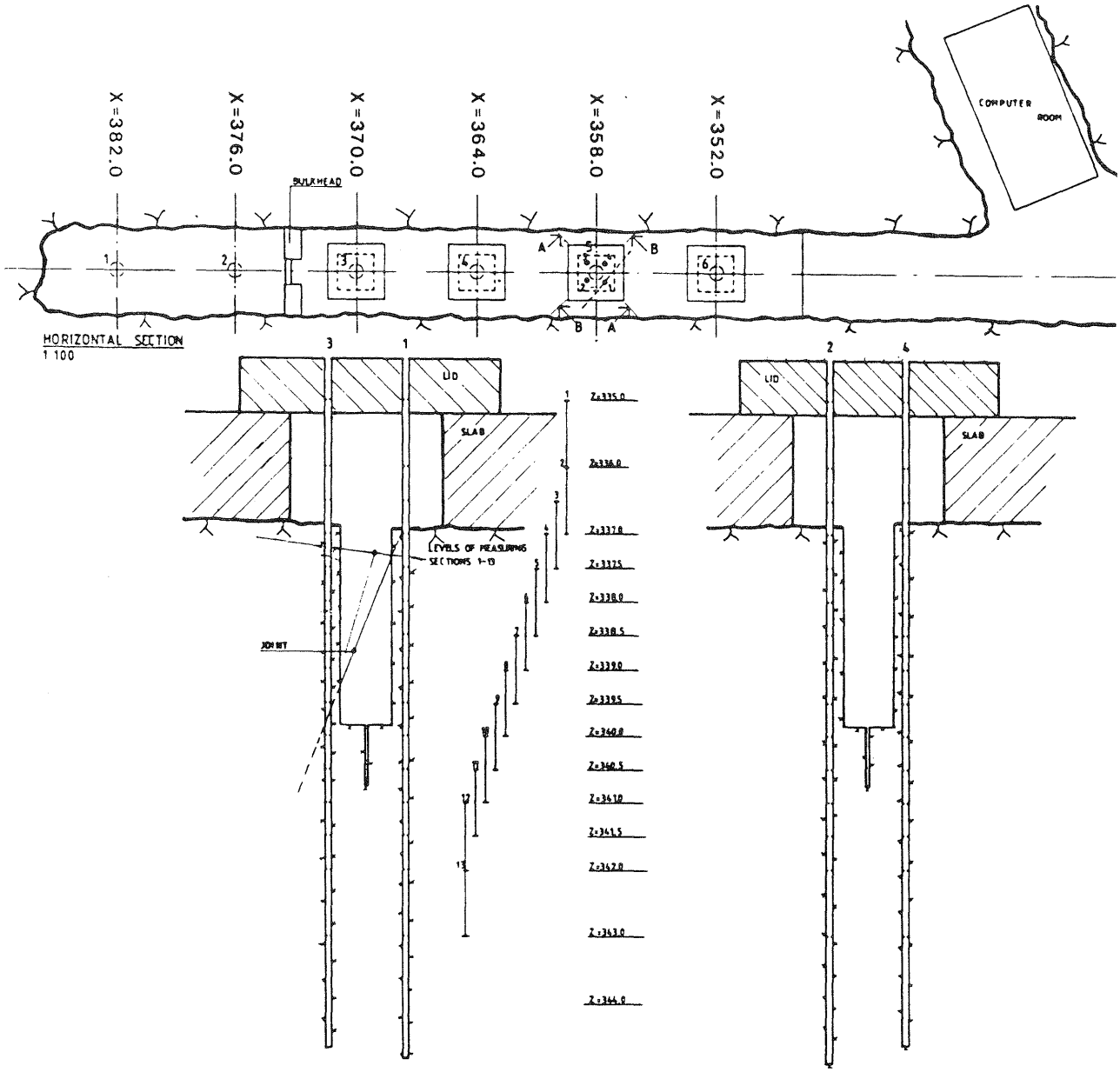

Fig 2.99. The "Kovari" holes intersecting main fractures

3 GENERAL CONCLUSIONS

3.1 Generalized BMT model

3.1.1 Heater holes

The determinant of the development of temperature fields, swelling pressures and displacements is the uptake and redistribution of water. In this respect all the heater holes behaved similarly, the main processes being the ones described below.

I "Wet" holes (no 1, 2 and 5)

1 The approximately 50 liters of water which filled the initial 1 cm wide slot between the rock and the bentonite blocks, were quickly absorbed by the dense bentonite whereby a clay gel formed, which was soon consolidated by the expanding dense clay. This yielded a tight clay/rock contact and an early build-up of a substantial, uniformly distributed swelling pressure.

2 Immediately after the start of the heater, the original pore water in the bentonite was redistributed because of the thermal gradient. Water migrated outwards, towards the peripheral part of the hole, where it contributed to the saturation of the dense bentonite there and to a continued fast increase in swelling pressure.

3 Inflowing water from the rock through larger discontinuities caused local infilling of bentonite which sealed them off and directed the water to finer fractures, which in turn became tight and caused redistribution of the water to the fissures and microscopic discontinuities of the crystal matrix. The frequency of effectively water-bearing fissures in the "wet" holes was sufficient to let more water pass the rock/bentonite interface than the bentonite could absorb and the water uptake

was therefore entirely determined by the suction power of the bentonite. The rate of absorption was found to correspond well to that of diffusion with unlimited access to water at all the boundaries, which means that the counteracting thermal gradient had no substantial effect. The laboratory-determined diffusion coefficient $D=4 \cdot 10^{-10}$ m^2/s applied well indicating no major scale effects.

4 Parallel to and after the saturation of the bentonite blocks, which became "welded" together, the upper part of the dense bentonite expanded upwards displacing the overlying sand/bentonite backfill by 5-7 cm, which was almost exactly the predicted deformation.

The rather special conditions in the BMT with obvious difficulties in compacting the backfill effectively around the heater shaft probably made it more compressible than expected and it may also have offered passage-ways for evaporation of pore water from the close vicinity of the heater. This effect should have been stronger in hole no 5 where there were many more possible leakage paths for water vapor than in the holes located in the closed, inner part of the tunnel. This may have contributed to the slightly lower water content in hole no 5 than in holes no 1 and 2 although the shorter testing time of hole no 5 is an equally possible explanation.

The power increase from 600 to 1400 W in hole no 1, which induced an increase in heater surface temperature by as much as $62^{o}C$ and a thermal gradient of about $3^{o}C/cm$ was not sufficient to drive water from the clay adjacent to the heater.

II "Dry holes" (no 3, 4 and 6)

1 The 3 cm slot between the rock and the bentonite blocks that was filled with loose bentonite powder absorbed water from the rock primarily by capillary suction. Where much water entered through the few clearly water-bearing joints and fractures, local swelling and tightening occurred. It cannot have caused very effective sealing of these joints until a rather late stage had been reached, however, since a significant increase in density did not appear until several months after the test start. Still, the local wetting and saturation of bentonite powder must have contributed to a redistribution of water to adjacent rock areas that led to the observed, remarkably uniform moistening of the entire periphery of the heater overpacks.

The rather dry conditions in the holes did not yield the same early saturation of the overlying sand/bentonite backfill that took place in the "wet" holes. This may have caused some evaporation of pore water along the heater shafts from the bentonite located close to the heaters, the surface temperature of which rose to more than 75°C in the first week. The resulting drop in heat conductivity may in turn have increased the temperature and thereby affected the water content distribution.

2 As in the "wet" holes, the thermal gradient initiated a redistribution of the initial pore water so that the water content dropped close to the heater and increased at the periphery. The latter effect was probably the main reason for the rather early build-up of swelling pressures in the "dry" holes. The radial distribution of water reached a relatively stable state, which can be reasonably well predicted by applying the "thermo-

capillary" hypothesis with the empirically derived k_2 -factor adapted to axi-symmetric conditions (cf. Figs 2.89-2.91). While the slightly greater access to water at the top and base of the holes allowed for a faster uptake of water by the bentonite than at the central parts of the holes, the water discharge capacity of the rock was still low and the moistening was very moderate also at their ends. Thus, the water content of the entire overpack changed very slowly but as indicated by the high-temperature test in hole no 3, the rate of moistening increased when the tunnel floor became wetter in the last phase of the test. If the "dry" hole tests had been prolonged the moistening would therefore probably have proceeded and ultimately reached the same state of practically complete saturation as in the "wet" holes. Water overpressure in the adjacent rock would not be a necessary prerequisite since the suction power of the bentonite would be sufficient to create the required hydraulic gradient to bring water through the rock. The appearance or non-existence of significant positive piezometric heads in the surrounding rock can actually be taken as a measure of whether the capacity of the rock to give off water is a determinant of the moistening rate or not.

Close to heater, i.e. where the water content was below about 8 %, more or less continuous pore systems probably existed in which cyclic water flow through the vaporization/condensation mechanism took place. This contributed to the heat transfer and resulted in a higher heat conductivity than under isothermal conditions.

3 As in the case of the "wet" holes, expansion of the upper part of the dense bentonite overpack took place. The heave in the 600 W tests in holes no 3 and 4 was smaller due to the shorter time for water uptake, the uniform expansion over the boundary indicating that most of the water migrated vertically from the overlying backfill.

3.1.2 Tunnel backfill

The blasting operations are assumed to have increased the frequency and apertures of the virgin rock within a peripheral zone of about 0.5 m thickness, particularly in the tunnel floor as implied by the fracture mapping and the applied blasting technique. This effect, and the removal of the blasted rock mass, probably tended to reduce the stresses in the peripheral zone, by which its hydraulic conductivity must have been somewhat increased. The tangential stress in the rock beyond this zone was increased to within a few meters distance and this probably had a tightening effect on the rock with respect to radial inflow into the tunnel, which was further reduced by the increased temperature in the short inflow tests that preceded the BMT. Joints and fractures outside the fractured zone and oriented more or less parallel to the tunnel walls are expected to have been somewhat widened and extended by the stress redistribution and this resulted in a net increase in axial hydraulic conductivity along the drift. The net result of this would naturally be an increased outflow from the close vicinity of the backfilled part of the tunnel when the piezometric heads in the rock surrounding the backfill finally rose due to the successive saturation of the fill.

The actual proof of the increased outflow from the inner part of the tunnel was obtained by measuring the water inflow into heater hole no 3 after the excavation in late May 1984. As shown by Fig 3.1 this inflow tended to increase in the course of the test and reached a maximum shortly before the bulwark was opened. After this operation the inflow dropped rapidly because of the strongly reduced piezometric heads in the water-bearing fracture zone at the tunnel periphery, which was then drained due to the removal of bulwark and backfill.

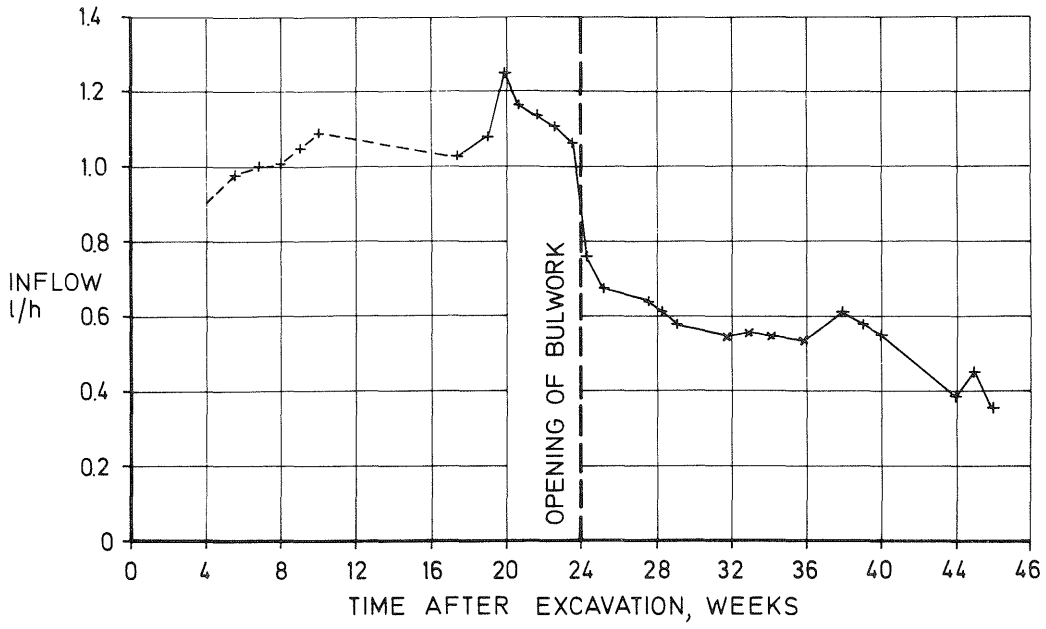

Fig 3.1. Measured inflow into hole no 3 after the excavation of this hole following the high-power test

As in the heater holes local swelling and tightening of the primary water-bearing rock structures took place, which directed the water to adjacent, less conductive zones, which in turn tended to be sealed. The initial moistening of the backfill was thus very heterogeneous but it became rather uniform in less than a year.

With the present low water content of the sand/bentonite backfill, the major driving force in the moistening process was probably capillary suction. Since it produces negative pore pressures of several hundred kilopascals in the present type of soil material, the water uptake became very rapid although the external water pressures remained low. The air enclosed in the pores was moved by the advancing water front to the central upper part of the backfill where it formed isolated non-saturated zones. The main direction of water migration in the wetting process was upward from the floor and lower parts of the tunnel since water naturally was more abundant here as was also manifested by the distribution of piezometric heads around the tunnel periphery.

3.2 Practical experience

3.2.1 Application of buffer materials

Insertion of HLW canisters with bentonite overpack in tightly fitting holes, tunnels, or vertical shafts needs to be conducted in a well planned and continuous manner since longer stops or intermittent operations lead to strong local bonds between rock and bentonite by which planned rearrangement and adjustment of bentonite blocks and canisters may become difficult. Also, exposed surfaces of bentonite-based buffer materials which are wetted soon become slippery and give off semi-liquid clay that flows to the floor and makes all transportation and handling operations difficult.

Much experience with respect to the application of buffer materials in deposition holes extending downwards from the floor of tunnels was gained through the Buffer Mass Test. Thus, it was demonstrated that the insertion of a whole set of a canister surrounded by tightly fitting bentonite blocks is a feasible technique. Likewise, successive application of bentonite blocks to form a brickwork with a central space left open for the lowering of a canister, was shown to be practical. In the former case, the load of the canister and bentonite blocks needs to be carried by using a base plate to which removable rods are attached at the edge. This arrangement was not tested but it is assumed to be a simple matter as long as there is a slot with a width of about 1-2 cm between the rock and the bentonite package. As indicated by the BMT study it is possible to fill this space with air-dry bentonite powder by which the stack of bentonite blocks is offered a certain mechanical support and a reasonably effective heat transfer to the rock. However, it is felt that filling the slot with water of low salinity would be the best solution since it is known to create rapid uniform swelling and a tight bentonite/rock contact over the entire hole periphery by which a high capacity to transfer heat to the rock is obtained soon after canister emplacement.

If the second technique for application is used, i.e. that bentonite blocks are piled-up to form a brickwork before the canister is inserted, a very rough shape of the rock surface can be accepted which allows for the use of slot-drilling technique as an alternative to full-face drilling. The slot between the brickwork and the rock is suitably filled with water if it is narrow, while it is probably more practical to fill wider slots of varying width with bentonite powder that is compacted parallel to the piling work. Since the application and compaction work can be effectively controlled, the homogeneity

and density of the compacted powder is expected to be very satisfactory. Thereby, the heat conductivity becomes reasonably high and it can be further improved by adding quartz powder. This would mean that the ability of the highly compacted bentonite to penetrate into fractures is largely reduced but this negative effect can be eliminated by a preceding fracture sealing through injection.

Either water is or is not introduced in the slot between the bentonite package and the rock in the deposition holes, the saturation of the highly compacted bentonite will be so slow that no noticeable displacement of the interface between the pile of bentonite blocks and the overlying sand/bentonite backfill will take place in the first few months. Thus, with a simple cover of the backfill in the form of a thin concrete layer, which is removed shortly before the application of the tunnel backfill, the dry density of the bentonite components is largely preserved until the start of the backfilling operation even if this takes place half a year after the canister emplacement.

While the BMT experiment demonstrated that the various ways of emplacing canisters and bentonite overpacks is sufficiently wellknown to be applied today already, the technique of backfilling tunnels from which deposition holes are drilled, has to be improved. Thus, the layer-wise application and compaction of sand/bentonite mixtures in the BMT study did not yield the high bulk density that can be obtained when using very effective compaction methods. Thus, when vibrating rollers with a weight of 5 tons are used to compact a mixture of 10 percent bentonite by weight and 90 percent suitably graded ballast, the resulting dry density should be at least 1.95 t/m^3, which corresponds to a bulk density of slightly more than 2.2

t/m^3 after complete saturation. These densities can be reached either by compacting well mixed components with water added to yield the optimum water content, or by mixing and compacting without adding water (Fig 3.2). Since the admixture of water yields a quality control problem and more expensive and difficult handling, the "dry" mixing and compaction is recommended.

As demonstrated by the BMT study, the upper 1.6-2.0 m space in tunnels cannot be filled and compacted very effectively by use of shotcreting, and new techniques have to be developed. One possible treatment is to use shotcreting for application, and large, low-frequency pounders driven by compressed air or combustion technique for compaction. The goal should be to arrive at a bulk density of at least 2.2 t/m^3 at saturation of the entire tunnel backfill since this would yield a strong support of the surrounding rock and a minimum vertical expansion of the highly compacted bentonite in deposition holes extending downwards from the tunnel floor.

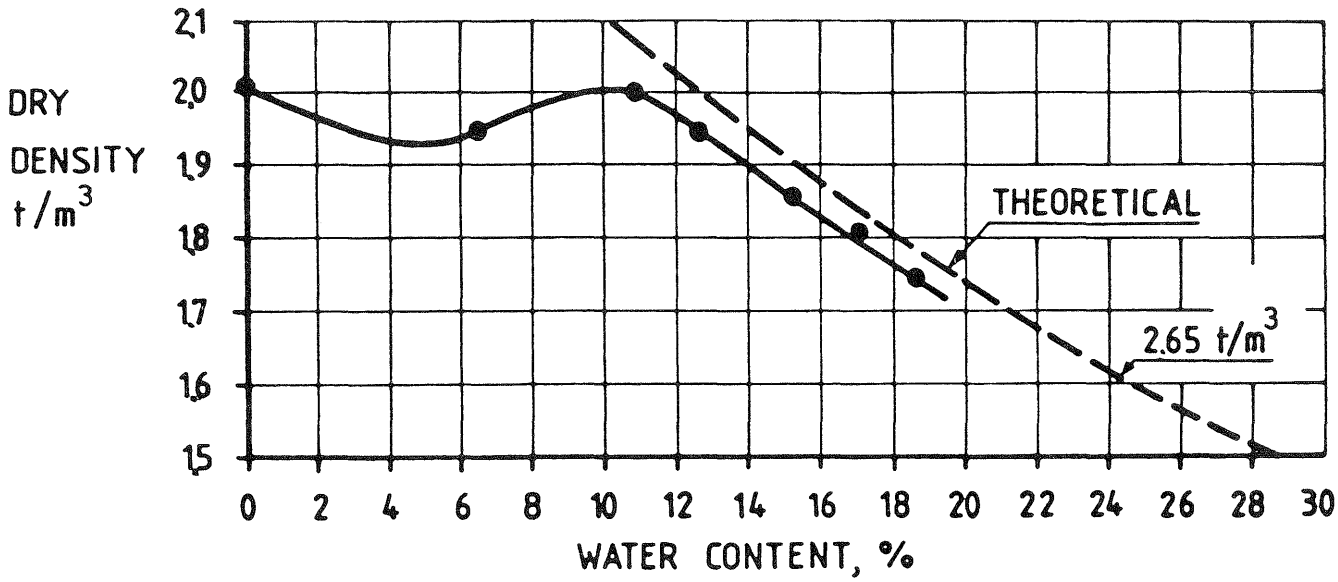

Fig 3.2. Dry density versus water content of mixture of 10 percent commercial bentonite (Laviosa) and 90 % graded ballast (Modified Proctor compaction). Notice that compaction at a very low water content gives approximately the same density as that at optimum water content.

3.3 Scale dependence, geometry

3.3.1 General

The size of the heater holes and heaters in the Buffer Mass Test are approximately 50 % of the full size deposition holes and canisters of the Swedish KBS 3 concept, while they represent about 25 to 40 % of the corresponding constituents of the Swiss concept. Since it is not immediately clear if the BMT results are relevant to such full-scale applications, it is of interest to find out whether there is any scale dependence of the major processes in the bentonite. Possible anomalies may primarily appear with respect to the magnitude and distribution of the temperature, and the heating of the bentonite will therefore be focused on here.

It is concluded from the BMT study that the rate of water uptake in the bentonite is of profound importance for the temperature evolution in the system and we therefore have to assume proper hydraulic boundary conditions before considering the geometrical scale effects. One extreme case is that of unlimited access to water over the entire rock/bentonite interface in the deposition holes. This corresponds to the "wet" holes in the BMT study, while the opposite condition, i.e. that of no water uptake, roughly corresponds to the "dry" hole no 6. We will consider here the two theoretical cases of unlimited access to water, and no uptake at all, both applied to the special case of KBS 3 as a practical example (Fig 3.3). For proper evaluation of the scale dependence the heat load will be taken the same as that in the BMT study, i.e. 400 W per meter length of canister, which corresponds to a total power of about 1800 W. The temperature for any other power with the same hole/canister geometry is easily derived since it is almost directly proportional to the power.

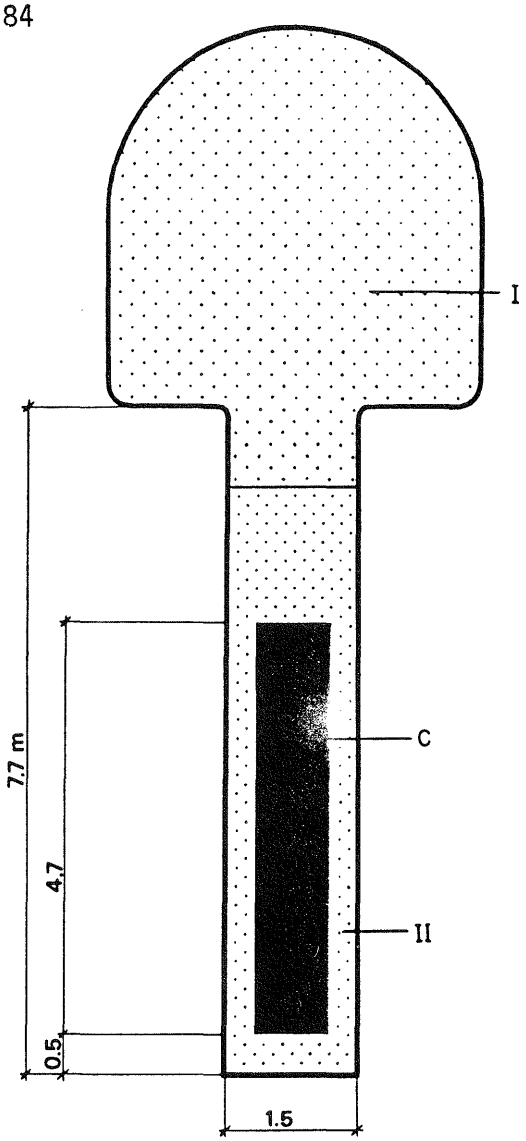

I Sand/bentonite
II Highly compacted bentonite
C Canister

Fig 3.3. Main geometrical features of the KBS 3 concept

3.3.2 Temperature development

3.3.2.1 The wetting process

The bentonite annulus of the KBS concept is 100 % thicker than that of the BMT case, which means that the arrival at a high degree of water saturation even in richly water-bearing rock will require much more than the 2-3 year period in which the bentonite became largely saturated in the "wet" Stripa holes. Using the same calculation procedure as for the heater holes and applying the same parameters for the water uptake, the moistening of the KBS 3 bentonite overpack will be as shown in Fig 3.4., i.e. 12-15 years will be required to raise the average water content from the assumed original 13 % to almost complete saturation.

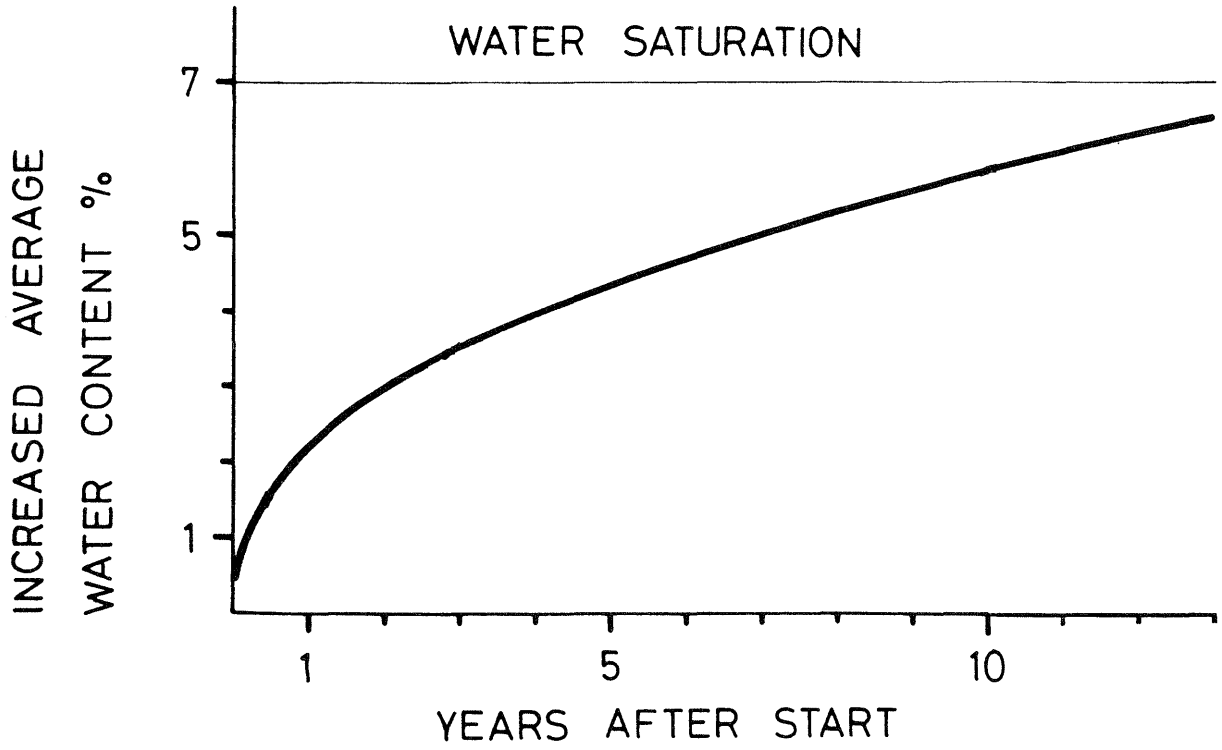

Fig 3.4. Moistening rate of the KBS 3 overpack in richly water-bearing rock

The distribution of the water content after 5 months, 3.2 years and about 10 years is illustrated in Figs 3.5-3.7. The diagram in Fig 3.7 demonstrates that the bentonite at the top of the canister will be the last part that becomes saturated and this suggests that the canister will tend to be pressed upwards during the saturation process due to the slower build-up of swelling pressures at the top. The upheaval is expected to be very slight, probably a few centimeters only, and it will be partly compensated for by the subsequent secular settlement.

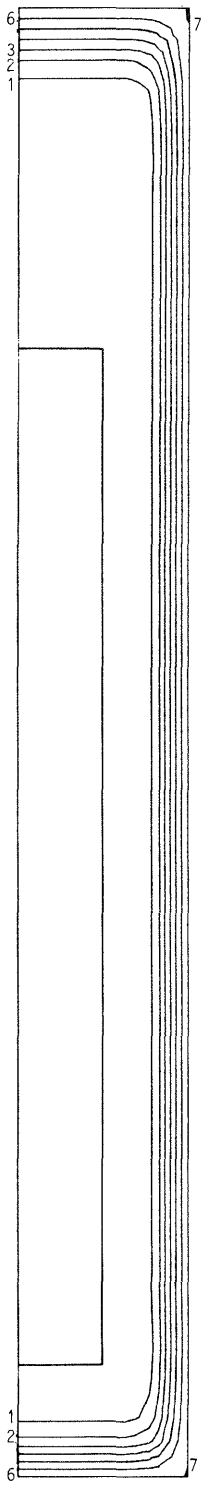

VATTENUPPT KBS3 V1

ISO-LINE NO	ISO-LINE LEVEL	EQUI-DISTANCE
1	1.0000	
2	2.0000	1.0000
3	3.0000	1.0000
4	4.0000	1.0000
5	5.0000	1.0000
6	6.0000	1.0000
7	7.0000	1.0000

MAX VALUE 6.9338
MIN VALUE -0.1745

LENGTH SCALE: 1 MM= 0.2000E-01

0 10 20 MM

Fig 3.5. Predicted increase in water content in the KBS 3 canister overpack applying the general BMT model for unlimited access to water. State after 5 months

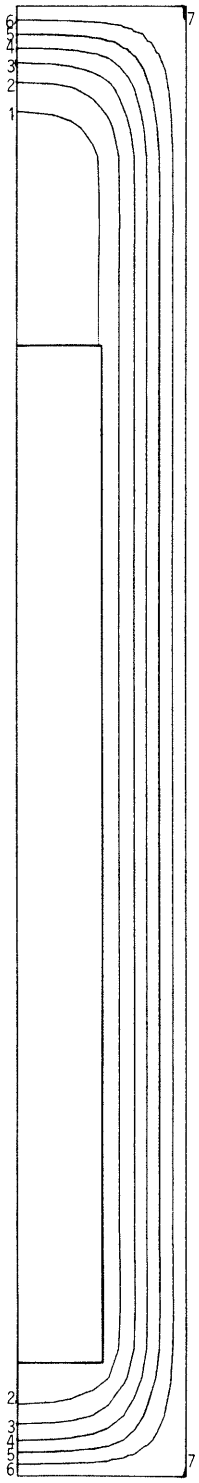

VATTENUPPT KBS3 V1

ISO-LINE NO	ISO-LINE LEVEL	EQUI-DISTANCE
1	1.0000	
2	2.0000	1.0000
3	3.0000	1.0000
4	4.0000	1.0000
5	5.0000	1.0000
6	6.0000	1.0000
7	7.0000	1.0000

MAX VALUE 6.9803
MIN VALUE -0.0039

LENGTH SCALE: 1 MM= 0.2000E-01

0 10 20 MM

Fig 3.6. Predicted increase in water content in the KBS 3 canister overpack applying the general BMT model for unlimited access to water. State after 3.2 years

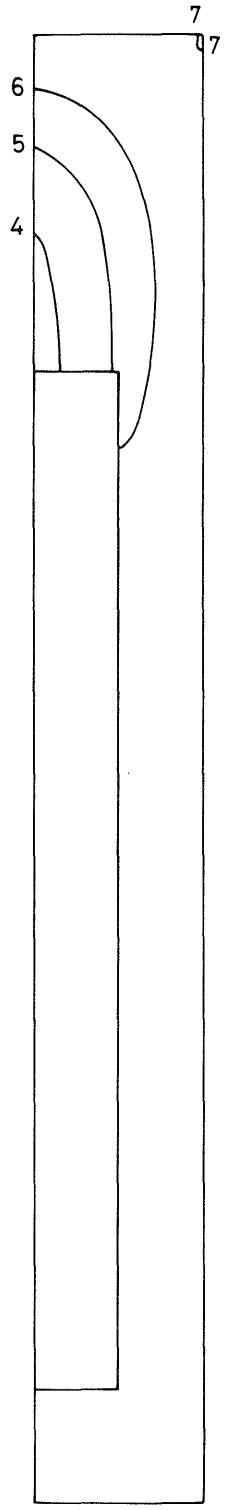

VATTENUPPT KBS3 V1

TIME = 0.3164E+09 10y
TEMPERATURE

ISO-LINE NO	ISO-LINE LEVEL	EQUI-DISTANCE
4	4.0000	1.0000
5	5.0000	1.0000
6	6.0000	1.0000
7	7.0000	

MAX VALUE 6.9980
MIN VALUE 3.7837

LENGTH SCALE: 1 MM= 0.2000E-01

0 10 20 MM

Fig 3.7. Predicted increase in water content in the KBS 3 canister overpack applying the general BMT model for unlimited access to water. State after about 10 years

In the theoretical "dry" hole case no water uptake is foreseen and here the BMT model implies redistribution of the initial water to yield a stable water content gradient which is related to the thermal gradient. As will be shown later, this gradient (about $1^{o}C$ per centimeter) is approximately 50 % of that in the "dry" 600 W BMT heater holes, which is expected to yield a less steep water content gradient in the KBS 3 case. Thus, while the water content ranged between about 7 % to 14 % in the radial direction of the major part of the non-saturated bentonite annulus at mid-height of the "dry" BMT holes, the corresponding interval is expected to be about 8 to 13 %, taking the initial water content as 10 %. The practical consequence of this would be that the drying of the clay close to the hot canister will be less obvious and that the laboratory-derived thermal parameters will therefore apply better than in the BMT case. Furthermore, the possible cyclic vaporization/condensation process close to the canister will be even more moderate than in the low-power heater tests in Stripa.

3.3.2.2 Temperature

The derivation of the temperature development in the bentonite has been based on the successive increase in heat conductivity that follows from the wetting in the "wet" case. The initial, only partly wetted state and the final, completely saturated condition, were represented by the same thermal parameters as in the previous calculations (Chapters 2.2.1.1 and 2.2.1.3), while linear interpolation was applied to the intermediate stage.

The results obtained for a discrete deposition hole of the KBS 3 type with a 1800 W canister are given in Figs 3.8 to 3.10. The effect of moistening of the clay is obvious from the first two diagrams; the temperature increase of the bentonite close to the canister at its

mid-height will rise to about 60°C after 3 years in the theoretical case of no water uptake, while in the "wet" case, a maximum temperature increase of about 55°C is reached after slightly less than 1 year, whereafter cooling by slightly more than 5°C takes place. At an ambient rock temperature of 10°C the bentonite temperature will thus increase to about 70°C in 3 years in the "dry" case, while the maximum temperature for the successively wetted bentonite in richly water-bearing rock will be about 65°C. Since, in practice, wetting will always take place, albeit at a slower rate than in the case of unlimited access to water, the bentonite in a discrete hole with the given geometry and power will not experience a higher temperature than 70°C. The main conclusion from this analysis is that the thermodynamic conditions in a full scale application of the KBS 3 type will be in the same range as in the BMT tests and that the induced physical and chemical effects will be similar. This is of particular importance with respect to the integrity of the smectite component of the bentonite, a matter that will be discussed in detail in Volume III.

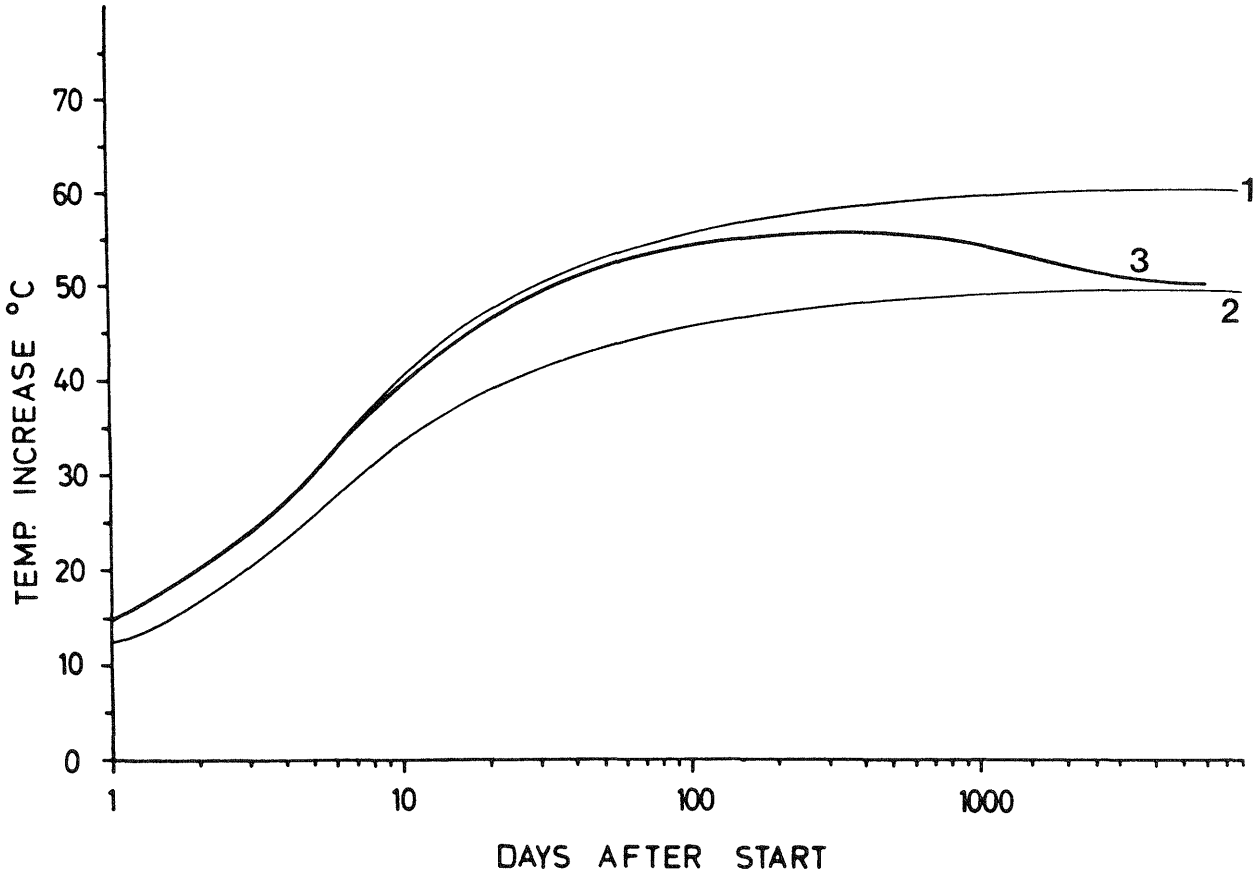

Fig 3.8. Predicted temperature increase in the bentonite close to the KBS 3 canister at its mid-height (assumed power 1800 W). 1) Initial water content preserved. 2) Complete saturation from start. 3) Successive wetting at unlimited access to water from rock

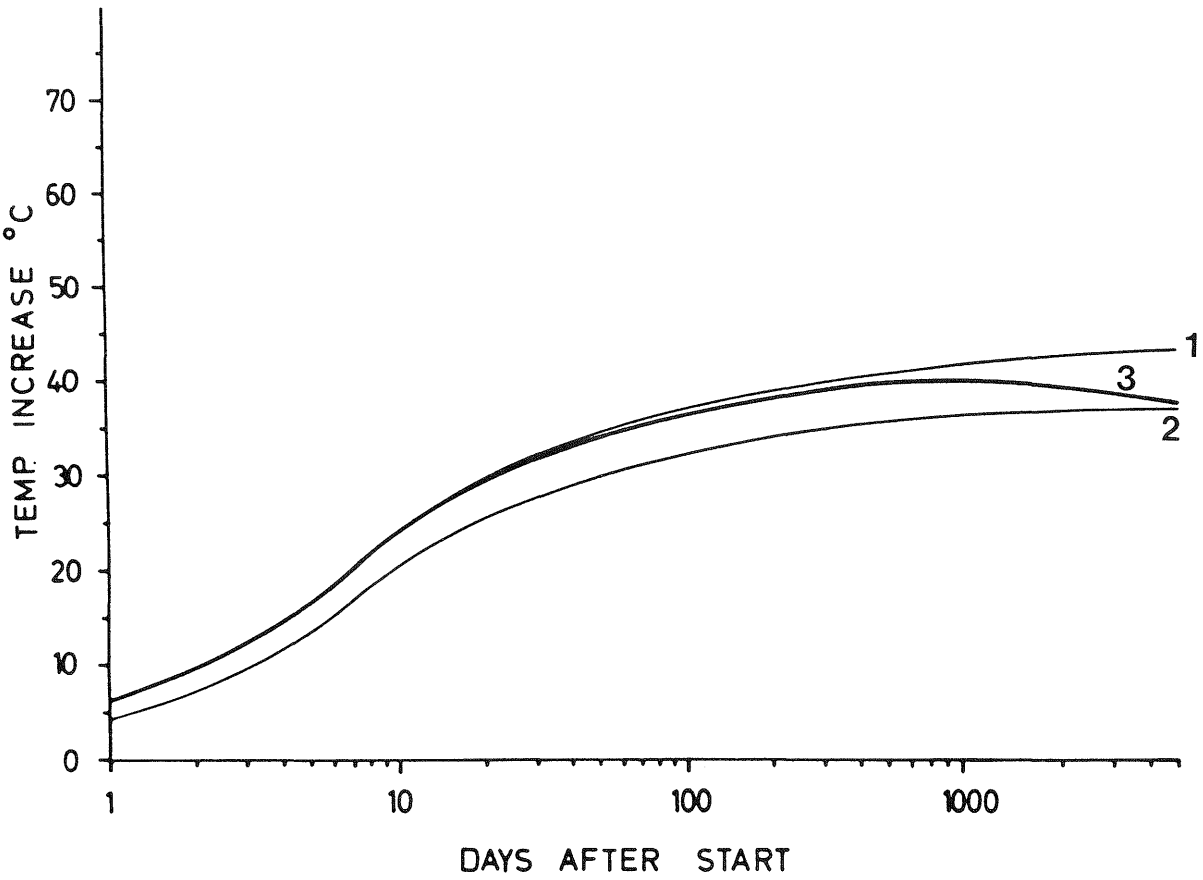

Fig 3.9. Predicted temperature increase at half distance between the rock and the KBS 3 canister at its mid-height (assumed power 1800 W). 1) Initial water content preserved. 2) Complete saturation from start. 3) Successive wetting at unlimited access to water from rock

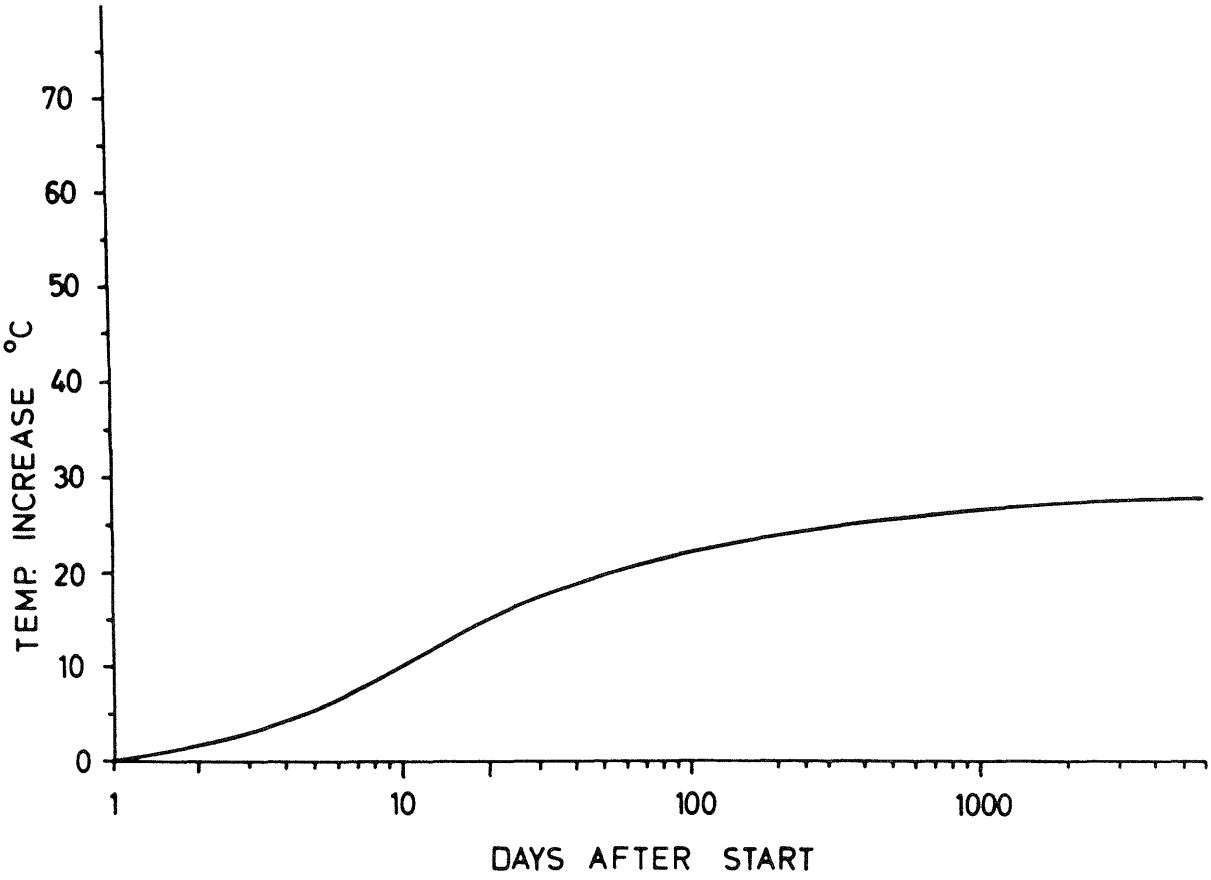

Fig 3.10. Predicted temperature increase the rock/bentonite at mid-height of the KBS 3 canister at 1800 W power

4 ACKNOWLEDGEMENTS

The authors are greatly indebted to all members of the field staff in Stripa who participated, with great skill, in the difficult backfill excavation and sampling operations. Special thanks are due to Thomas Forsberg and Björn Hagwall, University of Luleå, and Sven-Eric Tegelmark, Rockhammar, the latter two being responsible for much of the excellent treatment of the computer-logged data.

The authors also express their sincere gratitude to the members of the Technical Subgroup no 2, particularly to its chairman Paul Gnirk, for many valuable suggestions and fruitful discussions. The thanks are extended also to several colleagues at the SKB, particularly to Anders Bergström, Hans Carlsson and Lars Bertil Nilsson, for their support and help.

Finally, the authors wish to express their sincere appreciation to Mrs Jeanette Stenelo, SGAB, for the typing and for turning this activity into a noble art.

5 REFERENCES

1 "Heat Conductivity of Bentonite Buffer Materials". Knutsson, S., 1983. Int. report, University of Luleå.

2 "Buffer Mass Test - Thermal Calculations for the High Temperature Test". Knutsson, S., 1983. Stripa Project Internal Report 83-03.

3 "Water Uptake, Migration and Swelling Characteristics of Unsaturated and Saturated, Highly Compacted Bentonite". Pusch, R., 1980. SKBF/KBS Technical Report 80-11.

4 "Swelling Pressure of Highly Compacted Bentonite". Pusch, R., 1980. SKBF/KBS Technical Report 80-13.

5 "Use of Clays as Buffers in Radioactive Repositories". Pusch, R., 1983. SKBF/KBS Technical Report 83-46.

6 "Water Flow and Swelling Pressure in Non-saturated Bentonite-based Clay Barriers". Börgesson, L., 1984. Clay Barriers for Isolation of Toxic Chemical Wastes. Int. Symp., May 28-30, 1984, Stockholm, Sweden (in press).

7 "Structure of Water Adsorbed on Smectites". Sposito, G., and Prost, R., 1982. Chem. Rev. Vol. 82 (6), pp. 553-773.

8 "The Physical State of Pore Water of Na Smectite used as Barriers Component". Pusch, R., and Carlsson, T., 1985. Engineering Geology, Elsevier Publ. Co. (in press).

9 "Water Uptake and Swelling of Montmorillonitic Clay Seams in Rock". Pusch, R., 1979. Proc. 4. Int. Congr. on Rock Mechanics, Montreux, Vol. 2.

10 "Soil Physics". Marshall, T.J., and Holmes, J.W., 1979. Cambridge University Press.

11 "Proc. Int. Symposium on Water and its Conduction in Soils". Highway Research Board, Special Report 40, 1958. Wash. D.C.

12 "Hydrogen and Hydrogen Sulphide Diffusion in Compacted Bentonite". Eriksen, T.E., and Jacobsson, A., 1982. Internal Report.

13 "Diffusion of the Dyes, Eosin Yellowish, Bromophenol Blue, and Naphthol Green Bluish in Water Adsorbed by Montmorillonite". Anderson, D.M., Brown, R.L., and Buol, S.W., 1966. Soil Science Vol. 103, No. 4.

14 "Stability of Bentonite Gels in Crystalline Rock - Physical Aspects". Pusch, R., 1983. SKBF/KBS Technical Report 83-04.

15 "Borehole Sealing with Highly Compacted Na Bentonite". Pusch, R., 1981. SKBF/KBS Technical Report 81-09.